DYNAMICS AND THERMODYNAMICS OF GENETICALLY ENGINEERED ENZYMES

BY

BETH SANDERS, B.Sc.

PhD Thesis submitted, April 1989

Chemistry Department

University of Glasgow

1989

CONTENTS

Acknowledgements

This thesis is an account of original research work carried out in the Biophysical Chemistry laboratory, University of Glasgow, from October 1985 to October 1988 with funding from the Science and Engineering Research Council.

To Dr. A. Cooper I would like to extend my sincere thanks for his continual help and advice throughout this project. I also wish to extend my appreciation to Margaret Nutley for her technical assistance; Dr.A.Brown and co-workers for their advice and use of their lab facilities; Dr. L. A. Fothergill-Gilmore for the provision of the over-producing plasmids; Professors L.D. Barron and R.H. Pain for the use of Raman and fluorescence equipment, respectively;Isobel Freer and the Mycology Department for the use of their autoclaves and Drs. C.M. Johnson and D.T.F. Dryden for their instruction and assistance in obtaining calorimetric and fluorescence data. Finally I must thank my mother, father and John for their constant patience,support and encouragement during my time at University-I will always be grateful.

Beth Sanders

ABSTRACT

The possible effects of site-directed mutagenesis on the dynamic and thermodynamic properties of enzymatics have been studied using yeast phosphoglycerate kinase (PGK) as a test system. A variety of physico-chemical techniques have been used, including: isothermal and differential scanning microcalorimetry, fluorescence and fluorescence relaxation kinetics, Raman spectroscopy and depolarised Rayleigh scattering. The latter is a new technique, developed here, which shows promise in the study of dynamic properties of biological macromolecules.

Wild-type yeast PGK and the His388 $\longrightarrow$ Gln mutant, a mutant thought to induce significant changes in interaction in the "hinge" region of PGK, were compared by all techniques. Both forms of the enzyme were prepared in high yield by multi-copy plasmid techniques, using plasmids supplied by Dr. Fothergill-Gilmore (Edinburgh University).

Isothermal microcalorimetry was used to measure the thermodynamic parameters (K_{dis}, ΔH, ΔS) for binding of the three readily available substrates (ATP, ADP, 3-phosphoglycerate) to the enzyme. Although there were small differences in dissociation constants between the wild-type and mutant proteins, consistent with K_m differences observed by kinetic methods, there were no major differences in enthalpies of

binding. In the case of 3PG binding, however, there were significant differences with preliminary enthalpic data for the wild-type enzyme published by other workers. Enthalpic binding differences observed in various buffer systems are possibly due to a hitherto unrecognized protonation change associated with PGK-3PG binding.

Differential scanning calorimetry, performed for us at Yale University by Prof. J.M.Sturtevant, showed major differences in thermal stability between mutant and wild-type PGK, with the mutant being generally less stable to thermal unfolding. But, unfortunately, the thermogram of both forms of the enzyme shows some anomalies which, so far, have prevented detailed thermodynamic analysis of the thermal transition process.

Fluorescence emission, excitation and relaxation studies, performed in collaboration with Dr. D.T.F.Dryden (Newcastle University), shows significant differences between wild-type PGK and the His388 $\longrightarrow$ Gln mutant, though in neither case are these properties affected by ligand binding. Results indicate an interesting enhancement of fluorescence energy transfer between tryptophan residues in the mutant enzyme, possibly as a result of increased hinge flexibility in this mutant.

A new technique of depolarized Rayleigh scattering from dilute aqueous solution has been developed and shows promise in the study of protein dynamic effects. This technique

essentially probes the very low frequency (< 50 cm^{-1}) region of Raman scattering where large scale, highly damped, anharmonic motions of macromolecules are thought to occur. Trial experiments using lysozyme as a test system show significant low-frequency spectral shifts on binding of the tri-N-acetylglucosamine inhibitor, consistent with a "stiffening" of the protein induced by ligand binding in the active site cleft. The routine and reproducible application of this technique to larger macromolecules has yet to be perfected, but interesting and suggestive preliminary data have been obtained for the mutant PGK. Ligand binding to the ATP domain induces global "stiffening" effects similar to those observed with lysozyme. But, in contrast, binding of 3PG on the opposing domain of this enzyme results in shifts to lower frequencies consistent with a significant "loosening" of the entire structure. No such effects have been detected for the wild-type enzyme.

The general conclusion that may be drawn is that although short-range protein-substrate interactions in the active sites of PGK are relatively unaffected by this mutation, replacement of His388 by glutamine in a region remote from the active sites but in a key position to control inter-domain motion, results in measurable differences in large-scale dynamic processes in this protein which may be related to overall function.

Additional work (reported in Appendix D) includes an examination of the possible use of Surface Enhanced Raman Scattering (SERS) to study the vibrational spectra of proteins in dilute aqueous solution.

CHAPTER 1

CHAPTER 1

1.1 Introduction

1.1.1 Protein Function

Proteins are very large molecules which play a crucial role in virtually all biological processes. They are involved in the transport and storage of small molecules and ions. For example, haemoglobin and myoglobin transport oxygen in erythrocytes and muscle, respectively. Co-ordinated motion such as muscle contraction is accomplished by the sliding movement of the protein filaments actin and myosin. Proteins also play a vital role in distinguishing between self and non-self within the body's immune system. Antibodies are highly specific proteins that recognize and combine with foreign molecules and substances such as viruses, bacteria and cells from other organisms. As well as these functions, the high tensile strength of skin and bone is due to the presence of collagen, a fibrous protein and the response of nerve cells to specific stimuli is mediated by receptor proteins. For example, rhodopsin is the photoreceptor protein in retinal rod cells. The sequential expression of genetic information essential for the orderly growth and differentiation of cells is also controlled by proteins. One example of this involves the repressor proteins in bacteria which are important in the control of elements that silence specific segments of the DNA of a cell. But the most ubiquitous function of proteins, and the one which is of most relevance to this thesis, is that of enzymatic recognition, control and catalysis.

1.1.2 Enzymatic Catalysis

Chemical reactions in biological systems rarely occur at an appreciable rate, nor in a well-controlled manner, in the absence of enzyme catalysts. These catalysts are proteins which may accelerate a specific reaction by factors of at least a million.

Unlike most inorganic catalysts, enzymes are characteristically very specific in two ways. Firstly, most enzymes will interact only with one set of reactants (substrates) and secondly they will speed up only one of the various possible reactions of these substrates.
Familiar examples include the digestive enzymes that degrade foodstuffs to simple ingestable compounds and the biosynthetic enzymes that build complex molecules from simpler compounds. Even a reaction as simple as the hydration of carbon dioxide must be catalysed by an enzyme, carbonic anhydrase.

Given the functional diversity of proteins, one would expect to observe a corresponding complexity in the detailed structure of these molecules. This expectation has been confirmed by X-ray diffraction studies of these very large polypeptide molecules. The basic component of these molecules is the polypeptide chain, an unbranched polymer normally consisting of a sequence of a few hundred amino acid residues. Protein molecules will consist of one or a small number of such polypeptide chains, complemented in some cases by one or more prosthetic groups such as metal ions or special organic molecules.

For a given protein, the polypeptide chain of each molecule is folded compactly into a characteristic three dimensional structure. This conformation and the stability of a protein is heavily dependent upon non-covalent forces between the various amino acid side-chains comprising the primary structure (see section 1.1.4). It is these non-covalent forces that are responsible not only for the formation of the structures and complexes but also for chemical reactions themselves.

The first step in enzymatic catalysis is usually the formation of the enzyme-substrate complex and it is evident that this can only form when the enzyme and substrate are chemically compatible and capable of reacting with one another.The region that binds the substrates (and the prosthetic group, if any) and contributes the residues that directly participate in the making and breaking of bonds is known as the active site of the enzyme. This active site is an intricate three dimensional structure made up of groups that come from different parts of the amino acid sequence and usually exists in the form of a cleft or a crevice. A given enzyme will only interact with those substrates whose structure will "fit" both the stereochemistry and the interactions within the this site. It is in such a way that the enzyme provides a microenvironment which has the special properties essential for the role of catalysis.

Fundamental questions, however, regarding the nature of the forces involved when a substrate binds to an enzyme remain to be answered and so to help facilitate this an examination of the thermodynamic and dynamic changes which occur upon

substrate binding must take place (see sections 1.1.3 and 1.1.4, respectively).

1.1.3 Thermodynamic Parameters of Enzyme-Substrate Binding

The relationship between structure and thermodynamics is a fundamental physical key to the understanding of a variety of biological processes involving macromolecules. While the mechanism of such processes will differ from case to case, determination and rigorous interpretation of the thermodynamics are necessary. This requires the experimental evaluation of the principle thermodynamic quantities describing an interacting system, the apparent standard Gibbs energy change, ΔG^{o}, enthalpy change, ΔH^{o}, entropy change, ΔS^{o} and heat capacity change, ΔC_{p}.

Consider the binding equilibrium between an enzyme and its substrate or ligand, where a 1:1 enzyme-substrate complex forms. If the process is reversible then it can be described by equation 1.1 (assuming that no reaction is taking place).

$$E + S \rightleftharpoons ES \qquad (1.1)$$

If (E) is the concentration of free enzyme

(S) is the concentration of free substrate

(ES) is the concentration of enzyme-substrate complex at equilibrium

the situation at equilibrium may be described by:-

$$K_{ass} = \gamma (ES) / (E)(S) \qquad (1.2)$$

where K_{ass}, the equilibrium constant, gives a value for the relative proportions of E, S and ES. γ is the ratio of the activity co-efficients of ES to those of E and S and the value of γ will equal unity if the solutions are assumed to be ideal - as will be assumed henceforth. (This is usually a reasonable approximation for very dilute aqueous solutions). The free energy change, ΔG for a chemical reaction at constant pressure can be written as

$$\Delta G = \Delta G^{o} + RT\ln\frac{\Pi(\text{activities of products})}{\Pi(\text{activities of reactants})} \qquad (1.3)$$

where R is the gas constant and T is the absolute temperature For the enzyme-ligand binding system described above equation 1.3 becomes

$$\Delta G = \Delta G^{o} + RT\ln((ES)/(E)(S)) \qquad (1.4)$$

As a reaction proceeds its capacity to perform work, as measured by G, diminishes until finally, at equilibrium, the system is no longer able to supply additional work. This means that both reactants and products possess the same free energy and therefore $\Delta G=0$. Hence, the change in free energy for standard states of one molar can be related to K_{ass} by equation 1.5

$$\Delta G^{o} = -RT\ln K_{ass} \qquad (1.5)$$

The Gibbs free energy change (ΔG^{o}) represents a composite of two factors contributing to spontaneity, enthalpy (ΔH^{o}) and

entropy (ΔS^{o}). At a constant pressure this can be represented as

$$\Delta G^{o} = \Delta H^{o} - T\Delta S^{o} \qquad (1.6)$$

ΔH^{o} is the enthalpy (or heat content) change between initial and final states under standard conditions. In general

$$\Delta H = U + P\Delta V \qquad (1.7)$$

where ΔU equals the change in internal energy, P is the pressure and ΔV is the volume change. ΔU represents changes in overall internal energy of the entire system during ligand binding and includes contributions both from dynamic effects (molecular kinetic, rotational energies and so on) and from inter- and intramolecular interactions (potential energy). Both these will, of course, involve solvent molecules as well as the enzyme and ligands themselves. $P\Delta V$ represents an energy correction term to account for any work done by volume changes during the binding process. This is usually relatively small for protein interactions (Kauzmann, 1959).

As observed from equation 1.6, however, the evolution of energy is not the only criterion to be considered if a reaction is to be spontaneous. The degree of disorder of a system is represented by the thermodynamic entropy (S).

Various direct methods for determining thermodynamic binding parameters will be described later (section 2.1.3) but one

important indirect indicator of substrate affinity comes from simple kinetic measurements.

1.1.3.1 Enzyme Kinetics and the Michaelis Constant

If the substrate binding equilibrium is rapid compared to the subsequent reaction to form products, then the kinetics of the reaction may be described by the simple Michaelis-Menten scheme:-

$$E + S \overset{K_s}{\rightleftharpoons} ES \xrightarrow{K_{CAT}} E + P$$

so that the observed rate $V = K_{cat}(ES) = V_{max}((S)/(S)+K_m)$

At low substrate concentration,when (S) is much less than K_m, $V=(S)V_{max}/K_m$; that is, the rate is directly proportional to the substrate concentration,when (S) is much greater that K_m, $V=V_{max}$; that is, the rate is maximal and independent of the concentration of substrate.

The Michaelis constant and the maximal rate, V_{max}, can be readily derived from rates of catalysis at different substrate concentrations. To do this, it is convenient to transform the Michaelis-Menten equation into one that gives a straight line plot. This can be done by taking the reciprocal of both sides of the Michaelis-Menten equation to give:

$$1/V = 1/V_{max} + K_m/(V_{max}.(S))$$

A plot of 1/V versus 1/(S) yields a straight line with an intercept of $1/V_{max}$ and a slope of K_m/V_{max}.Values of K_m,

however, must be interpreted with caution and are not necessarily identical to the substrate binding affinity.

More complex enzymic mechanisms involving additional equilibrium processes and different rate-limiting steps may still obey Michaelis-Menten kinetics,but with a K_m unrelated to the primary binding step.

1.1.4 Non-covalent Forces Determining Protein Structure

The interpretation of thermodynamic data for the binding of substrate to enzyme is still speculative but potentially it can provide valuable insight as to the nature of the macromolecular-ligand complexes. For, while spectroscopic and crystallographic studies of such complexes can provide information concerning the microenvironment of the ligand or substrate and even a direct picture of the interacting system, it is not possible to obtain information to describe the strength of the various forces involved in the interaction. Having access to values for enzyme-ligand binding from sources, such as calorimetry and knowing that it is specific non-covalent interactions that are responsible for the binding process, it is important now to be able to evaluate the relative strength and importance of these forces between the enzyme and the ligand.

Although several model systems have been analysed (involving the transfer of solute from one solvent to another),(Kauzman, 1959;Tanford,1973), to help describe the thermodynamic changes which take place when ligand binds to enzyme, the

extrapolation to macromolecular systems can be dangerous. One main area of discrepancy lies in the fact that the binding of ligand to macromolecule involves a change in at least three species, the macromolecule, ligand and the solvent water. In the model systems, however, one is primarily interested in the interaction of the solute with for example water and the thermodynamics of transfer of this solute from water to some other phase, like organic solvent. Since ligand binding will involve the transfer of ligand from water to a binding site on the enzyme, and may involve a change in the degree of solvent exposure of various parts of the enzyme as well, studies of the nature of solute-water interactions are extremely valuable. These model systems have been important in providing a description of some of the non-covalent interactions within protein systems, such as hydrogen bonds and the hydrophobic effect. These forces and electrostatic and dispersion or van der Waal's interactions will be discussed within this section, with emphasis on the associated Δ H and ΔS values.

Many non-covalent interactions are important for protein structure formation, stability and activity. As well as being involved in the interaction between enzyme and its substrates, cofactors or inhibitors,they may be the forces which govern the folding of the polypeptide chain and stabilise the native structure of the protein. They are probably also responsible for the adherence of two or more protein molecules leading to aggregation or the formation of an oligomeric species.

The aim therefore of studies on the thermodynamic parameters involved in protein-ligand complex formation is to gain knowledge of the nature of the forces involved in a particular protein interaction.

These non-covalent forces can be subdivided, as shown in Table 1.1,into several types.

Hydrophobic forces

The hydrophobic bond is a way of describing the tendency of non-polar compounds, such as hydrocarbons,to transfer from an aqueous solution to an organic phase, as may occur when a protein folds. This is due not so much to the direct interaction between solvent and solute molecules but to the reorganization of the normal hydrogen bonding network in water by the presence of a hydrophobic compound. Since water consists of a dynamic, loose network of hydrogen bonds, the presence of a non-polar compound causes a local rearrangement in this and the water molecules line up around the non-polar molecule. The hydrophobic solute therefore causes only minor enthalpy changes in the solvent but instead produces large decreases in entropy due to the increase in local order. A hydrophobic molecule is driven into the hydrophobic region of the protein by the regaining of entropy by water. This effect usually results in the amino acids with non-polar side chains (Phe, Tyr, Trp, Leu, Ile, Met, Val) aggregating on the inside of the protein, shielded from the solvent. The ionized hydrophilic side chains are nearly always on the outside and help to maintain solubility. A high packing density - the fraction

Table 1.1 Types of non-covalent forces important for protein structures.(Schulz and Schirmer,1979.)

TYPE	EXAMPLE	
Dispersion forces	Aliphatic hydrogen	-C-H ··· H-C-
Electrostatic interaction	Salt bridge	$-COO^{-} \cdots H_3N^{+}-$
	2 dipoles	$>\overset{\delta+}{C}=\overset{\delta-}{O} \cdots \overset{\delta-}{O}=\overset{\delta+}{C}<$
Hydrogen bond	Protein backbone	>N-H ··· O=C<
Hydrophobic forces	Side chain of Phe	

of total space occupied by the atoms - is usually observed, indicating that non-covalent forces are efficiently used and in fact, the interior is normally as tightly packed as crystalline amino acids (Klapper,1971; Richards,1974; Chothia, 1975). Packing density is about 0.75 for proteins compared with values of 0.7 to 0.78 found for amino acid crystals.

One way of evaluating the hydrophobicity of a model system is to measure a molecule's partition between an organic and an aqueous phase when shaken with an immiscible mixture of an organic solvent and water (Fujita et al,1964; Leo et al, 1971). The distribution of the solute between the two phases depends on the competing tendencies of the hydrophobic regions to be squeezed into the organic phase by the hydrophobic bond, and the polar regions which require solvation, to be drawn into the aqueous phase.Various other experiments involving solutions of hydrocarbons in water have been used in an attempt to obtain a better understanding of the interaction of small organic molecules with biomacromolecules (Frank and Evans,1945; Krishnan andFriedman,1969; Reid et al, 1969; Wadso,1972).

Hydrogen bonds

This is a particularly important bond in biological systems and is a special case of electrostatic interaction. Hydrogen bonding arises if a hydrogen atom has a large positive partial charge and if its contact partner has a large negative partial charge. These charges attract each other. Since the entire electron shell of hydrogen is appreciably shifted onto the atom to which hydrogen is covalently bound,the shell

repulsion between contact partners is small, and the attracting charges can approach each other more closely. Such short distances give rise to a high attractive coloumb energy which is intermediate between the energies of covalent bonds and van der Waal's contacts (see later). Bonds of this strength are of particular importance since they are stable enough to provide significant binding energy but of sufficiently low strength to allow rapid dissociation.

Several model experiments have been used to investigate the nature of these bonds. In particular, in view of the tendency for peptide groups to associate with each other in native proteins, as for example, in helical regions, there has been considerable interest in finding model systems that permit evaluation of the association constant for dimerization of such groups and of the effect of environment upon it. This has been carried out by studying the self association of model compounds containing a peptide group, for example N-alkylacetamides. Kresheck and Klotz (1969) for example, used a calorimetric system involving the transfer of N-methylacetamide molecules from CCl_4 to H_2O. This simulated the enthalpy change when an amide hydrogen bond in a non-polar environment is exposed to aqueous solvent, as may occur in the unfolding of proteins. ΔG transfer was calculated and found to be negative due to the enthalpy and entropy changes being negative. This implied that internal hydrogen bonding did not contribute largely to stabilization of for example, helical structure within the interior of proteins.Other experiments in solvents such as C_6H_6 and CCl_4 indicate that

both the free energy and enthalpy for association between peptide units are negative. These refer to the interaction between unsolvated peptide groups (Tanford,1970). In water ΔH becomes zero and the free energy; positive. These results indicate that the strength of interpeptide hydrogen bonds is greater than the strength of hydrogen bonds between peptide groups and water.When other models are used, the greater tendency for interpeptide association in organic solvents,as compared to water,is confirmed. The opposite conclusion however is reached when similar data is derived from studies of the helix-coil transition of synthetic polypeptides in aqueous media (Tanford,1970). These results indicate that interpeptide hydrogen bonds are more, rather than less, stable than free peptide groups in contact with water.
Hence description of the nature of these bonds appears to be strongly dependent upon the type of model applied and any attempt to resolve this conflict is hypothetical and may be attributed to stabilizing side chain interactions within the helical polypeptide.

Electrostatic interactions

Since covalent bonds between different types of atoms lead to an asymmetric bond electron distribution, most atoms of a molecule carry partial charges.

As a neutral molecule has no net charge, it contains only dipoles or higher multipoles and the interaction energy of these depends on the dielectric constant of the surrounding medium.

Free charges are rarely observed inside the protein except as salt bridges and ion pairs and all partial charges form di- or multipoles.

Several varieties of electrostatic interactions exist,between ions with net charges, between permanent dipoles, between an ion and a dipole induced by it and between a permanent dipole and a dipole induced by it.

It is thought that an entropy effect is responsible for the stabilization of ionic bonds. This effect arises due to the fact that a lone ion in aqueous solution is surrounded by ordered water molecules. The association, therefore, of two oppositely charged ions will release bound water thus giving rise to an increase in disorder, or in other words, a gain in entropy.

Dispersion or van der Waal's forces

These forces occur between any pair of atoms, even between totally apolar ones. Each atom behaves like an oscillating dipole generated by electrons moving in relation to the nucleus.In a pair of atoms each dipole polarizes the opposing atom and as a consequence the oscillators are coupled, giving rise to an attractive force between the atoms.(These attractive forces are, however, counter-balanced by the repulsion of the electronic shells).

Although these attractive forces are weak and the energies low, they are additive and make significant contributions to

binding when summed over the whole molecule. One must also remember, however, to consider the balance of forces due to changes in solvation.

1.1.5 Structure and Dynamics of Proteins

Increasing attention has been focused on the dynamic aspects of protein structure and function and it has long been inferred from a variety of experimental studies that structural fluctuations occur in these molecules which are essential to biological activity (Linderstrom-Lang and Schellman,1959). Hence although X-ray crystallography gives the impression that proteins are static molecules, the fact is that individual macromolecules are dynamic objects undergoing various forms of intramolecular motion (Cooper,1976 and 1984). These motions range from rapid localised, sub-Ångstrom atomic librations and vibrations to slower processes which involve the correlated motion of large masses, for example, helice vibration causing openings in the arrangement or the motion of entire subunits producing a change in the overall conformation (Careri et al,1979;Gurd and Rothgeb,1979;Karplus and McCammon,1981).

Evidence for mobility within proteins comes from numerous physical methods including phosphorescence experiments (Saviotti and Galley,1974), electron microscopy (Valentine and Green,1967), mossbauer spectroscopy (Parak et al,1981), flash photolysis (Beece et al,1980;Stein,1985) and X-ray techniques (Artymiuk et al,1979; Frauenfelder et al,1979). More widely used to study the dynamic nature of protein

structure are the techniques of nuclear magnetic resonance spectroscopy (nmr), fluorescence spectroscopy and hydrogen exchange techniques.

Nmr experiments involving ^{13}C (Doddrell et al,1972;Richarz et al,1980) and proton spectra (Wagner,1983) have been used. ^{1}H nmr studies have been used to investigate dynamic aspects of globular proteins and so far have mainly concentrated on measurements of the internal mobility of aromatic rings, exchange of internal amide protons with the solvent (Richarz et al,1979; Wagner and Wuthrich,1979; Wuthrich and Wagner, 1979) and thermal denaturation (Wagner and Wuthrich,1978; Wuthrich,1979).These are relatively infrequent events with characteristic times of greater than 10^{-5} seconds, which consist of concerted motions involving sizeable fractions of the protein structure. Table 1.2 gives examples of some time events in globular proteins and enzymes.

In contrast, nmr relaxation studies (Doddrell et al,1972) have so far, for physical or practical reasons provided exclusively, information relating to much more frequent events in the time range 10^{-8} to 10^{-12} seconds.

In globular proteins the degree to which an amino acid side chain is exposed to solvent will depend on just how well it is shielded by the surrounding protein segments. The exposure of a residue can be judged by X-ray crystallographic information (Lee and Richards,1971) but this only provides a static view of the positioning of various groups.

In solution, protein molecules are subject to a wide range of

Table 1.2 Time events in globular proteins and enzymes.

DETERMINANTS	TIME (secs)
PROTEIN SURFACE	
Bound water relaxation	10^{-9}
Side chains rotational correlation	10^{-10}
Proton transfer reaction of ionizable side chains	$10^{-7} - 10^{-9}$
PROTEIN CONFORMATION	
Local motion	$10^{-8} - 10^{-9}$
Isomerization process	$10^{-2} - 10^{-7}$
Folding-unfolding transition	$10^{+2} - 1$
ENZYME-SUBSTRATE COMPLEX IN SOLUTION	
Encounter rate	diffusion controlled
Estimated lifetime of the transition state in covalent reactions	10^{-10}
Change in metal ion coordination sphere in metalloenzymes	$10^{-6} - 10^{-9}$
Enzyme-substrate local conformational motion	$10^{-2} - 10^{-4}$
Covalent enzyme-substrate intermediate lifetime	$10^{-2} - 10^{-4}$
Enzyme-substrate complex conformational isomerization	$10^{+2} - 1$
Enzyme-substrate complex unfolding transition	

conformational fluctuations (Linderstrom-Lang and Schellman, 1959; Weber,1975).As a result of this mobility, a residue that appears buried in the crystal may become periodically exposed in the solution state. The frequency at which such residues become "dynamically exposed" will depend on the nature of the surrounding protein fabric.If several layers of protein fabric blanket a residue or if the layers are very resistant to disruption, encounters between the buried group and solvent molecules may be very infrequent.

An excellent way to experimentally determine the degree of exposure of tryptophan residues and hence characterize the dynamics of the protein is by fluorescence quenching (Lehrer, 1971; Lakowicz and Weber,1973; Eftink and Ghiron,1975 and 1977).This method follows the argument that in order for buried tryptophans to be quenched,fluctuations in the protein matrix must facilitate the inward movement of the quencher. This proposal is also supported by hydrogen exchange experiments since it has been found that most of the interior backbone protons of folded proteins have measurable accessibility to solvent (Woodward and Hilton,1979).

Hydrogen exchange kinetics are generally measured by chemical or spectroscopic assay of the hydrogen isotope exchange from a macromolecule into the solvent (Hvidt and Nielsen,1966; Byrne and Bryan,1970; Englander and Englander,1972; Englander et al,1972). The labile protons which are measured are predominantly backbone -NH, and a few are buried side chain protons.(The exchange of exposed labile side chain protons is

too fast to be detected by the usual methods (Hvidt and Nielsen,1966; Englander et al,1972).

As well as experimental proof of the dynamic nature of proteins, considerable advances have been made in describing their motion using computer simulations by molecular dynamics and normal mode calculations (Gelin and Karplus,1975;Careri et al,1979;Karplus and McCammon,1979;Levitt,1983a and 1983b; McCammon and Harvey,1987). These results have clarified some features of the dynamics of proteins, but only in the short time scale (picosecond region). The possibility of reaching a complete understanding of enzymic catalysis however, by computer simulation of atomic motions in proteins, lies very far in the future. This is because enzymic catalysis involves conformational motions in the larger time scale as well as solvent effects and more than pairwise interactions at the active site, for which the descriptions of events are well beyond the possibilities now available.

A newly developed technique involving low frequency Raman scattering was utilised in an attempt to detect changes in the dynamic properties of enzymes. Further details of this method are discussed in chapter 6 of this thesis.
Vibrations in the low frequency region - less than $200cm^{-1}$ - have many interesting and specific properties different from the group vibrations that are normally observed in Raman and infrared measurements. The concept of group frequencies, that is, of the vibrations of a particular chemical group of atoms

in a molecule such as a peptide group or a $-CH_2$ group is not applicable to these low frequency modes. These particular modes appear to involve a collective motion of a large number of different atoms in the polymer or protein molecule (McCammon et al,1976).Although small molecules do not exhibit low frequency modes they can, in a crystal, vibrate or rotate relative to one another so as to produce low frequency crystal modes (Genzel et al,1976).

The low frequency modes in proteins arise due to the fact that when many atoms are coupled together in a macromolecule they can move collectively,like small molecules in a crystal, so that the effective mass involved in the motion is quite large. Furthermore, the forces between the non-bonded atoms involve such interactions as hydrogen bonding, torsional or van der Waal's forces. Thus the forces holding the distant molecules in a specific conformation are weak relative to chemical bonds so that the resulting vibration frequency is low because it corresponds to a total mass moving under the action of weak but specific forces.

It has been proposed that these low frequency modes of proteins are related to the overall dynamics of the protein system (Painter and Mosher,1979; Cooper and Dryden,1984) which, in turn, is thought to play an important role in biological function. The major question of interest, however, is what the role of these vibrations,in particular the low frequency modes, play during enzymatic catalysis.

Brown et al (1972) made the original observation of low freq-

uency modes within the proteins chymotrypsin and pepsin,using the technique of laser Raman spectroscopy. Since then similar results have been observed for several other proteins (Genzel et al,1976; Painter and Mosher,1979; Painter et al,1981 and 1982). As well as applying Raman scattering to record these modes, several other methods have been attempted or proposed, including Brillouin scattering (Devlin et al,1971), X-ray scattering and neutron scattering (Bartunik et al,1982). Theoretical studies have also been carried out with the aim of describing the low frequency modes of proteins (McCammon and Karplus,1977; Go,1978). While, however,the calculation of the vibrational properties of proteins at high frequencies is reasonably easy (Peticolas,1979), there is really no uncomplicated method of determining the low frequency vibrations. A method involving the calculation of the potential energy between atoms (Wilson et al,1955) has been accurately used in the estimation of the frequencies of vibrations of small molecules and more recently has been applied to simple helical homopolypeptides (Itoh and Shimanouchi,1970 and 1971; Small et al, 1970; Fanconi and Peticolas,1971; Fanconi et al,1971). The application of this method to proteins however has not yielded quite so accurate results.

In addition there are several approximate procedures for calculating the low frequency motion of proteins. One method involves the calculation of the frequencies for only certain structurally recognizable parts of the protein, such as the helix or β-structures and to simplify the actual molecular structure by a ball and spring model. The globular mass

approximation introduces solvent viscosity parameters while the double-lobe model considers the movement of large sub-units within multi domain proteins. These models have been devised in an attempt to overcome the inaccuracies and difficulties encountered when describing vibrations at low frequency. While some progress has been made, additional investigation must take place.

In addition it has been noted in some experiments (Genzel et al,1976) that there is a disappearance of low wavenumber bands in going from the crystalline protein to solution.These bands have been assigned to intermolecular crystalline modes. However, a more likely suggestion for the disappearance of these bands is that the band simply becomes so highly damped in aqueous solution that it is no longer visible by the Raman technique (McCammon et al,1976).This is an important point to bear in mind when attempting to visualize the large scale dynamic motion of protein molecules. Although theoretical calculations may give the impression that a macromolecule might oscillate harmonically with a well-defined normal mode spectrum, the approximation involved and the neglect of damping effects make this somewhat unlikely. More realistically the low frequency motion of protein domains is more likely to consist of complex,uncorrelated anharmonic and damped motions which only loosely approximate to harmonic trajectories. An experimental consequence of this is that we should not necessarily expect to see well-resolved "vibrational" bands in the low frequency Raman spectra of proteins in solution.

1.2 Protein Engineering

As yet it is still not known precisely what contribution particular amino acids and the interactions between amino acids, within the tertiary structure, make to the activity and the thermodynamic and dynamic properties of the protein. Recently developed methods, however,for the specific replacement of amino acid residues in enzymes by genetic manipulation have provided important new tools for enzymology (Cohen, 1975).These methods can be used to study the roles of individual residues in substrate binding and catalysis (Craik et al,1985; Fersht ,1985).

Chemical techniques have also been used to modify the active site of enzymes (Kaiser and Lawrence,1984).

In principle both these methods could be used to produce modified enzymes with activities and stabilities tailored for specific applications (Ulmer,1983; Thomas et al,1985). In addition it would be of great commercial value to be able to engineer enzymes used in industrial processes so as to give them improved properties, such as better rate and binding constants, changed reaction and substrate specificities and increased thermostability and stability in organic solvents. It should also be possible to generate rules for the forces present in these macromolecules under a variety of conditions.

Hence using recombinant DNA technology and nucleic acid chemistry it is now possible to synthesize new enzymes de novo

via the synthesis of their genes, and to tailor and redesign existing enzymes by mutating their genes. This new technology is called protein engineering.

1.2.1 Site-Directed Mutagenesis

Given the gene of a protein, it is possible to mutate it by a variety of methods. Many of these are relatively nonspecific and nonsystematic, for example, involving the breaking of DNA chains using nucleases to produce a single-stranded gap. This gap may be repaired by a polymerase or ligase under mutagenic conditions to generate a range of substitution or deletion mutants. Alternatively, sodium bisulphite treatment which deaminates cytosine residues to uracil, leads to a change of coding. Other techniques can be used (Fersht,1985) but they cannot generally be targeted against particular codons and there are usually difficulties in screening for the desired mutant. Oligonucleotide-directed mutagenesis, however, allows the systematic replacement of every single amino acid residue in a protein in turn (Schott and Kossel,1973; Hutchinson et al,1978;Razin et al,1978;Wallace et al,1980). This technique usually involves the insertion of the piece of DNA carrying the gene encoding for the required protein into a DNA molecule called a vector. The most common vectors are called plasmids and these are small pieces of double-stranded circular DNA found in bacteria and some other organisms which can replicate independently of the host cell chromosome.
One of the single stranded DNA circles must be isolated and annealed to a short oligonucleotide which has been synthesized to be complementary to the region of the gene to be

mutated, except for a single or double- base mismatch.The aim of this mismatch is to change the sequence of bases coding for the target amino acid into the code for the required mutant residue. The rest of the single-stranded DNA is replicated and ligated, resulting in a duplex containing one strand of mutant and one strand of wild-type DNA. This vector is introduced into a host where colonies of cells are produced which contain either the vector with the mutant or the vector with the wild-type gene. The introduction of DNA into living cells is known as transformation.

1.2.2 Transformation

This procedure allows a large number of the vector molecules containing the wild-type or mutant protein gene, also called recombinants, to be produced from a limited amount of starting material. This situation arises because the plasmid replicates autonomously within the host cell to produce numerous copies that can be passed to the daughter cells.
Transformation in cells is an inefficient procedure and a method must be used to distinguish a cell that has taken up a plasmid from the many thousands that have not been transformed. The answer is to make use of selectable markers usually carried by the plasmids (Cohen,1975). One example is the plasmid pMA27 (see section 2.1.1) which contains a leu2 gene coding for β-isopropyl malate dehydrogenase, one of the enzymes involved in the conversion of pyruvic acid to leucine. In order to make use of this marker, a host organism which has a non-functional leucine gene must be used. Such a $leu2^-$ organism will be unable to synthesize leucine and will

only normally survive if this amino acid is supplied as a nutrient in the growth medium. Hence if the recombinant pMA27 is used to transform leu2$^-$ host cells, selection is possible because transformants will contain a plasmid-bourne copy of the leu2 gene, and so will be able to grow in the absence of the amino acid.Using this technique therefore, gene mutation can be controlled to a single specific site and then the transformed host cells can be selectively isolated. A further advantage of some plasmids arises from the fact that many copies may exist in each cell, and so these plasmids are termed multicopy plasmids. Partly because of this high copy number, a gene cloned into such a plasmid may produce large amounts of enzyme (see section **3.1**). All of these benefits make site-directed mutagenesis potentially an invaluable technique in any study involving proteins and undoubtedly without it, the experiments described within this thesis could not have proceeded. As mentioned previously, to be able to selectively alter enzymes in ways to suit specific requirements, it is necessary to first understand the nature of thermodynamic forces involved when a substrate binds to the enzyme and the dynamic changes which take place. One method of investigating this is by examining the effects of selected amino acid mutations, within a particular enzyme, upon these properties of the enzyme. If an enzyme is to be used for this purpose, however, it must comply with certain requirements. The enzyme phosphoglycerate kinase (PGK) is ideally suited to the kind of study described above, using site-directed mutagenesis. PGK is a good model protein to use to investigate the dynamics and thermodynamics since it

exhibits many of the characteristics relevant to most proteins - it is large, it consists of more than one domain and it is flexible, undergoing constant dynamic motion. Upon the binding of substrate to PGK, the enzyme recognizes it and responds by undergoing major domain movement. This recognition of substrates is a property possessed by almost all enzymes and so PGK provides a relatively simple system to allow the investigation of the way in which this recognition is translated so as to effect major molecular change. As well as these aspects, other advantages of studying PGK are that the amino acid sequences of eight PGK's have been determined (Mori et al,1986) and the wild-type enzyme has had its kinetic and structural properties well documented. The structure of the substrate binding site is also known to high resolution.

Mutant and wild-type enzyme is easy to prepare in gram quantities using a high expression, multi-copy, plasmid system.

1.3 Phosphoglycerate kinase

Phosphoglycerate kinase, "PGK" (E.C.2.7.2.3.) is an enzyme in the glycolytic pathway (Fig.1.1) responsible for the formation of adenosine triphosphate (ATP) by reversible phosphoryl transfer between 1,3-diphosphoglycerate and adenosine diphosphate (ADP) in a wide variety of organisms (Bucher,1955; Scopes,1969,1971 and 1975; Krietsch and Bucher, 1970). It is PGK isolated from bakers yeast (saccharomyces cerevisiae) which is the subject of interest in the

Fig.1.1 The Glycolytic Pathway

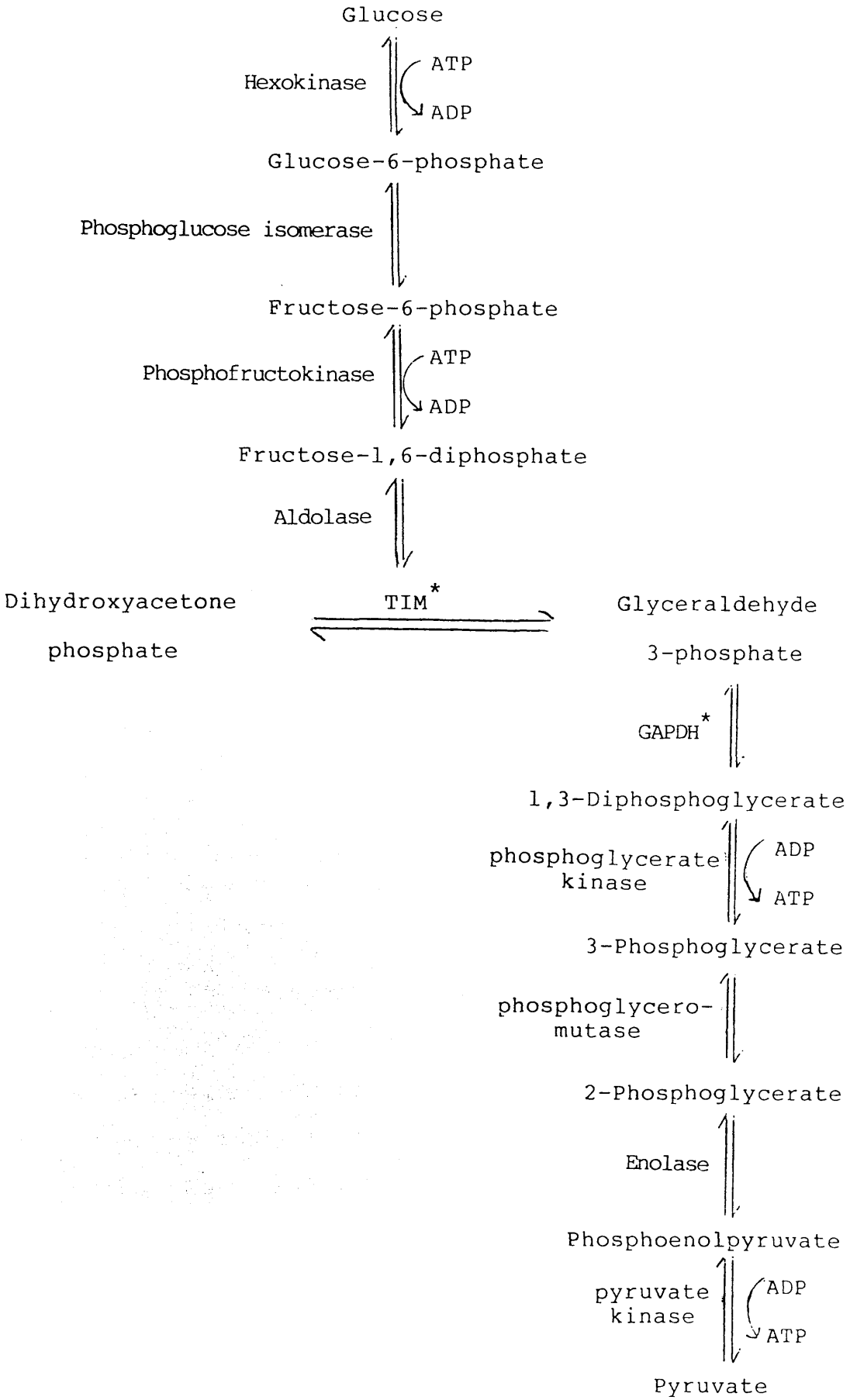

* TIM:Triose phosphate isomerase

GAPDH:Glyceraldehyde 3-phosphate dehydrogenase

following chapters.

PGK catalyses the transfer of the phosphoryl group from the acyl phosphate of 1,3-diphosphoglycerate to ADP. ATP and 3-phosphoglycerate are the products.

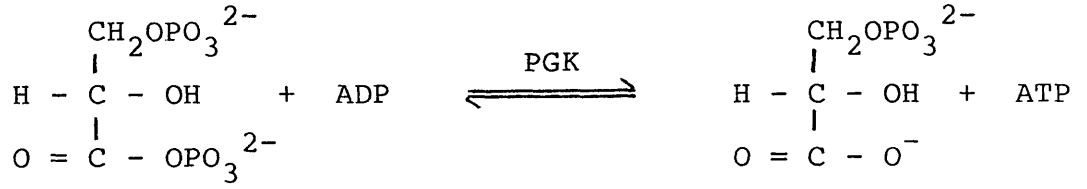

1,3-diphosphoglycerate 3-phosphoglycerate

There is a requirement for bivalent cations (Mg^{2+} or Mn^{2+}) since the metal ion complexes of the nucleotides are the true substrates (Larsson-Raznikiewicz,1964 and 1970b).

The enzyme is a monomer of molecular weight about 45,000 (Larsson-Raznikiewicz,1970a; Watson et al,1982) comprising a single polypeptide of 415 amino acids (Perkins et al,1983; Fig.1.2).

X-ray studies of the enzyme (Bryant et al,1974) have shown that the enzyme consists of two lobes, each containing about 200 amino acids, which correspond to the N-terminal and C-terminal halves of the polypeptide chain. Twelve C-terminus residues however pass back into the N-terminal domain in the form of an α-helix (Fig.1.3).

Difference electron density maps have shown that the MgADP binding site is located in the C-terminal lobe (Blake and

Fig.1.2 Primary sequence of yeast phosphoglycerate kinase

S L S S K L S V Q D L D L K D K R V F I R V D F N V P L D G

K K I T S N Q R I V A A L P T I K Y V L E H H P R Y V V L A

S H L G R P N G E R N E K Y S L A P V A K E L Q S L L G K D

V T F L N D C V G P E V E A A V K A S A P G S V I L L E N L

R Y H I E E E G S R K V D G Q K V K A S K E D V Q K F R H E

L S S L A D V Y I N D A F G T A H R A H S S M V G F D L P Q

R A A G F L L E K E L K Y F G K A L E N P T R P F L A I L G

G A K V A D K I Q L I D N L L D K V D S I I I G G G M A F T

F K K V L E N T E I G D S I F D K A G A E I V P K L M E K A

K A K G V E V V L P V D F I I A D A F S A S A N T K T V T D

K E G I P A G W Q G L D N G P E S R K L F A A T V A K A K T

I V W N G P P G V F E F E K F A A G T K A L L D E V V K S S

A A G N T V I I G G G D T A T V A K K Y G V T D K I S H V S

T G G G A S L E L L E G K E L P G V A F L S E K K

A=Alanine
C=Cysteine
D=Aspartic acid
E=Glutamic acid
F=Phenylalanine
G=Glycine
H=Histidine
I=Isoleucine
K=Lysine
L=Leucine
M=Methionine
N=Asparagine
P=Proline
Q=Glutamine
R=Arginine
S=Serine
T=Threonine
V=Valine
W=Tryptophan
Y=Tyrosine

Fig.1.3 Structure of yeast PGK (Watson et al,1982).

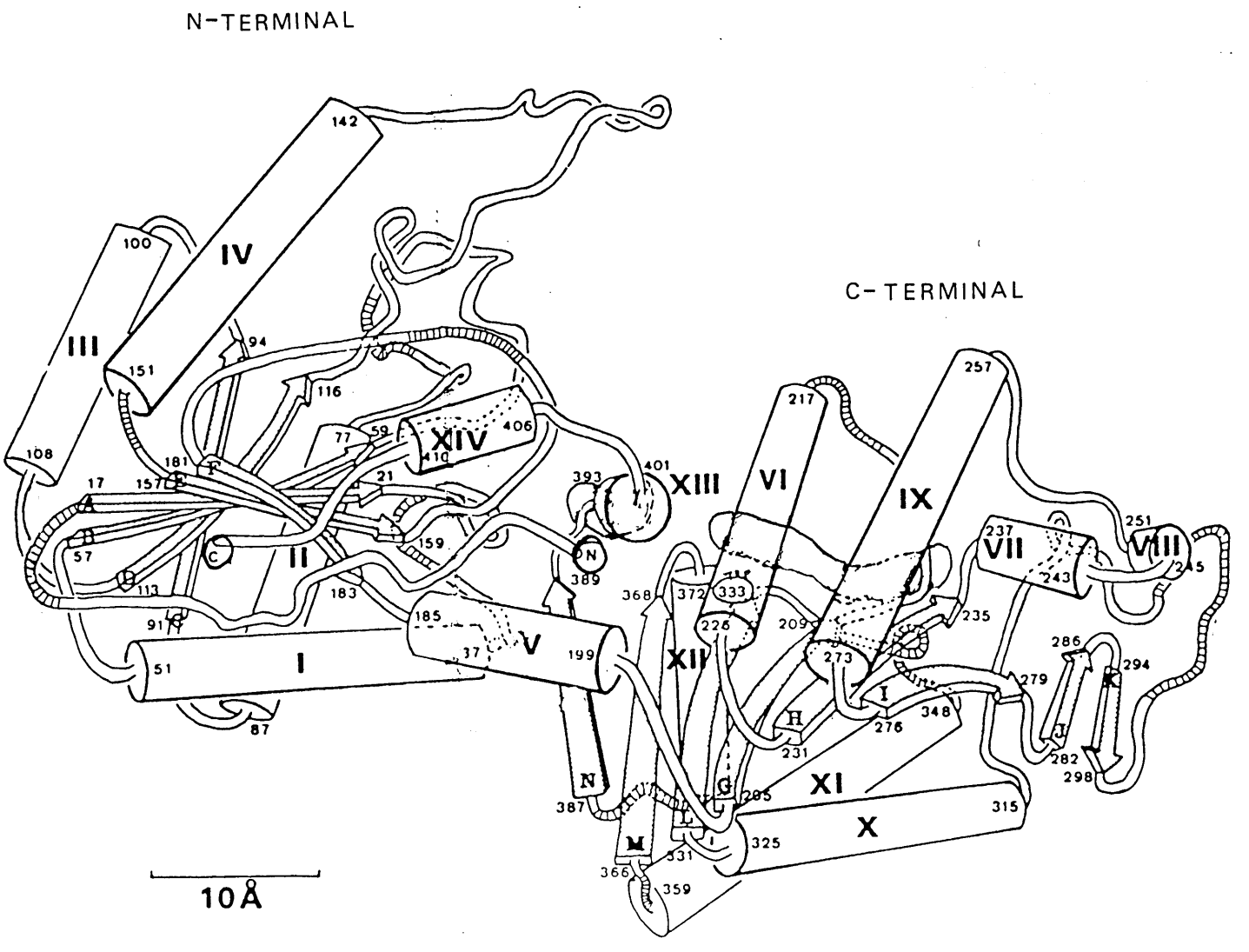

Evans,1974; Lesk and Chothia,1984) with the phosphate chain extending towards the neck region of the molecule (Bryant et al,1974). The α and β phosphate groups of ATP are thought to be in contact with the main chain of the enzyme and are specifically linked to lysine residues. The transferable γ phosphate, on the other hand, binds to the amino end of an α-helix where two of its oxygens are hydrogen bonded to the first and second peptide nitrogens of a sequence of three consecutive glycines (369-371). The remaining oxygen is exposed to the solvent and probably interacts with an arginine residue extending from the amino domain during catalysis. It is also thought that a main chain carbonyl oxygen forms a hydrogen bond with the N6 nitrogen of the ATP's adenosine group and that the hydroxyl groups of the ribose ring form similar bonds to side chain carboxyl groups. The use of labeled phosphate on ATP by Webb and Trentham (1980) showed that the catalytic reaction proceeded by inversion of configuration,consistent with the direct transfer of the phosphoryl group from 1,3-diphosphoglycerate to ADP. Difference maps of 3-phosphoglycerate binding to PGK have provided no definite feature corresponding to bound substrate. However the most probable binding site for 3-PG is located on the N-terminal domain between residues Arg-38 and Arg-170 in an area which has a high concentration of basic residues. As a consequence of the salt link between 3-PG and the Arg-38 side chain, the phosphate of ATP is directly in line with the attacking carbonyl oxygen of the other substrate.

The location of the two ligand binding sites on the two diff-

erent lobes, at a distance of 12-15Å apart, has led to the suggestion that substantial relative movement of the two domains towards one another must occur to bring the substrates together and at the same time to expel the solvent that lies between them (Bryant et al,1974; Anderson et al,1979; Banks et al,1979; Adams and Pain,1986; Tompa et al,1986). There is evidence that this is indeed the case for yeast PGK from kinetics experiments (Larsson-Raznikiewicz and Jansson, 1973; Scopes,1978a and 1978b, nuclear magnetic resonance spectroscopy (Tanswell et al,1976), small-angle X-ray scattering (Pickover et al,1979),substrate binding reactions (Adams and Pain,1986) and chemical modification results (Markland et al,1975, Hjelmgren et al,1976).

Until recently, the results obtained by Roustan et al (1980) from hydrodynamic studies of yeast PGK were quoted as firm evidence to support the domain movement theory. It has since been concluded that these results are too large to be simply due to a confomational change and that other processes, such as, aggregation may be responsible (Dr.H.C. Watson, personal communication).

The conformational change that occurs upon substrate binding to PGK (Scopes and Algar,1979) is best described as a rotation of the relative orientation of the two domains by between 10 and 20 degrees - also known as a "hinge-bending" motion.

Kinetics experiments have led to the conclusion that PGK has

a rapid equilibrium random order mechanism in which the binding of one substrate does not affect the binding of the other (Larsson-Raznikiewicz,1967 and 1970a). The results of several other kinetics studies have proved difficult to understand, some of them implying the presence of multiple binding sites (Ali and Brownstone,1976; Beissner and Rudolph,1979; Schierbeck and Larsson-Raznikiewicz,1979). Nmr experiments however (Tanswell et al,1976) and X-ray diffraction (Blake and Evans,1974;Bryant et al,1974) reveal only a single,strong binding site for nucleotides, and gel filtration studies have established a single phosphoglycerate binding site (Scopes, 1978b).

Other anomalous kinetics data has been collected for PGK (Scopes,1978a and 1978b) in the presence of varying concentrations of some anions and it was suggested that this was due to an effect on the rate of dissociation of 1,3-diphosphoglycerate from PGK, this being the rate limiting step of the back reaction because of very tight binding of this ligand (k_{dis} approximately equals $5X10^{-8}M$).
Various other studies of PGK have been made including association and sedimentation experiments (Spragg et al,1976), binding studies (Conroy et al,1981) and fluorescence spectroscopy (see chapter 8).

There has also been considerable interest shown in various mutant forms of PGK (Roustan et al,1976; Mas et al,1986) and site-directed mutagenesis has been a useful technique in studying the importance of interactions between certain amino

acids on the activity and stability of the enzyme. For example, it has been suggested (Watson et al,1982; Wilson et al,1984; Mas et al,1987 and 1988) that there is critical involvement of a histidine-glutamate interaction at the waist region of the PGK molecule in permitting the hinge-bending conformational change to take place. It is known that the imidazole group of His-388 extends from the carbonyl domain towards the carbonyl group of Glu-190 in the amino terminal domain and a salt link is formed. This occurs when the enzyme is in the open conformation and the two residues are in close van der Waal's contact.If the above suggestion is true, an interesting question is posed - what would happen to the dynamics, the thermodynamic parameters of binding and to the catalytic efficiency of the enzyme, if the waist region was changed in some way? In particular, what would be the effect of altering the inter- action between His-388 and Glu-190? This alteration has in fact been achieved by site-directed mutagenesis (Mas et al, 1987 and 1988; Wilson et al,1987) where the glutamate and histidine residues have been replaced individually.

The mutant which will be studied in detail within this thesis is the replacement of His-388 by a glutamine residue (Wilson et al,1987).

1.4 Aims of this Thesis

As yet, complete understanding of the processes involved and the changes which take place when ligands bind to proteins has not been established. It is thought however that the non-

covalent interactions occurring between amino acid side chains, providing the protein with a stable three dimensional structure, also play an important role in the binding of substrate and the ensuing catalytic process, as well as the various forms of major conformational change that may take place. In an attempt to elucidate the importance of these side chain interactions, and in particular the role of the His388-Glu190 electrostatic interaction in PGK, the thermodynamic and dynamic properties exhibited by the wild-type and mutant (His388 → Gln388) form of the enzyme are compared in the following chapters of this thesis.

Details of the procedures used for site-directed mutagenesis, and the isolation and purification of mutant and wild-type PGK are reproduced in chapter 3 along with details of kinetics and activity measurements.

CHAPTER 2

Introduction to Experimental Techniques

2.1 Isothermal Microcalorimetry

- 2.1.1 Introduction to calorimetry
- 2.1.2 Calorimetric instrumentation
- 2.1.3 Calorimetric principles

2.2 Differential Scanning Calorimetry

- 2.2.1 Introduction to differential scanning calorimetry
- 2.2.2 Interpretation of DSC curves

2.3 Raman Spectroscopy

- 2.3.1 Introduction to Raman spectroscopy
- 2.3.2 The Raman spectrometer
- 2.3.3 Low frequency Raman spectroscopy and the dynamics of proteins.
- 2.3.4 Conventional Raman spectroscopy and the conformation of proteins

2.4 Fluorescence Spectroscopy

- 2.4.1 Introduction to fluorescence spectroscopy
- 2.4.2 Fluorescence lifetimes
- 2.4.3 Protein fluorescence

CHAPTER 2

INTRODUCTION TO EXPERIMENTAL TECHNIQUES

This chapter provides an introduction to the principles and techniques involved in each of the methods employed in the following chapters of this thesis.

2.1 Isothermal Microcalorimetry

2.1.1 Introduction to Calorimetry

In all life sciences there can be noted a marked trend towards an increased use of physical instrumentation.Calorimeters, which are instruments for measurements of heat quantities or heat effects, offer one approach in this respect. Calorimeters were first employed as scientific instruments at the end of the eighteenth century (Armstrong,1964) when combustion phenomena and the nature of heat were intensively studied. Calorimetry has now reached a degree of development which makes it a promising research tool as a general analytic tool, for example in kinetic investigations (Berger et al,1968) or as an instrument for the determination of thermodynamic data. It is the latter use which will be described more fully throughout this chapter.

There is no sharp difference between "ordinary" calorimetry or "macrocalorimetry" and "microcalorimetry". However the micro- prefix usually indicates very sensitive calorimeters capable of measuring total heat quantities of a few millijoules with small sample quantities - (of the order of a few

nanomoles of reagent). Hence, it is only because of the development of these sensitive microcalorimeters in recent years that thermodynamic experiments involving heats of association of proteins and inhibitors (about $\pm$50kJmol^{-1}) can be carried out.

The most common thermodynamic property to be determined calorimetrically is the enthalpy change, ΔH. The enthalpy is determined at a fixed temperature so that the disadvantages of averaging over a range of temperatures (as is inherent in the Van't Hoff procedure for determining Δ H from the temperature dependence of K, for example) is eliminated. Δ H can be measured with an accuracy of a few percent and since it can be measured with such precision, calorimetry is also the best method for finding Δ S and ΔG (see section 1.1.3).

2.1.2 Calorimetric Instrumentation

Currently LKB Productor, Inc., Tronac and Beckman account for the majority of commercially available microcalorimeters,some being more specifically suited to certain applications than others (Langerman and Biltonen,1979; Wadso,1976).

There are several different calorimetric principles in use, but generally calorimeters can be classified under two major headings : adiabatic calorimeters and heat-conduction calorimeters.An ideal adiabatic calorimeter is perfectly insulated, thermally, and so there is no heat exchange between the calorimetric vessel and the surroundings. A quantity of heat is evolved or absorbed during an experiment (exothermic and endothermic, respectively) and gives rise to a temperature

change that is proportional to the heat capacity of the calorimetric system. This temperature change can be measured, usually by use of a thermistor or by use of one or more thermocouples.

The ideal heat-conduction calorimeter is perfectly connected, thermally, with its surrounding heat sink and this allows heat to be quantitatively transferred from the reaction vessel to the heat sink (exothermic reactions) or vice versa (endothermic reactions). With calorimeters of this type it is the heat flux, dQ/dT, that is measured.

Several types of calorimeters have come into use that are based on concepts between these two extreme calorimetric principles - descriptions of which may be found in several review articles (Skinner,1969; Wadso,1970 and 1976).
Heats of binding are generally measured using either a batch calorimeter (Wadso,1968) or a flow calorimeter (Monk and Wadso,1968). With a batch calorimeter a solution of enzyme and a solution of substrate or inhibitor are allowed to reach thermal equilibrium separately in a reaction cell, then these mixtures are combined and the total heat evolved is measured. On the other hand, with the flow technique, the two solutions are pumped separately through a heat exchanger to reach equilibrium very quickly and then the two solutions are mixed giving a continuous evolution of heat.

The use of flow calorimetry is restricted to fast reactions which occur in a time, short compared with the retention time

of the liquid in the flow cell. The flow method has several advantages over batch calorimetry since its operation is exceedingly simple and equilibration time prior to the experiment is short. As well as this, mixing of reactants can be achieved without the presence of a gaseous phase, which is of great importance when experiments are performed with volatile liquids or in microcalorimetric experiments where very small condensation-evaporation effects may affect the results. Surface adsorption effects which may cause serious errors in microcalorimetry can be neglected if a steady liquid flow is allowed to continue until possible wall reactions have occurred. It is a calorimeter of the latter type - an LKB 2107-121 flow microcalorimeter (a modified version of that described by Monk and Wadso (1968) - which was used for the purpose of the experiments described in this chapter and chapter4.

The main components of the LKB flow microcalorimeter are shown in Fig.2.1 and consist of a heat sink assembly, two detector units,two heat exchangers,a heater and a temperature sensor which are all mounted in an insulated box. The heat sink assembly comprises of the main heat sink which lines the inside of the insulated box and two pairs of smaller heat sinks which conduct heat from the thermopiles to the main heat sink. These thermopiles are in thermal contact with two separate reaction vessels in which heat reactions can take place.

The microcalorimeter is designed on the heat leakage

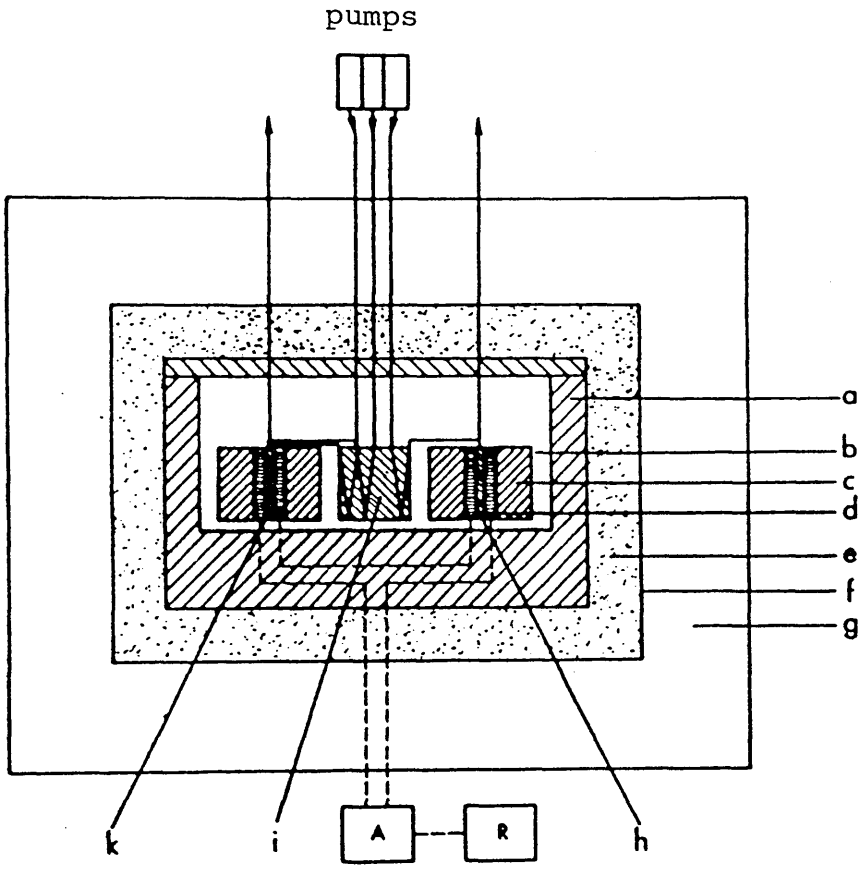

Fig.2.1 Flow Microcalorimeter

(a)main heat sink,(b)air space,(c)aluminium block, (d)semiconductor thermopiles,(e)insulation,(e)insulation, (f)stainless steel container,(g)thermostated water bath, (h)flow-through vessel,(i)heat-exchanger unit,(k)mixing reaction vessel.A ia an amplifier and R is the recorder/ integrator.From Wadso (1976).

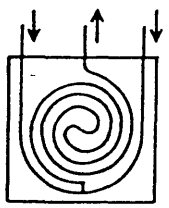

mixing vessel

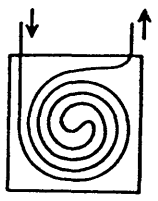

flow-through vessel

principle - that is to say,if heat is generated by a reaction in a vessel, heat flows from the vessel to the heat sink assembly or if heat is absorbed by a reaction in a vessel, heat flows from the heat sink to the vessel. In each case, the temperature difference creates a heat flow across the thermopiles, which are located between the vessel and the heat sink assembly,and an electromotive force proportional to the temperature difference is generated (see section 2.1.3). The output voltage from the thermopiles is amplified and directed to a chart recorder and an integrator system with a digital display.

Also attached to the apparatus was a built-in heater unit which was used for calibration purposes (see section 4.1).

2.1.3 Calorimetric Principles

In a conduction calorimeter like the LKB 2107-121 there is a controlled transfer of heat from the calorimeter vessel to the surroundings. Most simply this can be achieved by placing a thermopile wall between the vessel and the surrounding heat sink. For each thermocouple both the voltage, v and the heat flow, dq/dt are proportional to the temperature difference between the calorimeter wall and the heat sink.This generates the relationship:

$$v = c.dq/dt$$

where c is a constant.

In the ideal case all heat is transported through the thermocouple leads and so

$$v_1 + v_2 + \ldots\ldots = c.dq_1/dt + c.dq_2/dt + \ldots\ldots$$

$$V = c.dQ/dt$$

where V is the thermocouple voltage and dQ/dt is the total heat flow through the thermopile. Integration of this leads to:

$$Q = 1/c \int V dt$$

So the heat evolved is proportional to the area under the voltage-time curve:

$$Q = \varepsilon A$$

ε is the calibration constant for the calorimetric system and its value may be determined by electrical or chemical calibration experiments (section 4.1).

The experiments described in chapter4 are steady state experiments. An idealised recorder output, as a function of time, for an experiment of this type is shown in Fig.2.2. In a steady state experiment the reaction rate in the vessel is constant and a uniform recorder deflection E results,Fig.2.2. If Q is the heat quantity, corrected for dilution processes, evolved in the calorimetric experiment and Q_m is the corrected heat quantity for the hypothetical process where all enzyme is complexed by inhibitor, then the association constant, K_{ass}

$$K_{ass} = (EI)/(E)(I)$$

can be expressed as

$$K_{ass} = (E_t)(Q/Q_m)/((E_t)-(E_t)Q/Q_m).((I_t)-(E_t)Q/Q_m)$$

where (E_t) and (I_t) are the total enzyme and inhibitor concentrations, respectively.

This equation can be converted to

Fig.2.2 Typical response-time curve of the heat effects in a thermopile conduction calorimeter.

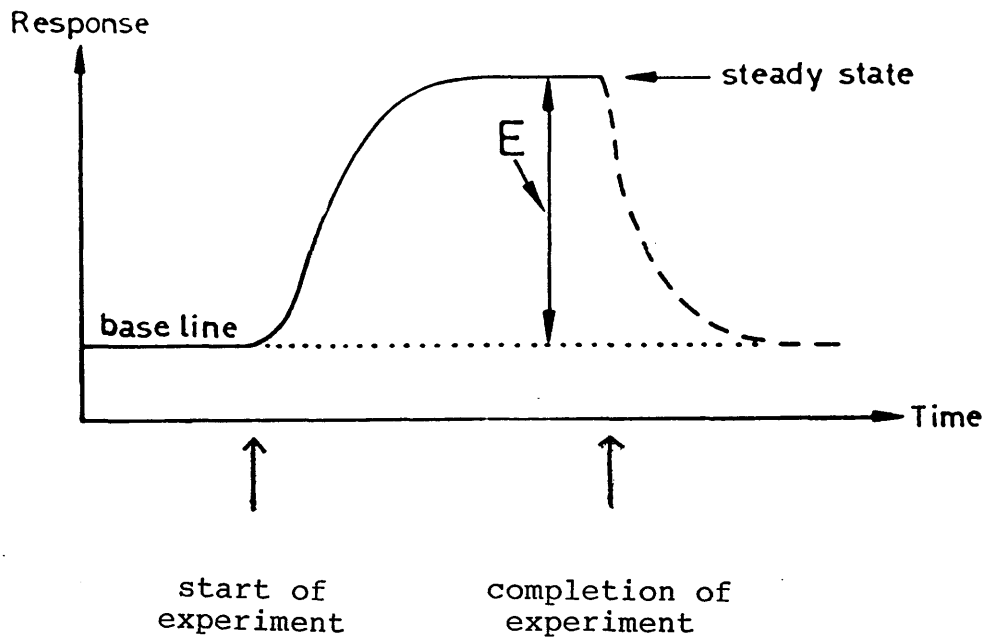

$$1/Q \cong 1/Q_m + K_{dis}/Q_m . 1/(I)$$

where K_{dis} is the dissociation constant, the reciprocal of K_{ass} and (I) is the concentration of free inhibitor in the final calorimetric solution.

Using this equation the calorimetric results are presented in the form of a double reciprocal plot of 1/Q versus 1/(I) (chapter4). ΔH is obtained from the intercept $1/Q_m$, after which K_{dis} can be calculated from the slope of the line (K_{dis}/Q_m).

When the results are plotted as a graph of Q against (I) the points are given equal weight. However when the same points are plotted as 1/Q against 1/(I) the points of lowest (I) are effectively given a higher weighting, and since these can be determined less accurately another, more exact form of calculating ΔH and K_{dis} was employed. This was done by fitting the thermal binding data by iterative least-squares procedures to the complete hyperbolic binding equation:

$$Q = - \frac{\Delta H}{2(E_t)} ((E_t)+(I_t)+K_{dis}) \; X \left\{ 1 - \sqrt{1 - \frac{4(E_t)(I_t)}{((E_t)+(I_t)+K_{dis})^2}} \right\}$$

In addition it should be noted that the double-reciprocal method of analysis requires knowledge of the free inhibitor (ligand) concentration at equilibrium, and this only approximates to the known total concentration (I_t) in cases of very weak binding. In practice, therefore, analysis using

the full hyperbolic binding equation is much more reliable. Evaluation of ΔH and K_{dis} using both of these methods is reported in chapter4.

2.2 Differential Scanning Calorimetry

2.2.1 Introduction to Differential Scanning Calorimetry

When a material undergoes a change in its physical state, or when it reacts chemically, heat may be either absorbed or liberated, corresponding to endothermic or exothermic changes respectively. The importance of calorimetric studies of the changes in the state of proteins induced by various factors stems from the fact that calorimetry is the only method for the direct determination of the enthalpy associated with the process of interest.

Calorimetry acquires special significance in the studies of temperature-induced changes in the state of the protein,since temperature-induced alterations in macroscopic systems must proceed with a corresponding change in enthalpy. In other words, these changes are accompanied by heat absorption if the process is induced by a temperature increase or, by the evolution of heat if it is caused by a temperature decrease. The functional relationship between enthalpy and temperature usually includes all the thermodynamic information on the macroscopic states, accessible within the considered temperature range and thus information can be extracted from the enthalpic function by its thermodynamic analysis. This temperature dependence of the enthalpy can be determined experimentally by calorimetric measurements of the heat capacity of

the studied system over the temperature range of interest. Microcalorimeters measure this heat capacity not in a discrete way of stepwise sample heating by discrete energy increments as do classical calorimeters but constantly with continuous heating or cooling of the sample at a constant rate. In other words, they scan along the temperature scale by measuring continuously small changes in the heat capacity of the samples and as a result these instruments are usually called scanning microcalorimeters (Dodd and Tonge,1987). Continuous heating and measurement has a great advantage over the discrete procedure, since it provides more complete information on the heat capacity function and it permits the complete automation of all measurement processes. Its disadvantage is that the studied sample is never in complete thermal equilibrium.

Commercial DSC has been applied extensively in the study of lipids (Singer and Nicolson,1972), biological membranes (Steim et al,1969; Blazyk and Steim,1972), polysaccharides (Norton et al,1983) and nucleotides (Breslauer et al,1986). However perhaps the most important application of DSC is concerned with the thermal unfolding of proteins (Beck et al, 1965; Donovan and Ross,1973;Hu and Sturtevant,1987 and 1988), since the calorimetric analysis can give information concerning the fundamental nature of this process and the forces involved in the stabilization of the native structures of proteins (Privalov,1979).

The most commonly used instruments for work with biochemical

systems are the DASM-1M (Privalov et al,1975; Privalov and Potekhin,1986), the DASM-4 (Privalov,1980) and the Microcal 2 (Privalov and Potekhin,1986). These scanning calorimeters measure not the absolute but the difference heat capacity, that is to say they are differential instruments with two identical calorimetric cells and measurements consist of a comparison of their heat capacities. The heat capacity difference of the cells is usually measured by a compensation method in which the sensors automatically monitor the power in the electric heaters to both cells to maintain identity of their temperatures to within 10-20 μdegrees at heating (Danforth et al,1966). The difference in these powers is recorded as a function of temperature (Gill and Beck,1965). A schematic representation of the thermal analysis system used to monitor such changes is reproduced in Fig.2.3.
One of the cells is loaded with the solution to be studied and the other one with some standard liquid. Thus, the heat capacity of the studied liquid is determined relative to the chosen standard.In studying dilute solutions it is convenient to take the solvent as the standard since, in this case, the measured difference heat capacity will correspond directly to the heat capacity contribution of the molecules dissolved in the solution. This is an important consideration since in general a significant fraction of the total change in apparent specific enthalpy is due to the simple heating or cooling of the solvent.

2.2.2 Interpretation of DSC Curves

The curves produced record the differential heat input to the

Fig.2.3 Schematic representation of the DSC analysis system.

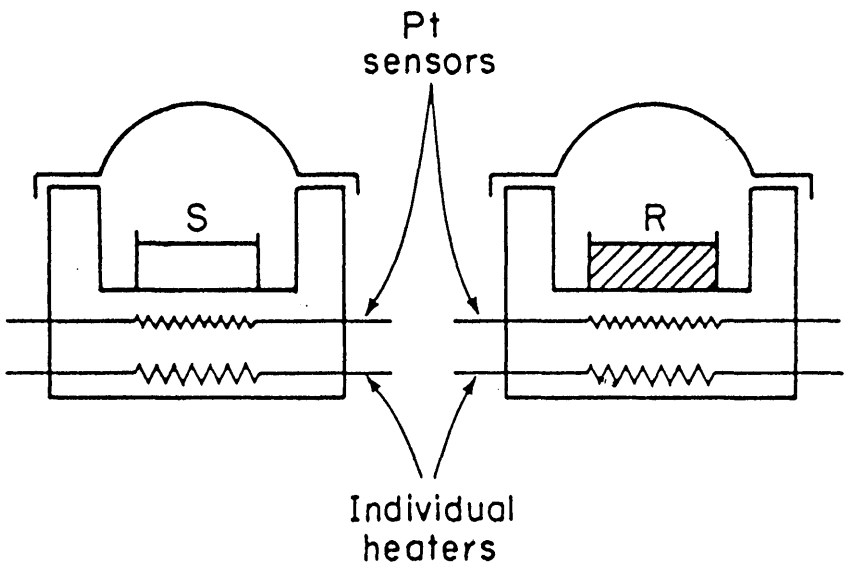

S = Sample cell
R = Reference cell

sample, expressed as excess specific heat in $mJdeg^{-1}$ on the ordinate, against temperature on the abscissa. The so-called excess apparent specific heat being the amount by which the apparent specific heat during a transition involving the solute exceeds the baseline specific heat.

An idealised representation of the three major processes observable by DSC are given in Fig.2.4.

When the enthalpy change (ΔH) for a reaction is greater than zero, the sample heater of the calorimeter is activated to equilibrate the sample and reference temperatures again. The corresponding signal obtained is called an endotherm. For an exothermic change ($\Delta H < 0$) it is the reference heater which must be activated to restore ΔT to zero. This gives a signal in the opposite sense, known as an exotherm. Since these energy inputs are proportional to the magnitude of the thermal energies involved in the transition, the records give measurements directly.

Peak areas in DSC therefore are proportional to the thermal effects experienced by the sample as it is subjected to the temperature variations, where the peak area is defined as that area enclosed between the peak on the DSC record and the interpolated baselines. The peak area is most commonly measured by one of the following methods.Firstly,there is the "cut and weigh" method in which the area of the peak can be obtained by comparison with the weight of a square of known area, cut from the same paper. This method is accurate to

Fig.2.4 An idealised representation of the processes observable by DSC.

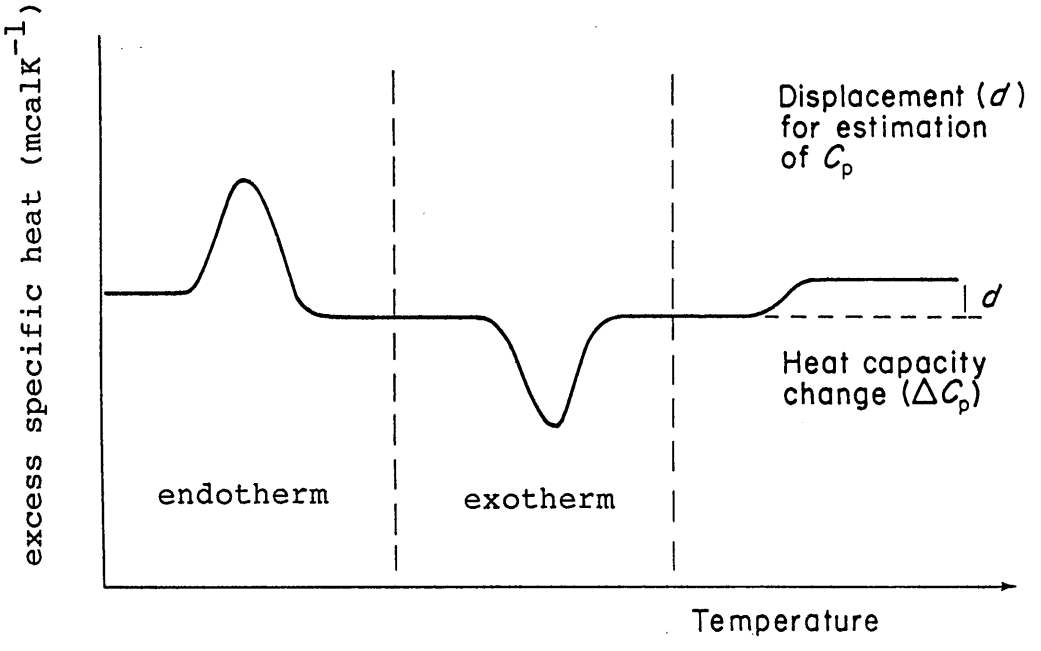

within $\pm$5%. A second technique uses a planimeter which involves carefully tracing the perimeter of the peak on the DSC record with the stylus of the planimeter arm,resulting in the area being registered on the planimeter dial. Accuracy is thought to be within $\pm$1%. The most accurate method of all involves the use of an integrator unit connected to the calorimeter or, nowadays, continuous data acquisition and integration by on-line computer. Both computer and planimeter methods were employed in calculating the peak areas of the DSC curves obtained in chapter5.

When a sample is subjected to a heating programme in DSC, the rate of heat flow into the sample is proportional to its heat capacity (C_p) and many chemical/physical processes involve a change in the value of C_p for the sample. In DSC this can be detected by the displacement of the baseline from one near horizontal position to another. Fig.2.4 denotes this displacement as being equal to some value d, and from this measurement C_p may be determined.

$$C_p = d/(\text{heating rate X m})$$

where m is the sample mass.

Interpretations of DSC data are usually based on the van't Hoff equation,

$$(\partial \ln K/\partial T)_p = \Delta H_{vH}/(R.T^2)$$

where K is the equilibrium constant for the process under study, T is the absolute temperature and ΔH_{vH} is the apparent or van't Hoff enthalpy. This equation is directly applicable to two-state processes in which, when a protein sample is heated through a temperature range, there are no

significantly populated intermediate states at equilibrium. When such a situation exists $\Delta H_{vH} = \Delta H_{cal}$, where ΔH_{cal} is the true or calorimetric enthalpy, obtained by integration of the DSC curve. A ratio of $\Delta H_{vH} / \Delta H_{cal}$ of less than unity indicates a significant population of one or more intermediate states between the native and denatured state whereas a ratio greater than unity indicates intermolecular cooperation (Sturtevant,1987).

ΔH_{vH} can be calculated using the expression:

$$\Delta H_{vH} = (ART^2_{1/2} \cdot C_{ex,1/2}) / \Delta H_{cal}$$

where the constant A has the value 4.00 for a simple two state process not involving association or dissociation, $T_{1/2}$ is the absolute temperature of half denaturation, $C_{ex,1/2}$ is the excess apparent heat capacity at $T_{1/2}$ and R is the gas constant.

2.3 Raman Spectroscopy

2.3.1 Introduction to Raman Spectroscopy

Raman spectra provide detailed information on the vibrational motions of atoms or groups of atoms in a molecule and because these vibrations are sensitive to chemical changes, the vibrational spectrum can be used as a monitor of molecular chemistry. Very low frequency spectra may also provide information relating to the molecular rotations of the sample (Genzel et al,1976;see section 1.1.5,chapter 5 and Table2.1).

The origin of Raman scattering lies in inelastic collisions between the molecules composing the sample and the irradiat-

Table 2.1 Spectral Ranges

REGION		APPROXIMATE RANGE λ	APPROXIMATE RANGE $\tilde{\nu}$ (cm^{-1})
UV	electronic vibration		
Far		10 - 200nm	50,000 - 1,000,000
Near		200 - 400nm	25,000 - 50,000
VISIBLE	electronic vibration	400 - 800nm	13,000 - 25,000
INFRARED	molecular vibration		
Near		0.8 - 2.5 μm	4,000 - 13,000
Middle		2.5 - 50 μm	200 - 4,000
Far		50 - 1000 μm	10 - 200
RAMAN	molecular vibration	2.5 - 1000 μm	10 - 4,000
MICROWAVE	molecular rotation	0.01 - 10cm	0.1 - 100
NMR	nuclear precession	10 - 100cm	0.01 - 0.1

ing photons. Since total energy is conserved during the scattering process, the energy gained or lost by the photon must equal an energy change within the molecule.This exchange in energy results in a frequency change of the photon which can be detected by a corresponding change in wavelength of the scattered light (Fig.2.5). The kind of molecular information provided by Raman spectroscopy hence is namely the frequencies, usually expressed as wavenumbers (cm^{-1}), and the spectroscopic intensities due to molecular vibrations, rotations and other kinds of motion.

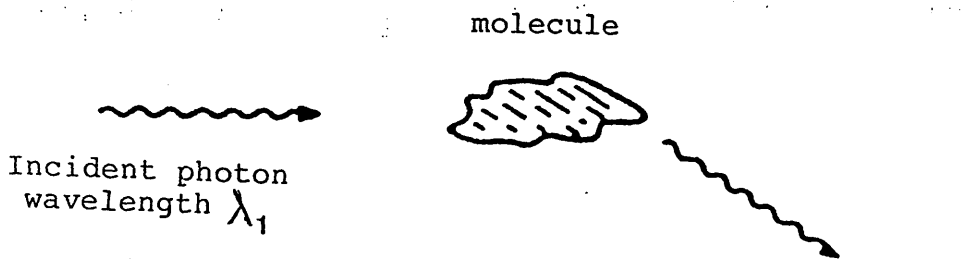

For Raman scattering $\lambda_1 \neq \lambda_2$

Fig.2.5 An inelastic collision between a photon and a molecule

2.3.2 The Raman Spectrometer

Light provided by a laser is used to irradiate the sample being investigated. Since they produce well-collimated, monochromatic beams of narrow band width, lasers have become the standard excitation sources for Raman scattering experiments (Mooradian,1970).

A scattering geometry of 90^{o} (see Fig.2.6) was used to collect the scattered light, although different geometries can be employed (Gilson and Hendra,1970; Tobin,1971).The collected light is directed to a triple monochromator which separates spatially the scattered light on the basis of

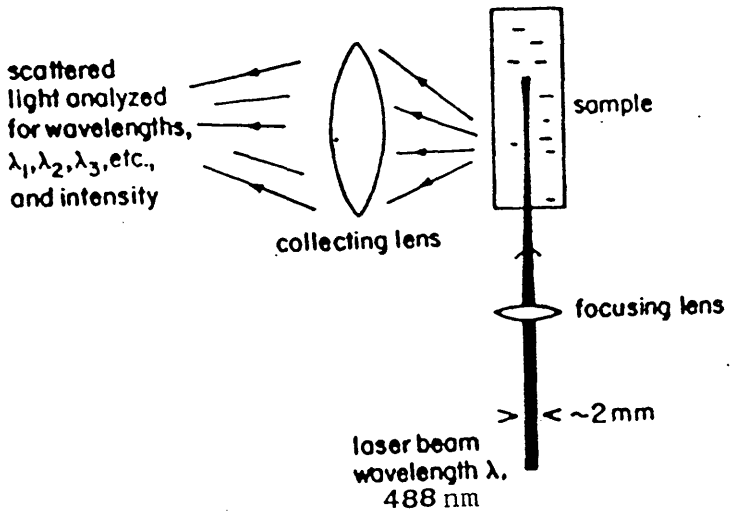

Fig.2.6 Schematic of a Raman experiment

frequency. A double or triple monochromator, as used in this case, is necessary to separate the Raman photons from the overwhelming number of Rayleigh photons. Rayleigh photons are of the same frequency as the photons of the incident radiation and they arise when the incident beam is scattered without a change of wavenumber. Rayleigh scattering always accompanies Raman scattering.

At the exit port of the monochromator the Raman spectrum forms an image in the form of a series of very faint lines which are detected by a photomultiplier. Detection of the spectral lines is carried out by slowly turning the gratings of the monochromator, thus allowing the lines of the spectrum to move in succession across the slits of the photomultiplier tube.The photoelectron current from the photodetection system is converted to an output voltage and stored by one of various methods.

Hence there are five basic components of the Raman spectrometer;the laser,the sample compartment and associated optics, the monochromator, a photoelectric detection system and an output device with options for data handling. A schematic diagram of the arrangement used for the subsequent Raman experiments is shown in Fig.2.7.

2.3.3 Low-Frequency Raman Spectroscopy and the Dynamics of Proteins

The technique of laser Raman spectroscopy has been used with considerable success to obtain the Raman active vibrations of

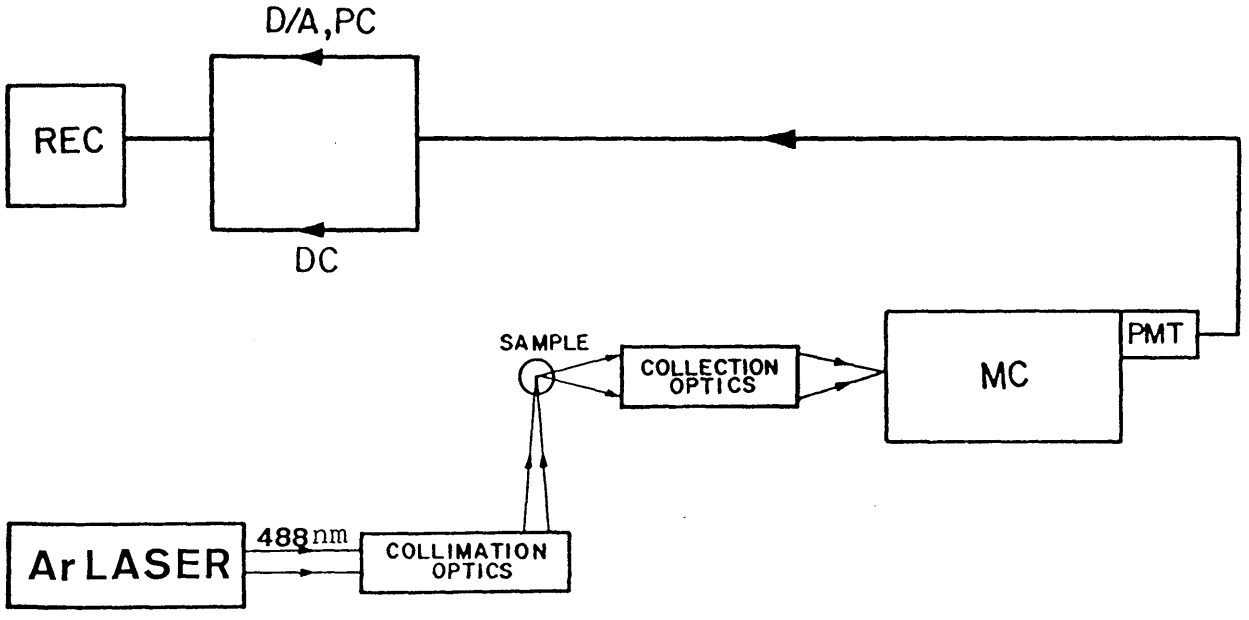

Fig.2.7 Schematic diagram of Raman spectrometer : MC, monochromator; PM, photomultiplier; DC, direct current amplification; D/A, digital to analog converter; PC, photon counting detector; REC, recorder/computer

several proteins (Lord and Yu,1970a and 1970b;Yu,1977; Carey, 1982; section 1.1.5). Until recently however, it has been impossible to obtain Raman spectra below 150cm^{-1}. Now, with the abundance of spectrometers fitted with triple grating monochromators and the development of other techniques (Brown et al,1972), it is possible to discriminate against the Rayleigh scattering and hence record spectra to below 5cm^{-1}. Elastic scattering of the laser incident light should produce an infinitely narrow peak at zero wavenumbers shift. This however is not what is observed, instead there is a fairly broad peak - the spread of the signal depending upon the physical nature of the sample being studied. The origin of this additional scattering is not well understood. Whereas Blatz (1967 and 1968) and others (Gross and Vuks,1935; McDevitt and Fateley,1970) interpret the "peaks" in terms of low frequency Raman modes, Litovitz and coworkers (Bucaro and Litovitz,1971a and 1971b; Dardy et al,1973) argue that the wing must be considered an integral part of the Rayleigh line which reflects the short-time orientational behaviour of the molecules. Certainly, when analysing solutions, the buffer itself exhibits a weak Rayleigh wing and this is one of the advantages of using Raman spectroscopy in the study of biological materials-water is a very weak scatterer.However, when protein is added the intensity of the wing increases greatly (see Fig.2.8). This additional contribution is probably due to many vibrational (some of which are damped) and rotational signals from the protein. In fact there are so many "peaks" that they are not individually distinguishable and they simply merge to produce the "bell-shaped" Rayleigh

Fig.2.8 Comparison of the low frequency spectra of buffer and buffer + 3% wild-type PGK.

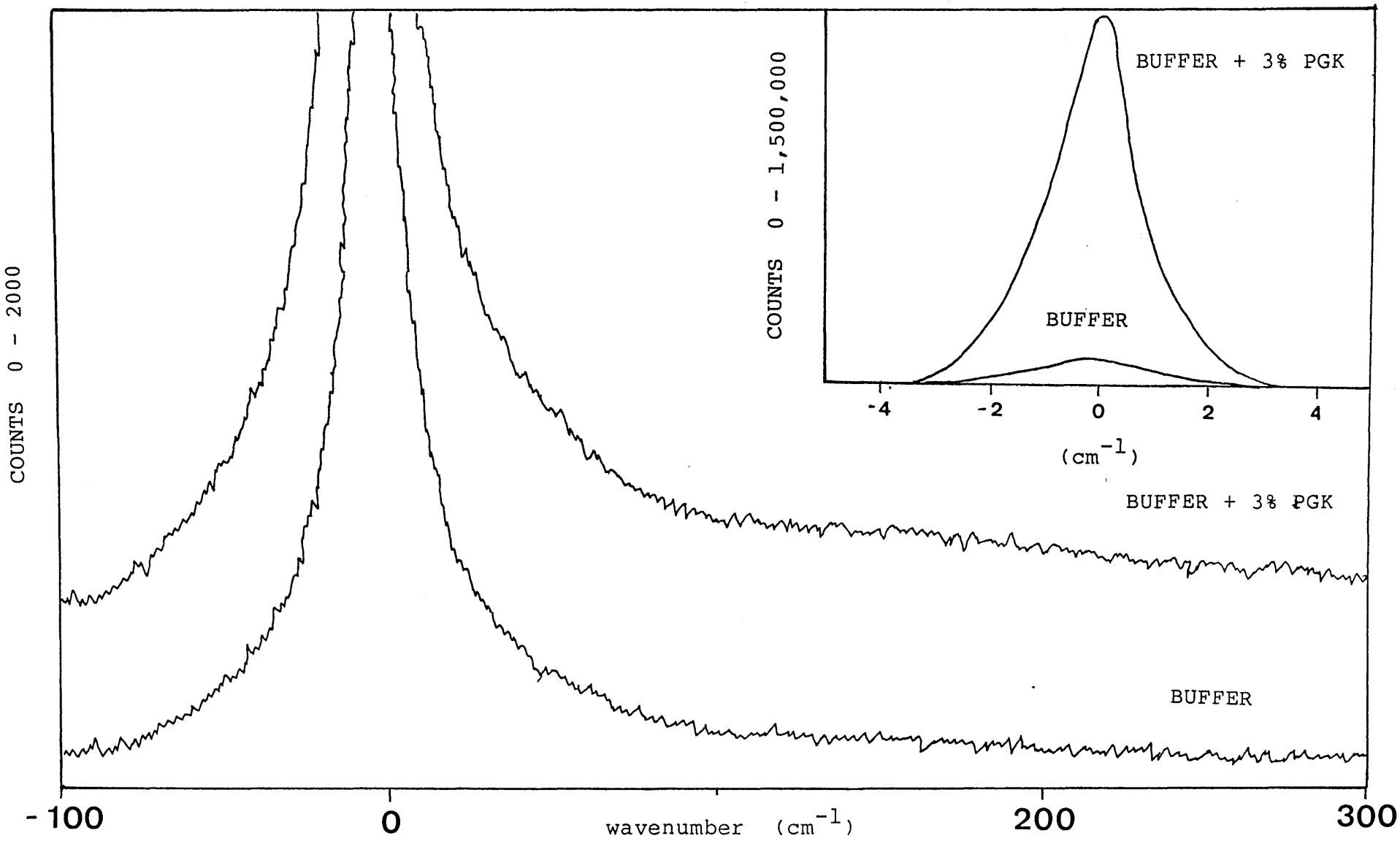

wing.

Since the low frequency Raman spectrum (0-300cm^{-1}) is thought to be closely related to the dynamical behaviour of the protein in question (see section 1.1.5), any change in this spectrum upon for example, substrate binding or alteration of the protein structure, will indicate a change in the dynamics of the system.

It must be noted that in the experiments detailed in chapter 6,instead of analysing the spectra to look for characteristic peak changes, it is necessary to inspect for differences in the distribution and intensities of the collective frequencies.

By recording the low frequency spectra of mutant and wild-type PGK, with and without substrate, it is primarily thought to be changes in the vibrations/rotations associated with the dynamics which control catalysis that are being observed. These results may then provide an indication as to the role which the dynamic properties of the system play in enzymatic catalysis - as yet an unanswered question.

2.3.4 Conventional Raman Spectroscopy and the Conformation of Proteins

Site-directed mutagenesis of proteins may not only affect their dynamic properties but may also, no matter how carefully the mutation is selected, alter the mean conformation of the polypeptide. Such effects can make interpretation of

experimental data difficult, and it is important to establish what changes, if any, have been induced by mutation. One possible way to probe this is to compare Raman spectra of mutant and wild-type proteins in the conventional, high frequency region where particular group frequencies may be identified. Bands associated with amide groups are particularly useful here because they are readily resolved and are sensitive to conformational environment.

It is known that the conformation of the amide group is of overriding importance in determining the backbone structure of polypeptides. This arises from the partial double bond character of the CO-NH bond composing the backbone which results in a planar conformation of the amide groups. In addition to planarity,the amide bonds in linear or open-chain polypeptides adopt the trans conformation exclusively (Donahue,1953), while the cis planar conformation has been proposed for some residues of fibrous proteins (Pauling and Corey,1951).

Vibrational assignments of the various amide bands which exist appear in Table2.2. and by far the most important modes in the Raman study of the structure of proteins are the amideI and amideIII vibrations. (Although the amideII band is strong in IR absorption, it is virtually unseen in the non-resonance Raman effect). As a result, these modes are widely used to characterize the various forms of secondary structure which exist in polypeptides. Examples of this include the α-helix and β-sheet which are organized, hydrogen bonded

Table2.2 Vibrational modes of the trans secondary amide group

BAND TERMINOLOGY	APPROXIMATE $\tilde{\nu}_{C=O}$ (cm^{-1})	ASSIGNMENT
AMIDE I	1650[a]	Primarily C=O stretch
AMIDE II	1550[b]	Primarily N-H in-plane bending with a C-N stretching contribution.
AMIDE III	1250[c]	Primarily C-N stretching with N-H in-plane bending. (The coupling phases are opposite to Amide II).
AMIDE IV	630[d]	O=C-N bending
AMIDE V	700[d]	N-H out-of-plane bending
AMIDE VI	600[d]	C=O out-of-plane bending
AMIDE VII	200[d]	Internal rotation about the peptide C-N bond related to the barrier hindering internal rotation.

[a] cis - 1650
[b] cis - 1450
[c] cis - 1350
[d] weak in Raman

structures found in proteins. In these ordered regions, any buried carbonyl oxygen forms a hydrogen bond with an amide -NH group. This is done in two major ways; by forming α-helices or by forming β-sheets. The α-helix is a stable structure, each amide group making a hydrogen bond with the third amide group away from it in either direction and so there is approximately 3.6 amino acids in each turn of the helix. The C=O groups are parallel to the axis of the helix and point almost straight at the NH groups to which they are hydrogen bonded. Side chains of the amino acid point away from this axis.

β-sheet structures arise from the fact that an extended polypeptide chain can make complementary hydrogen bonds with a parallel extended chain. This in turn can match up with another extended chain to build up a sheet. Two stable arrangements exist: the parallel β-sheet in which all the chains are aligned in the same direction, and the anti-parallel β-sheet in which the chains alternate in direction. Residues which are involved in neither α-helical or β-pleated structures are called "random coil", even though their structure may be far from random.

The use of amideI and amideIII regions of the Raman spectrum to characterize the structure of a protein however, depends firstly upon the determination of characteristic frequencies for the various common forms of secondary structure that exists - namely, helical, β-sheet and random protein conformations. This has been accomplished by using polypeptide

models and proteins of known conformation (Carey,1982) and the characteristic Raman bands produced by α-helical, β-sheet and random-coiled conformations are summarised in Table2.3.

Hence the normal Raman spectrum of a protein probes structural details such as average backbone conformation.
As well as this it is also possible to probe some amino acid side chains, particularly those of tyrosine and tryptophan.It is normally not possible however, to focus on a single molecular group.

2.4 Fluorescence Spectroscopy

2.4.1 Introduction to Fluorescence Spectroscopy

When a molecule absorbs light to form an electronically excited species, radiative deactivation can occur by two mechanisms - fluorescence and phosphorescence.In fluorescence the emitted radiation ceases almost immediately when the exciting source is removed but, in phosphorescence, it may persist for long periods (even hours, but characteristically seconds, or fractions of seconds).The difference of behaviour suggests that fluorescence is an immediate conversion of absorbed light into re-emitted energy, but that in phosphorescence the energy is stored in some kind of reservoir, from which it slowly leaks. The sequence of steps involved in fluorescence and phosphorescence is depicted in Figs.2.9a and 2.9b.

Table 2.3 Approximate positions (cm^{-1}) of the most intense Amide I and III bands in Raman spectra for various forms of secondary structure.

	AMIDE I	AMIDE III
α - helix	1645 - 1660	1265 - 1300
β - sheet	1665 - 1680	1230 - 1240
unordered	1660 - 1670	1240 - 1260

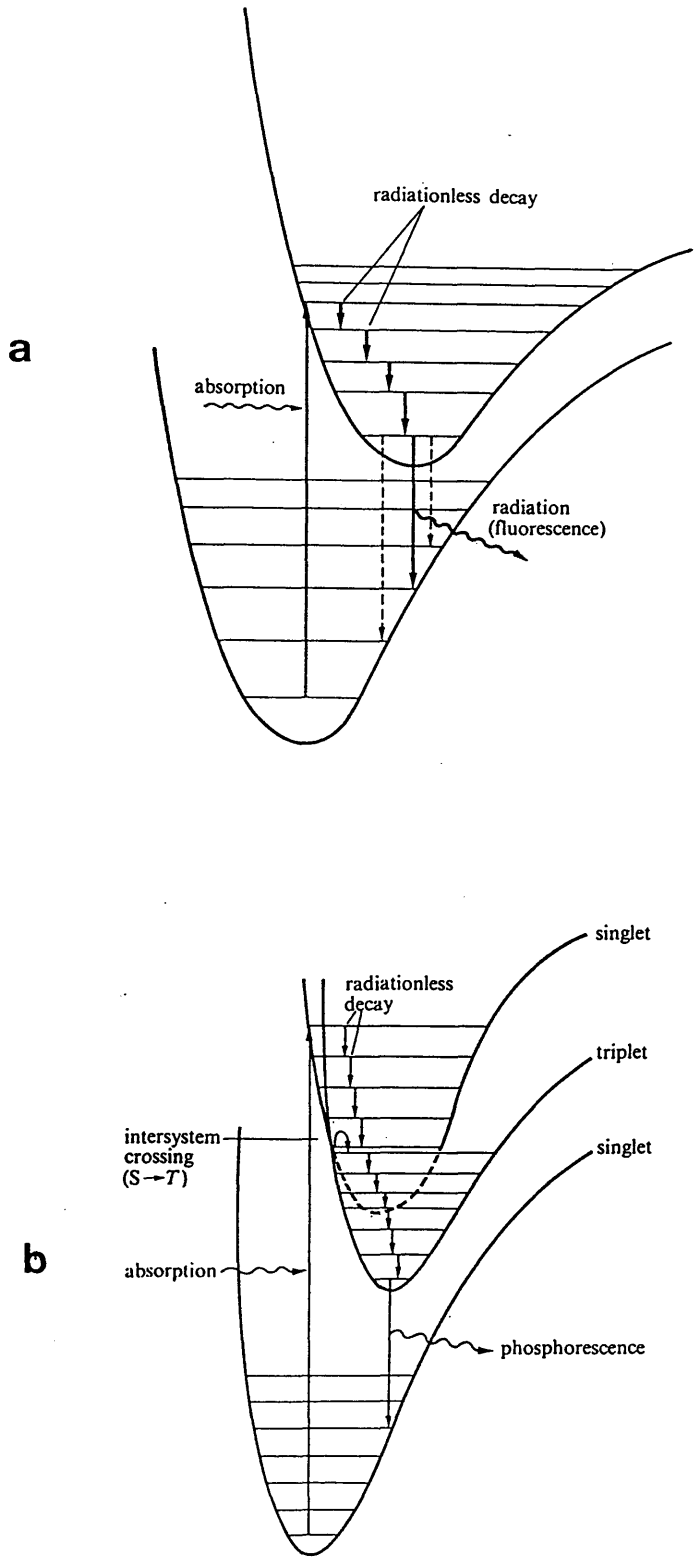

Fig.2.9 The sequence of steps leading to (a) fluorescence and (b) phosphorescence. (From Atkins,1983)

Initial absorption of light, in the fluorescence process, carries the molecule into the vibrational energy levels of the upper molecular state. In the excited state the molecule is subjected to collisions with its environment (for example, solvent molecules) and its thermal energy is discarded as thermal motion of the surroundings. The collisions succeed in lowering the molecule down its ladder of vibrational energy levels, but they may be unable to withdraw the larger electronic energy difference and quench the electronic excitation energy. The molecule might therefore live long enough to undergo a spontaneous emission, and to emit the excess energy as radiation as it drops to the lower electronic state.This mechanism accounts for the observations that fluorescence radiation has a lower frequency than the incident radiation - the fluorescence occurs after some energy has been discarded into the solvent.

The successful application of fluorescence methods requires an understanding of the instrumentation involved.Considerable attention to the experimental details is necessary since fluorescence is a highly sensitive method.

Generally, both excitation and emission spectra are recorded. An emission spectrum is the wavelength distribution of the emission measured with a single constant excitation wavelength. It is this form of spectrum which will be analysed within chapter8, where the spectra are presented on a wavelength scale.

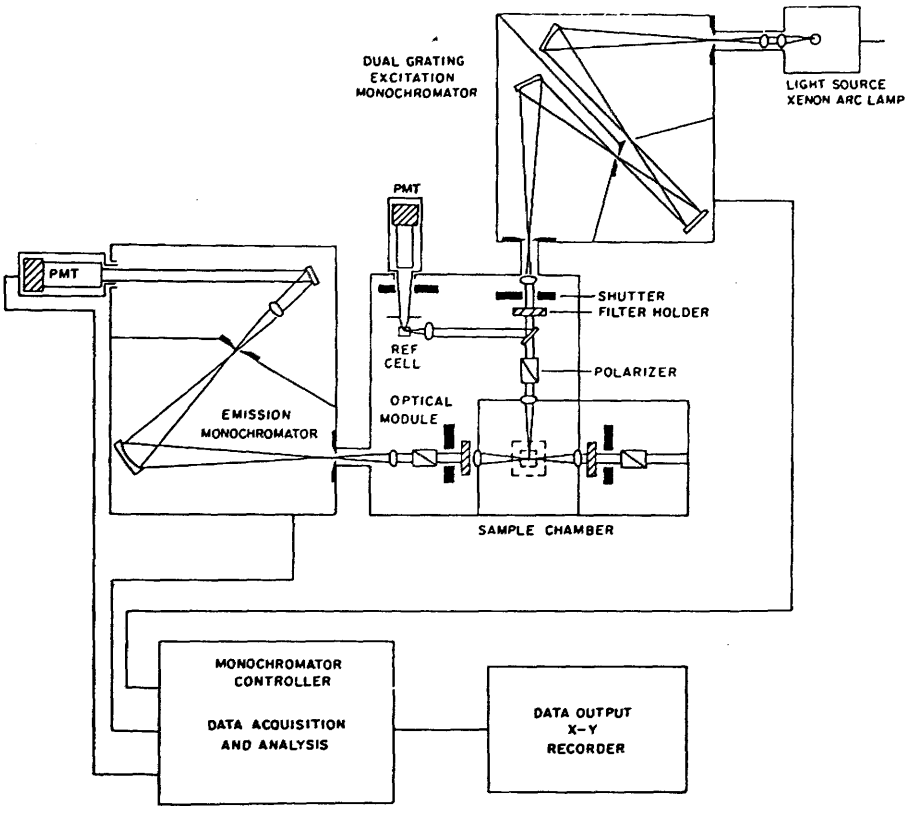

Fig.2.10 Schematic diagram of a spectrofluorometer.

(From Lakowicz,1983)

For an ideal instrument, the directly recorded emission spectra would represent the photon flux emitted at each wavelength. Fig.2.10 shows a schematic diagram of a general purpose spectrofluorometer. The spectrofluorometer used for the experiments detailed in this thesis was a Perkin Elmer Fluorescence Spectrometer connected to a xenon power supply. Xenon arc lamps are, at present, the most versatile light sources to provide continuous light output from 270nm to 700nm. Light is emitted as a result of the recombination of electrons with ionized Xe atoms. The instrument is equipped with monochromators to select both the excitation and emission wavelengths. Fluorescence is detected by photo-multiplier tubes and quantified with the appropriate electronic devices. Hence, the output can be presented graphically and may be stored in a computer memory.

2.4.2 Fluorescence Lifetimes

The fluorescence lifetime of a substance usually represents the average amount of time the molecule remains in the excited state prior to its return to the ground state. The precise nature of the fluorescence decay can reveal details about the interactions of the fluorophore with its environment. For example, multiple decay constants can be the result of a fluorophore being in several distinct environments,or as a result of excited state processes. The measurement of fluorescence lifetimes is difficult because these values are typically near 10nsec, necessitating the use of high speed electronic devices and detectors. There are two widely used methods for the measurement of fluorescence lifetimes - the

pulse method and the harmonic or phase-modulation method. The equipment used for the lifetime experiments described in chapter8 functioned by the pulse method in which the sample was excited with a brief pulse of light and the time-dependent decay of fluorescence intensity was measured. F(t), the fluorescence intensity, which is proportional to the excited state population N(t), decays exponentially. The fluorescence lifetime is generally equated with the time required for the intensity to decay to 1/e of its initial value. Alternatively, the lifetime may be determined from the slope of a plot of the logF(t) versus t (see Fig.2.11). Since the measurement of the entire time-resolved decay using only a single excitation pulse is technically very difficult, the sample is generally excited with repetitious pulses and from this the decay can be reconstructed by two methods-the pulse sampling method or the photon counting method. The latter technique was used by the instrumentation for the following data collection and involves measurement of the time between the pulse when the sample is excited and the arrival of the first photon at the detection system. Only the first arriving photon is counted, therefore, the system must be adjusted so that no more than one photon arrives per pulse. This time difference is measured for a large number of photons, usually 10^6 and the resulting distribution of arrival times represents the decay curve.

The expression,

$$F(t) = F_o.e^{-t/\tau}$$

where F_o is the fluorescence intensity at t=0, describes the

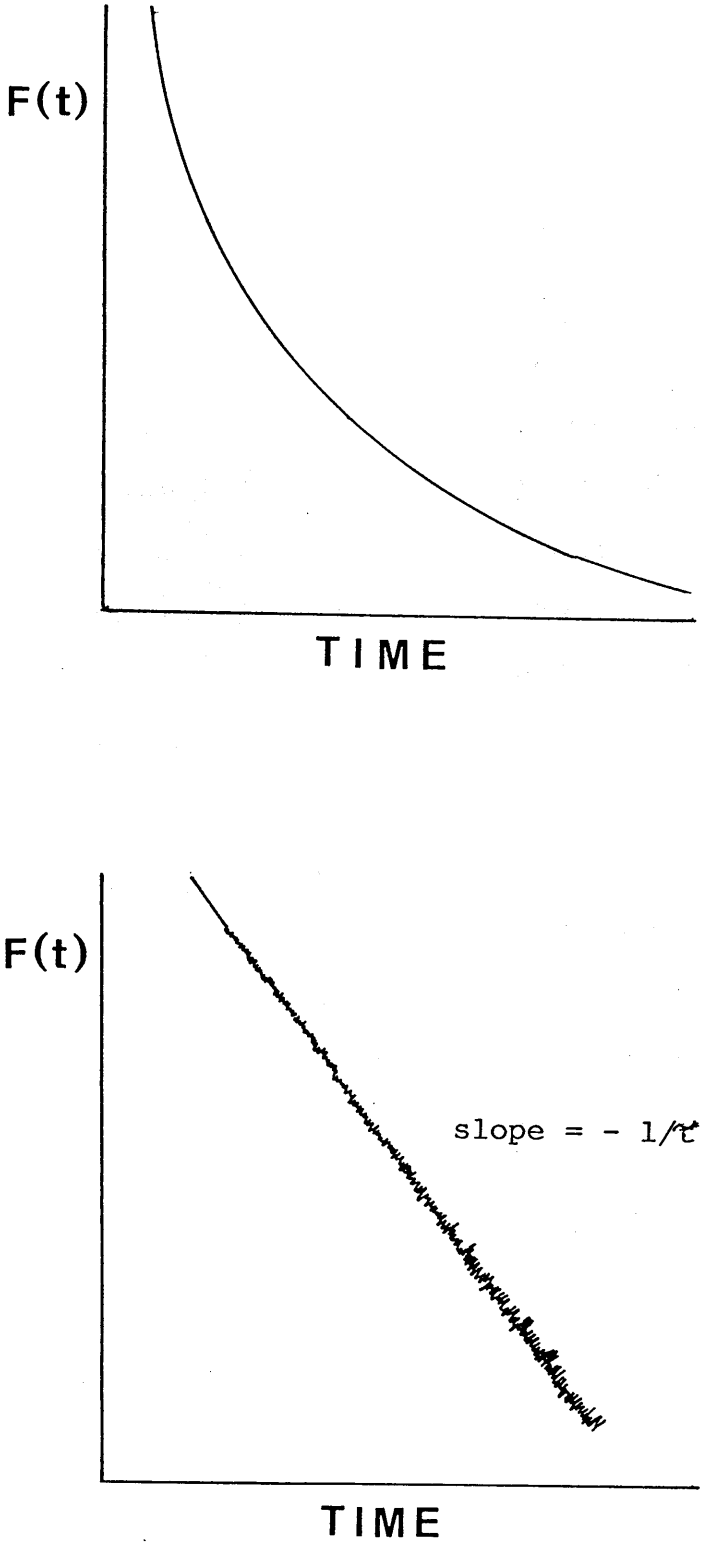

Fig.2.11 Schematic diagram of pulse lifetime measurements

time-resolved decay of the fluorescence intensity, F(t), for a single fluorophore which decays exponentially. Frequently however the decays are not adequately described by a single exponential and in these instances the observed decay is generally fitted to a sum of exponentials,

$$F(t)=\sum_i \alpha_i . e^{-t/\tau_i}$$

where α_i is a preexponential factor representing the fractional contribution to the time-resolved decay of the component with a lifetime τ_i. This equation is of significance where the species being excited is a mixture of several different fluorophores or one fluorophore in several different environments. Hence τ_i values represent the lifetimes of the individual species.

The object of measuring the time-resolved decays is to determine F(t). However, the presence of a signal due to the lamp pulse complicates matters and so the time distribution of the lamp pulse, L(t) must be measured in a separate experiment.

The observed decay of fluorescence is called R(t).F(t) can be calculated using the known values of L(t) and R(t) (Badea and Brand,1971; Yguerabide,1972).

$$R(t) = \int_o^t L(t').F(t-t')dt'$$

A variety of methods have been proposed for estimation of F(t) from the measured decay curve R(t) and the lamp profile L(t) (O'Connor et al,1979). A least squares method (Grinvald and Steinberg,1974) was applied in the following calculations and carried out with the help of a PDP 11/23 computer. The

basis of this method is the calculation of the expected value of R(t) given assumed values of α_i and τ_i. The fitting function used by the computer is:

$$R_c(t) = A + \alpha_1 . e^{-i/\tau_1} + \alpha_2 . e^{-i/\tau_2} + \alpha_3 . e^{-i/\tau_3}$$

where c is the channel number, τ_i is the lifetime of component i, α_i equals the amplitude of component i and A is the residual fluorescence (usually very small). Using these values and the measured time-profile of the lamp pulse, the calculated values $R_c(t)$ are compared to the observed values R(t) and the goodness-of-fit (χ^2) is calculated. A minimum value of χ^2 indicates the best fit. If the χ^2 value is larger than 2 this indicates a poor fit whereas a χ^2 value of less than 1.2 indicates a good fit.

The α_i and τ_i values are varied by the computer until the best fit is obtained. The closeness of the fit is illustrated when the actual and the calculated fluorescence decay curves are superimposed. Visual inspection of these curves is often difficult, however and to overcome this, examination of the residuals is useful. The residuals plot is a graph of the standard deviation between the observed and calculated curves versus time. A "good-fit" is indicated by a small standard deviation range and a plot which is symmetrical about zero.

2.4.3 Protein Fluorescence

Almost all proteins contain phenylalanine, tyrosine and tryptophan and these natural fluorophores contribute to their ultraviolet fluorescence. Protein fluorescence is generally excited at the absorption maximum near 280nm, or at longer

wavelengths. Consequently, phenylalanine is not excited in most experimental situations. Furthermore, the quantum yield of phenylalanine is small, so that emission from this residue is rarely observed (Figs.2.12 and 2.13 and Table2.4). It has been found that the quantum yields of tyrosine and tryptophan fluorescence in proteins is considerably lower than those of the free amino acids (Table2.4) - this is probably due to various quenching processes involving photon transfer and environmental effects occuring within the protein (Radda and Dodd,1968).

Simple proteins can be divided into two groups on the basis of their fluorescence properties. Proteins which only contain phenylalanine and tyrosine exhibit fluorescence spectra indistinguishable from that of free tyrosine (with λ_{max} = 303nm). This reflects the insensitivity of tyrosine fluorescence to the polarity of the environment-insensitivity which is due to the low polarity of its excited state.
Normally proteins containing both tyrosine and tryptophan show a fluorescence spectrum which is characteristic of tryptophan alone. The maximum of emission is dependent upon the protein and while the emission maximum of tryptophan in water occurs at 348nm it is highly dependent upon polarity.It must be noted that PGK is one of the proteins in which this is not the case and the emission spectrum of this enzyme, excited at 280nm, is dominated by tyrosine emission (section 8.1).Unlike tyrosine emission however,tryptophan fluorescence in proteins was found by Teale (1957) to have quantum yields which could be higher, lower or about the same as that of the

free amino acid. These phenomena are discussed at great length by Chen (1967) with examples of many proteins. The tryptophan fluorescence lifetimes of proteins are dependent upon the protein and its tertiary structure, and not the amino acid sequence, that is responsible for the variation in lifetimes among native proteins (Grinvald and Steinberg, 1976). It must be noted that in proteins where there is more than one tryptophan residue or where the protein exists in more than one conformation, multi-exponential decay of the fluorescence may occur.This has indeed been observed for wild -type PGK (Stryjewski and Wasylewski,1986).

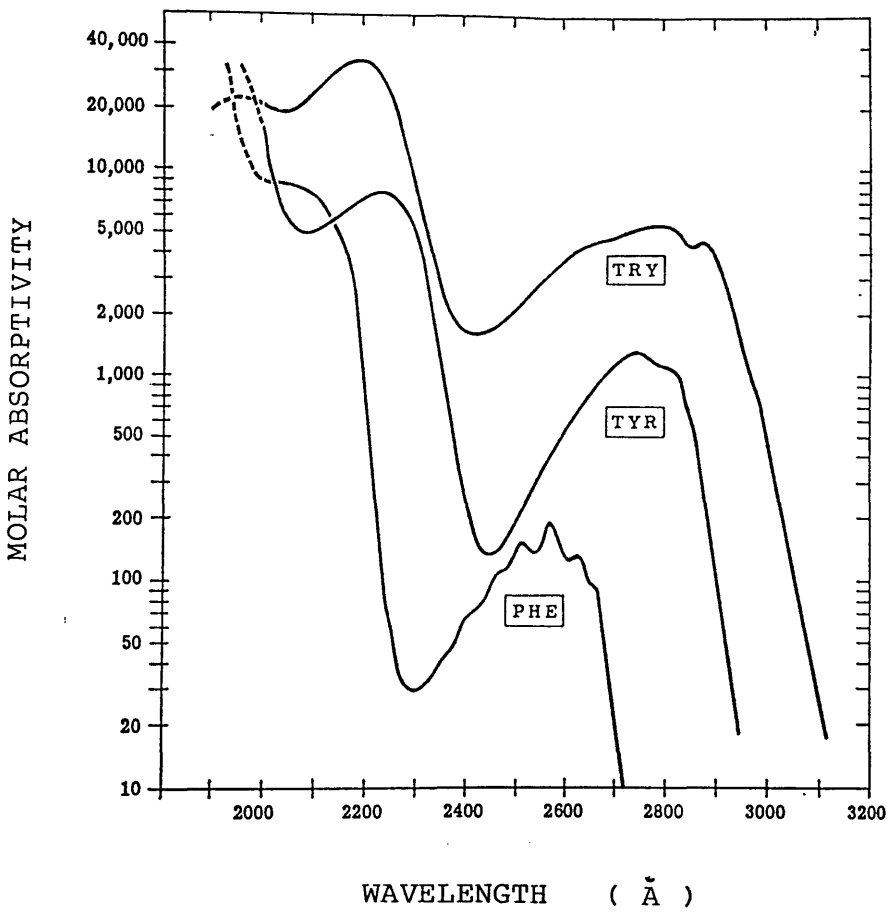

Fig.2.12 Absorption spectra of the aromatic amino acids at pH6

(From Wetlaufer,1962)

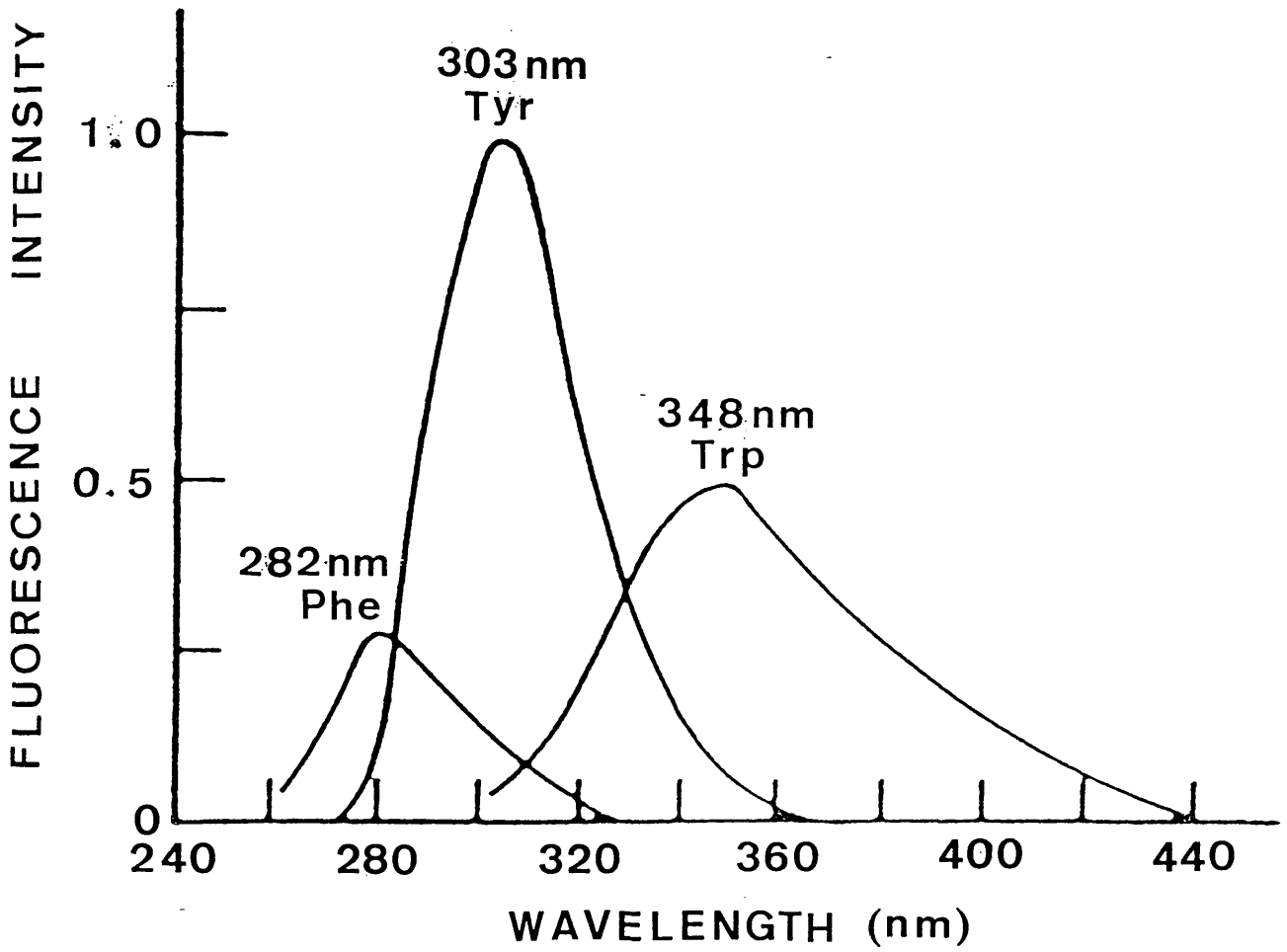

Fig.2.13 Fluorescence emission spectra of the aromatic amino acids.

Table 2.4 Absorption and emission spectra of aromatic amino acids in water.(From Radda and Dodd,1968)

AMINO ACID	ABSORPTION		EMISSION	
	λ_{max} (nm)	ε (litre mol^{-1} cm^{-1})	λ_{max} (nm)	QUANTUM YIELD
PHENYLALANINE	257 206 187	200 9,000 58,000	282	0.036
TYROSINE	275 222 192	1,200 8,000 47,000	303	0.21
TRYPTOPHAN	280 220 196	5,500 32,000 21,000	348	0.20

CHAPTER 3

Experimental Details

3.1 Isolation of Wild-Type and Mutant PGK by Genetic Engineering Techniques

- 3.1.1 Plasmid preparation
- 3.1.2 Transformation of yeast with plasmids pMA27 and pMA40b*-PGK
- 3.1.3 Growth of yeast
- 3.1.4 Isolation and purification of yeast PGK

3.2 Comparison of Kinetic Measurements for Wild-Type and Mutant PGK

- 3.2.1 Calculation of Michaelis constant, K_m
- 3.2.2 Measurement of catalytic activity

CHAPTER 3

EXPERIMENTAL DETAILS

3.1 Isolation of Wild-Type and Mutant PGK by Genetic Engineering Techniques

Initially, several methods were used to isolate wild-type PGK from dried bakers yeast (see Appendix A) but due to the low yield of enzyme from this source it was necessary to use genetic engineering techniques in order to obtain the required amounts of enzyme. Using multi-copy plasmid systems provided a method for not only isolating large amounts of wild-type PGK but also obtaining mutant PGK by site-directed mutagenesis (see section 1.2).

It has been found that the glycolytic enzyme genes of saccharomyces cerevisiae encode for some of the most abundant mRNA and protein species in the cell, with each gene contributing up to 5% of the total mRNA and protein (Holland and Holland,1978).Over-expression yeast vectors pMA27 and pMA40b have already been used to produce wild-type and mutant PGK respectively, in quantities which represent between 50 and 80% of the total cell protein.

3.1.1 Plasmid Preparation

Plasmid vectors pMA27 and pMA40b*-PGK stored in yeast and E.coli hosts respectively, were kind gifts from Dr.L.A. Fothergill-Gilmore, Biochemistry Department, University of Edinburgh.

pMA27

The gene for yeast PGK has been isolated from chromosome III on a 2.95 kilo-base pair HindIII DNA restriction fragment (Dobson et al,1982). This fragment, containing the PGK gene, is covalently linked to plasmid pBR322 with a 3.3kb double EcoRI fragment containing the yeast Leu2 gene and the 2μ plasmid origin of replication (Broach,1982). The plasmid formed is denoted pMA27 (see Fig.3.1). This acts as a vector which can replicate independently of the host chromosome when it is incorporated into an appropriate host,such as yeast. Plasmid pMA27 is also an integral part of the formation of the over-producing plasmid vector pMA40b*-PGK,for mutant PGK.

pMA40b*-PGK

Plasmid pMA27 and phage M13mp9 were digested with HindIII restriction enzyme. The 2.95kb pair fragment containing the PGK gene was ligated to the now linear form of M13mp9.(M13 is an example of a small, filamentous phage, usually about 6500 nucleotides long, and several features make it attractive as the basis for a cloning vehicle. One advantage arises because the genome of this phage which is a covalent circle of single -stranded DNA, goes through a covalent circular duplex of DNA termed RF - replicative form). This form of the M13 genome behaves very much like a plasmid and can be treated as such for experimental purposes. It can be easily isolated from a culture of infected E.coli, manipulated and then can be re-introduced into E.coli.

Single-stranded DNA was prepared from the products of the

ligation reaction and this was allowed to anneal with linear HindIII/BamHI fragment from another M13mp9. The double-stranded DNA circle formed was used as a template to direct mutagenesis and at this point an oligonucleotide specifying a single thymine to adenine replacement is incorporated into a gap in one of the strands. Upon this step being successful the residue His-388, normally expressed in the wild-type enzyme, will be changed to Gln-388.

The 2.95kb pair HindIII fragment with the mutant PGK gene was removed from the M13 plasmid and ligated to the large HindIII fragment comprising most of plasmid pMA40b (Fig.3.2) to produce a new plasmid pMA40b*-PGK.

3.1.2 Transformation of Yeast with Plasmids pMA27 and pMA40b*-PGK

Yeast transformation was carried out by the genetics department, University of Glasgow, following the method used by Beggs (1978). Details of all media used in the following sections are reproduced in Appendix B.

An identical transformation procedure was followed for both vectors, in which they were used to transform yeast cells of the Leu2$^-$ (section 1.2.2) strain X4003/5b and the transformed cells isolated by leucine selection.

A single yeast colony was used to innoculate 2.5ml YPG medium and this was grown to a stationary culture at 30^{o}C for 48hours with vigorous shaking. 25-100 μl of this was trans-

Fig.3.1 Plasmid pMA27

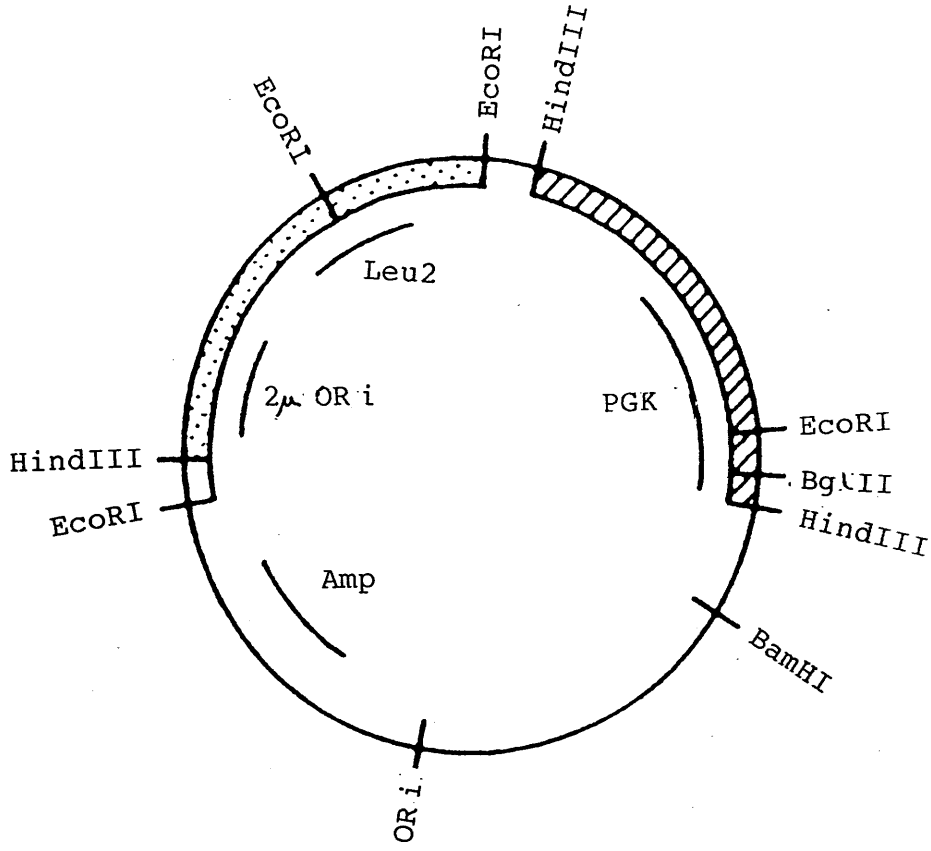

HindIII fragment containing the PGK gene

double EcoRI fragment derived from yeast 2μ plasmid

The remainder of plasmid pMA27 consists of plasmid pBR322

(From Wilson et al (1984))

Fig.3.2 Plasmid pMA40b

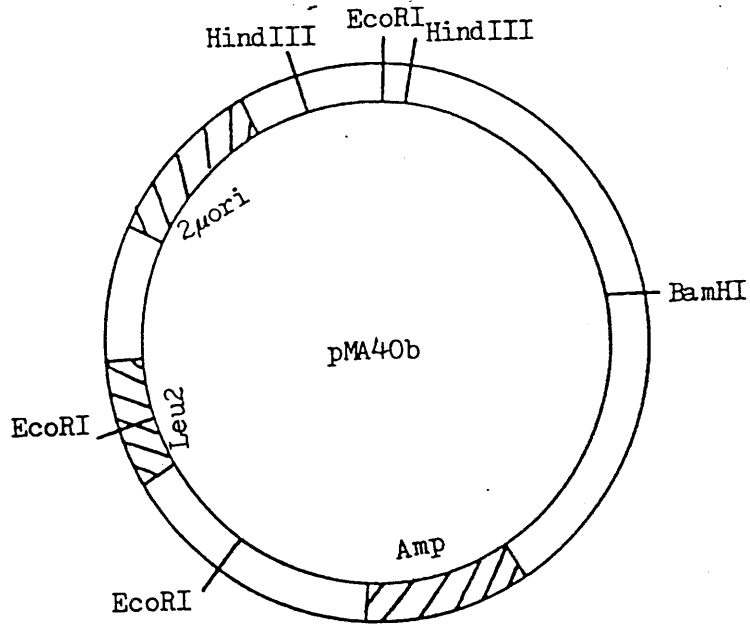

ferred to 100ml YPG and allowed to grow overnight with vigorous agitation at 30°C. The optical density was checked to be between 0.6 and 0.9 before harvesting. After centrifugation at 2,500 rpm for 5minutes at room temperature, the cells were resuspended in 50ml of the sorbitol/EDTA solution containing freshly added 50mM DTT and incubated (30°C) with gentle shaking. After 20minutes the cells were collected by centrifugation and resuspended in 50ml sorbitol/EDTA/citrate containing 3% β-glucuronidase. This solution was incubated at 30°C for 15-20minutes with gentle shaking. The β-glucuronidase breaks down the yeast cell walls and since the cells are present in hypertonic solution, protoplasts - cells devoid of walls - can form. Protoplast formation was monitored by light microscopy, by adding dilute detergent to burst the cells. Once the protoplast had formed, the solution was centrifuged at 2,500rpm for 2.5minutes and washed three times with 1.2M sorbitol at room temperature. (Resuspension of the protoplasts was carried out very gently at each washing step). Finally the cells were suspended on 100μl sorbitol/$CaCl_2$ to give a thick suspension. These cells were in such a condition that the plasmid vector could be added to the cell suspension and it would be incorporated into the yeast cells. 15μl of plasmid DNA, pMA27, was added to 50μl of protoplasts and left for 15minutes at room temperature. To this solution was added 1ml of freshly dissolved 20% polyethylene glycol (PEG) in $CaCl_2$/Tris and after 30-60seconds the mixture was spun in an Eppendorf centrifuge until pelleted.The PEG was removed and the protoplasts suspended in 100μl of YPG/sorbitol before leaving the solution for 30minutes at

30°C. About 0.2ml of this solution was plated with about 10ml of top agar and incubated at 30°C for about 3days.

3.1.3 Growth of Yeast

Preparation of shake culture/innoculum

5ml batches of YO medium, containing 50µg/ml of each of the amino acids mentioned in part (1), Appendix B, were innoculated with a single transformed yeast colony and then grown with shaking for 48hours at 30°C. These cultures were used to innoculate 2l batches of the same medium, prewarmed, and grown at 30°C for about 24hours or until a dense culture was obtained. This was transferred to the chemistry department where batches were stored at 4°C until required by myself for the following yeast growth and PGK purification steps.

Continuous culture

Since large amounts of enzyme were required (several grams), it was necessary to culture many litres of the transformed yeast. The volume of the fermentor used was 10litres and since it was found that approximately 1gram of PGK was obtained from each 10litre batch, several batches of yeast were harvested.

9litres of GYNB medium was placed in the fermentor vessel and autoclaved at 15lb/in^2 for 30minutes. The fermentor was placed in a waterbath (30°C) and allowed to equilibrate to this temperature before addition of 200ml sterile innoculum. Air was pumped through the fermentor, serving both to aerate the medium and to keep the yeast cells evenly distributed.

The yeast was allowed to ferment until the stationary phase was reached - usually about 48hours - and then the yeast cells were harvested. As much of the slurry as possible was removed from the fermentor without actually exposing the interior parts of the apparatus to the non-sterile outside environment.

To the fermentor, 9litres of freshly autoclaved GYNB medium was then added, along with a further 200ml of transformed yeast. The 48hour growth and harvest cycle was again started. This procedure was repeated several times and each harvest was checked by microscope for the presence of contaminating species.

3.1.4 Isolation and Purification of Yeast PGK

Upon harvesting the medium containing the yeast cells, this was centrifuged at 13,500rpm for 20minutes to collect the yeast pellet. The accumulated pellet was added to the same volume of 0.75M ammonia solution and stirred for 3hours at room temperature before storing at $4^{o}C$ for a further 20hours. 30ml, 0.5M lactic acid was stirred into the autolysis mixture and then the pH was lowered to 7.0 using 5M lactic acid.
The cell debris was removed by centrifugation (13,500rpm for 20minutes). The pH of the supernatant was adjusted to 6.0 with 5M lactic acid and solid ammonium sulphate (300g/l of extract) was added, with stirring,over a period of 20minutes. Stirring was continued for a further 30minutes before the solution was centrifuged and the resulting precipitate discarded. A further 100g/l of ammonium sulphate was added to

this supernatant as before and then centrifuged and the precipitate discarded.The pH of the supernatant was adjusted to 4.3 with 5M lactic acid (previously adjusted to pH3.5 using ammonia solution) and stirred for 20minutes before centrifugation. The supernatant was discarded and the precipitate taken up in approximately 20ml of 0.5M Tris. Adjustment of the pH to between 6.0 and 7.0 was made using 5M lactic acid. The enzyme suspension was stored in 400g/l ammonium sulphate at $4^{o}C$. After each purification step a sample of the supernatant was tested by gel electrophoresis. At this stage in the purification of PGK there was still a large amount of impurity present - the identity of which was unknown. Since the absorption spectrum of the enzyme solution showed a high intensity absorption peak at 260nm this implied that the impurity could be nucleic acid. This proposition was also supported by gel filtration experiments using mini-columns which indicated that the contaminating species was of high molecular weight- higher than that of PGK (see Fig.3.3). It was also noted from the gel electrophoresis results that no bands of protein of higher molecular weight than PGK were present.

The fractions collected from the gel-filtration column were tested for PGK activity using the following procedure:

Assay for PGK activity

PGK activity was assayed according to the method of Scopes (1975).

Fig.3.3 Elution pattern of crude PGK mixture from mini Sephadex G-100 column

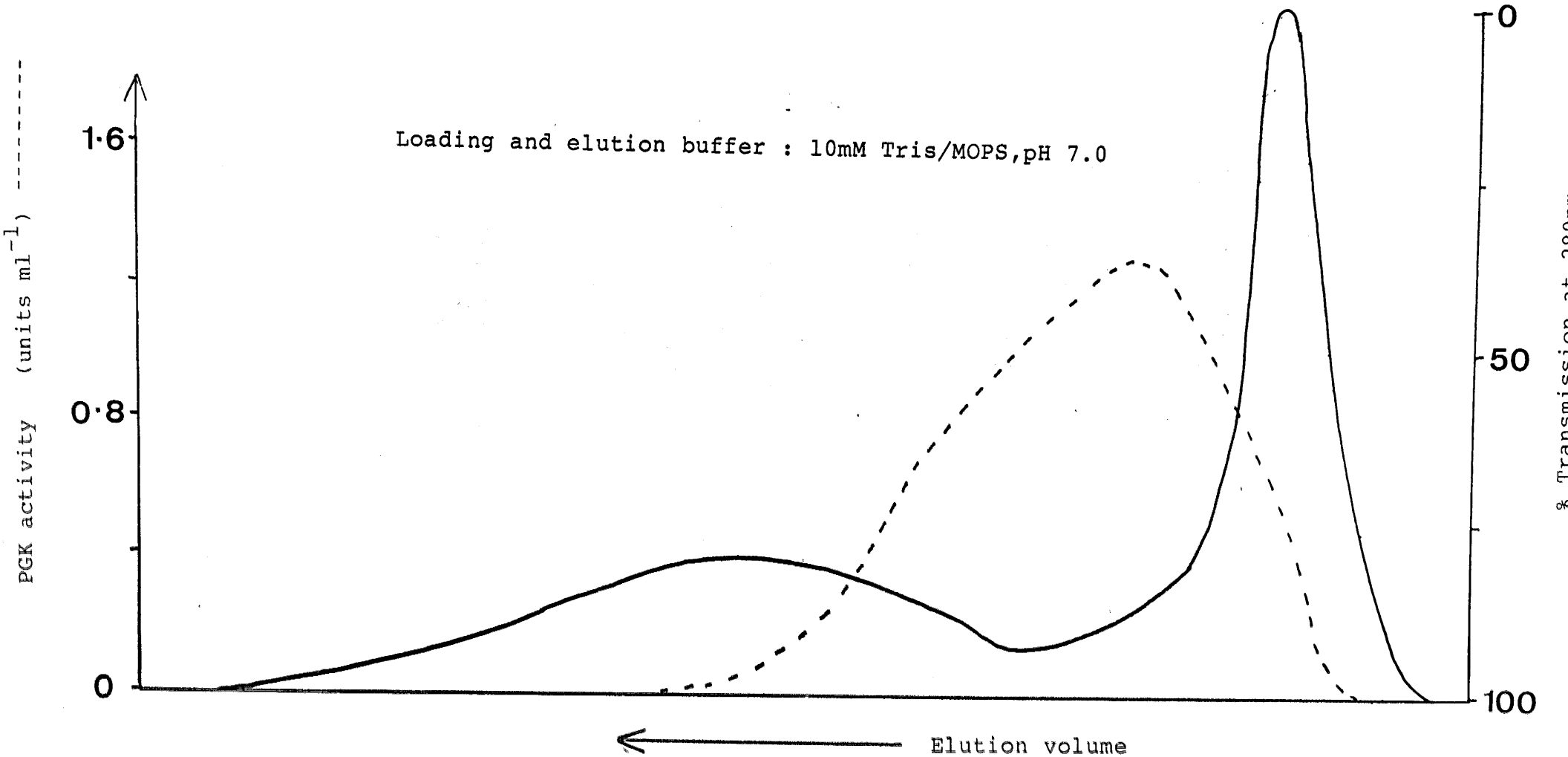

materials

Glyceraldehyde 3-phosphate dehydrogenase (E.C.1.2.1.12.), ATP (disodium salt), β-NADH and bovine serum albumin (BSA) were purchased from Sigma Chemical Co. Ltd.,Poole,England and used without further purification.D(-)3-PG (barium salt) also came from this source but could not be added directly to the assay medium since the barium salt has very low solubility in aqueous solution. The free acid was generated by adding the salt to water containing Amberlite IR120 ion-exchange resin (Hopkin and Williams).

Potassium chloride and EDTA.Na_2 were both obtained from Koch-light Ltd. and magnesium sulphate from Fisons.

PGK was assayed in the direction of 1,3-diphosphoglycerate formation, coupling with GAPDH (Bucher,1947). The reaction was followed by monitoring the decrease in absorbance at 340nm due to the oxidation of NADH.

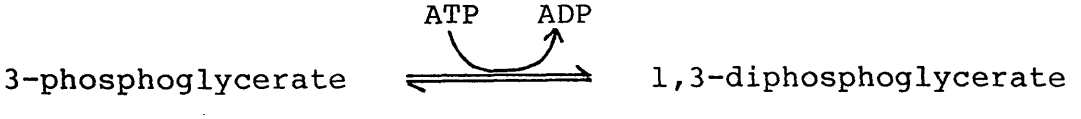

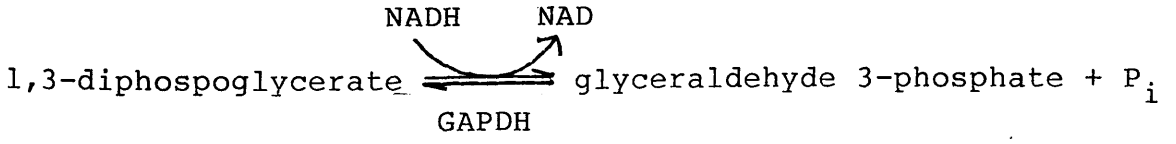

solutions

STOCK BUFFER (freshly prepared each day):

Triethanolamine,30mM
3-PG,10mM
KCl,50mM
$MgSO_4$,5mM
Na_2EDTA,0.2mM

} adjusted to pH7.5 with HCl

To this was added,

BSA,0.2mg/ml
NADH,0.1mM
GAPDH,40μg/ml of enzyme of specific activity 110units/mg

Magnesium ions are present to form the Mg-nucleotide complex, which is the true substrate, while the triethanolamine/HCl provides buffering capacity.

2.2ml of stock buffer was placed in a quartz cuvette and 100 μl of 1mg/ml GAPDH and 0.2ml of 50mM ATP were added. The cuvette + solution was left to equilibrate to 30^{o}C.
The absorbance at 340nm was observed for several minutes to determine whether the assay solution contained any contaminating PGK. Then 50μl of suitably diluted PGK solution was added, with thorough mixing, and the A_{340} recorded until a baseline was reached.
PGK activity was calculated using the molar extinction coefficient for NADH, at 340nm, of $6.22X10^3$ $mol^{-1}lcm^{-1}$ by the following equation:

$$\text{Number of enzyme units added to cuvette} = \frac{\text{Absorbance change/min}}{6.22} \times \text{volume of cuvette}$$

Tubes indicating PGK activity showed absorbance spectra with λ_{max}=280nm. All other fractions however, which have an absorbance have λ_{max} near 260nm. Hence it would appear that there are high and low molecular weight impurities. To determine if nucleic acid was the impurity present in the enzyme solution, several techniques were applied to detect phosphate esters and hence distinguish between protein and nucleic acid (see Appendix C).

When several of the fractions eluted from the G-100 column and showing λ_{max}=260nm were tested in this way, a positive result was obtained. Hence it appears that the impurity was indeed nucleic acid. To separate nucleic acid and PGK, a DEAE Sephadex ion-exchange column was used. PGK in pH7.0 buffer, being positively charged, passed straight through the column whereas the nucleic acid,which was negatively charged,became adsorbed to the column and remained there until eluted-using high salt concentration buffer.

The use of DEAE-Sephadex for the purification of PGK

DEAE-Sephadex A-25-120 (purchased from Sigma Chemical Co.) was swollen to approximately 100ml in 10mM Tris/MOPS, pH7.0, containing 10^{-5}M PMSF, $2X10^{-5}$M benzamidine and 6mM mercaptoethanol and carefully packed into a 4.6cm diameter column. Before the crude PGK solution was loaded onto the ion-exchanger, the ammonium sulphate mixture was dialysed against running tap water for about 3hours. Dialysis was continued at 4^{o}C against several changes of 10mM Tris/MOPS, pH7.0 + 1mM EDTA.Na_2, over a period of 48hours. (Dialysis tubing was pre-

boiled in water containing EDTA and sodium bicarbonate - to remove impurities).

The dialysed solution was centrifuged,if necessary,to remove any precipitous material present and the resulting clear supernatant was pumped onto the DEAE column at a rate of 100ml/hour. Once all of the protein solution had been loaded onto the column,it was washed through with several volumes of column buffer. Nucleic acid was deadsorbed from the column using column buffer + 0.2M KCl.

The eluate passed through a U.V. spectrometer flow cell,where the $\%T_{280nm}$ was recorded before being collected as 100 drop fractions (about 6ml) by automatic fraction collector (see Fig.3.4). PGK activity measurements were found for the collected fractions. The U.V. absorption spectrum was also recorded and each fraction under the first elution peak was shown to have an absorption maximum at 278nm - the λ_{max} expected for PGK. This indicates that the nucleic acid impurity is no longer present. This is substantiated when these fractions are also tested for the presence of phosphate esters using the techniques described in Appendix C - a negative result was obtained.

Fractions containing greater that 5mg PGK/ml were pooled together and a small sample was removed to test the purity of the solution by gel electrophoresis.The gel consisted predominantly of one band at the position PGK would be expected. PGK concentration was determined using the value of A_{280}=

Fig.3.4 Elution pattern of dialysed PGK mixture from DEAE ion-exchange column

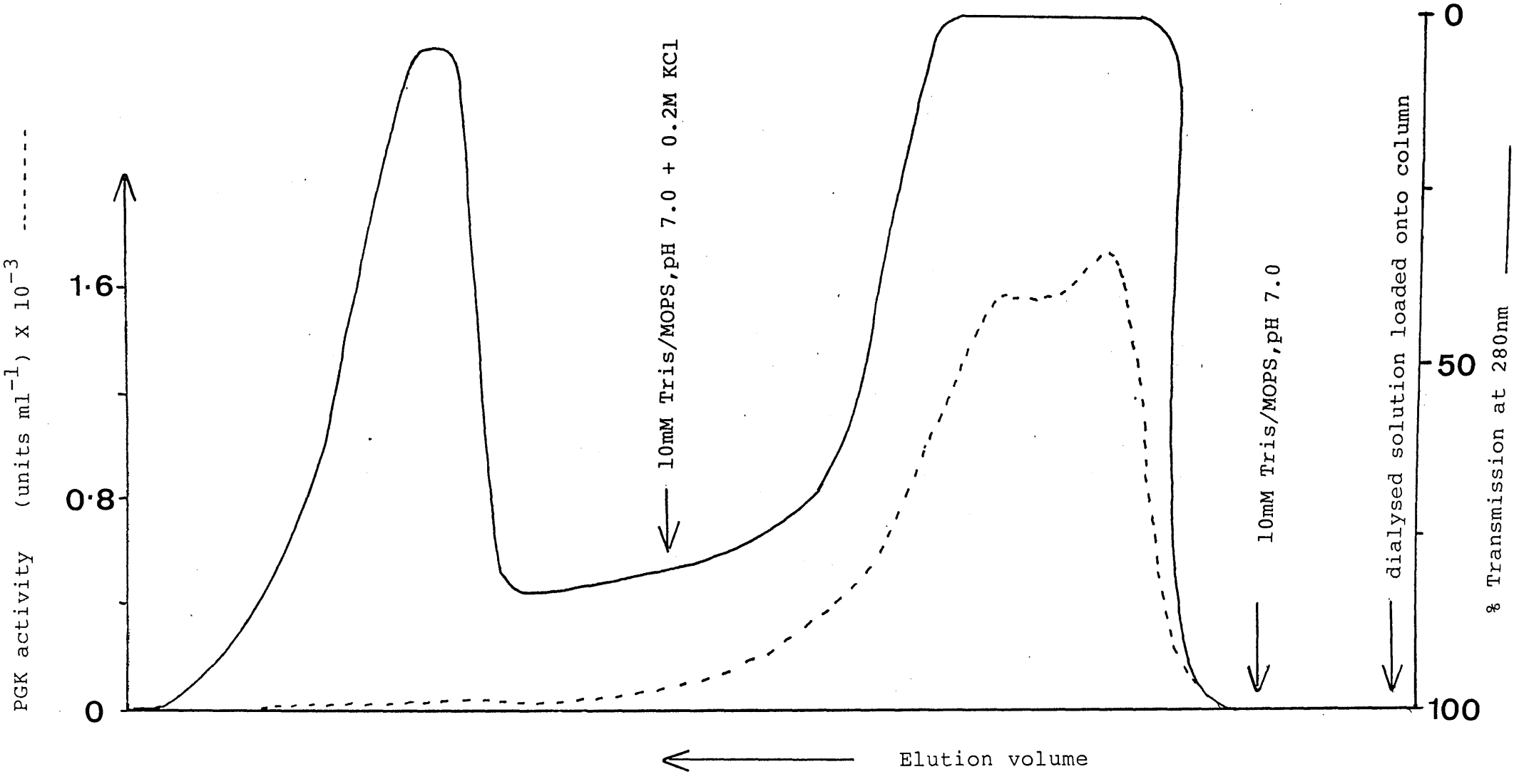

0.495 for a 1mg/ml solution - an average of published values (Bucher,1947 and 1955; Spragg et al,1976; Scopes,1978). Using this absorbance value, specific activity measurements were made of the pooled samples. The values obtained for wild-type and mutant PGK are given in section (3.2.2) and are very similar to those reported by Wilson (1985) for the pure enzyme. The results are also consistent with those published by Adams et al (1985) for wild-type PGK. These authors obtained a single band on an SDS polyacrylamide gel and presumed from this observation that their PGK was 100% pure. Hence the preparation was considered pure enough for experimental use after relatively few purification steps as compared with the method for the isolation of PGK from dried bakers yeast.
The wild-type and mutant PGK was stored at $4^{o}C$ in 60% (w/v) ammonium sulphate.
The entire purification procedure is recorded in Fig.3.5.

3.2 Comparison of Kinetic Measurements for Wild-Type and Mutant PGK

Parallel kinetic measurements have been made with both the mutant and wild-type enzymes.

3.2.1 Calculation of Michaelis Constant, K_m

An introduction to this subject has already been provided in section 1.1.3.1.
The information required to calculate K_m is V, the rate of catalysis and S, the substrate concentration. This enables a straight-line plot of 1/V versus 1/S to be drawn which has an intercept of $1/V_{max}$ and a slope of K_m/V_{max}.

Fig.3.5 Purification of wild-type and mutant PGK

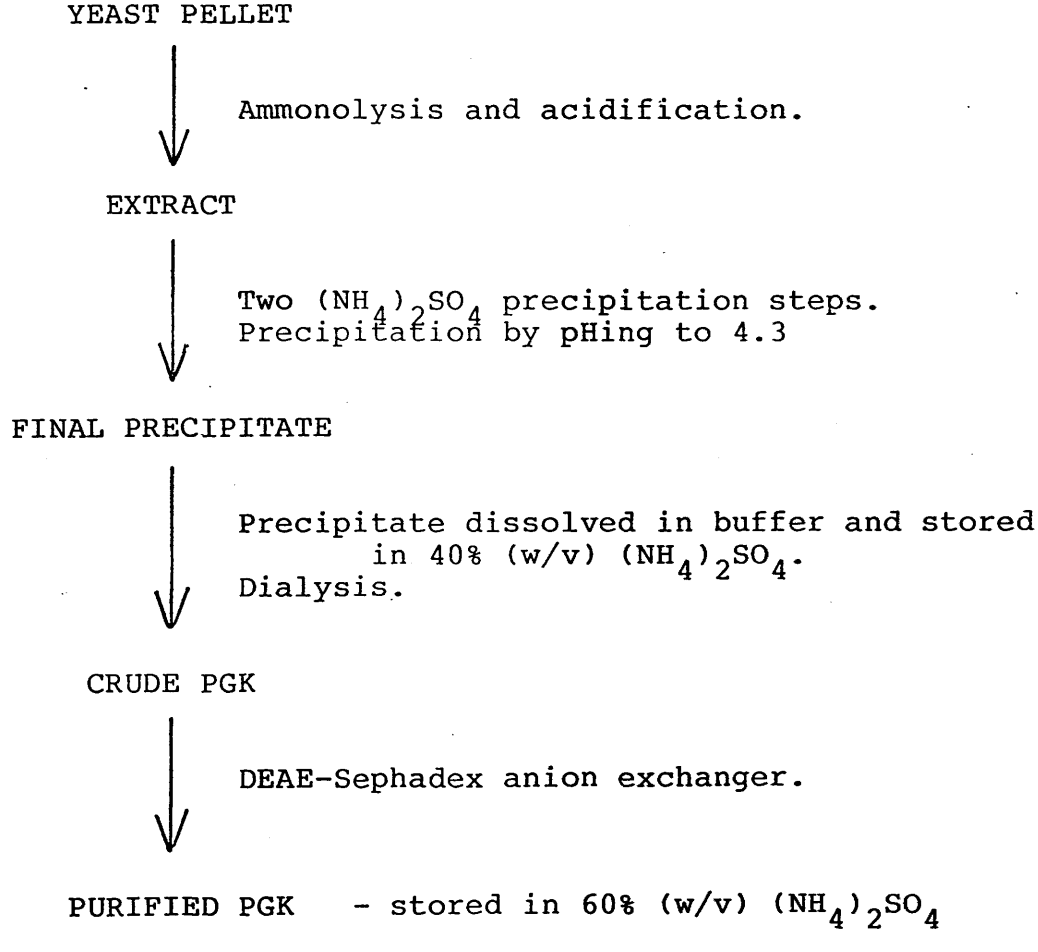

Experimental

Two sets of assay experiments were performed, one in which the 3-PG concentration was varied (0.045mM to 9.03mM) and the other in which the concentration of ATP was varied (0.008mM to 3.87mM). All other components of the assay solution were the same as those stated in section 3.1.4 and all solutions were equilibrated at 25°C before the activity measurements were taken.

Results

The results obtained are reproduced in Table3.1. The mutation of His-388 to a glutamine has had the effect of reducing the Michaelis constant for ATP by a factor of about three to 0.07mM compared with 0.23 for wild-type PGK. The K_m value however for the binding of 3-PG has not been significantly altered. These results are similar to the findings of Wilson et al (1987).

3.2.2 Measurement of Catalytic Activity

The specific activity of both the mutant enzyme and wild-type enzyme was calculated.

After dialysis of a portion of the PGK samples stored in 60% (w/v) ammonium sulphate, the absorbance of the enzyme solutions was found at 280nm and from this the concentration of PGK present was calculated.

Using the procedure outlined in section 3.1.4 the enzyme activity of each solution was assayed at 30°C and the answer expressed in units/ml of enzyme solution. By combining this

result with that for the known PGK concentration the specific activity (units/mg) was calculated (Table3.2). Catalytic activity has been reduced by a factor of four by introducing the glutamine residue to replace the histidine residue. This observation is in agreement with those results found by Wilson (1985).

While the effects on the K_m value for ATP binding and the catalytic constant might easily be described as a consequence of the lack of neutralization of the negative charge on Glu-190 in the mutant enzyme, previous work implies that the explanation is probably not quite so clear-cut. For example, nitration of Tyr-193 (Markland et al,1975; Hjelmgren et al,1976) which prevents the formation of the His388-Glu190 salt bridge (Watson et al,1982),leads to partial inactivation of the enzyme but no change in the K_m values for the 3-PG and MgATP substrates.The binding of MgATP however can protect the Tyr residue from nitration by perturbing the domain interface thus making Tyr-193 inaccessible or by attaching to a second nucleotide binding site nearby (Khamis and Larsson-Raznikiewicz,1981).

Kinetic experiments (Wilson et al,1987) studying the effects of sulphate on mutant and wild-type activity imply that the Glu190-His388 interaction does not control the complicated activation/deactivation patterns demonstrated by the enzyme. Since the amino acid sequence around the interface of the N and C domains is highly conserved in PGKs from many different sources, the only firm conclusions which can be made at this

Table 3.1 K_m values for wild-type and mutant PGK.

	SUBSTRATE		
PGK	3PG (mM)	ATP (mM)	SOURCE
wild-type	0.4	0.55	Tompa et al (1986)
	---	0.4 or 0.35	Larsson-Raznikiewicz (1964)
	---	0.2	Fifis and Scopes (1978)
	0.38	0.60	Vas and Batke (1984)
	0.42	0.30	Mas et al (1986)
	---	0.32	Wilson et al (1987)
	0.42 $\pm$ 0.07	0.23 $\pm$ 0.04	Present work
mutant	*	0.11	Wilson et al (1987)
	0.39 $\pm$ 0.06	0.07 $\pm$ 0.01	Present work

* unchanged from wild-type value

Table 3.2 Measurement of the specific activity of wild-type and mutant PGK.

SPECIFIC ACTIVITY (units mg^{-1})		
wild-type	mutant	
600 $\pm$ 51	150 $\pm$ 37	Present work
607	167	Wilson (1985)

moment suggest that the domain interface sequence is critical for the activity and stability of the enzyme. This is supported by the fact that even though these residues may be spatially distinct from the active site even minor modifications have an effect on catalytic activity.

CHAPTER 4

Investigation of the Thermodynamics of Enzyme-Ligand Binding by Microcalorimetry

CHAPTER 4

INVESTIGATION OF THE THERMODYNAMICS OF ENZYME-LIGAND BINDING BY MICROCALORIMETRY

4.1 Instrumental Details

The calorimetric instrumentation used is described in section 2.1.2. However, before any experimental work was carried out the calorimeter was allowed to equilibrate at 25°C (±0.1°C) for several days, in a temperature-controlled room. Initially the temperature was regulated by the calorimeter's own thermo-statically controlled air bath for heating purposes and an external water flow when cooling was required. The flow rate of the mains cooling water was extremely variable and frequently caused the thermostat output to oscillate between high and low values. This situation was totally unsuitable since the internal temperature of the calorimeter was not remaining constant. A new temperature control system was devised which did not involve the air-bath's thermostat. A new heating unit and cooling water - mains water via a temperature-controlled water bath - were connected externally to the calorimeter.This system performed more satisfactorily.

4.2 Determination of Calibration Constant

Regardless of the type of calorimetric experiment, it is necessary to convert the observed signal to a heat quantity by the use of the predetermined calibration constant, ε. ε can be found by chemical or electrical methods (sections 4.2.1 and 4.2.2).

4.2.1 Electrical Method of Calibration

This involves passing a continuous current through the 50 Ω calibration resistor within the calorimeter. An LKB 2107-310 control unit connected to the calorimetric apparatus was used for this purpose and it provides a current in the range 0.1 to 100mA which corresponds to an approximate heat effect of $5X10^{-7}$ to $5X10^{-1}$W.

The heat effect, Q was calculated using the equation:

$$Q = I^2R \quad \text{Watt}$$

where I was the calibration current and R was the resistance of the calibration heater - the exact value of R for the instrument used was 49.881 Ω.

The calibration constant was then obtained from the expression:

$$\varepsilon = Q/E \quad \text{Watt/division or Watt/integrated unit}$$

where E was the recorder deflection, in divisions or in integrated units, during the steady state of the experiment. The calibration was repeated with and without solution (water) flowing through the mixing vessel on the 3 μV, 10 μV and 1mV amplifier ranges.

The integrating unit was directly connected to the chart recorder and it provided a digital readout at one minute intervals,this is directly proportional to the heat produced. This is a more accurate method for calculating heat values since it rules out errors which may arise due to human judgement. (In a more recent version of the instrument, developed late on in this project, full computer interfacing,

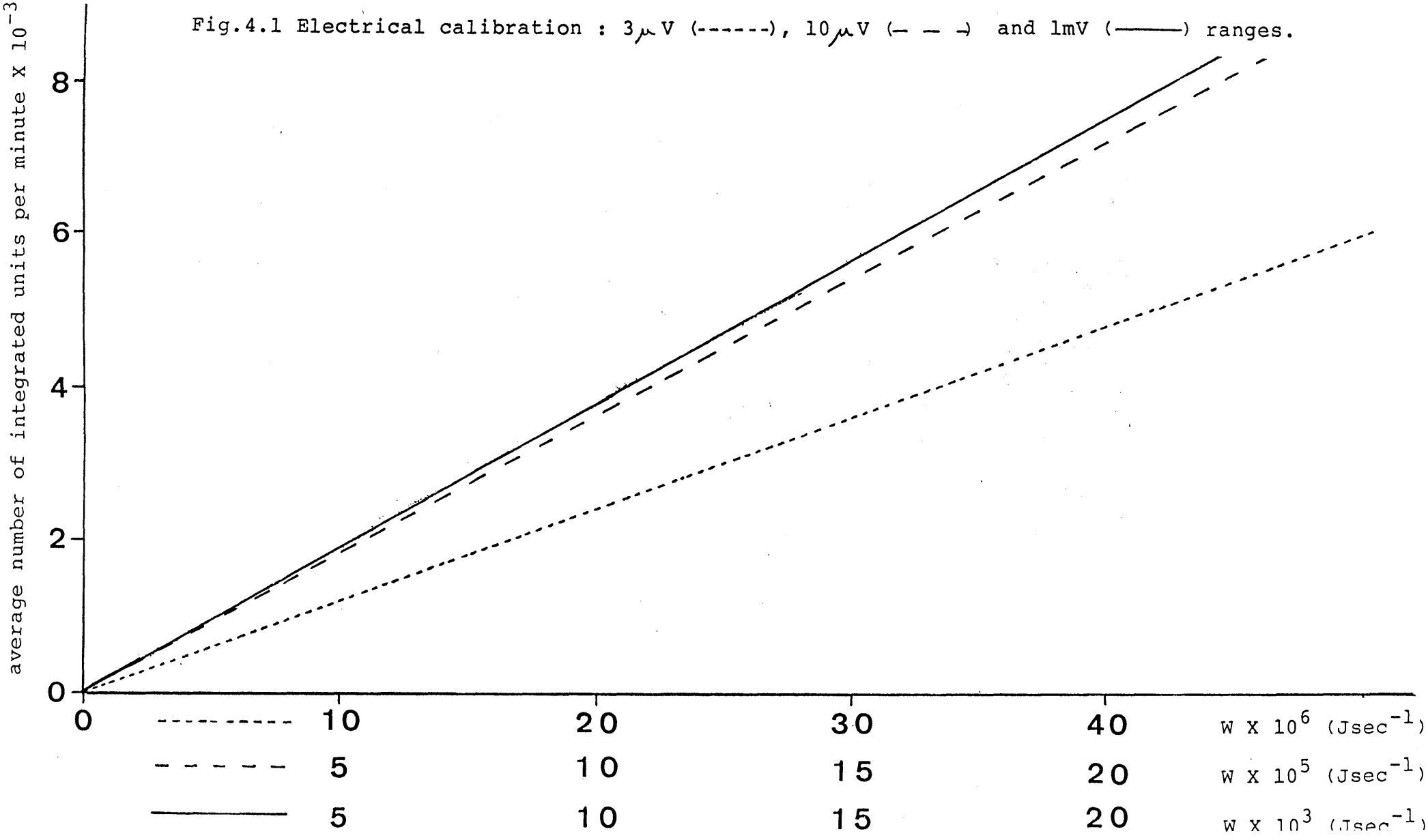
Fig.4.1 Electrical calibration : 3μV (------), 10μV (— — —) and 1mV (———) ranges.
average number of integrated units per minute X 10^{-3}
0
2
4
6
8
0
10
20
30
40
W X 10^6 ($Jsec^{-1}$)
5
10
15
20
W X 10^5 ($Jsec^{-1}$)
5
10
15
20
W X 10^3 ($Jsec^{-1}$)

data collection and analysis has been introduced).

The results obtained are presented in Fig.4.1 and values for ε are tabulated in Table4.1. (The straight-line calibration plots depicted in Fig.4.1 for each amplifier range is an average of the results obtained, with and without H_2O flowing at that particular amplifier range. In all cases however, the plots obtained with solution flowing and without were coincident).

4.2.2 Chemical Method of Calibration

Chemical calibration can be carried out using one or more of several standard reactions - the heat of dilution of sucrose (Gucker et al,1938) and the enthalpy of protonation of Tris and the enthalpy of ionization of water (Grenthe et al,1970). It was the latter two experiments which were used for the purpose of calculating the calibration constant.

Heat of neutralization of Tris

This experiment was carried out on the 3 μV,10 μV and 1mV amplifier ranges using 0.4mM Tris reacting with 0-0.6mM HCl, 1mM Tris reacting with 0-2.5mM HCl and 50mM Tris reacting with 0-100mM HCl, respectively.

All Tris solutions were stored under nitrogen since preliminary calibration experiments showed steadily decreasing deflection heights during the supposedly steady state of the experiment. This was indicative of CO_2 dissolving in the solution and reacting with the Tris.

The Tris solution and the particular HCl solution of interest were allowed to equilibrate to approximately 25°C before being pumped into the calorimeter through separate inlets at a rate of 0.1mlmin^{-1}. When these solutions met and mixed within the mixing vessel, a curve similar to that of Fig.2.2 was observed and the average number of integrated units "generated" by the heat produced noted at the steady state phase. This procedure was repeated several times with a different HCl concentration on each occasion.

Since the pump rates and the concentrations of the reacting solutions were known accurately, it was possible to calculate the number of moles of Tris being neutralized per minute. By equating this with the known ΔH for the reaction - taken to be -47.4kJmol^{-1} (Grenthe et al, 1970) - the expected heat produced per minute upon neutralization could be calculated. Furthermore, by plotting the average number of integrated units per minute against the corresponding calculated heat produced (Jmin^{-1}), a value for the calibration constant in J per integrated unit was determined (see Figs.4.2,4.3,4.4 and and Table4.1).The results obtained at all amplifier ranges were comparable and consistent with those established using the electrical calibration method (section 4.2.1).

Heat of Ionization of Water

This experiment was carried out on the 100μV amplifier range and involved the reaction of 10mM sodiun hydroxide with various concentrations of hydrochloric acid (0-25mM) by the previously described technique.

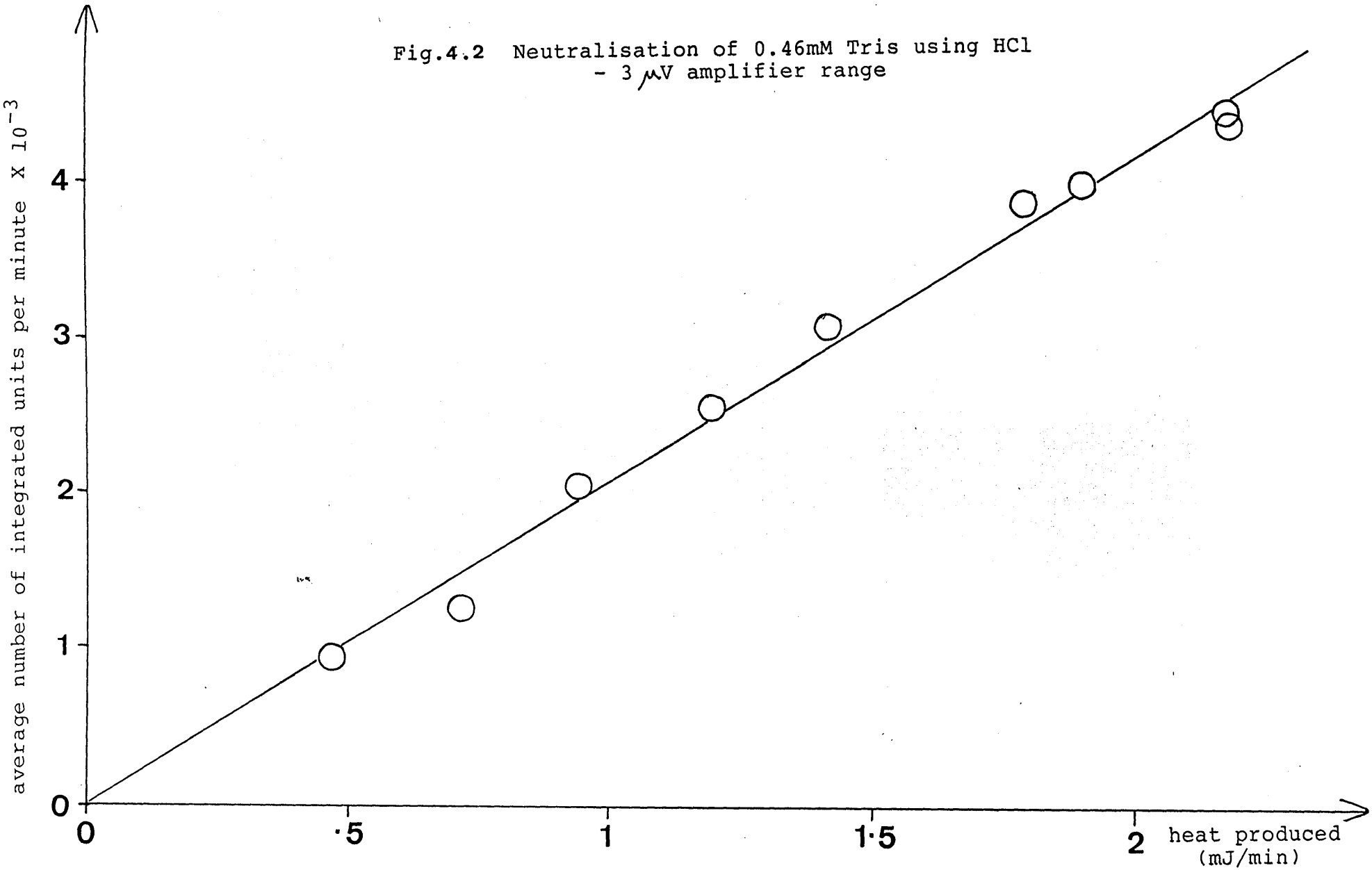
Fig.4.2 Neutralisation of 0.46mM Tris using HCl
- 3 μV amplifier range
average number of integrated units per minute X 10^{-3}
0
1
2
3
4
0
·5
1
1·5
2
heat produced
(mJ/min)

Fig.4.3 Neutralisation of 1mM Tris using HCl
- 10 μV amplifier range

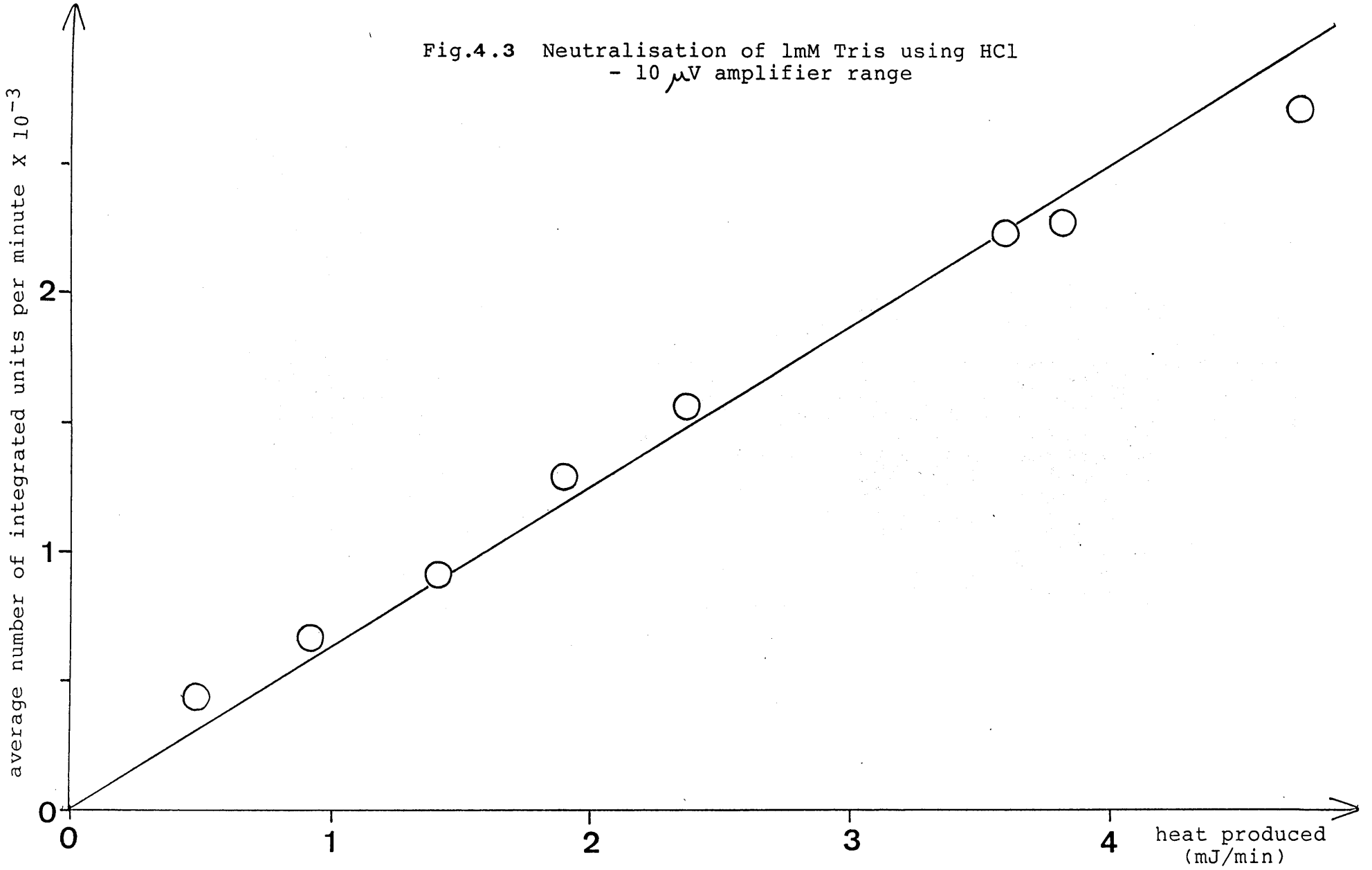

Fig.4.4 Neutralisation of 50mM Tris using HCl
- 1 mV amplifier range

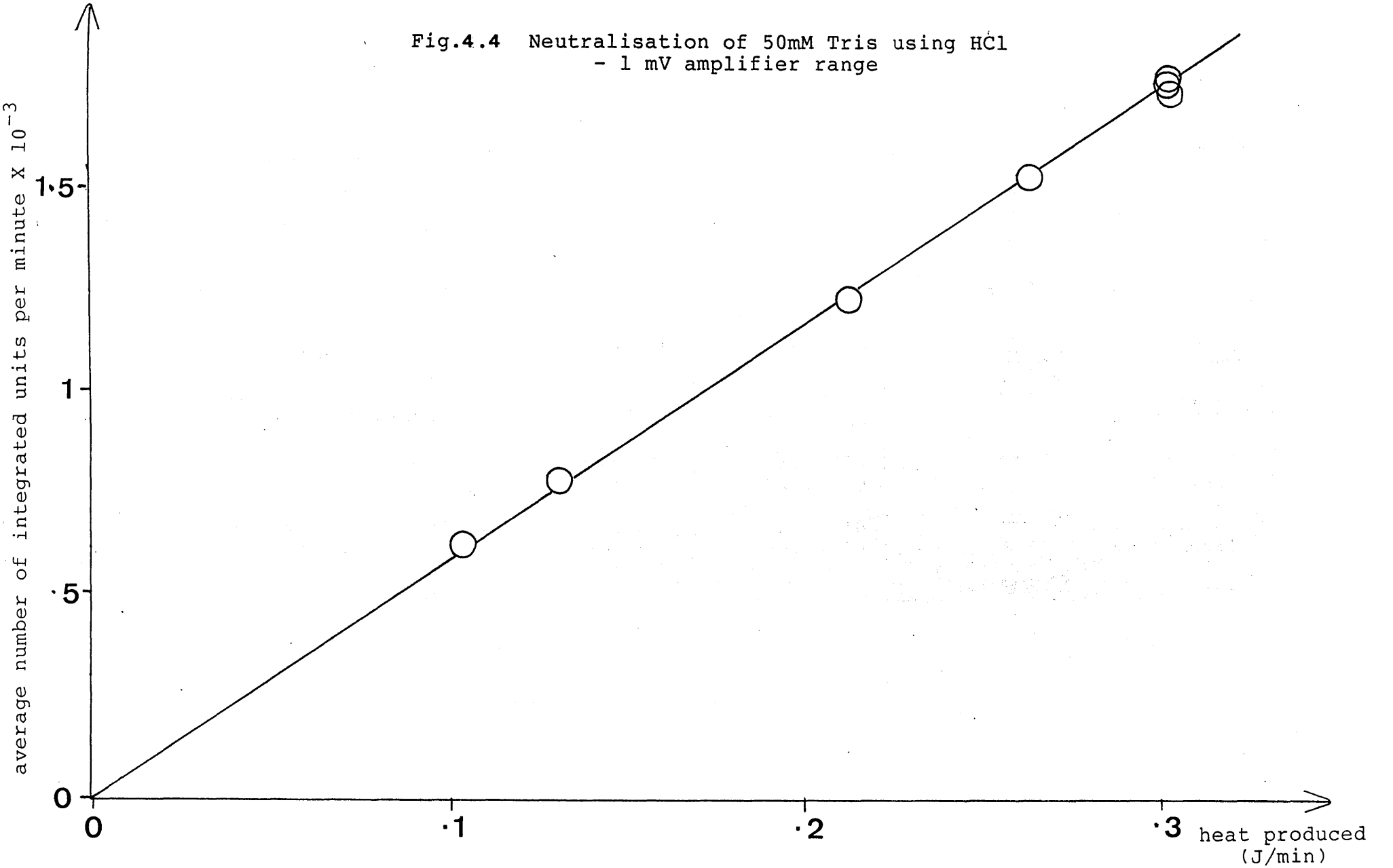

Table 4.1 Values of ε (J/integrated unit) as determined by the various methods of calibration.

	AMPLIFIER RANGE			
METHOD	3 μV	10 μV	100 μV	1mV
electrical (no water flowing)	4.88×10^{-7} *4.88×10^{-7}	1.62×10^{-6} *4.86×10^{-7}	---	1.62×10^{-4} *4.86×10^{-7}
electrical (water flowing)	4.99×10^{-7} *4.99×10^{-7}	1.66×10^{-6} *4.98×10^{-7}	---	1.58×10^{-4} *4.74×10^{-7}
heat of neutralisation of Tris	4.82×10^{-7} *4.82×10^{-7}	1.69×10^{-6} *5.07×10^{-7}	---	1.55×10^{-4} *4.65×10^{-7}
heat of ionization of water	---	---	1.57×10^{-5} *4.71×10^{-7}	---

*corresponding ε value on the 3 μV range

Using a ΔH value of $-55.84 kJmol^{-1}$ for the reaction, a calibration constant of $1.57X10^{-5}J$ per integrated unit was calculated (Fig.4.5).

NaOH solutions were all stored under nitrogen gas to prevent CO_2 dissolving in solution.

All calibration experiments - electrical and chemical - gave sufficiently consistent results for the calibration constant of the calorimeter that it can be certain that the value used in subsequent experiments is fairly accurate. A value of $\varepsilon = 1.61X10^{-6}J$/integrated unit (10$\mu$V) range and $\varepsilon = 4.95X10^{-7}J$/integrated unit (3$\mu$V range) was used in all the following experiments - averages of all the experiments carried out.

4.3 Preliminary Experiments with Lysozyme

The binding of inhibitors to lysozyme has been studied in depth over the past few years (Bjurulf et al,1970;Bjurulf and Wadso,1972; Cooper,1974) and so this system was used to test the performance of the calorimeter and its suitability for enzyme-ligand studies.

4.3.1 Introduction

Lysozyme (E.C.3.2.1.17) hydrolyses polysaccharides in certain bacterial cell walls and various inhibitors which resemble the natural substrate have been found, notably N-acetyl-D-glucosamine ("NAG"), di-N-acetyl-D-glucosamine ("NAG_2") and tri-N-acetyl-D-glucosamine ("NAG_3"). The structures of the complexes between the inhibitors NAG and NAG_3 have been

Fig.4.5 Ionisation of water - reaction of 10.57mM NaOH with HCl
-100 μV amplifier range

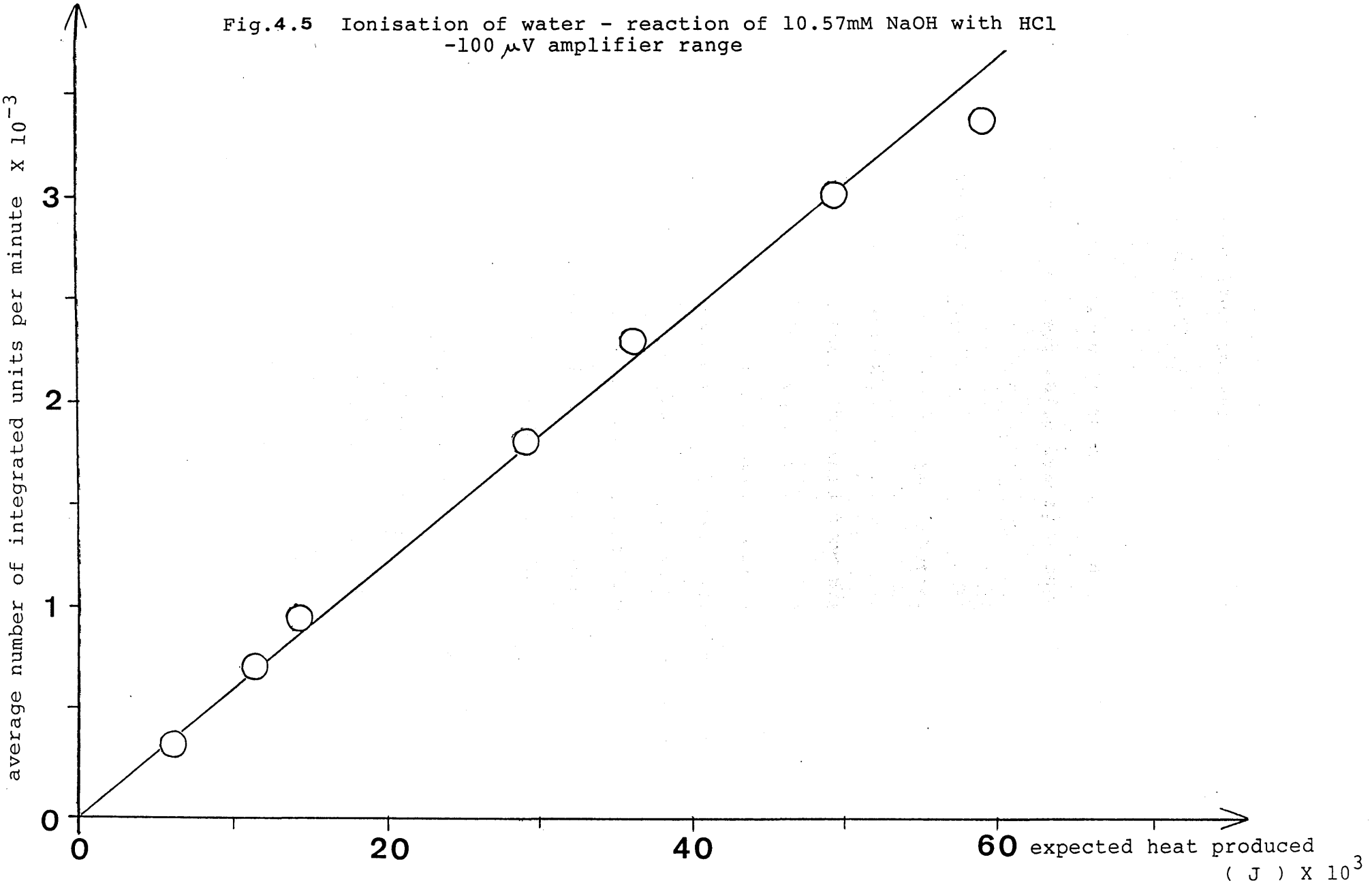

determined (Blake et al,1967) and a mechanism for the catalytic action of this enzyme has been proposed on the basis of these structural studies.

Subsequent work described in this section is concerned with the association of hen egg-white lysozyme and NAG.

4.3.2 Experimental

All enzyme solutions and substrate solutions were made up using 0.1M acetate buffer,pH5.0.

The NAG solutions (α form, obtained from Sigma Chemical Co. Ltd.) were made up a few hours prior to the start of the experiment - to allow the mutarotation equilibrium of the two forms of NAG to be established. The half time of conversion from α to β at 25°C and neutral pH is about 30minutes (Kowalski and Schimmel,1969) and the equilibrium mixture was found to contain 60% α and 40% β -NAG. The concentration of NAG, after mixing, varied from 0mM to 125mM.

Lysozyme solutions were generally made up on the day of the experiment using freeze-dried protein from Sigma.The concentr -ation (molarity) was obtained for both NAG and lysozyme solutions by weighing the solutes and measuring the volume of solvent used.Lysozyme concentration was also calculated using A_{280nm}=25.5 for a 1% solution and a 1cm path length, and a molecular weight of 14,600 (Bjurulf et al,1970).Comparison of the spectroscopically determined lysozyme concentration with that calculated by weight led to a finding of 5% salt in the protein samples.In some cases therefore,the lysozyme solution

was dialysed overnight against buffer before use. No differences however, were found between the results for experiments using the two types of preparation.

Calorimetric measurements were made on the 10 μV amplifier range and were performed with a fixed lysozyme concentration of 5mgml^{-1}-before dilution-and variable NAG concentrations. Separate experiments were carried out to find the heats of dilution for both the lysozyme and the NAG solutions - using the same range of concentrations as used in the binding experiments.

4.3.3 Results

The results are presented in the form of a binding curve of heat evolved, Q(kJmole^{-1}), corrected for heats of dilution of protein and inhibitor versus final inhibitor concentration, I (mM), in Fig.4.6.

As described in section2.1.3, the formation of a 1:1 enzyme-inhibitor complex is assumed and a value for $-\Delta H=23.5 \pm 1.9$ kJmol^{-1} and $K_{dis}=26.1 \pm 3.9$mM were calculated using the double reciprocal plot (Fig.4.7). These results are fairly consistent with those results obtained,using the same method, by Bjurulf and Wadso (1972); $-\Delta H=24.3 \pm 1.0$kJmol^{-1} and K_{dis} =26.5mM.As a double check,using the iterative least-squares method to analyse the results, the values obtained for $-\Delta H$ and K_{dis} were found to be 23.1 ± 1.6kJmol^{-1} and 24.6 ± 5.0mM, respectively, which are again close in value to those published.

Fig.4.6 Hyperbolic binding curve of lysozyme + NAG reaction

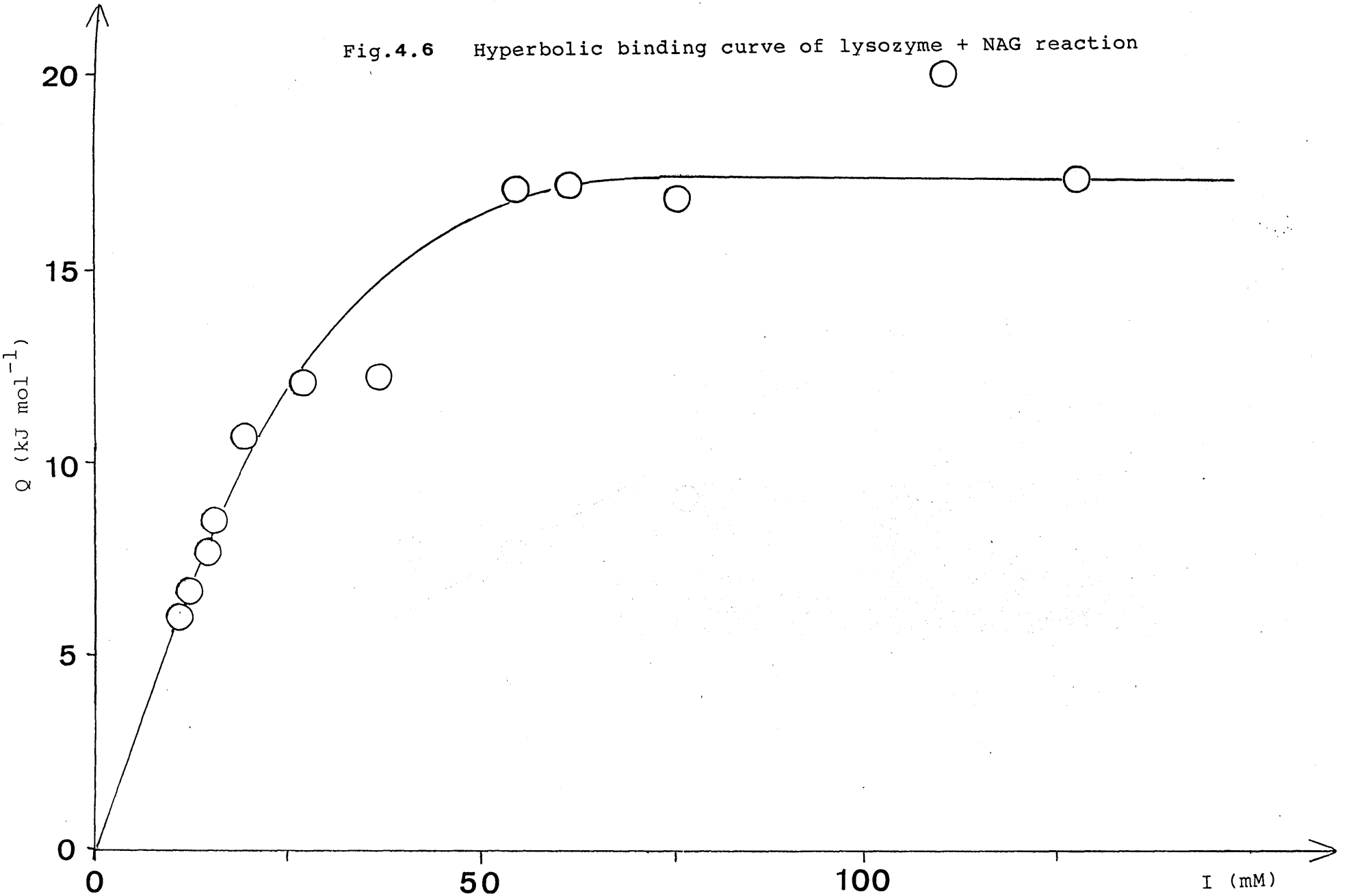

Fig.4.7 Double reciprocal plot of fig.4.6

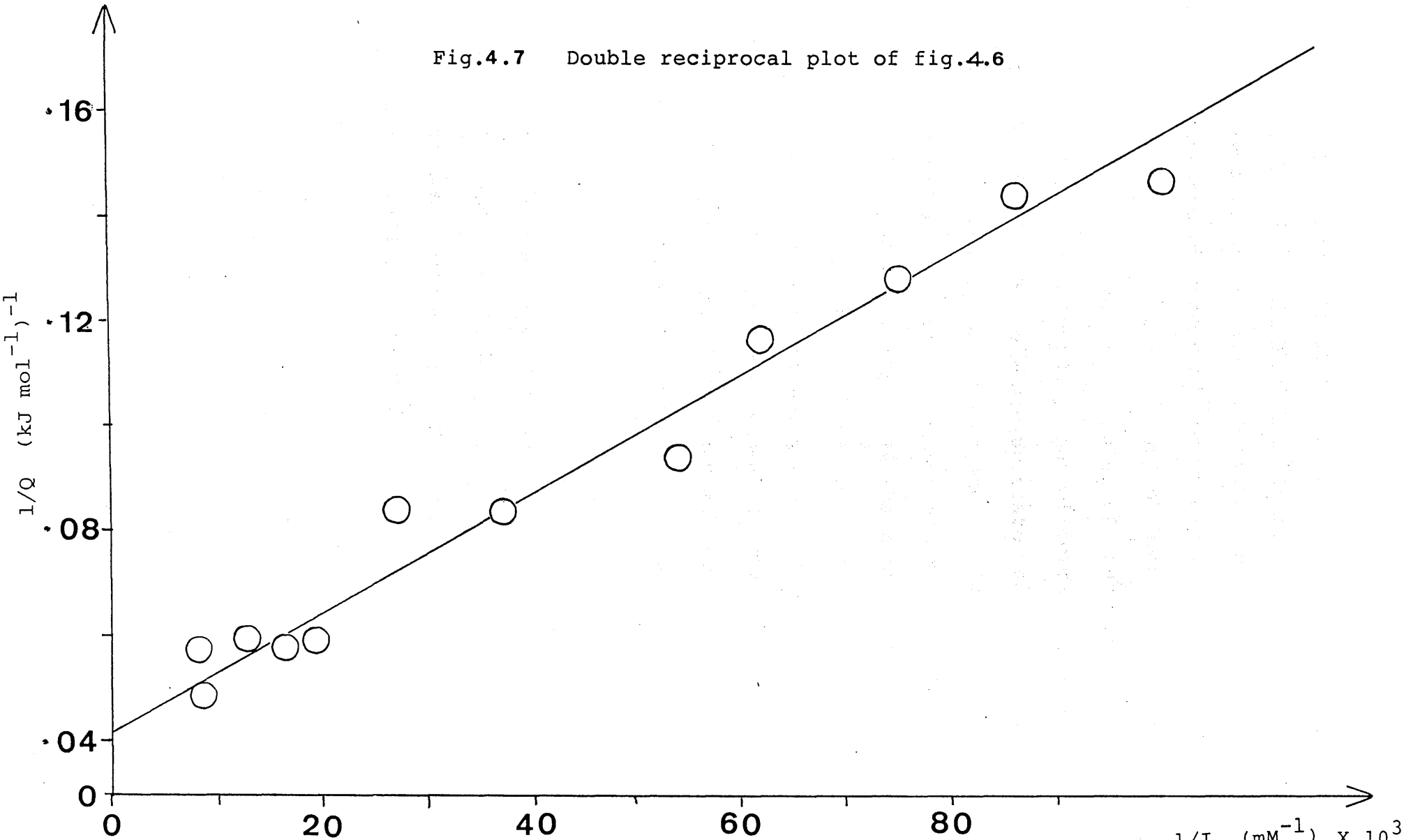

4.4 Calorimetric Experiments with PGK

4.4.1 Calorimetric Experiments Involving Substrates

When an enzyme binds to its substrate the total heat of reaction consists of the heat of catalysis (which involves all breaking and formation of covalent bonds) and a quantity which includes the heat of transfer of substrate from bulk solvent to the protein surface, heat of formation of non-covalent bonds in the enzyme-substrate complex, heat of conformational changes on binding etc. - called the heat of binding. In order to elucidate the nature of the forces between enzyme and substrate it is the heat of binding which must be measured. However, since the heat of catalysis is generally an order of magnitude greater, the heat of binding is obscured. It is for this reason that most attention in thermal experiments has been focused on the binding of competitive inhibitors since they are not broken down to form products.

In this section the heat effects which occur when the substrates ATP, ADP and 3PG bind to PGK (the mutant and wild-type forms) are analysed.The reason for doing so is two-fold. Firstly, this will provide basic details of the thermodynamic interactions when the enzyme-substrate complex forms, from which to expand upon in the future. In this instance there will be no contribution from the heat of catalysis since only one substrate will be bound to PGK at any one time. Secondly, by comparison of the results obtained for both forms of enzyme, it will determine the effect of this particular mutation on the thermodynamic properties of PGK, thus

providing further information relating to the mechanism of PGK catalysis.

4.4.2 Preparation of Enzyme Solutions

Preparation of the solutions of both forms of enzyme was carried out using the same procedure.

The PGK samples (both wild-type and mutant) had been stored as an ammonium sulphate precipitate in 10mM Tris/MOPS, pH7.0 buffer containing 0.1mM DTT. Prior to use, the ammonium sulphate precipitate was centrifuged and dissolved in a small volume (about 10ml) of buffer containing 10mM Tris/MOPS,pH7.0 and 0.1mM DTT. This solution was placed in dialysis tubing which had been pre-boiled to remove impurities and then dialysed exhaustively against 500ml of the same buffer for about 36hours.Several changes of buffer were made during this period.The buffer used for the final change consisted of 50mM Tris/MOPS, pH7.0 + 4mM $MgCl_2$ + 0.1mM DTT and dialysis was continued with this overnight. All dialyses were performed with stirring at $4^{o}C$. Upon completion of dialysis the protein solution was centrifuged to remove any precipitous material which was present and then diluted,using the dialysis buffer, to a suitable PGK concentration for use in the calorimetric experiment. PGK concentration was determined using the value $A_{280nm}=0.495$ for a $1mgml^{-1}$ PGK solution - an average of published values (Bucher,1947 and 1955; Spragg et al,1976; Scopes,1978b).A molecular weight of 44,500 was assumed for the PGK monomer molecule (Merret,1981).

When not in use the enzyme solution was stored at $4^{o}C$.

4.4.3 Preparation of Substrate Solutions

All substrate solutions were made up using the buffer which remained outside of the dialysis tubing.

adenosine-5'-triphosphate

Stock solutions of ATP ranging from 0mM to 2mM were prepared. The appropriate amount of ATP (disodium salt) was weighed out and then dissolved in buffer to produce a 2mM solution. This was then diluted to produce a series of solutions of different ATP concentrations.No pH adjustment was necessary.

adenosine-5'-diphosphate

ADP (Di-monocyclohexylammonium salt) stock solutions (0mM to 2mM) were made up in the same way as for ATP. Similarly, adjustment of the pH of the substrate solutions was not necessary.

3-phosphoglyceric acid

The insoluble barium salt of 3PG was converted to the free acid using Amberlite IR120 ion-exchange resin and the pH corrected to 7.0 with concentrated buffer and NaOH. Stock 3PG was diluted to provide a series of substrate concentrations (0mM to 2mM).

ATP, ADP and 3PG were all purchased from Sigma Chemical Company Ltd.

4.4.4 Results

All experiments were performed at 25^{o}C, following the

procedure described in section 2.1.2. PGK was pumped through one inlet and the substrate solution pumped through the other.

For each series of experiments, the inhibitor concentration was varied whereas the enzyme concentration was kept constant.

Baseline measurements,pumping buffer through the inlets, were carried out regularly throughout the experiment.
The heat of reaction of substrate, at a particular concentration,with wild-type and mutant PGK was calculated as described previously (section 2.1.3) taking into account baseline shifts and heats of dilution (negligible for ATP and ADP solutions but of a significant value for the 3PG solutions). Figs.4.8 to 4.19 depict the experimental heats of binding obtained as a function of final inhibitor concentration.From these results values for K and ΔH^{o} for the binding processes can be calculated and subsequently ΔG^{o} and ΔS^{o} values. Tables4.2 and 4.3 list the thermodynamic binding parameters, as calculated by the iterative least-squares method described in section 2.1.3.

It would appear that replacement of His388 with Gln388 has had little effect on the binding sites of the substrates.This is what would have been expected since the mutation is at the hinge-bending region of the enzyme and not directly related to the substrate binding sites (Watson et al,1982). However, upon detecting a difference in the K_m value for ATP binding,

Fig.4.8 Hyperbolic binding curve of wild-type PGK + MgADP

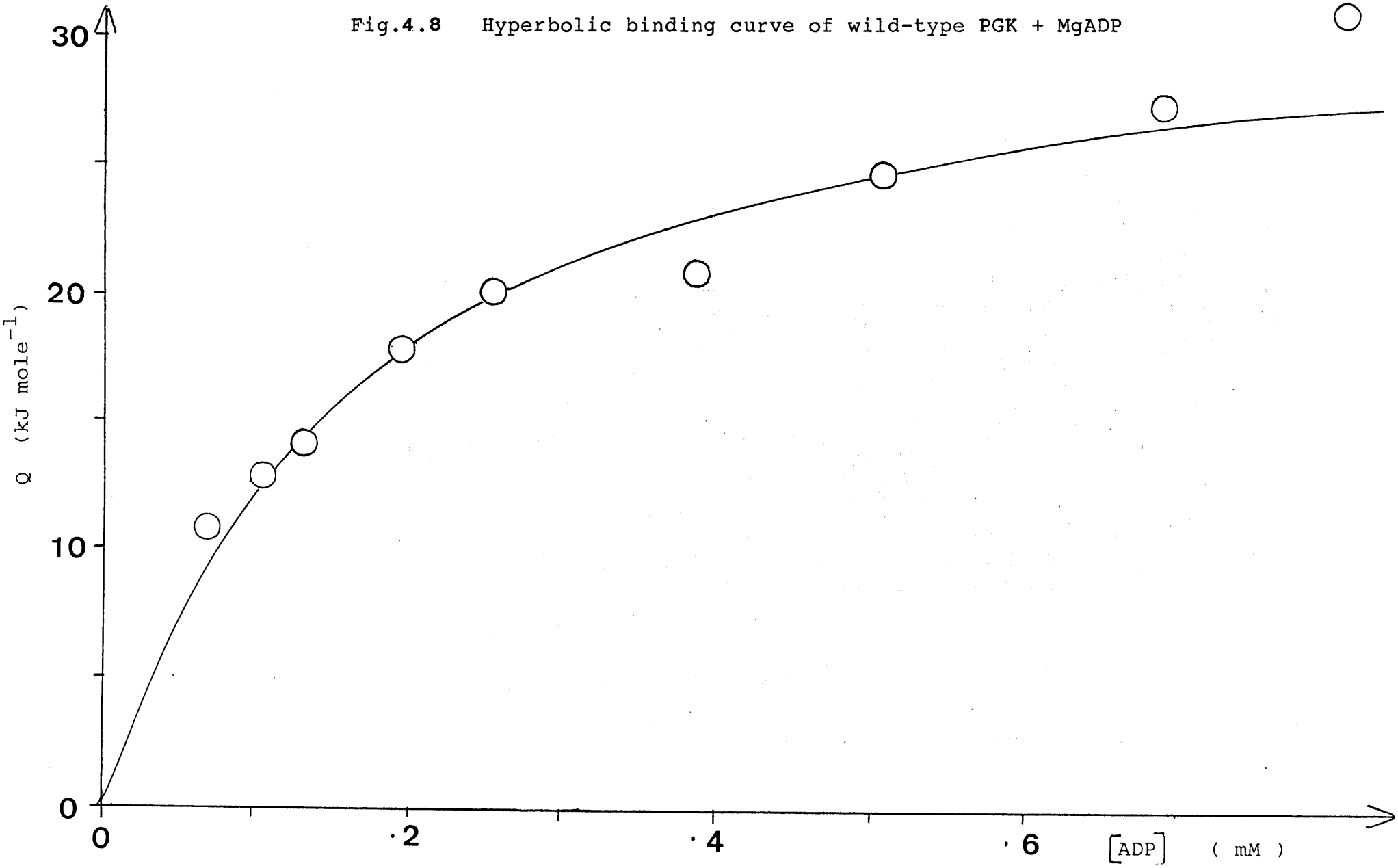

Fig.4.9 Double reciprocal plot of Fig.4.8

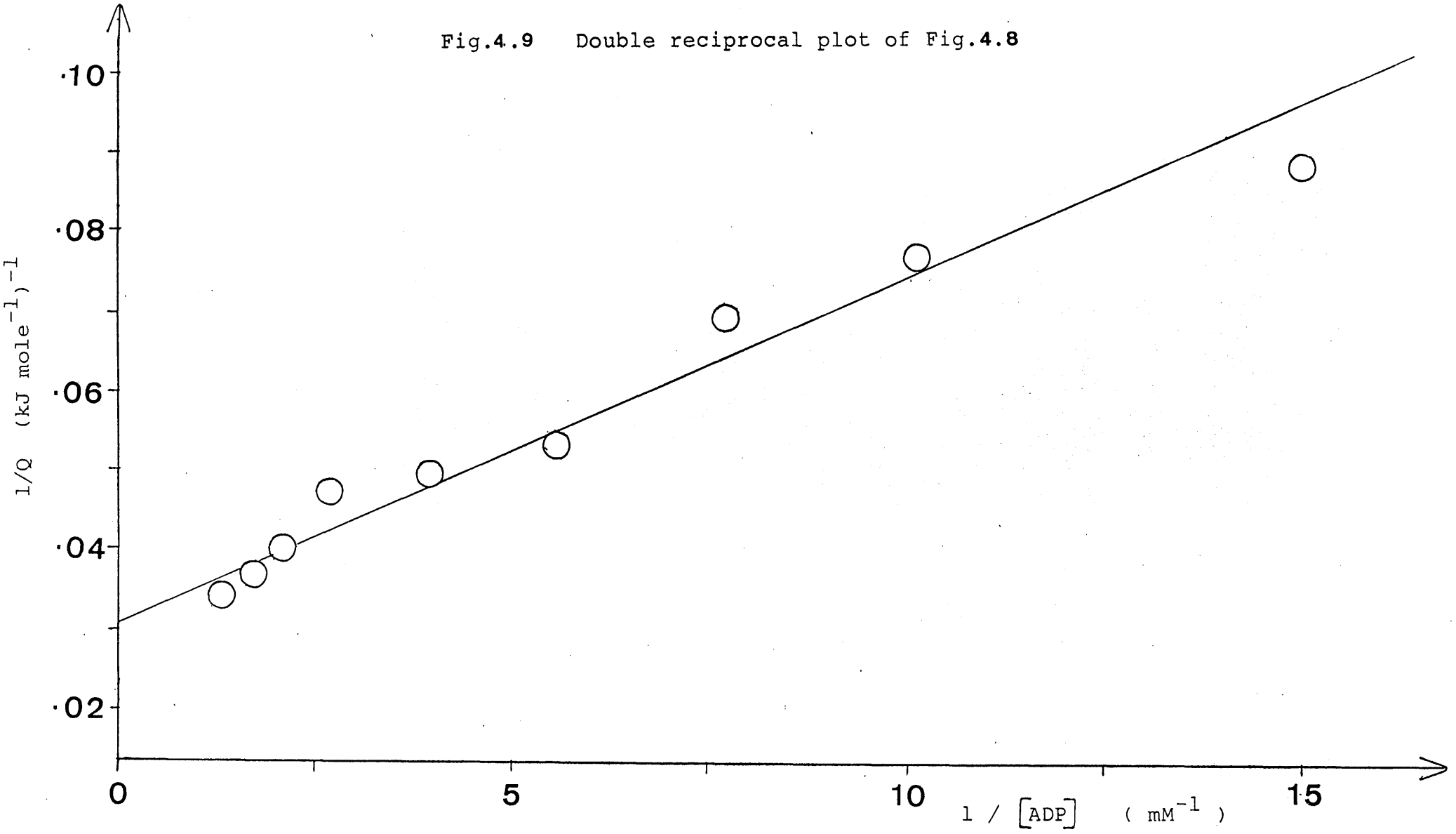

Fig.4.10 Hyperbolic binding curve of wild-type PGK + MgATP

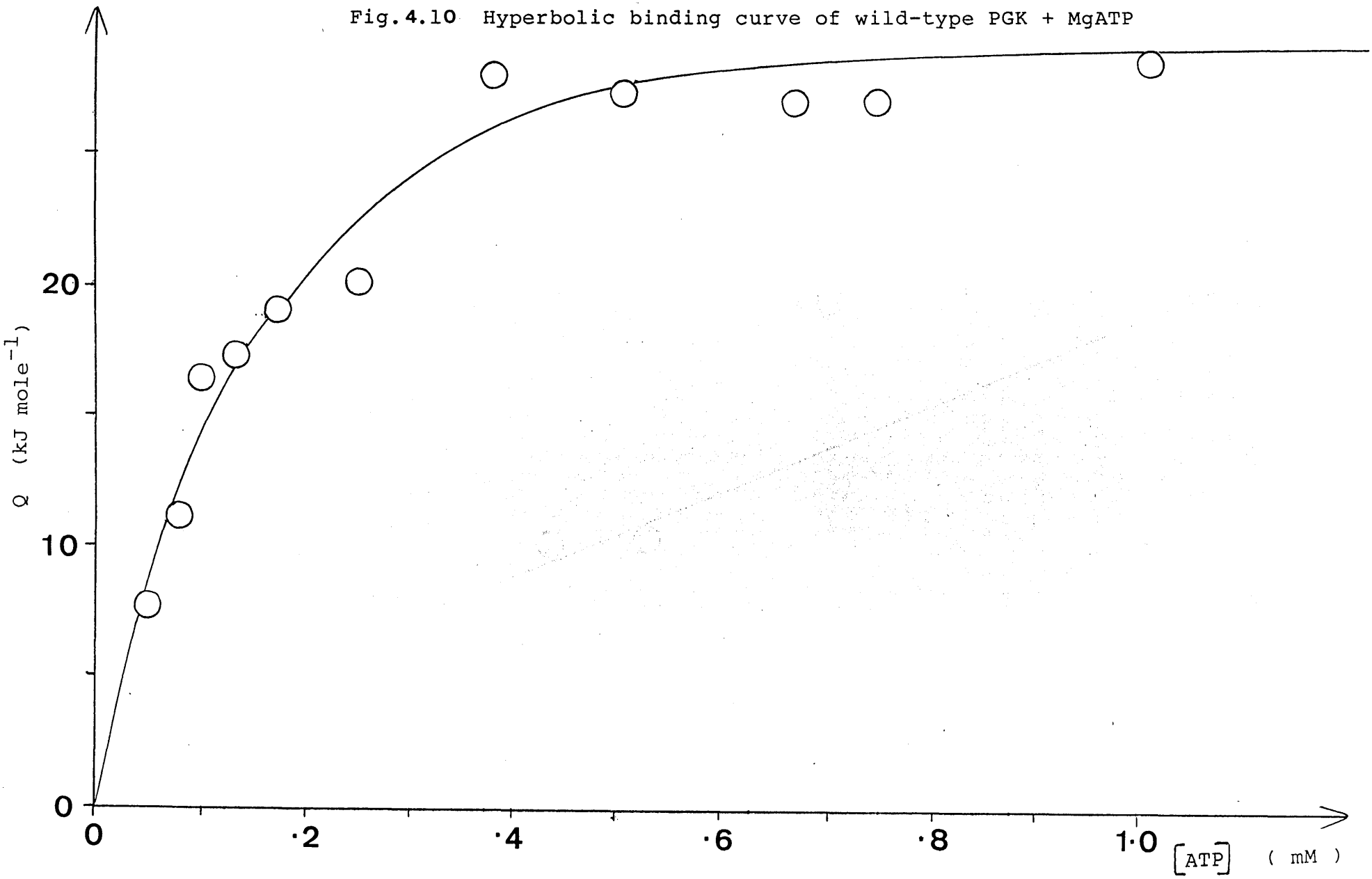

Fig.4.11 Double reciprocal plot of Fig.4.10

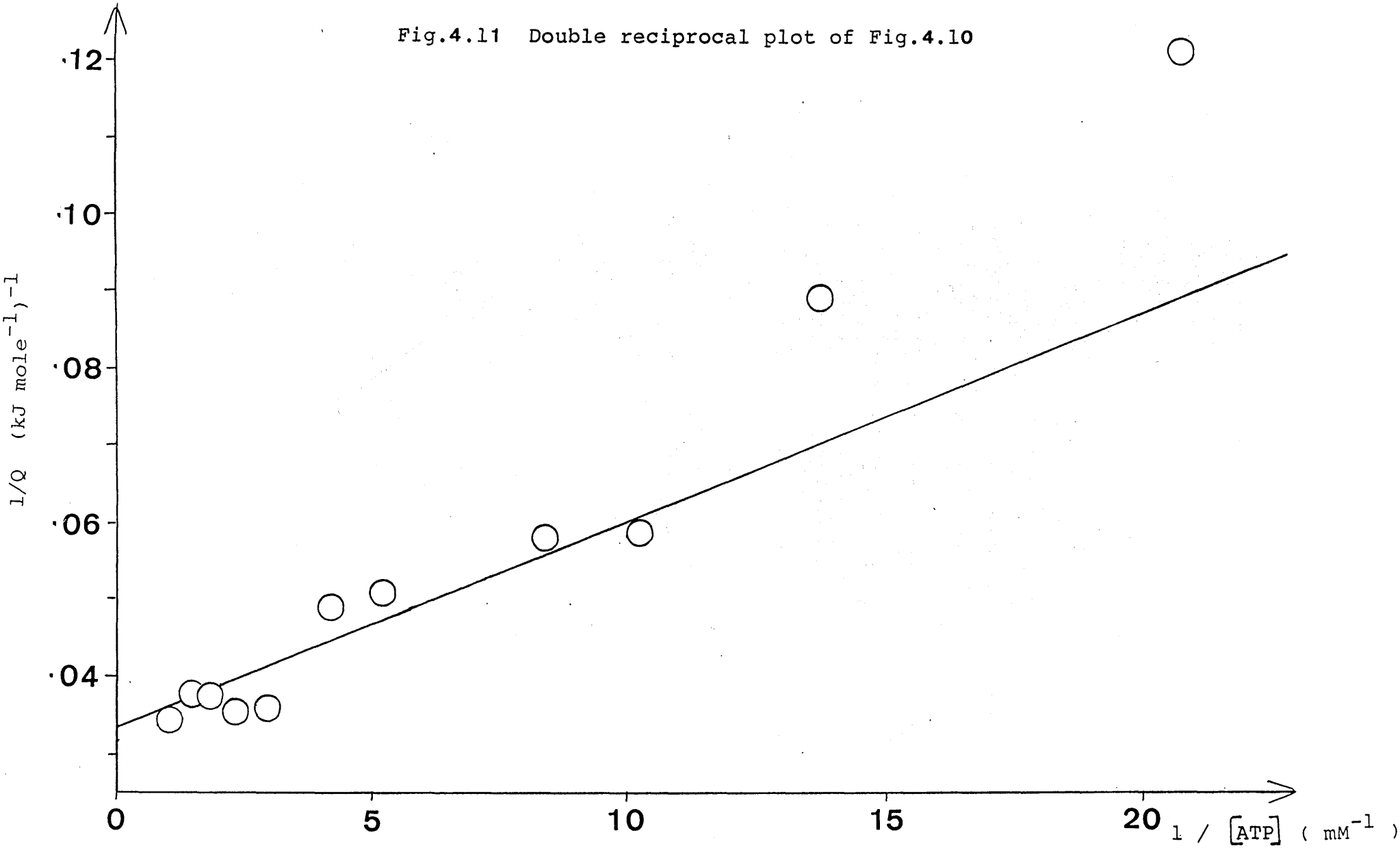

Fig.4.12 Hyperbolic binding curve of wild-type PGK + 3PG

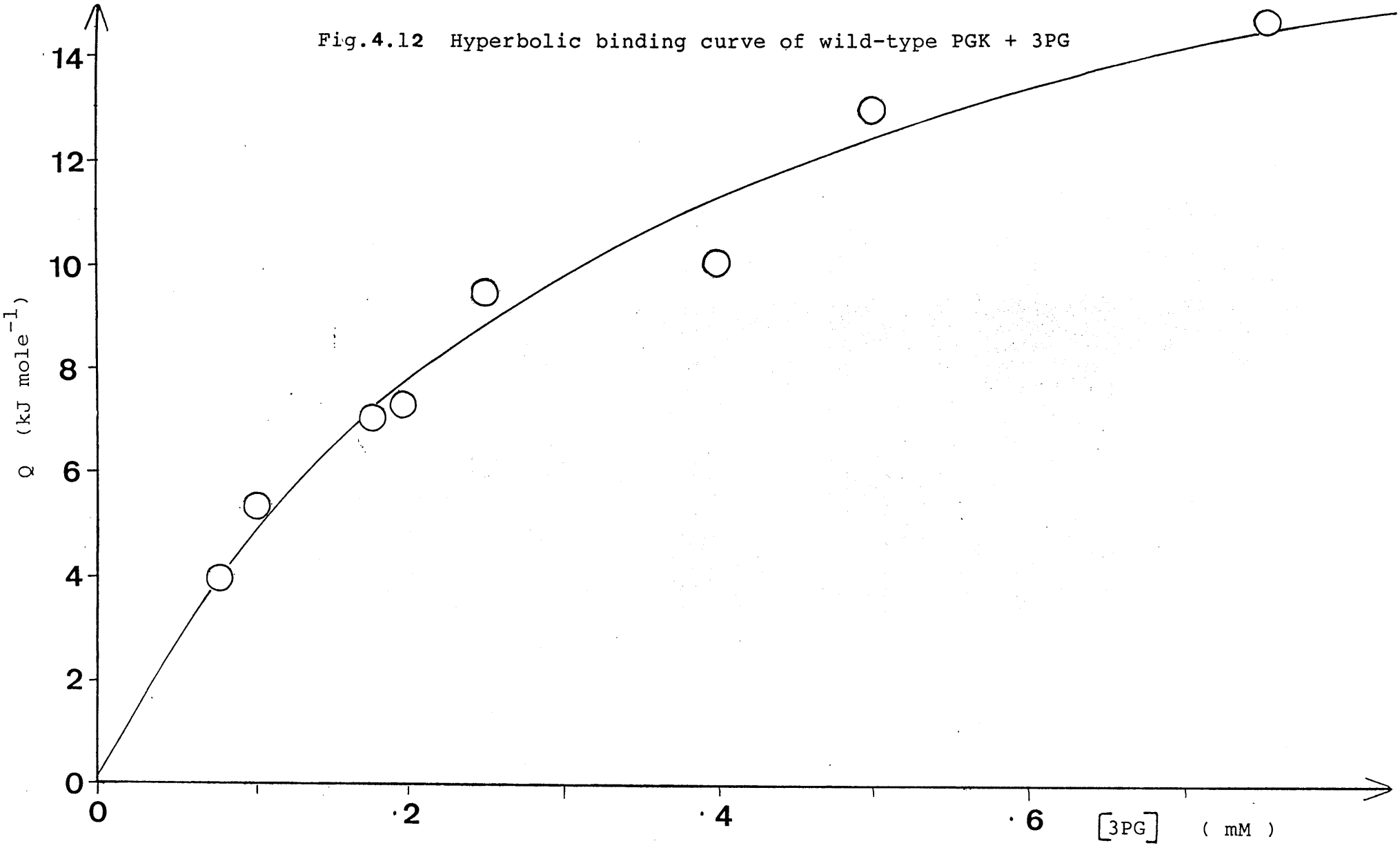

Fig.4.13 Double reciprocal plot of Fig.4.12

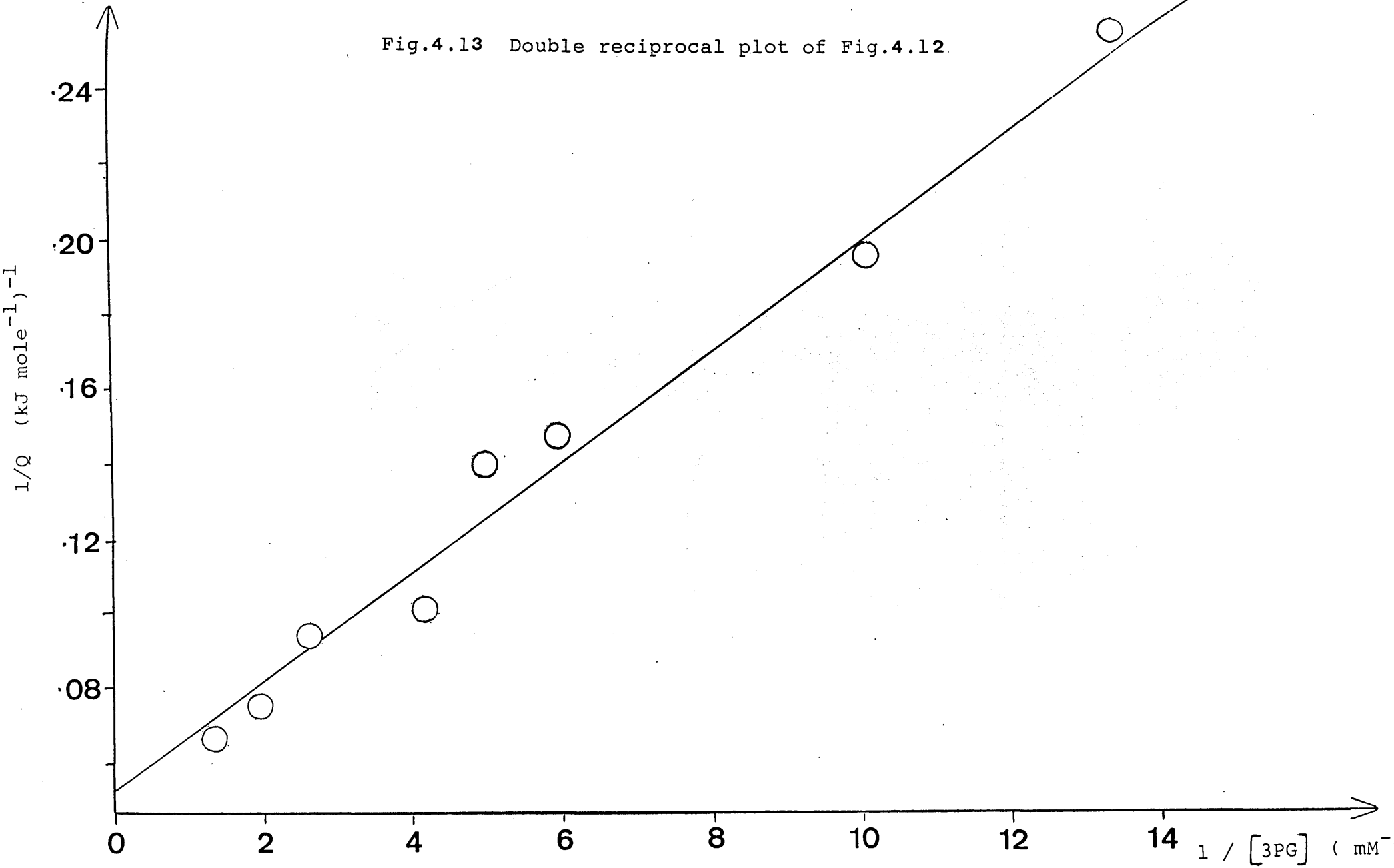

Fig.4.14 Hyperbolic binding curve of mutant PGK + MgADP

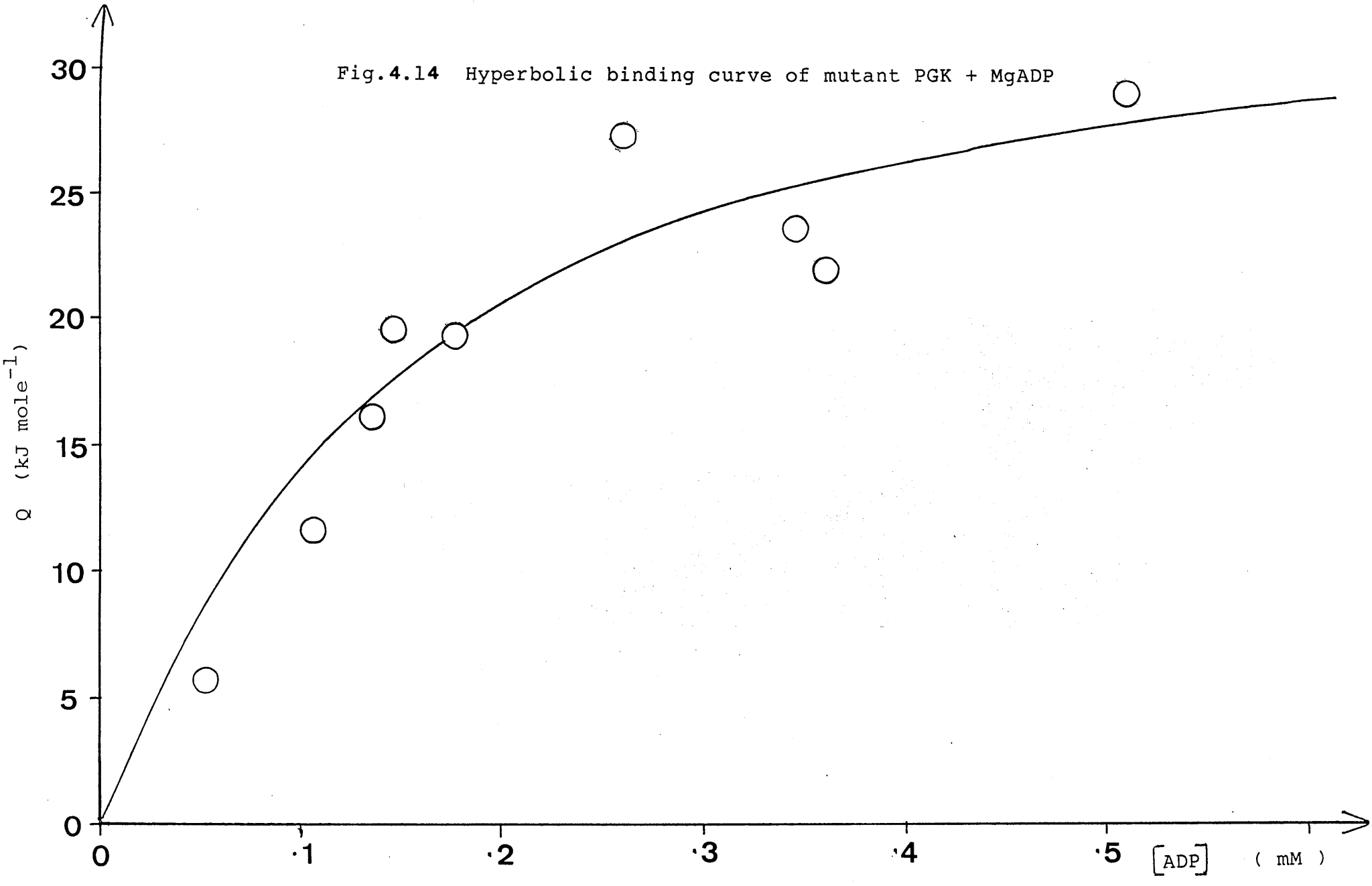

Fig.4.15 Double reciprocal plot of Fig.4.14

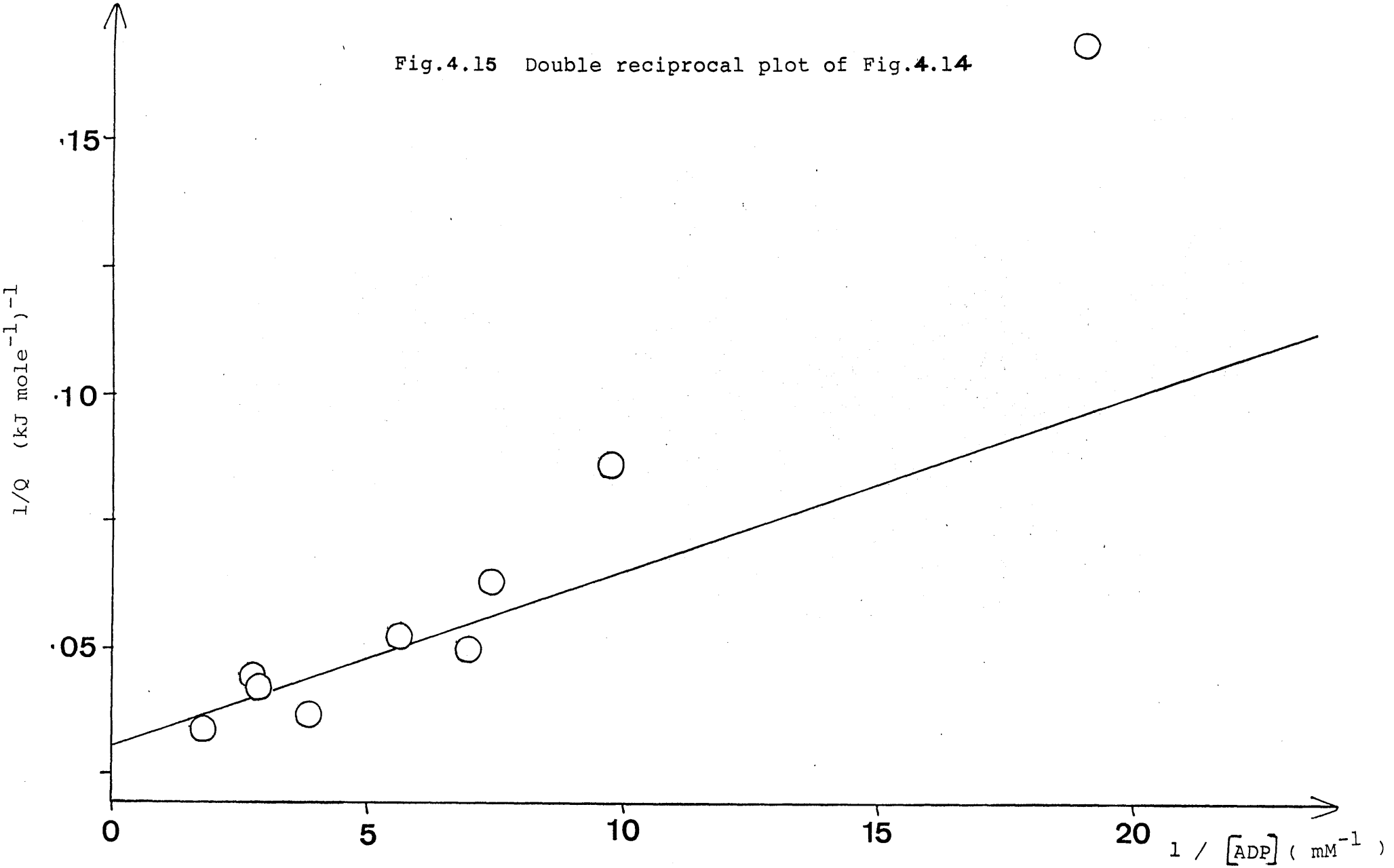

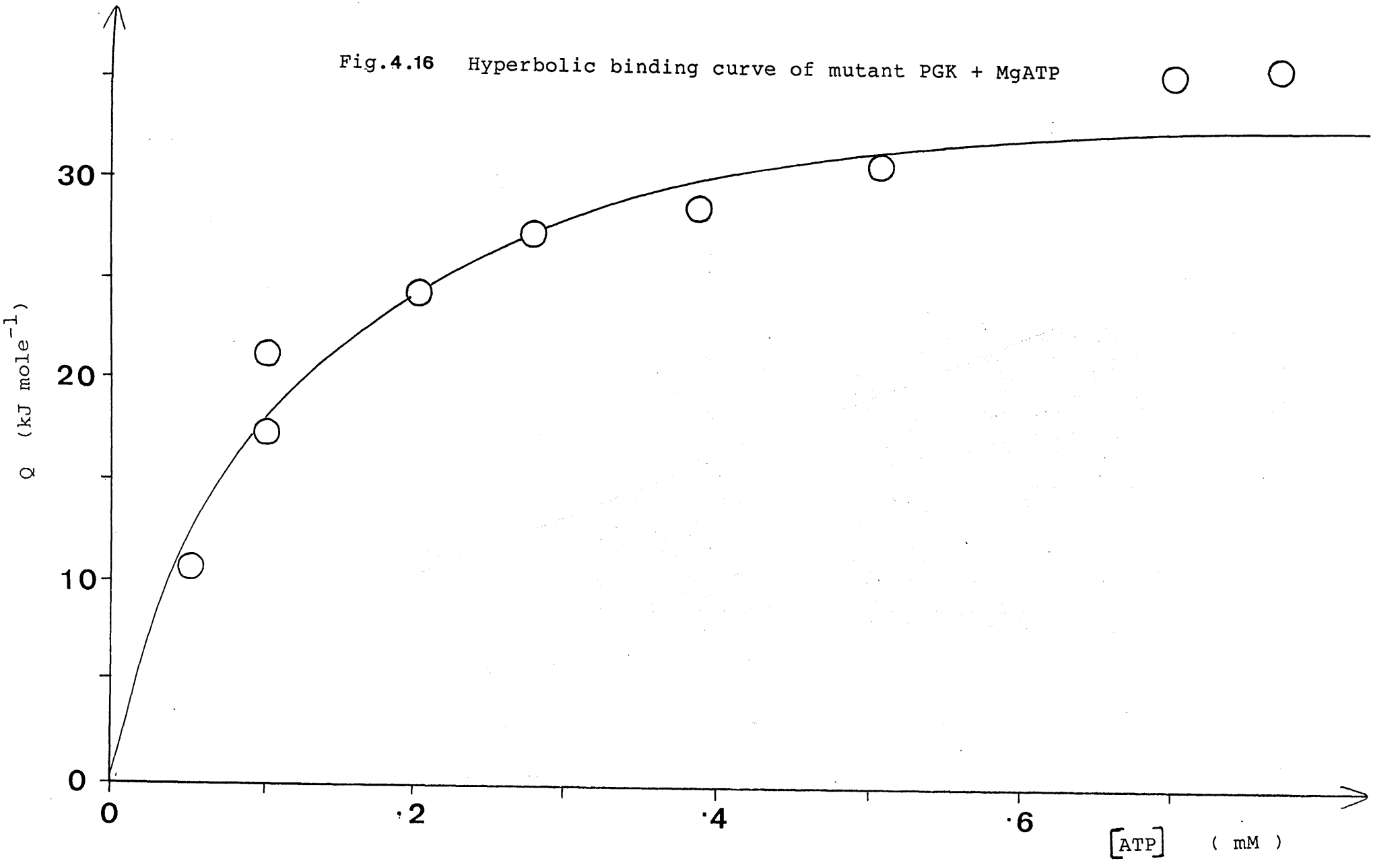
Fig.4.16 Hyperbolic binding curve of mutant PGK + MgATP
Q (kJ mole^{-1})
30
20
10
0
0
·2
·4
·6
[ATP] (mM)

Fig.4.17 Double reciprocal plot of Fig.4.16

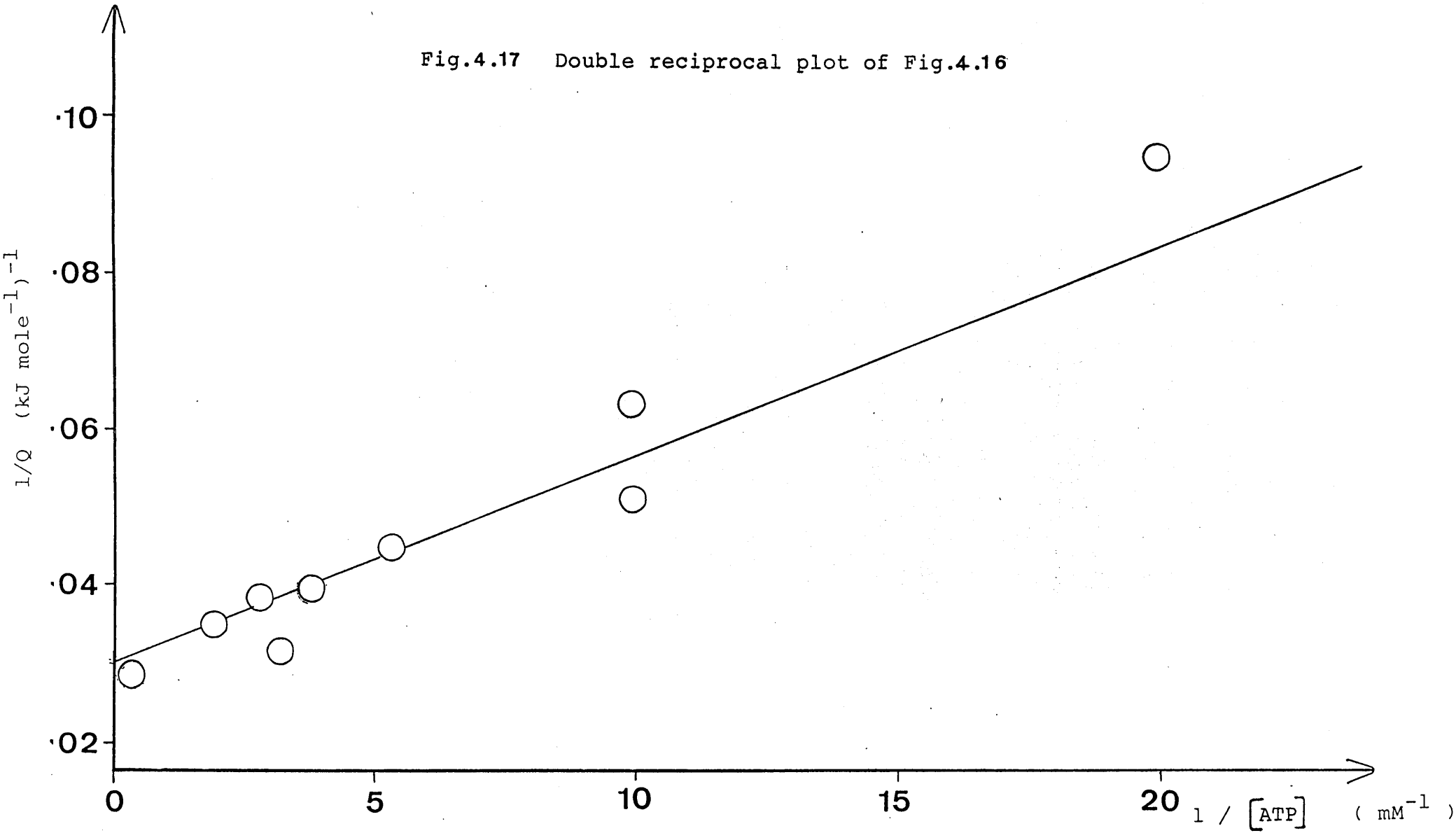

Fig.4.18 Hyperbolic binding curve of mutant PGK + 3PG

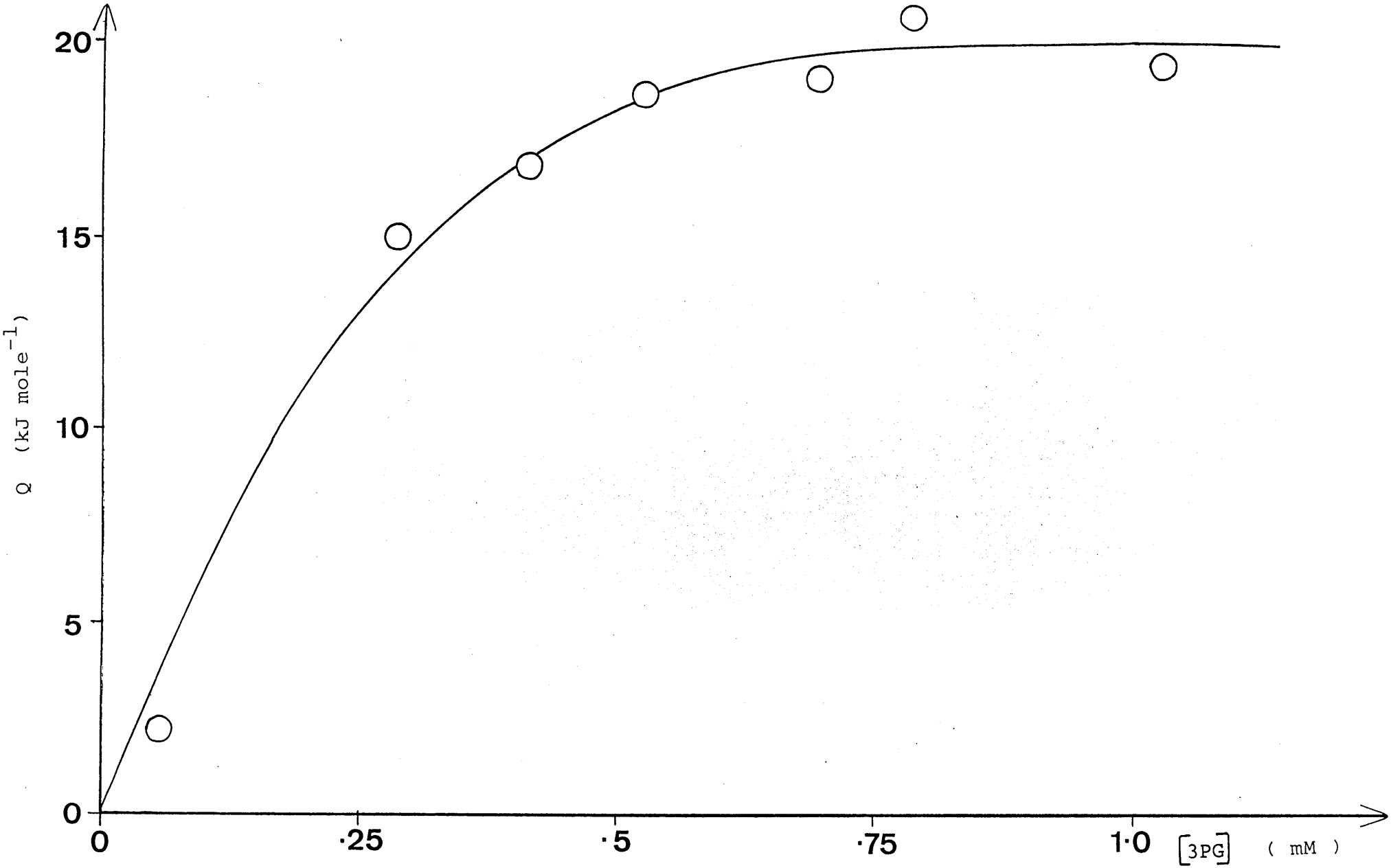

Fig. 4.19 Double reciprocal plot of Fig. 4.18

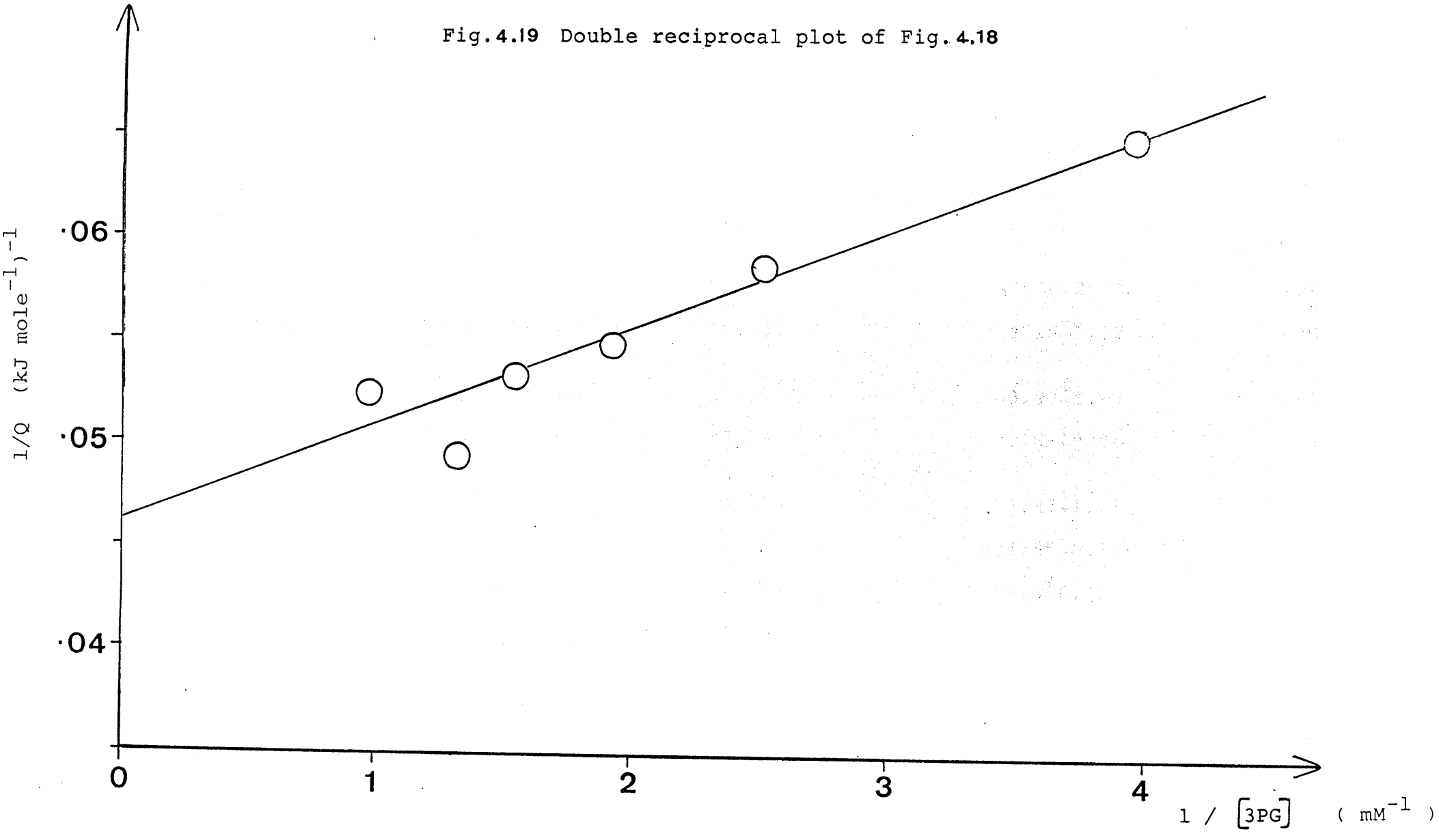

Table4.2 Thermodynamic Parameters for the Binding of MgADP, MgATP and 3PG to Wild-Type PGK at 25°C,pH7.0.

SUBSTRATE		K_{dis}(mM)	K_{ass}(M^{-1})	$-\Delta G^{o}$(kJmol^{-1})	$-\Delta H$(kJmol^{-1})	ΔS(JK^{-1}mol^{-1})
MgADP		0.169 ± 0.025	$(5.92\pm0.88)X10^{3}$	21.52 ± 0.31	33.70 ± 2.33	-29.66 ± 9.06
	*	0.010 ± 0.002	$(1.00\pm0.20)X10^{5}$	28.53 ± 0.50	39.16 ± 3.22	-35.64 ± 12.55
MgATP		0.047 ± 0.010	$(2.13\pm0.45)X10^{4}$	18.99 ± 0.52	30.93 ± 1.93	-40.07 ± 8.22
	*	0.009 ± 0.001	$(1.11\pm0.12)X10^{5}$	28.83 ± 0.29	31.63 ± 0.04	-9.54 ± 1.05
3PG		0.264 ± 0.018	$(3.79\pm0.26)X10^{3}$	20.47 ± 0.17	18.87 ± 1.21	5.20 ± 4.63
	*	0.110 ± 0.020	$(9.09\pm1.65)X10^{3}$	28.28 ± 0.46	-15.65 ± 0.33	147.27 ± 2.51
	**[1]	0.057 ± 0.005	$(1.75\pm0.15)X10^{4}$	24.21 ± 0.21	16.0 ± 0.28	27.55 ± 1.64
	**[2]	0.068 ± 0.001	$(1.47\pm0.22)X10^{4}$	23.77 ± 0.37	20.5 ± 0.06	10.97 ± 1.44

* values of Hu and Sturtevant (1987) in PIPES buffer
** values of Dr.C.M. Johnson (personal communication) in [1]Tris/MOPS and [2]PIPES buffers

Table4.3 Thermodynamic Parameters for the Binding of MgADP, MgATP and 3PG to Mutant PGK at 25°C,pH7.0.

SUBSTRATE	K_{dis}(mM)	K_{ass}(M^{-1})	$-\Delta G^{o}$(kJmol^{-1})	$-\Delta H$(kJmol^{-1})	ΔS(JK^{-1}mol^{-1})
MgADP	$(7.50\pm4.04)X10^{-2}$	$(1.33\pm0.71)X10^{4}$	23.53 ± 1.32	32.37 ± 4.57	-33.11 ± 19.87
MgATP	$(4.89\pm0.01)X10^{-2}$	$(2.04\pm0.04)X10^{4}$	24.59 ± 0.05	33.86 ± 1.86	-31.11 ± 6.31
3PG	$(1.87\pm0.01)X10^{-2}$	$(5.35\pm0.03)X10^{4}$	26.97 ± 0.01	20.12 ± 0.04	23.15 ± 0.17

for the mutant and wild-type forms of the enzyme, it might also have been expected that there would be a difference in the ATP binding energies.It is difficult though,to know what the magnitude of $\Delta H_{mut} - \Delta H_{w-t}$ would be if these parameters were directly related to the differing K_m values. By using the K_m values obtained for mutant and wild-type PGK, calculating the corresponding ΔG and then the difference in the two values, $\Delta G_{mut} - \Delta G_{w-t}$, gives some indication as to the magnitude of the difference that would be expected when comparing the ΔH values for both forms of enzyme. The result of this calculation is approximately $2.94 kJmol^{-1}$ which is within the limits of the difference, $\Delta H_{mut} - \Delta H_{w-t}$. Hence, while ΔH_{mut} and ΔH_{w-t} for ATP binding are approximately equal within limits, the difference observed, rather than being as a consequence of experimental error, may be related to the effects which caused the contradictory K_m results for ATP binding to mutant and wild-type enzyme.

Results found for ATP and ADP binding to wild-type PGK correlate well with those found by Hu and Sturtevant (1987) using flow calorimetry. The value found by these authors when the energetics of 3PG binding was investigated however,was an endothermic result and certainly not equivalent to the value stated here. In fact, upon looking at both the wild-type and mutant enzyme, similar exothermic results were observed in each case.Initially the explanation for the differing results was thought to lie in the fact that the buffer solutions used were not the same - Hu and Sturtevant used 50mM PIPES,pH7.0 + 4mM $MgCl_2$ + 0.1mM DTT. However upon correspondence with Dr.C.

M.Johnson (Chemistry Department, University of Glasgow), who was repeating the 3PG - wild-type PGK binding experiments in PIPES and Tris/MOPS buffers by batch calorimetry, he also reported obtaining an exothermic result ($-16kJmol^{-1}$ for PIPES and $-20kJmol^{-1}$ for Tris/MOPS). An explanation as to why the results obtained by myself and Dr.Johnson, by two different calorimetric methods, are in such contradiction to those of Hu and Sturtevant has still to be sought.

While comparison of the results obtained by myself with those of Dr.Johnson for formation of the 3PG-PGK complex in Tris/MOPS buffer are very similar, there is certainly a variation in the ΔH value when PIPES is used. This is possibly due to the fact that the buffer systems have different heats of neutralization. Hence, if upon binding of 3PG any protons are released from the substrate or enzyme into the buffer, then they will bind to the buffer molecules in an exothermic reaction. If this is in fact the case then the total enthalpy change occurring when 3PG binds is equal to the heat of binding of 3PG to PGK plus the heat of binding of the released proton to the buffer. (Recall that the function of a buffer is to bind and thereby neutralize the effect of the ions produced in solution, to maintain that solution at a constant pH).

Comparing those results observed for 3PG binding to wild-type PGK in PIPES buffer with those found for Tris/MOPS buffer,the enthalpy change will be due to differences in the heat of ionization of the buffers. Values for the heats of neutral-

ization of Tris/MOPS and PIPES buffers are -22kJ and -12 kJ per mole of protons (Dr.Johnson, personal communication), respectively. The ionization energy for Tris/MOPS buffer is certainly more exothermic than that of PIPES, probably therefore effecting the more exothermic result for PGK binding 3PG in the former buffer.

At this time it is not certain how many protons,if indeed any are released. However in a recent publication by Wilson et al (1988), nmr data is provided relating to the pk_a of 3PG when bound to PGK (pk_a=4.5) and free in solution (pk_a=6.84). One implication that can be taken from this result,recalling that in this thesis all calorimetric experiments were performed at pH=7.0, is that approximately half of the free 3PG will be ionized. Upon the binding of this substrate to PGK within the calorimeter - still at pH7.0 - almost all of the remaining protonated 3PG will become ionized. Presumably the "lost" protons will be scavenged by the buffer, thereby generating heats (of ionization) in addition to the enthalpy change for 3PG binding to the enzyme. Hence if 1mole of 3PG was to bind to enzyme, the pk_a data implies that 1/2mole of protons would be released and be taken up by buffer molecules.Recalling now the heats of neutralization of PIPES and Tris/MOPS buffers, the heats generated when the 1/2mole of H^+ bound would be -6kJ and -11kJ,respectively. A 5kJ difference would therefore be expected when carrying out the experiments in the two buffer systems - the Tris/MOPS data should be 5kJ more exothermic. This is almost exactly the difference observed in the 3PG binding reaction under the two buffer conditions and

supports the suggestion that there may indeed be loss of protons from the 3PG substrate molecules when they are bound by the PGK.

CHAPTER 5

Thermal Unfolding of PGK

5.1 Experimental Details

5.2 Results and Discussion

CHAPTER 5

THERMAL UNFOLDING OF PGK

5.1 Experimental Details

The following experiments were carried out by Professor J.M. Sturtevant (Department of Chemistry, Yale University, Connecticut, USA) on a Microcal MC-2 differential scanning calorimeter, using PGK samples provided by us.

Wild-type PGK,isolated in this lab by the method described in section 3.1.4 and stored in 60% (w/v) ammonium sulphate, was dialysed extensively against 50mM PIPES + 0.1mM DTE, pH7.0. The resulting enzyme solution was diluted with this buffer to a final concentration of 11.05mgml^{-1}. This solution was then loaded into the sample cell of the calorimeter, while buffer was placed in the reference cell and the experiment was performed at a scan rate of 1Kmin^{-1}.The experiment was repeated using a wild-type solution of concentration 2.76 mgml^{-1} and then a mutant PGK solution of 3.97mgml^{-1}.

Wild-type PGK experiments were also carried out in the presence of 20mM Na_2SO_4.

Integration of the resulting DSC curves was carried out by planimeter.

5.2 Results and Discussion

Examples of the DSC curves obtained for 11.05mgml^{-1} and 2.76 mgml^{-1} wild-type PGK and 3.97mgml^{-1} mutant PGK are reproduced

in Figs.5.1,5.2 and 5.3 respectively.

The process was apparently irreversible, as indicated by the fact that no endotherm was seen on rescanning any of the solutions. This corresponds to results observed by Hu and Sturtevant (1987).From these curves, values for $t_{1/2}$, $(T_{1/2}-273.15)$, ΔH_{cal}, ΔH_{vH} and ΔC_p were calculated and are tabulated in Table5.1, beside the corresponding values obtained by Hu and Sturtevant using yeast PGK purchased from Sigma Chemical Co.. For wild-type PGK ($11.05 mgml^{-1}$) alone, both ΔH_{cal} and ΔH_{vH} were smaller than those values reported by Hu and Sturtevant for PGK at the same concentration and whereas the results of these authors indicate a ΔC_p of $+1.4 kcalK^{-1}mol^{-1}$ for the thermal process, a change in the heat capacity for the PGK samples from this laboratory was barely detectable.$t_{1/2}$ values were also quite different. A comparison of the $\Delta H_{vH}/\Delta H_{cal}$ ratio showed that both results were approximately the same at a value of nearly 0.9 indicating that there may be one or more intermediate states occurring between the native denatured states.Sturtevant also found, by repeating the experiments at various PGK concentrations that there was no significant variation with protein concentration in any of the quantities observed from DSC data. This is not the same observation made upon comparison of the data derived from DSC results of the experiments using the PGK isolated in this lab ($11.05 mgml^{-1}$ and $2.76 mgml^{-1}$) and may imply that some form of aggregation occurs due to denaturation.

Fig.5.1 DSC curve observed with a solution of 11.05mgml^{-1} wild-type PGK

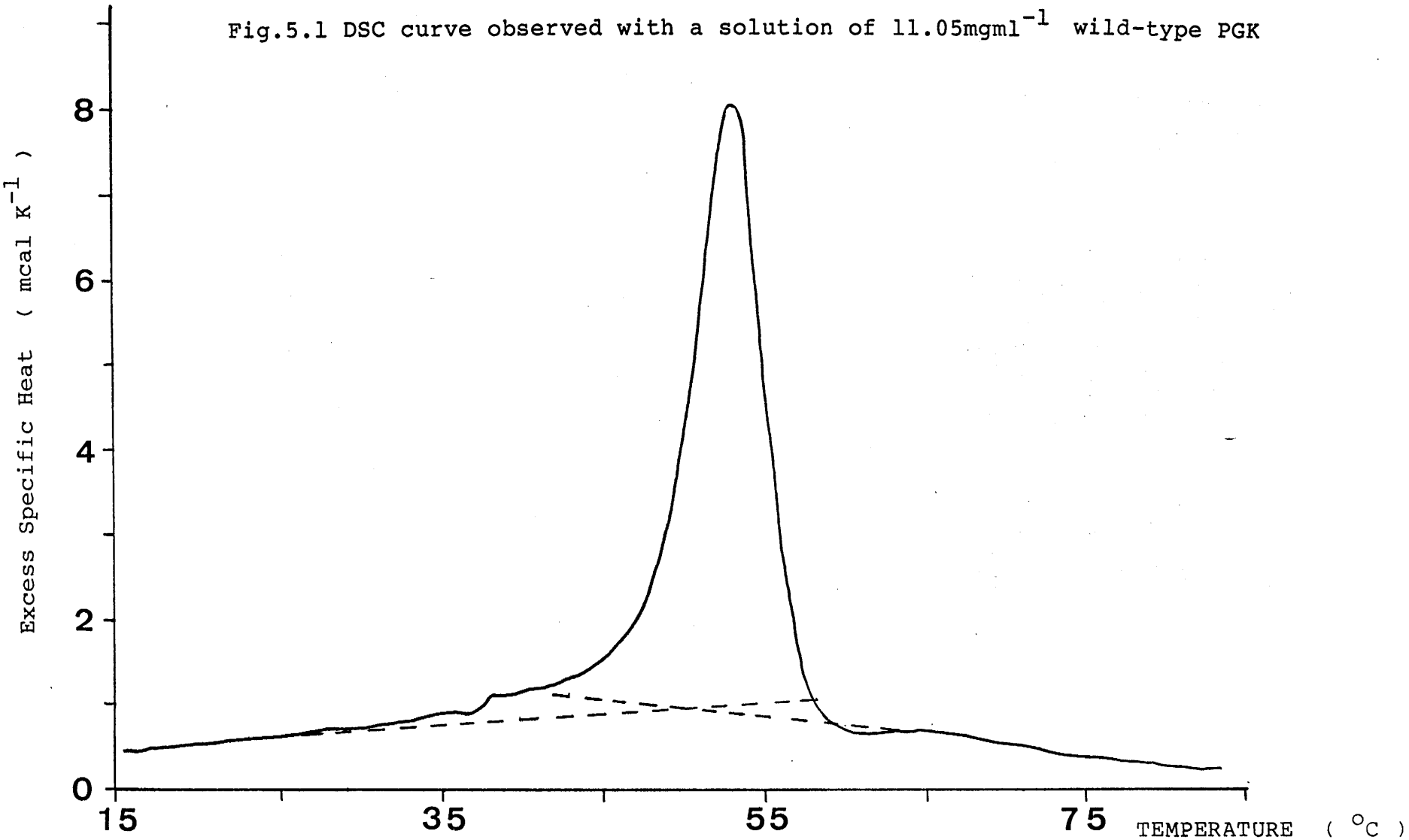

Fig.5.2 DSC curve observed with a solution of 2.76mgml^{-1} wild-type PGK.

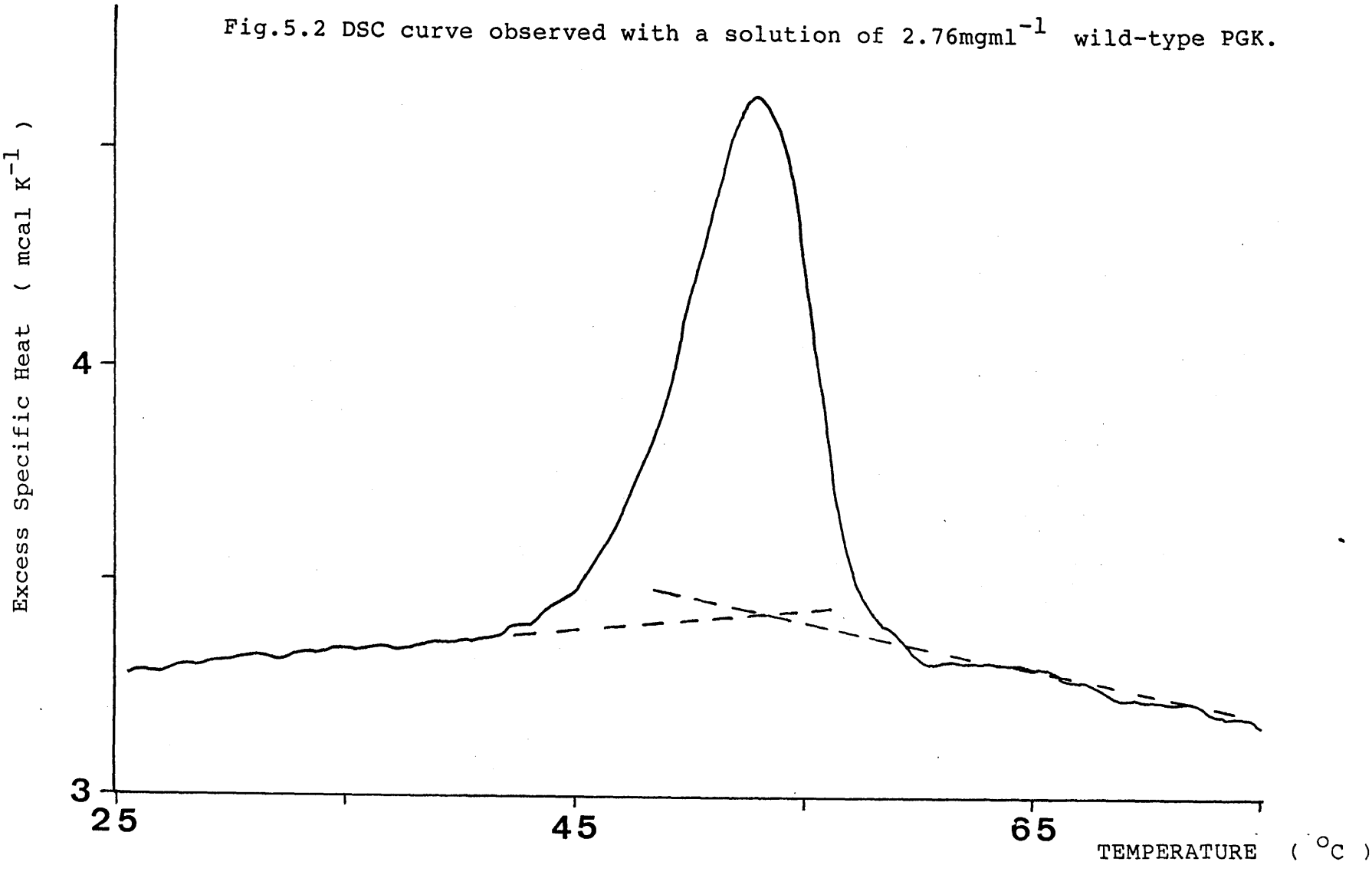

Fig.5.3 DSC curve observed with a solution of 3.97mgml^{-1} mutant PGK.

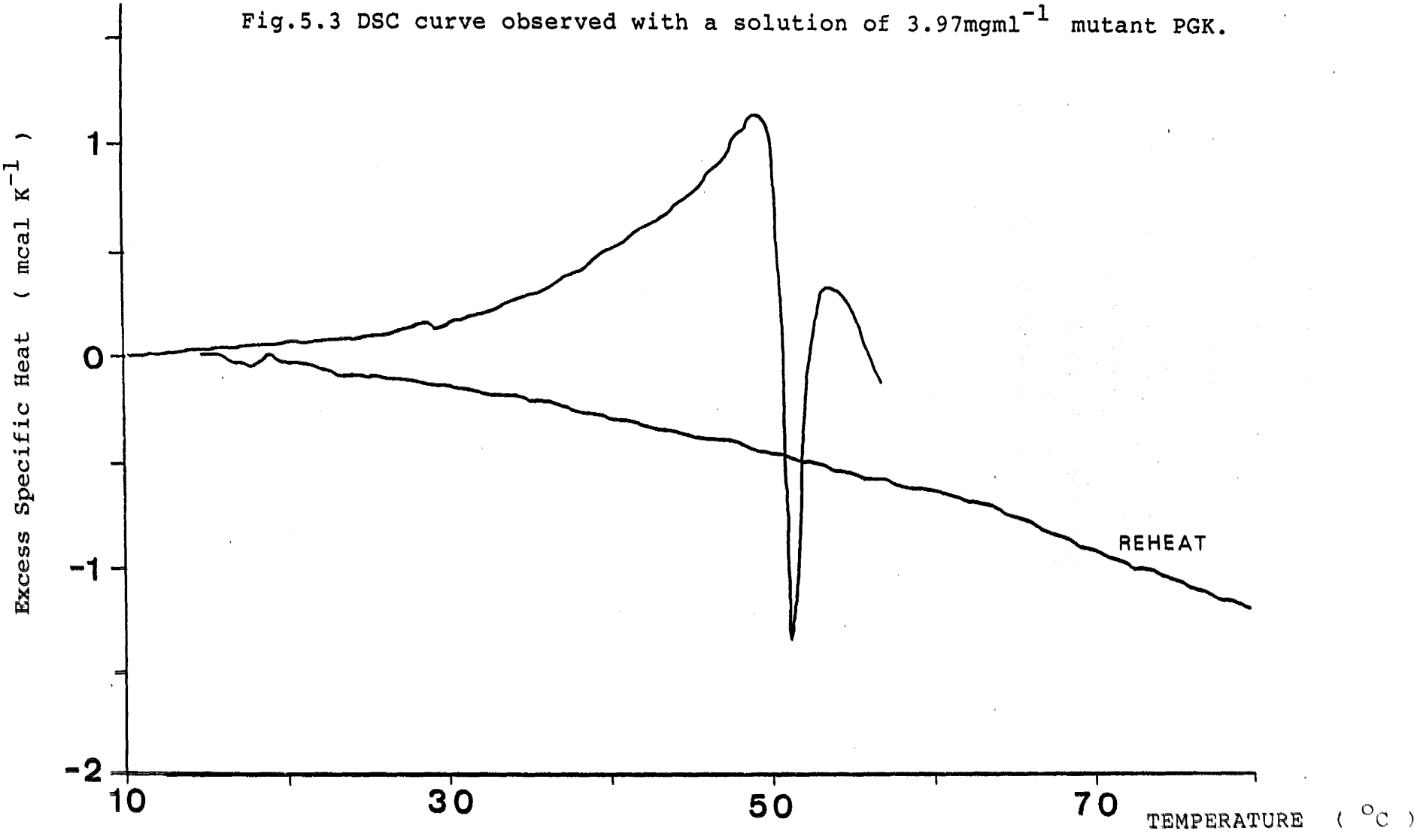

More recent work by Hu and Sturtevant (1988), involving the binding of sulphate to PGK, indicated that increasing the concentration of sulphate bound to wild-type PGK induced increases in the $t_{1/2}$, ΔH_{cal}, ΔH_{vH} and $\Delta H_{vH}/\Delta H_{cal}$ values. This was also the trend observed for the PGK data presented in Table5.1 and Fig.5.4, although direct comparison of both sets of data shows dissimilar thermodynamic values. The $\Delta H_{vH}/\Delta H_{cal}$ ratio, with sulphate present at a concentration of 20mM,has increased to over unity,implying that intermolecular cooperation might be occurring and this may require some degree of molecular association.This effect has probably been caused by the increase in ionic strength of the solution. An increase in $t_{1/2}$, with increasing sulphate concentration is to be expected for a reaction accompanied by dissociation of the ligand.

The large increase in ΔH_{cal} observed by Hu and Sturtevant (1988) with increasing sulphate concentration is thought to be in part due to an increase in $t_{1/2}$ coupled with the large ΔC_p value. A much smaller ΔH_{cal} is reported here, possibly due to the smaller ΔC_p observed.

Assuming therefore that both sets of experiments were carried out under identical conditions, the only difference between the PGK samples which may contribute to the conflicting results was the source and resultant purity. The cause of these inconsistent results is still a matter of contention (Prof.J.M.Sturtevant,private communication).

Table 5.1 Thermal denaturation of wild-type PGK at pH7.0.

Protein Concentration ($mgml^{-1}$)	Na_2SO_4 Concentration ($mgml^{-1}$)	$t_{1/2}$ (^{o}C)	$\triangle H_{cal}$ ($kcalmol^{-1}$)	$\triangle C_p$ ($kcalK^{-1}mol^{-1}$)	$\triangle H_{vH}$ ($kcalmol^{-1}$)	$\triangle H_{vH}/\triangle H_{cal}$
11.05	----	53.3	152	very small	138	0.908
*	----	56.3	204	+1.4	178	0.873
2.76	----	52.7	116	very small	121	1.043
1.50	20	57.0	153	----	210	1.373
**	20	58.9	242	+2.14	262	1.083

*Hu and Sturtevant (1987)
**Hu and Sturtevant (1988)

Fig.5.4 DSC curve observed with wild-type PGK + 20mM Na_2SO_4

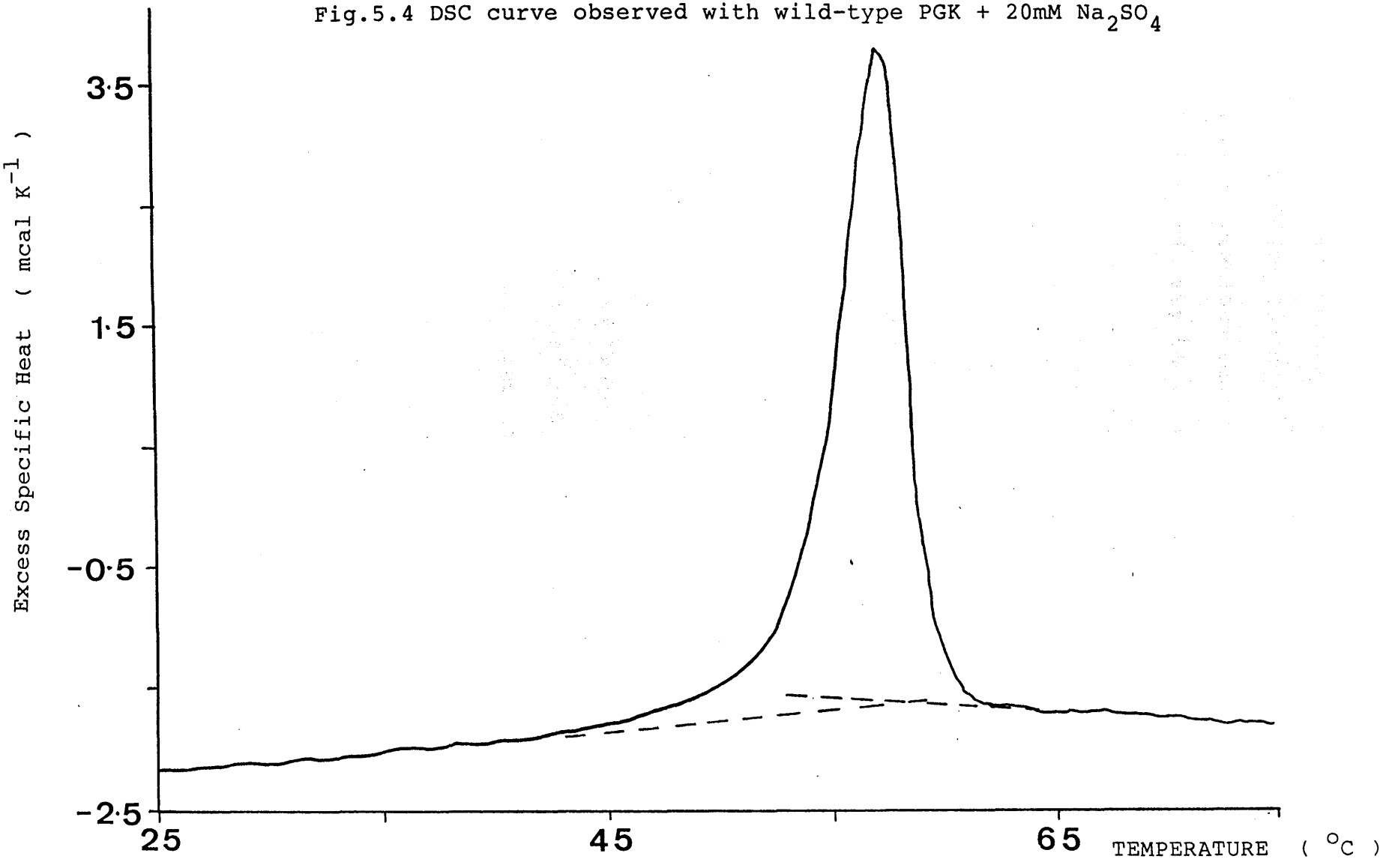

Fig.5.3 indicates the results for a scan of a mutant PGK sample of concentration 3.97mgml^{-1}. This plot shows a large exotherm similar to previous results observed by Sturtevant. It is thought that this may be an artifact resulting from the geometry of the cells of the MC-2, since such exotherms are not observed when using apparatus with a different cell configuration.

A reheat of the sample indicated that the process was irreversible, as with the wild-type enzyme.

Further experiments are being performed using wild-type and mutant PGK from this lab and it will be of considerable interest to obtain accurate results for mutant PGK-analysed by this technique.This will allow comparison of the mutant PGK results with the same values obtained for wild-type enzyme and hence may yield information relating to the effect of the mutation on the free energies of stabilization (Sturtevant,1987), as well as changes in the other thermodynamic parameters and folding/unfolding processes.This would also provide evidence to support the theories on the importance/insignificance of the replacement of His388 by Gln388 with particular reference to the stabilization of the enzyme structure and its effect on some of the enzyme's thermodynamic and non-thermodynamic (for example, the nature of the transition) properties.

These aspects of DSC highlight the reasons why it has been a technique, widely employed to study the conformational or

phase transitions which these complex structures undergo upon being heated.This can then provide information concerning the fundamental nature of the unfolding process and the forces involved.

CHAPTER 6

Investigation of Protein Dynamics by Low Frequency Raman Scattering

CHAPTER 6

INVESTIGATION OF PROTEIN DYNAMICS BY LOW FREQUENCY RAMAN SCATTERING

6.1 Introduction

Background details describing the techniques of Raman spectroscopy and the apparatus employed is provided in section2.3.

This chapter describes a potentially useful Raman method for examining the depolarized Rayleigh wing scattering from protein solutions. This portion of the Raman spectrum and the large-scale dynamic motions of the protein in question are thought to be closely related (section1.1.5). However, due to damping effects in solution, it is unlikely that the protein will be oscillating harmonically and so instead of observing well-defined vibrational bands in the low frequency spectrum, it is necessary to inspect the overall distribution and intensities of the collective frequencies within the range of interest,in order to obtain the desired information.A complex frequency distribution like this probably arises from uncorrelated anharmonic and damped motions of the protein and it is changes in this frequency spread,upon substrate binding to PGK (and lysozyme), which will be analysed.

6.2 Experimental Details

Arrangement of the apparatus used was as described in section 2.3.2,with modifications for depolarized Rayleigh scattering. Incident laser light was polarized vertically using a quartz polarization rotator. 90^{o} depolarized, scattered light was

selected by placing a Polaroid analyzer in front of the collection optics, followed by a quarter-wave polarization scrambler (to eliminate any effects due to polarization sensitivity of the triple-monochromator system).A 10% (transmission) neutral density filter was also placed in front of the collection lens during measurements at low wavenumbers,to avoid saturation of the photomultiplier tube due to high intensity Rayleigh scattering.Light was provided by a Spectra Physics continuous wave argon laser and scattered photons were detected by a Brandenburg Alpha series photomultiplier. In addition, the use of a photomultiplier cooling unit (Products for Research,Inc.) encircling the photomultiplier tube resulted in the successful reduction of "background noise",caused by thermal fluctuations,by a factor of 200. The photoelectric current obtained was initially displayed on a chart recorder.More recently however, the spectrometer photon counter was interfaced with a computer and this now facilitates collection, storage, manipulation and display of the spectral data.

6.2.1 Preliminary Low Frequency Raman Experiments with Lysozyme

An introduction to lysozyme has already been provided in section4.3.1.

Two 7.5% hen egg white lysozyme (Sigma Chemical Co. Ltd.) solutions were prepared in 0.1M acetate buffer, pH5.0, one containing 5.5mM of the lysozyme inhibitor tri-N-acetyl glucosamine (Sigma). Both solutions were filtered through 0.22μm Millipore filters, before placing in a clean Raman

cell. Raman spectra were recorded of both solutions,from -100 to +300cm^{-1}. The Raman spectrometer settings are outlined in Table6.1 and the spectra obtained are depicted in Fig.6.1 (the insert at the top right hand corner of the diagram depicts the part of the spectrum which is lost from the top of the main picture). Comparing the spectrum of lysozyme with and without tri-NAG bound gives the appearance that there has been an increase in the proportion of higher frequency modes present when inhibitor is bound,at the cost of losing some of the enzyme's lower frequency modes. These results are consistent with the inhibitor bound in the enzyme's cleft and blocking lysozyme hinge-bending and/or other low frequency motion - in other words - accordant with a general molecular stiffening. Control experiments comparing solutions of 7.5% lysozyme with identical solutions containing 0.18M glucose and 0.12M NAG,another inhibitor,provided results that showed no effect with glucose and a similar but smaller effect with NAG as that observed with tri-NAG. The fact that the Raman spectrum of lysozyme + glucose was identical to that of lysozyme alone, seems to rule out possible indirect causes of the observed effect, for example by changing the refractive index of the solution. Since lysozyme is thought to undergo a hinge-bending motion similar to that suggested for PGK, it seems possible that both enzymes will exhibit comparable dynamic properties.

6.2.2 Low Frequency Raman Experiments with Mutant and Wild-Type PGK

Identical procedures were followed for wild-type PGK and

Table 6.1 Spectrometer settings for the recording of low frequency Raman spectra of lysozyme.

Scan range (cm^{-1})	-150 to +150
Laser line (nm)	480
Power (mW)	300
PM voltage (kV)	1.2
Scan rate ($cm^{-1}min^{-1}$)	5
Slits (μm)	70,70,70,70
Count time (secs)	5

Fig.6.1 Low frequency Raman spectra of 5mM lysozyme and 5mM lysozyme + 5.5mM tri-NAG.

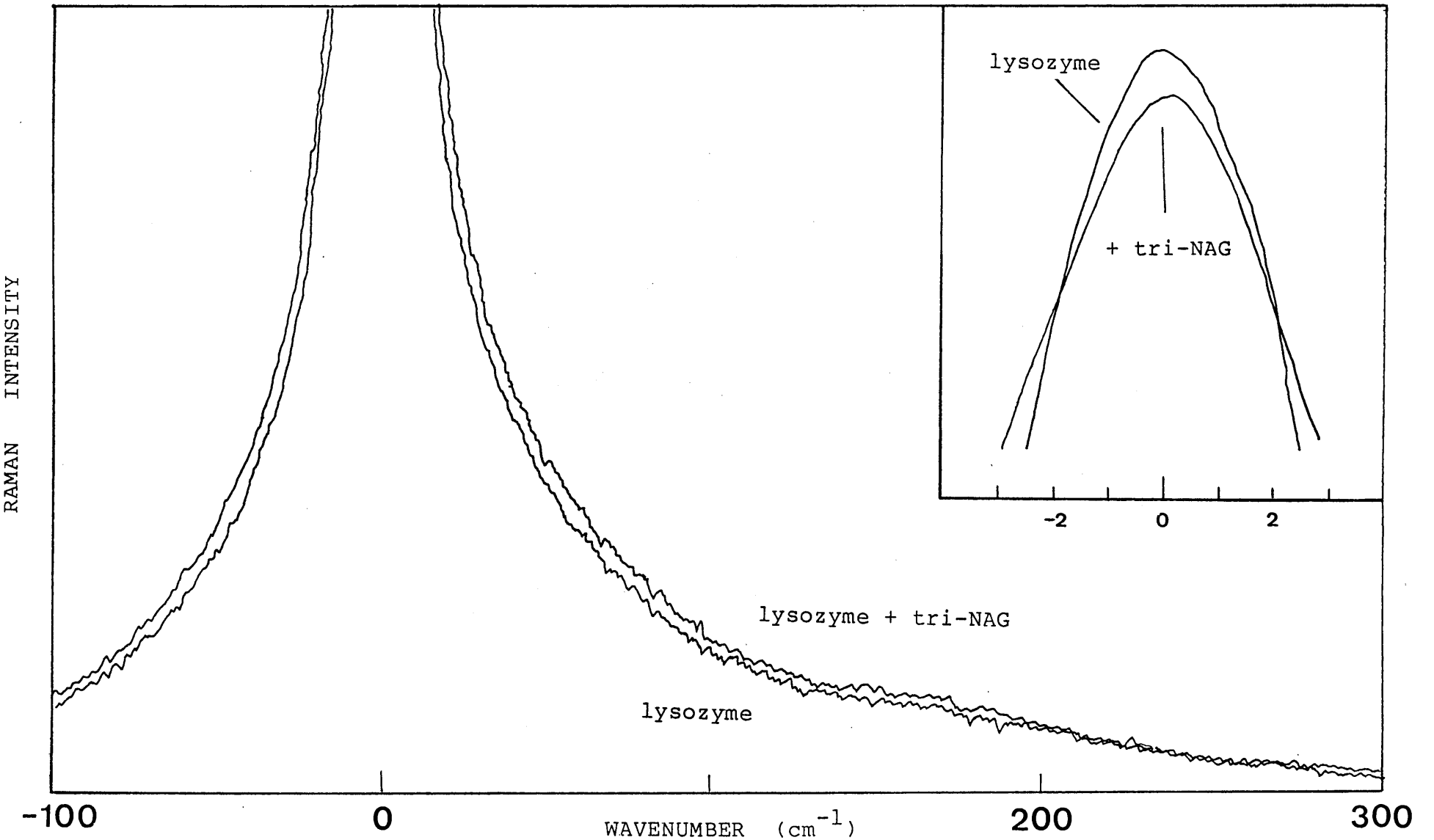

mutant PGK.

The PGK, stored at 4°C in a buffer solution containing 600g ammonium sulphate per litre, was centrifuged and the pellet of enzyme retained.(The supernatant,which still contained a significant amount of PGK, was dialysed extensively against water and the PGK isolated by freeze-drying). The pellet was dissolved in a small volume of 10mM Tris/MOPS, pH7.0 buffer containing 0.1mM DTT. This solution was placed in dialysis tubing (pre-boiled with EDTA and $NaHCO_3$) and dialysed for several hours against 10mM Tris/MOPS, pH7.0 + 0.1mM DTT + 4mM $MgCl_2$. After dialysis, the enzyme solution was centrifuged to remove any precipitous material present and then diluted using fresh buffer to provide a stock solution of PGK between 2% and 3%. The exact concentration was measured by the absorbance at 280nm, as detailed previously in section4.3.2. Stock substrate solutions were prepared of 50mM ATP (disodium salt), 50mM ADP (Di-monocyclohexylammonium salt) and by the procedure used in section3.1.4, 50mM 3PG (barium salt). All compounds were purchased from Sigma.Five, 1.2ml portions of the stock PGK were placed in five different vials and to them was added 50μl of 50mM ATP,50μl of 50mM ADP, 50μl of 50mM 3PG, 50μl of H_2O and to the fifth vial 25μl of both ATP and 3PG.

Two sets of Raman spectra were recorded for each of the five enzyme-substrate solutions - one set between -10 and +10cm^{-1} and the other -100 to +300cm^{-1}.At this point it must be noted that wavenumber and frequency differ by a factor of the speed

of light, c, where $\nu = c/\lambda$ and since c varies with the refractive index of the medium, values of $\Delta\nu$, expressed in cm^{-1}, do also. Hence, for very careful work $\Delta\nu$ should be calculated in vacuum wavenumbers (Strey,1969). However, since the difference between the values of $\Delta\nu$ for air and vacuum are small, they were neglected.

The individual spectrometer settings are shown in Table6.2. When recording -10 to $+10cm^{-1}$ spectra, a 10% neutral-density filter was situated between the sample and collecting lenses to prevent saturation of the PM tube which may occur at zero wavenumbers when scan speed is slow.

Spectra were recorded individually after the PGK solution in question was filtered through a Millex-GV_4 millipore filter (0.22μm pore size) into a very clean cuvette.

The results obtained are as indicated in Figs.6.2 and 6.3 where the insets represent the plots obtained from the -10 to $+10cm^{-1}$ spectra.

6.3 Low Frequency Spectra of Substrate Solutions

To check that the substrate solution is not causing any changes in the low frequency spectra, identical experiments were performed on each of the 50mM substrate solutions using the same settings as described in Table6.2. It was found upon comparing the resultant substrate solution spectra with the same spectrum for water alone that there is no significant difference. The substrate solution can therefore be regarded

Fig.6.2 Low frequency Raman spectra of 2.2% wild-type PGK and 2.2% wild-type PGK + substrates.

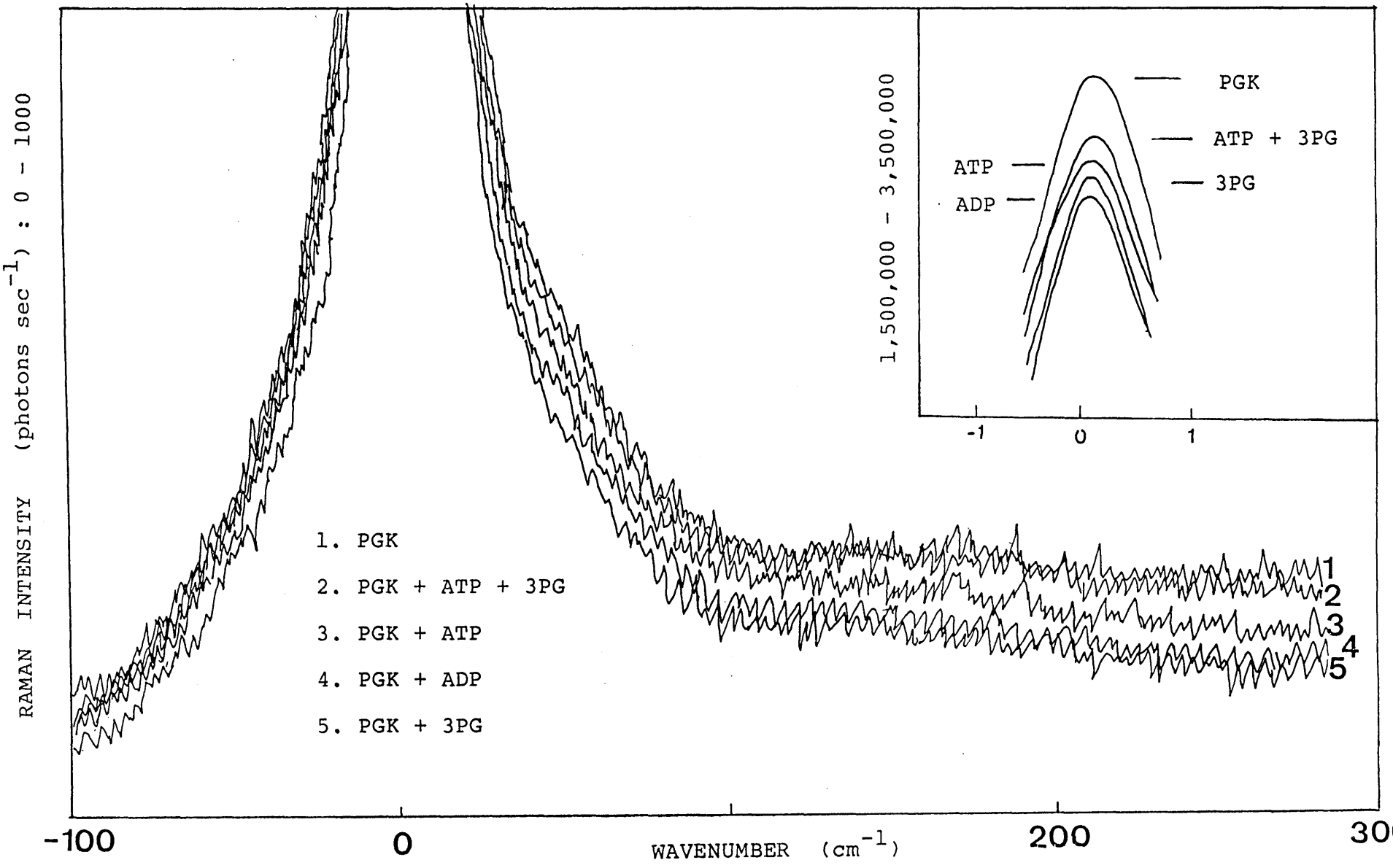

Fig.6.3 Low frequency Raman spectra of 2.2% mutant PGK and 2.2% mutant PGK + substrates.

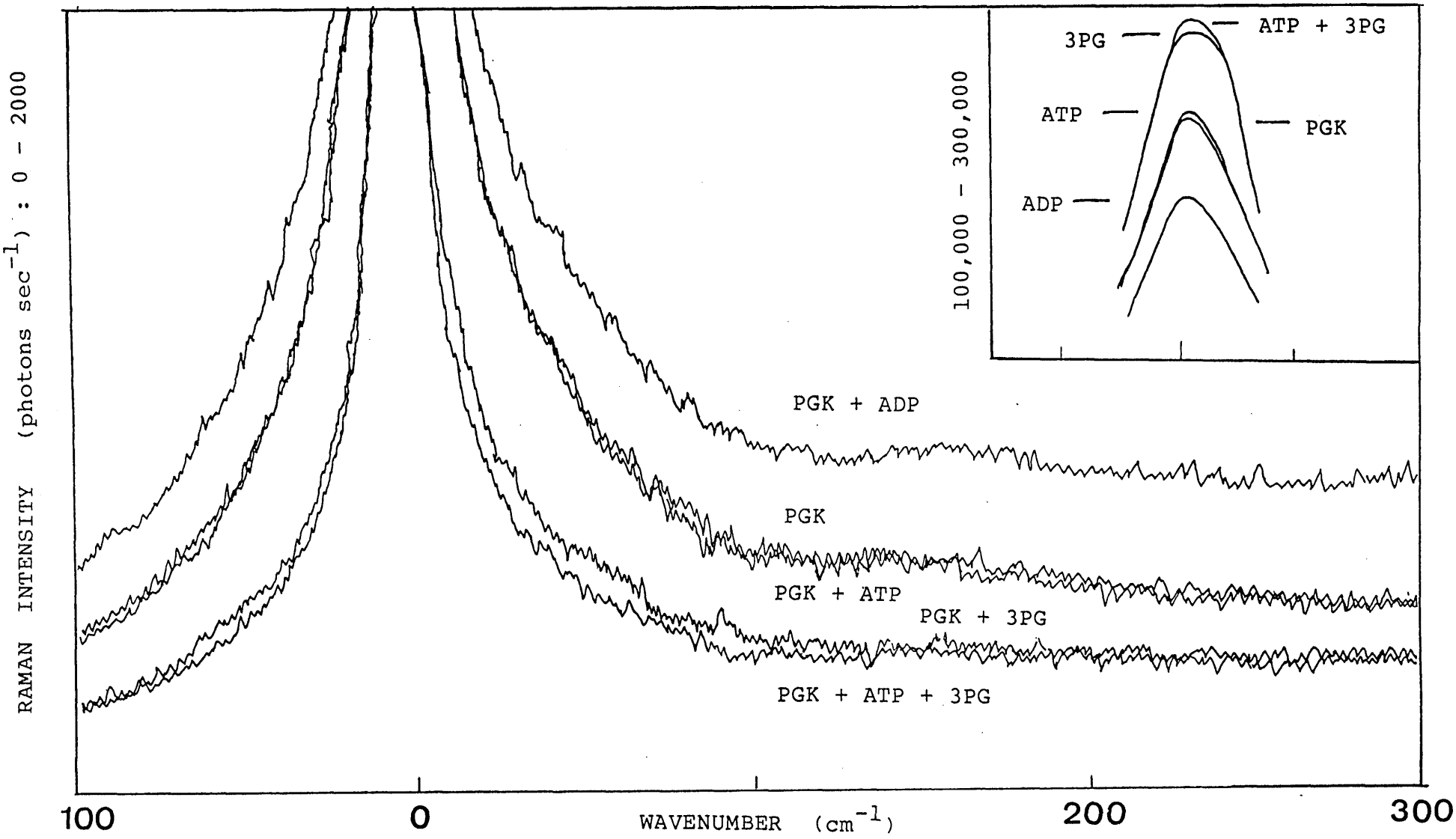

Table 6.2 Spectrometer settings for the recording of low-frequency Raman spectra.

scan range (cm^{-1})	-100 to +300	-10 to +10
laser line (nm)	488	488
power (mW)	50	50
scan rate (cm^{-1} min^{-1})	10	1
slits (μm)	250,250,250,250	70,70,70,70
count time (secs)	5	5
volume of sample in cuvette (ml)	1.2	1.2

Table 6.3 Raman Spectrometer settings

Scan range (cm^{-1})	fixed at 0000
Laser line (nm)	488
Power (mW)	50
PM voltage (kV)	1.1
Slits (μm)	250,250,250,250
Count time (secs)	5
10% filter	yes

as providing a negligible contribution to the Raman spectrum of the enzyme plus substrate solution.

6.4 Relationship Between Count Rate and the Concentration of PGK

During the course of these PGK experiments problems due to protein aggregation were encountered. The presence of these aggregates caused spurious peaks in the output signal as well as a general increase in the count rate,inconsistent with the previous experimental results. Hence, it was decided that it would be necessary to find out the effect of PGK concentration, and any accompanying aggregation effects, on the count rate.

2% PGK solutions (wild-type and mutant) were prepared as before (section6.2.1). Portions of each solution were diluted with buffer by between 0 and 100 times. The count rate was observed for each solution at zero wavenumber shift for several minutes and the average reading calculated. The instrument settings used are given in Table6.2 and the results obtained are reproduced in Figs.6.4 and 6.5, plotted as log of the average number of counts observed versus the log of the PGK concentration . Reasonable straight-line correlations were obtained over the concentration range investigated. Hence this would imply that the anomalous effects observed due to aggregation are caused by the presence of enzyme-bound substrate.

Fig.6.4 Relationship between the number of photon counts and wild-type PGK concentration.

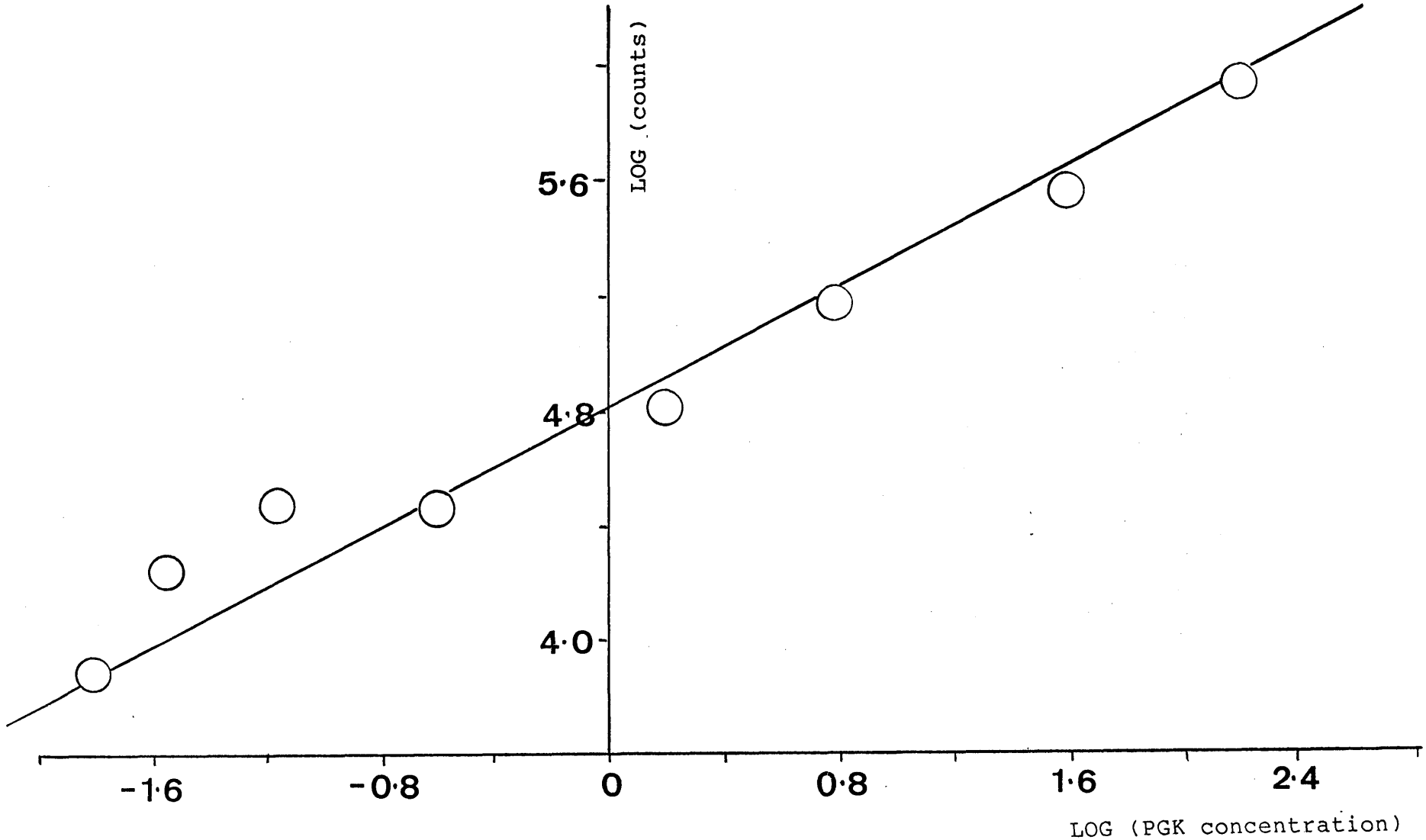

Fig.6.5 Relationship between the number of photon counts and mutant PGK concentration.

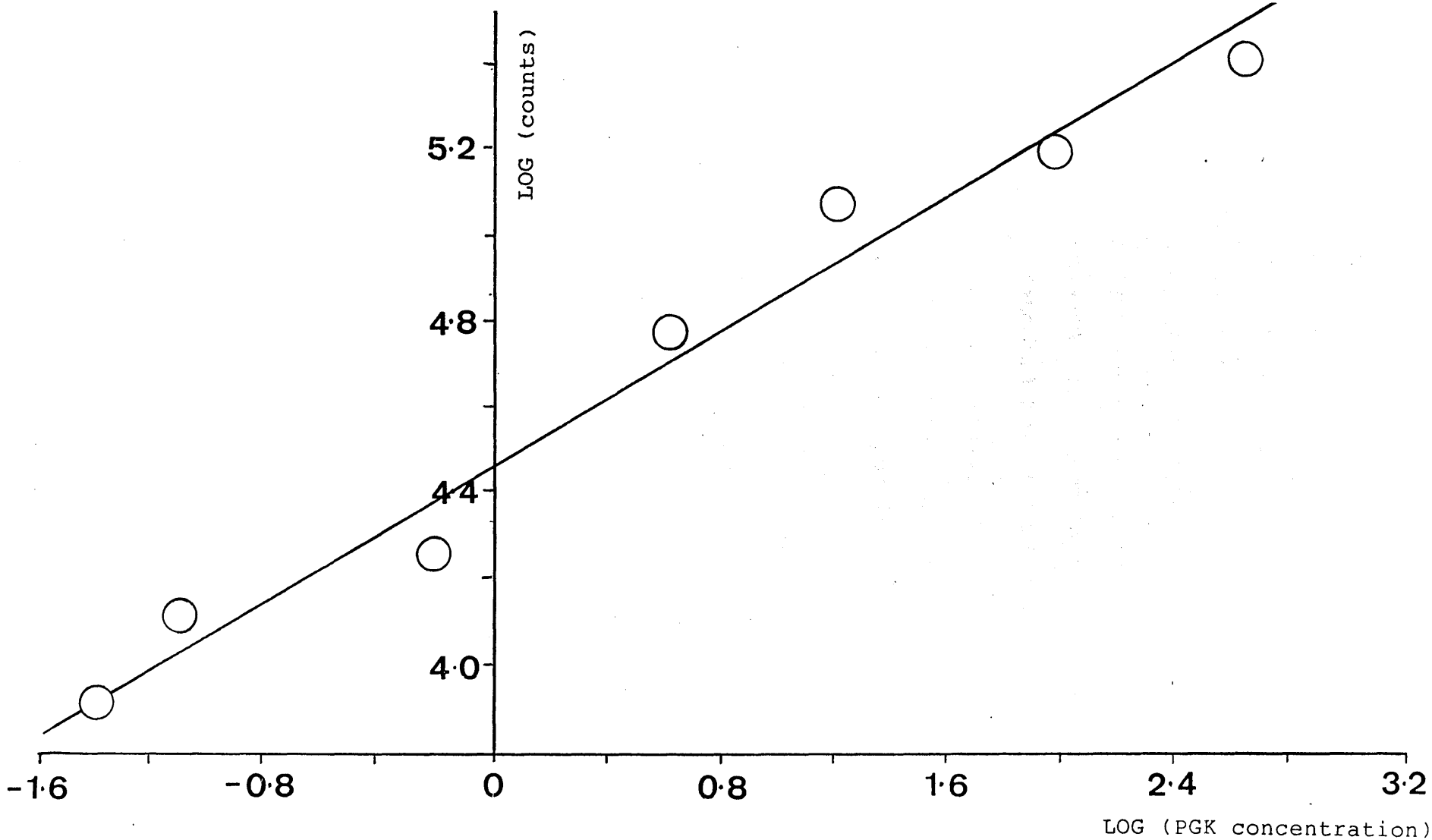

6.4 Results and Discussion

Recalling the spectra reproduced in Figs.6.2 and 6.3, it can be seen that in the former spectrum all five traces are very similar with no changes being observed upon binding of the substrate.These results, along with the arguments put forward in section2.3.3 imply that there has not been a change in the dynamics of the system when the enzyme binds substrate - none that is,that can be detected by this technique. When the same set of experiments,however,were carried out using mutant PGK some interesting results were obtained (Fig.6.3). As yet it is difficult to explain by looking at these results exactly what changes in the dynamic properties of PGK,if any, are occurring upon substrate binding. Speculative proposals would imply that the presence of ADP bound to PGK has the effect of increasing the number of higher frequency vibrations at the cost of losing a number of the lower freq-uency modes. Effectively the macromolecule has "stiffened". Upon binding 3PG the opposite effect is observed. Simultan-eous addition of ATP and 3PG produce a result similar to that when only 3PG is present. This is a reasonable observation since the presence of ATP alone, bound to PGK, has little effect on the spectrum of PGK by itself.

The fact that mutant PGK exhibits such properties but the wild-type does not, might be explained by the fact that the overall dynamics of the two forms of PGK are possibly quite different, due to the loss of the His388-Glu190 interaction in the hinge region. Not only is this interaction thought to be very important in the action of the enzyme by facilitating

domain movement (section1.3) but the movement itself characterizes the dynamic properties of the molecule which this technique of analysis is attempting to monitor. As mentioned previously though, these descriptions of dynamic alterations are entirely tentative because while the results reported here for the low frequency spectra of wild-type PGK plus substrates were highly reproducible, the results for the mutant enzyme were not quite as reliable. Nevertheless, in general it was found that the presence of substrate did alter the low frequency Raman scattering of the mutant enzyme solution - although in most cases the change was only by a very small amount. Observation of these trends was frequently confused by problems with maintaining the clarity of the samples - caused by aggregation of the protein sample and the unavoidable presence of interfering dust particles etc.

Since this is the first instance of using this method for analysing dynamics, any description of the changes in dynamic motion is entirely speculative until further experimentation and analysis of the results has occurred.

CHAPTER 7

Conventional Raman Spectroscopy of PGK

7.1 Experimental Details

7.2 Results and Discussion

CHAPTER 7

CONVENTIONAL RAMAN SPECTROSCOPY OF PGK

7.1 Experimental Details

An introduction to conventional Raman spectroscopy and its use in determining conformational details of proteins has already been given in section 2.3.4.

The same arrangement of apparatus was used as described in section 6.1.1, this time using solid samples. However, an additional problem arises when recording the spectra of solids - this involves the presence of plasma lines. It is found, when using the Ar laser for excitation, that in addition to the major lasing line, the laser beam contains other weaker plasma lines of the gas. Rayleigh scattering of these lines from the sample, particularly when the sample is in solid form, can give the appearance of spurious Raman bands.To remove these interfering lines, a narrow band interference filter, specific for the laser line in use (488nm), was placed between the laser and the sample. It was only necessary to use this instrument when solid samples were being investigated.

Initial allignment of the optics and sample, to obtain the optimum spectra, was done using sodium citrate. The Raman spectrum of this compound is well documented (Kerker et al, 1980a) and consists of several distinct and intense peaks and therefore it is ideal for allignment and calibration purposes.

Several sample handling techniques were tried in order to record the spectra of solid specimens. Samples in the form of powders or fine crystals were transferred into melting-point capillary tubes and positioned such that the laser beam was striking the packed, open end of the tube. If on the other hand the sample consisted of large crystals, these were mounted on the tip of a sharp object, such as a needle. The most satisfactory method however, involved compressing the sample into the concave depression on the head of an "Allan" screw, and mounting this such that the laser beam was striking the face of the solid at a 45^{o} angle. Using this technique to position the sample, to give optimum sample scattering was straight-forward and provided a relatively large specimen surface area. Good thermal contact with the metallic support also seemed to reduce radiation damage due to the sharply focused laser beam.

Once the equipment had been most suitably positioned, the resulting spectrometer settings used to record spectra of all the following samples, were as indicated in Table7.1.

7.2 Results and Discussion

The spectra obtained for sodium citrate closely resembled those previously published and exhibited distinct, intense bands.

A further test experiment was run using solid lysozyme. The spectrum obtained is reproduced in Fig.7.1 and this also correlates well with those reported in the literature (Chen

Table 7.1 Spectrometer settings for the recording of solid wild-type and mutant PGK.

Scan range (cm^{-1})	350 to 1750
Laser line (nm)	488
Power (mW)	30
PM voltage (kV)	1.1
Scan rate ($cm^{-1}min^{-1}$)	25
Slits (μm)	500,500,500,500
Count time (secs)	5
10% filter	NO

Fig.7.1 Raman spectrum of solid lysozyme

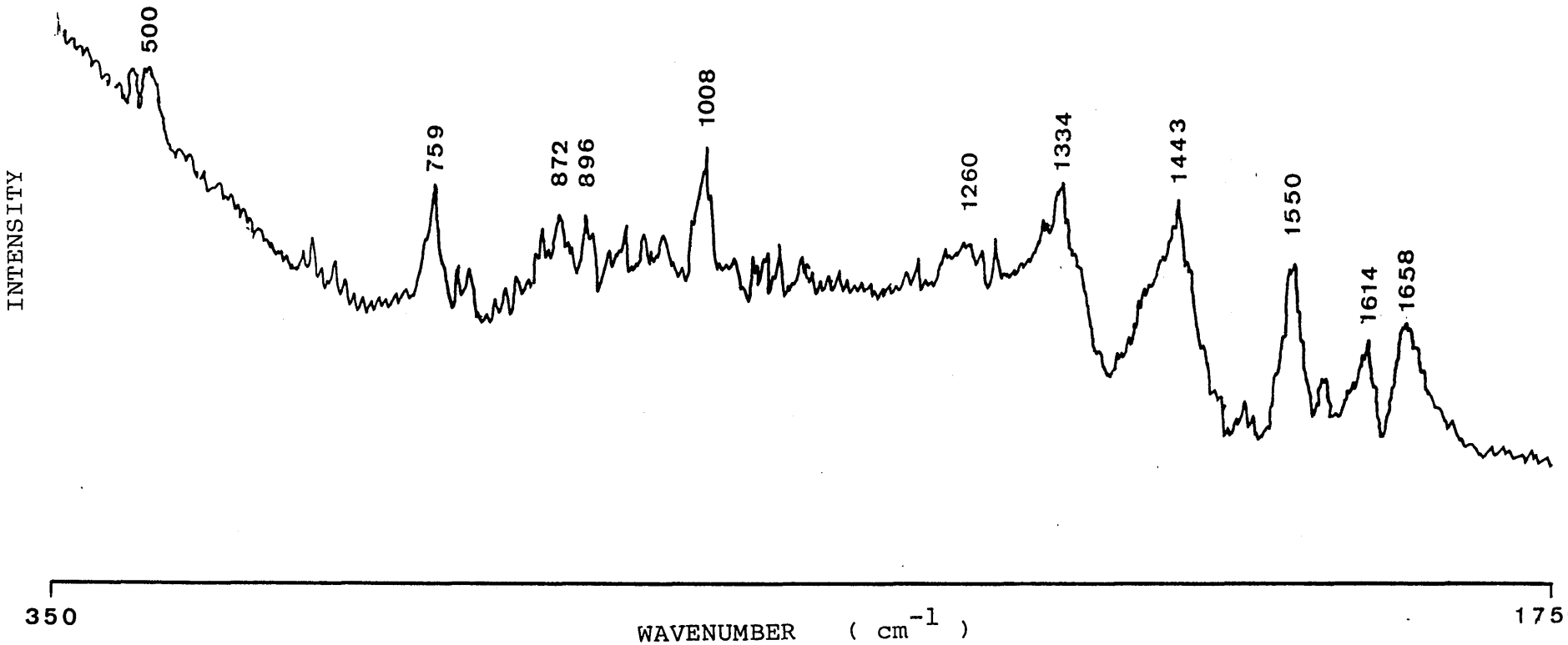

et al,1974).

The Raman spectra of freeze-dried (section 6.1.1) wild-type and mutant PGK were also recorded and the results are presented in Figs.7.2 and 7.3. Table7.2 outlines the main Raman bands for PGK and their tentative assignments. Band positions on the mutant and wild-type PGK spectra are very similar, implying that the exchange of the His388 for Gln388 has had little effect on the conformation of the PGK molecule. This however, does not mean that there has not been an alteration in the arrangement of the residues in the vicinity of amino acid 388 itself, since the normal Raman spectrum of a protein usually provides information about the average backbone conformation.

One outstanding difference is the peak intensities at 975cm^{-1} and 970cm^{-1} for wild-type and mutant PGK respectively. This peak however was subsequently found to be attributable to the presence of sulphate which had not been completely removed during the dialysis procedure.

Looking more closely at the 1250cm^{-1} and 1666cm^{-1} bands representing the amideIII and amideI bands, respectively for wild-type PGK, the bands are seen to be broad and this would suggest that PGK has a high proportion of each of the three forms of secondary structure mentioned previously. This correlates well with crystallographic information (Banks et al,1979) which implied that 25% and 42% of residues in PGK were located in β-structures and helices, respectively.These

Fig.7.2 Raman spectra of freeze-dried wild-type and mutant PGK

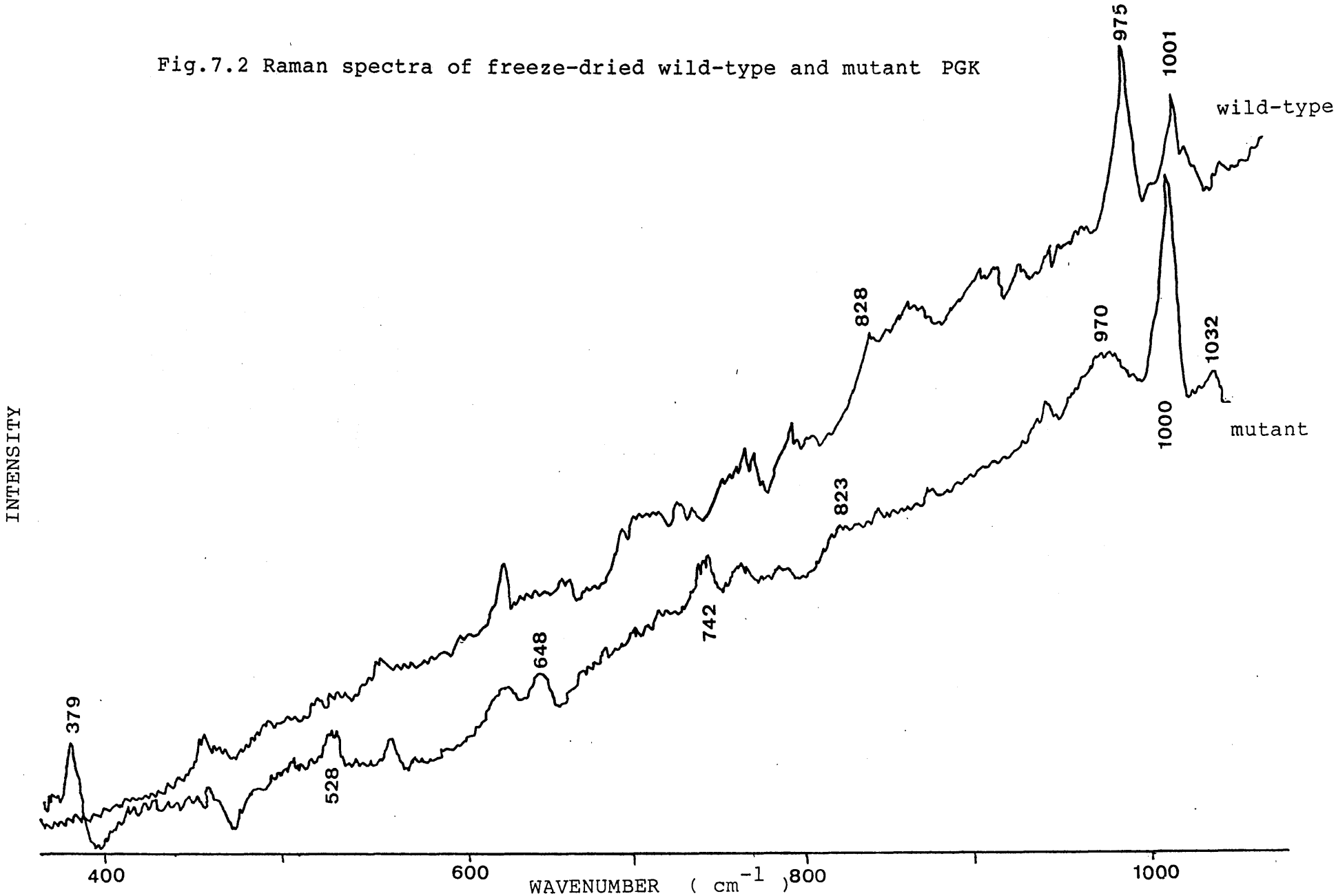

Fig.7.3 Raman spectra of freeze-dried wild-type and mutant PGK.

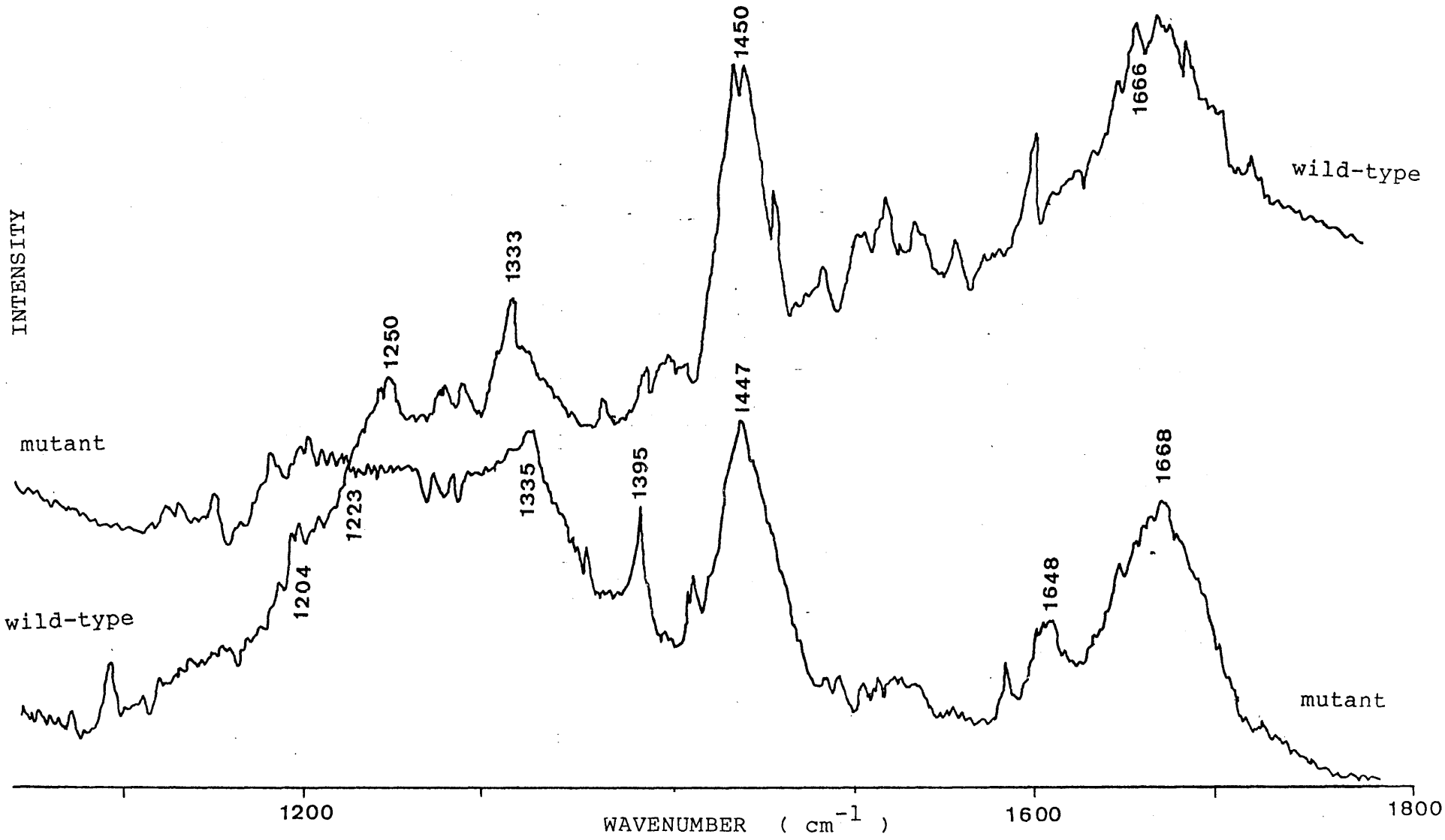

Table 7.2 Approximate positions (cm^{-1}) of the most intense bands in the Raman spectra of PGK.

WILD-TYPE	MUTANT	ASSIGNMENT
	379	
447		
	528	
621	621	Phe
	648	Tyr
700		
	742	
759		
785		
828	832	Tyr
975	970	SO_4^{2-}
1001	1000	Phe
	1032	
	1204	
	1223	AMIDE III
1250		AMIDE III
1333	1335	buried Trp
	1395	
	1424	ionized COO^-
1450	1447	ionized COO^- and CH_2 bending
1525		Trp
1606	1614	
1666	1667	AMIDE I

are similar to the observations made for mutant PGK, although the peaks at 1335cm^{-1} and 1525cm^{-1} representing tryptophan (Yu,1974) are weaker and broader than the corresponding signal for wild-type PGK. This indicates a possible change in the environment of the tryptophan residues.

Normal Raman spectroscopy is therefore useful for the determination of information about the secondary structure composition of polypeptide backbones, even if detail about specific residues is limited.

With reference to the comparison of wild-type and mutant PGK's investigated in this section, very little difference has been observed in the two spectra. The tryptophan bands may be the exception, implying a dissimilarity in the tryptophan environments - a proposal put forward in chapter8 because of the results from fluorescence spectrometric analysis of wild-type and mutant PGK. However differences in Raman background, due to broad-band fluorescence and unavoidable differences in sample packing, make detailed comparison of spectra difficult.

CHAPTER 8

Fluorescence Spectroscopy of PGK

CHAPTER 8

FLUORESCENCE SPECTROSCOPY OF PGK

8.1 Fluorescence Emission Spectra of Wild-Type PGK

An introduction to this experimental technique has already been covered in chapter2.

8.1.1 Experimental

The wild-type PGK for these experiments was supplied by Dr. Dryden (Biochemistry Department, University of Newcastle upon Tyne).

A solution of 2mg PGK per ml of 10mM Tris/90mM NaCl/1mM EDTA.Na_2, pH7.27 buffer, was used to study the fluorescence emission spectra. A sample of this solution was added to a 1cm fluorescence cuvette and then placed in the spectrometer. The sample was irradiated with light of wavelength 280nm and the resulting emission spectrum recorded, λ_{max}=306nm. This procedure was repeated with an excitation wavelength of 295nm and the resulting λ_{max} found to be equal to 329nm (see Fig. 8.1).

8.1.2 Results

Upon excitation at 280nm, the fluorescence emission of PGK is dominated by the tyrosine fluorescence-an anomally,peculiar to PGK (Dr.Dryden, personal communication)-see section 2.4.3. Since tyrosine fluorescence emission is relatively insensitive to the polarity of its surroundings, the λ_{max} obtained for the tyrosine emission of PGK (306nm) is fairly close to the λ_{max} of a solution of tyrosine in water (303nm).

Fig.8.1 Fluorescence emission spectra of 0.2% wild-type PGK

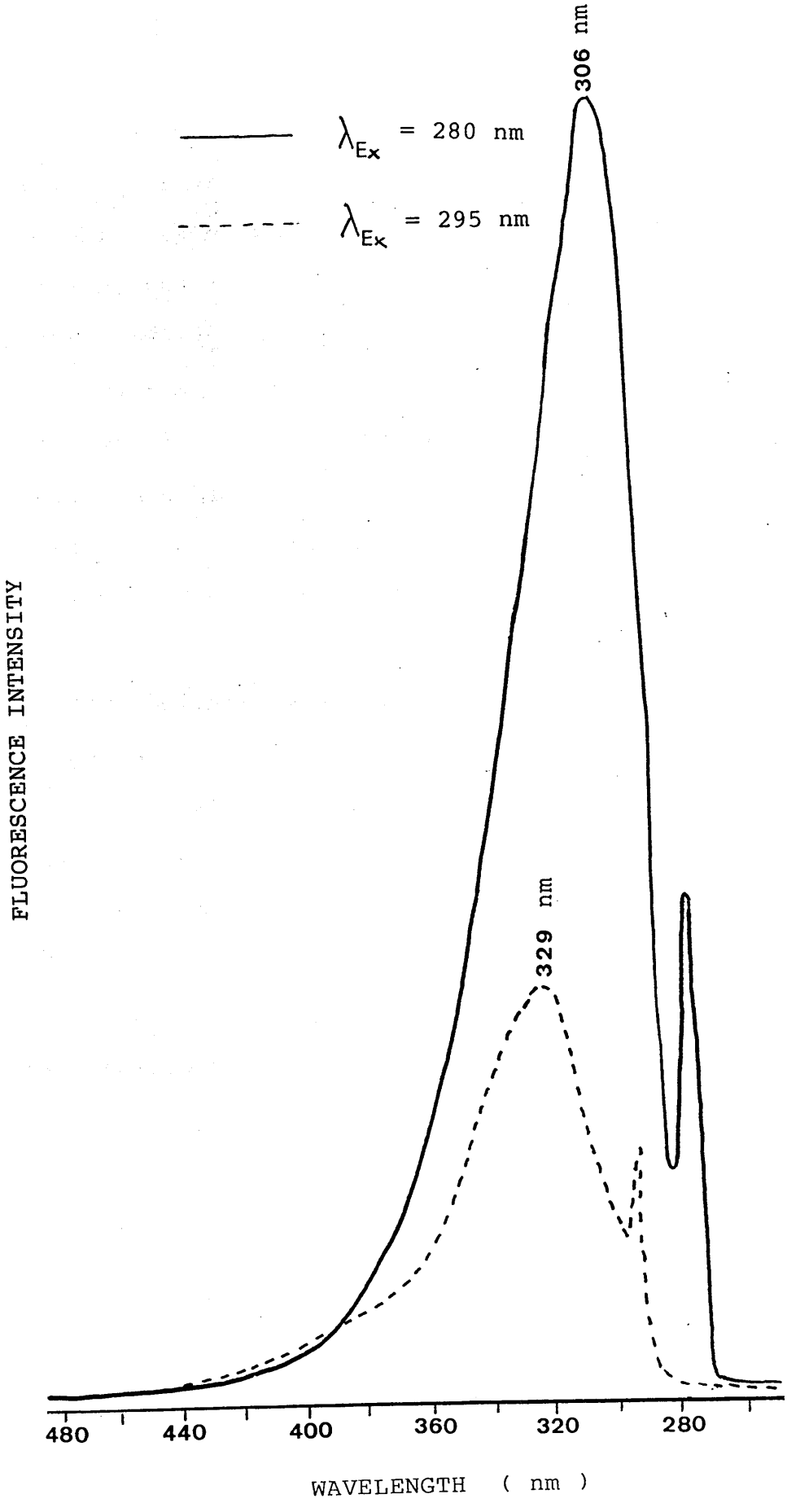

This is not so for the fluorescence emission spectrum representing tryptophan, upon irradiation by light of wavelength 295nm, where a λ_{max} of 329nm was obtained (see Table 8.1). This value is quite different from that of tryptophan in water (λ_{max}=348nm) and supports experimental findings which show that tryptophan fluorescence is greatly affected by the environmental conditions (for example, polarity, temperature) surrounding the fluorophore (Radda and Dodd,1968). The emission maxima of tryptophan fluorescence in proteins has been observed to vary from below 330nm to above 350nm (Teale,1960). This blue shift observed probably occurs as a result of shielding of the tryptophan residues from water by the protein matrix.

8.2 Fluorescence Emission Spectrum of Mutant PGK

8.2.1 Experimental

The emission experiments carried out in section 8.1.1 were repeated using a 2mg mutant PGK per ml of buffer (10mM Tris/ 90mM NaCl/1mM EDTA.Na_2,pH7.27).

Results

The results obtained are as shown in Fig.8.2 and Table8.1). The emission maximum at 328nm obtained for the tryptophan fluorescence is very similar to the value obtained for wild-type PGK. Tyrosine emission results, however, for mutated PGK and wild-type PGK are vastly different. It is found that irradiation of mutant PGK with light of wavelength 280nm induces the emission of light of maximum intensity close to that of the tryptophan emission value. A similar result was

Fig.**8.2** Fluorescence emission spectra of 0.2% mutant PGK

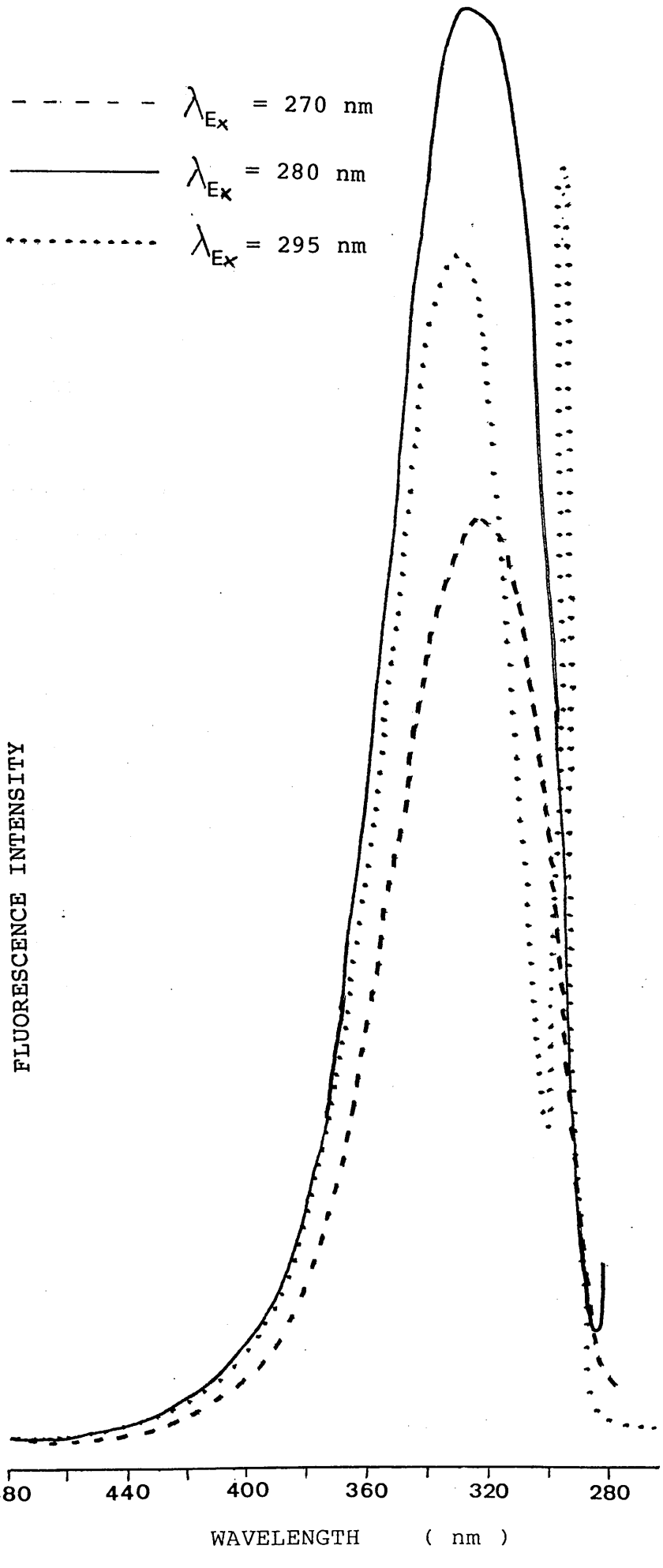

obtained when λ_{ex}=270nm. One possible explanation for this difference in λ_{max}, is that energy transfer from tyrosine to tryptophan is occurring, enhanced by the fact that the enzyme structure is less rigid in the mutated form of the enzyme. This transfer can occur without the intermediate appearance of an emitted photon, and is primarily the result of dipole-dipole interactions between the excited state donor and an acceptor. The rate of energy transfer depends upon the extent of overlap of the emission spectrum of the donor with the absorption spectrum of the acceptor, the relative orientation of the donor and acceptor transition dipoles and the distance between these molecules.

Fig.8.3 shows a graph of emission maximum as a function of the excitation wavelength. This indicates that wild-type PGK exhibits tyrosine emission below 290nm and tryptophan above this.The effect is dramatically reduced for the mutant enzyme indicating, as mentioned previously, a large amount of efficient energy transfer below 290nm, from excited tyrosine to tryptophan. This results in a tryptophan-like emission spectrum at all excitation wavelengths,possibly due to a more flexible hinge, allowing favourable energy transfer orientations to occur.

8.3 Effect of Substrate Binding on the Fluorescence Emission Spectrum of PGK

8.3.1 Experimental

Two, 980 μl solutions of mutant PGK in buffer (2mg PGK per ml of 10mM Tris/90mM NaCl/1mM EDTA.Na_2,pH7.27) were prepared. To

Fig.8.3 Variation of emission maximum wavelength versus excitation wavelength for wild-type and mutant PGK

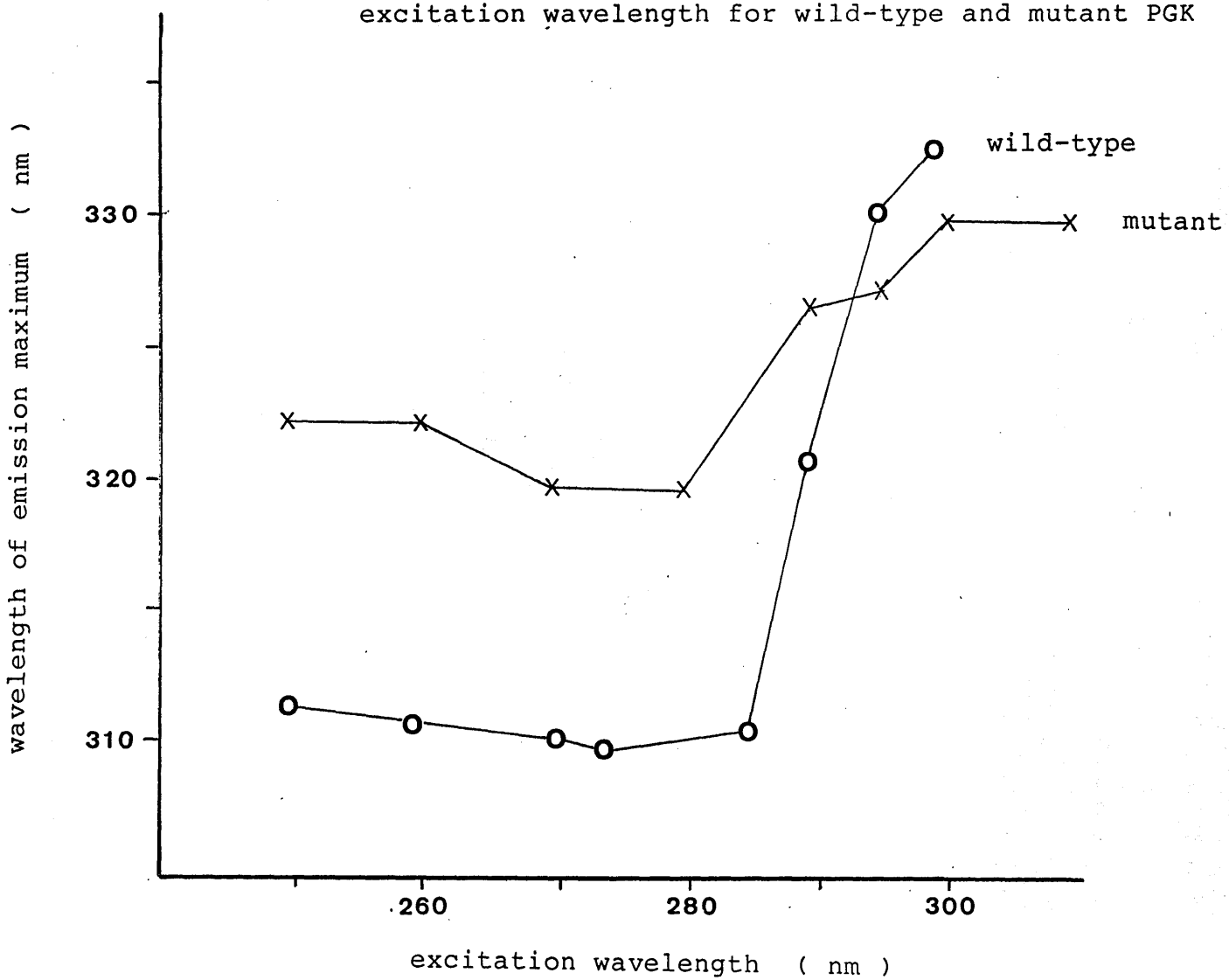

one sample was added 20μl, 100mM ATP and 20μl, 125mM $MgCl_2$ and to the other PGK sample, 20μl, 100mM 3PG. Substrate solutions were initially prepared in the same buffer as the enzyme solution.

Steady state emission spectra were recorded for each solution using excitation wavelengths of 280nm and 295nm.

8.3.2 Results

The results obtained are reproduced in Figs.8.4 and 8.5 and in Table8.2. Table8.2 indicates that there is little or no alteration of the fluorescence emission spectra of mutated PGK upon binding of the substrates MgATP and 3PG. This is in agreement with the same comparison when wild-type PGK is investigated (Dr.Dryden, personal communication).

8.4 Fluorescence Lifetimes of PGK

8.4.1 Experimental

All lifetime experiments were carried out using an Edinburgh Instruments Fluorescence Spectrometer, at the University of Newcastle upon Tyne, in collaboration with Dr.Dryden. The experiments were all repeated several times and it was found that the results were closely reproducible.

A solution of 2mg PGK per ml of buffer (10mM Tris/90mM NaCl/ 1mM EDTA.Na_2, pH7.27) was pipetted into a 1cm fluorescence cell and placed in the fluorescence spectrometer.

The flash lamp used to irradiate the sample was contained in

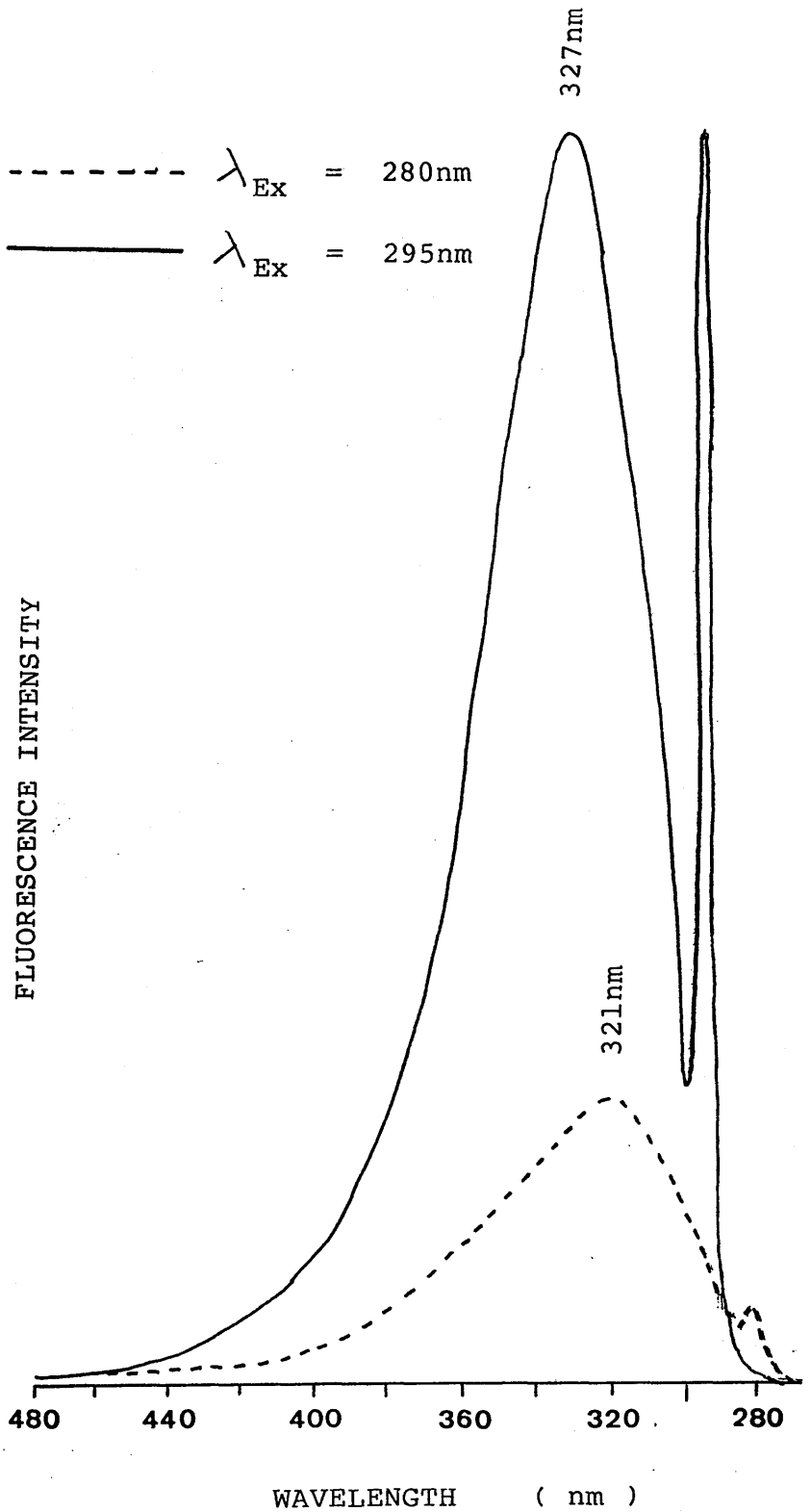

Fig.8.4 Fluorescence emission spectra of 0.2% mutant PGK + 2mM MgATP

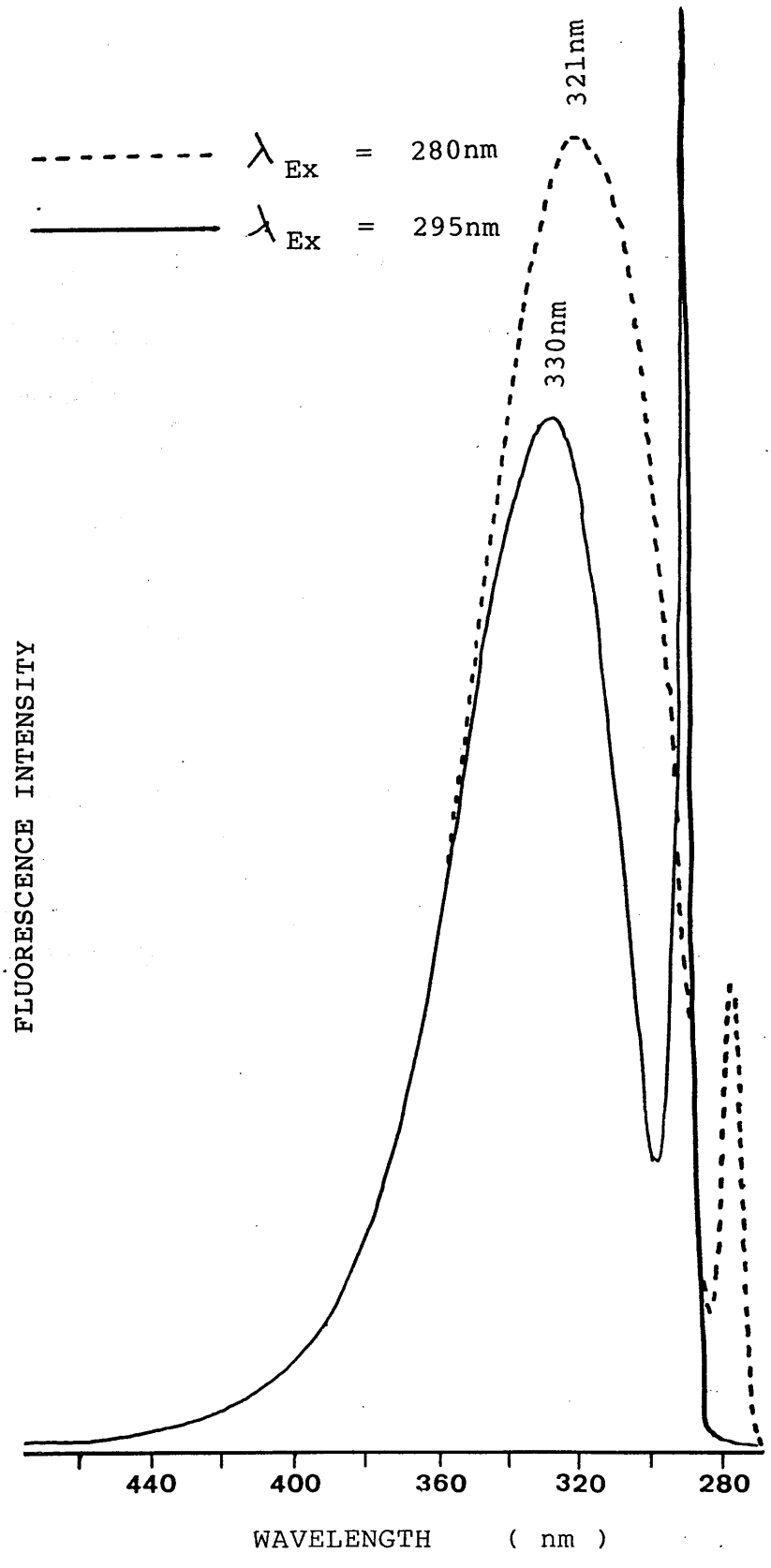

Fig.8.5 Fluorescence emission spectra of 0.2% mutant PGK + 2mM 3PG

Table 8.1 Emission maxima of wild-type and mutant PGK.

	EXCITATION WAVELENGTH		
	270nm	280nm	295nm
wild-type	---	306nm	329nm
mutant	320nm	321nm	328nm

Table 8.2 Emission maxima upon substrate binding to mutant PGK.

	EXCITATION WAVELENGTH	
SUBSTRATE	280 nm	295 nm
Mg-ATP	321 nm	327 nm
3PG	321 nm	330 nm
no substrate	321 nm	328 nm

0.5 atmospheres of hydrogen and pulsed at a rate of 50kHz. (The type of gas determines the spectral distribution of the output. Whereas nitrogen provides a number of high-intensity lines, a continuum of lines extending into the ultraviolet is available using hydrogen or deuterium). The pulse rate of the lamp was controlled by a thyratron tube, the voltage (7.5kV) of which was suitably adjusted to produce a pulse with a 1.5 nsec signal width at half height.

All experiments were performed at a temperature of 25^{o}C.

The data necessary to produce the fluorescence decay curve for the PGK solution was accumulated by the photon counting method described in section 2.4.2. As soon as possible after this measurement the time-resolved fluorescence decay of the lamp pulse must be recorded, since the lamp profiles change with time. Ludox - a very dilute solution of finely dispersed silica - was used for this purpose. Fig.8.6 is a typical diagram of the fluorescence decay of PGK and the flash lamp. From this data the computer calculates the impulse response function F(t), the decay which would be observed for an infinitely sharp excitation pulse, having first been given estimated α_i and τ_i values.

It was thought for a long time that wild-type PGK had three fluorescence lifetimes (Privat et al,1980; Stryjewski and Wasylewski,1986).More recently,however,fluorescence quenching experiments carried out by Dryden and Pain (1988) indicate that the three lifetimes observed previously are in fact an

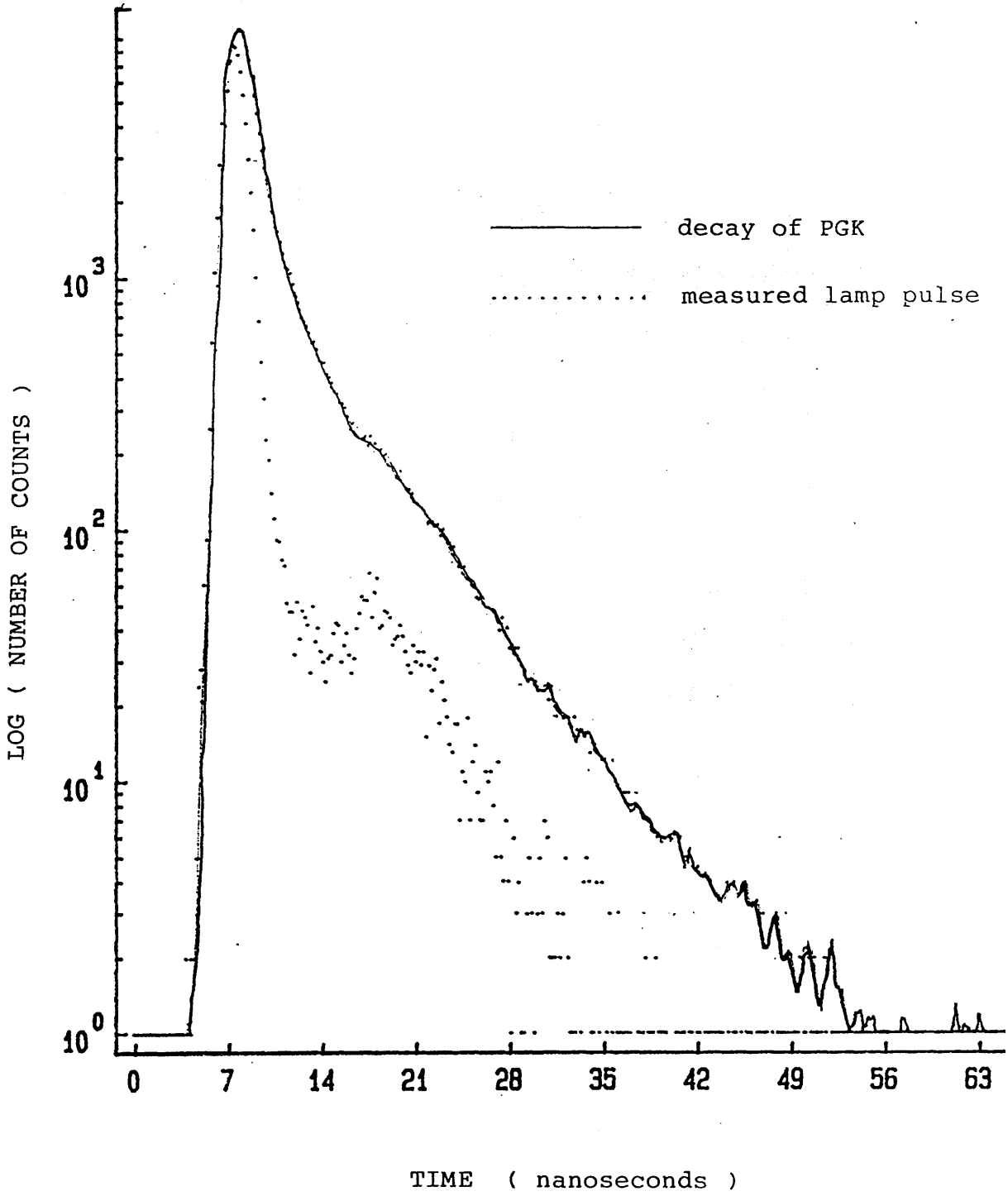

Fig.8.6 Fluorescence decay of mutant PGK-excited at 295nm

average of three unquenchable decay times exhibited by the buried Trp333 and three longer times from the surface Trp308 which can be quenched.

It was assumed that the mutated enzyme's fluorescence decay would show similar characteristics. The data therefore was fitted with three exponentials using a least-squares "Fit 3" program on the PDP 11/23 computer.

8.4.2 Results

The fitting of the fluorescence decay data for mutant PGK with three exponentials appears to have been the correct assumption, since the resulting χ^2 and residuals plots indicate a good agreement between the observed and calculated fluorescence decay curves. Fig.8.7 is an example of a typical set of results.Parallel experiments using wild-type PGK under the same conditions as for mutant PGK, were carried out. This permitted the observation of any differences between the results for the two forms of the enzyme-caused by the assumed increased flexibility of the molecule due to the replacement of His388 by Gln388.

The results using wild-type PGK were also very reproducible and a typical example of this is shown in Fig.8.8.Super-impositions of the mutant and wild-type decay curves are reproduced in Fig.8.9.

For both sets of results the lifetimes τ_1 and τ_2 are similar in value, even though the fractional contribution of

Fig.8.7 Fluorescence decay of mutant PGK-excited at 295nm

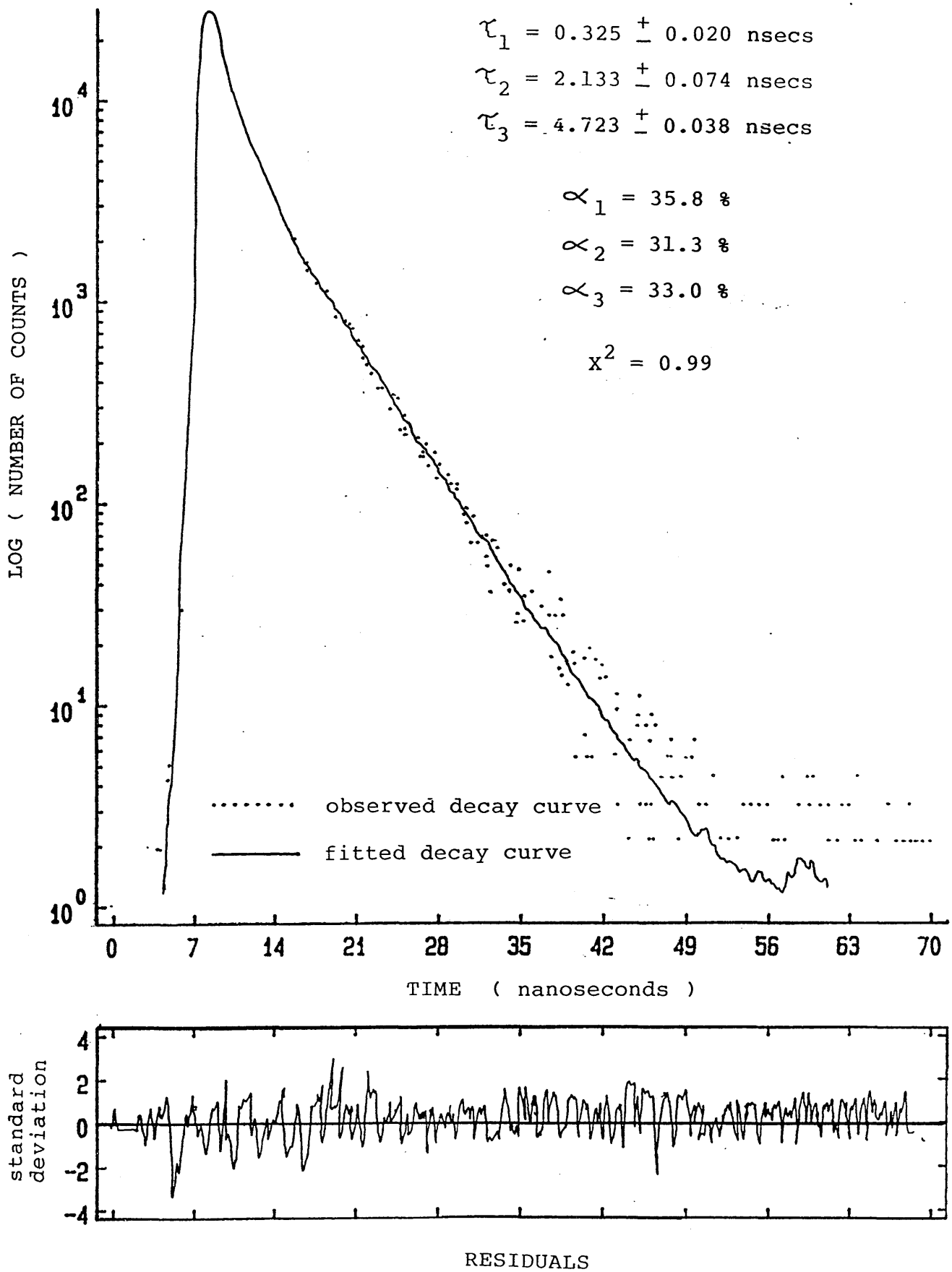

Fig.8.8 Fluorescence decay of wild-type PGK-excited at 295nm

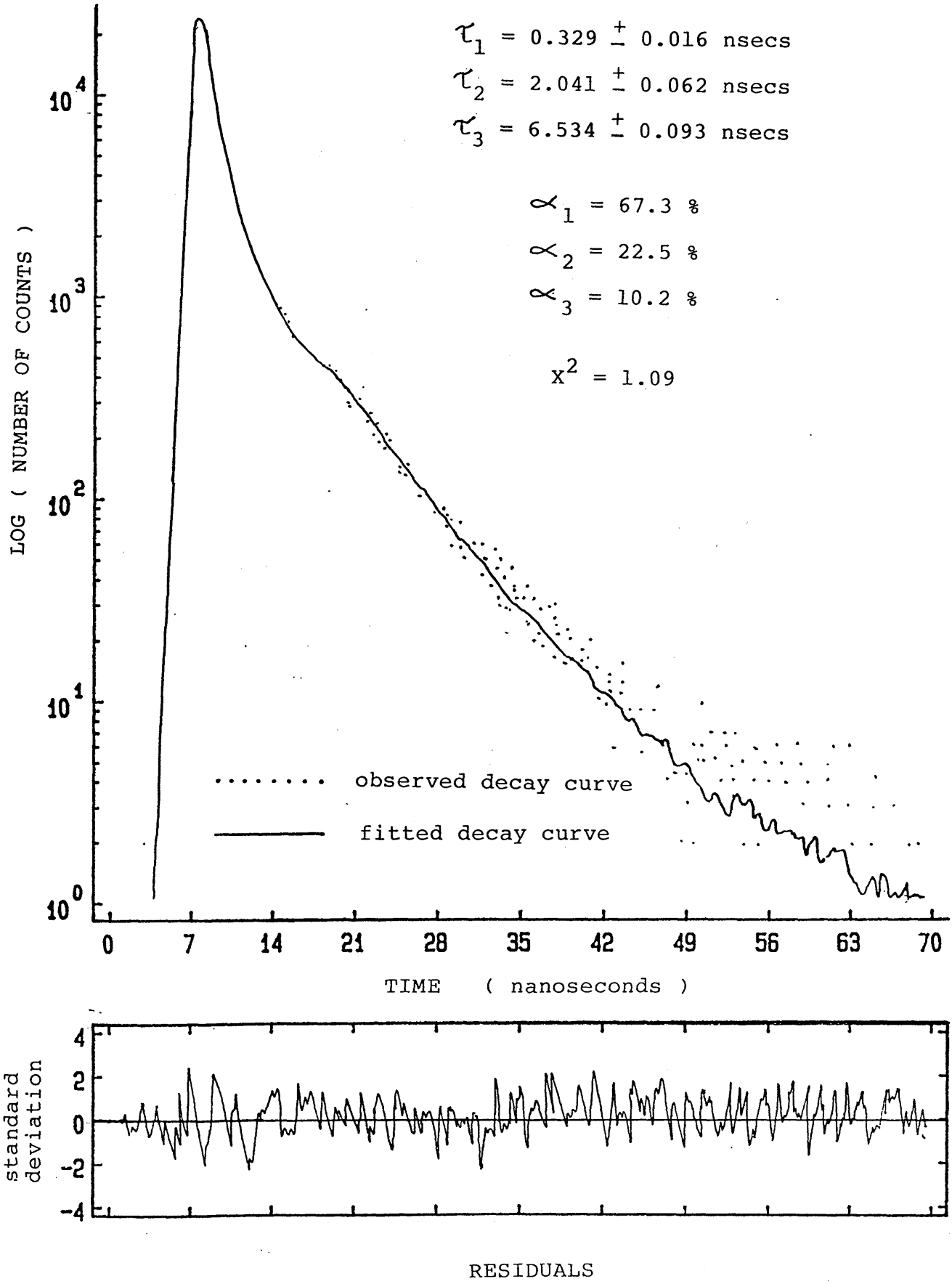

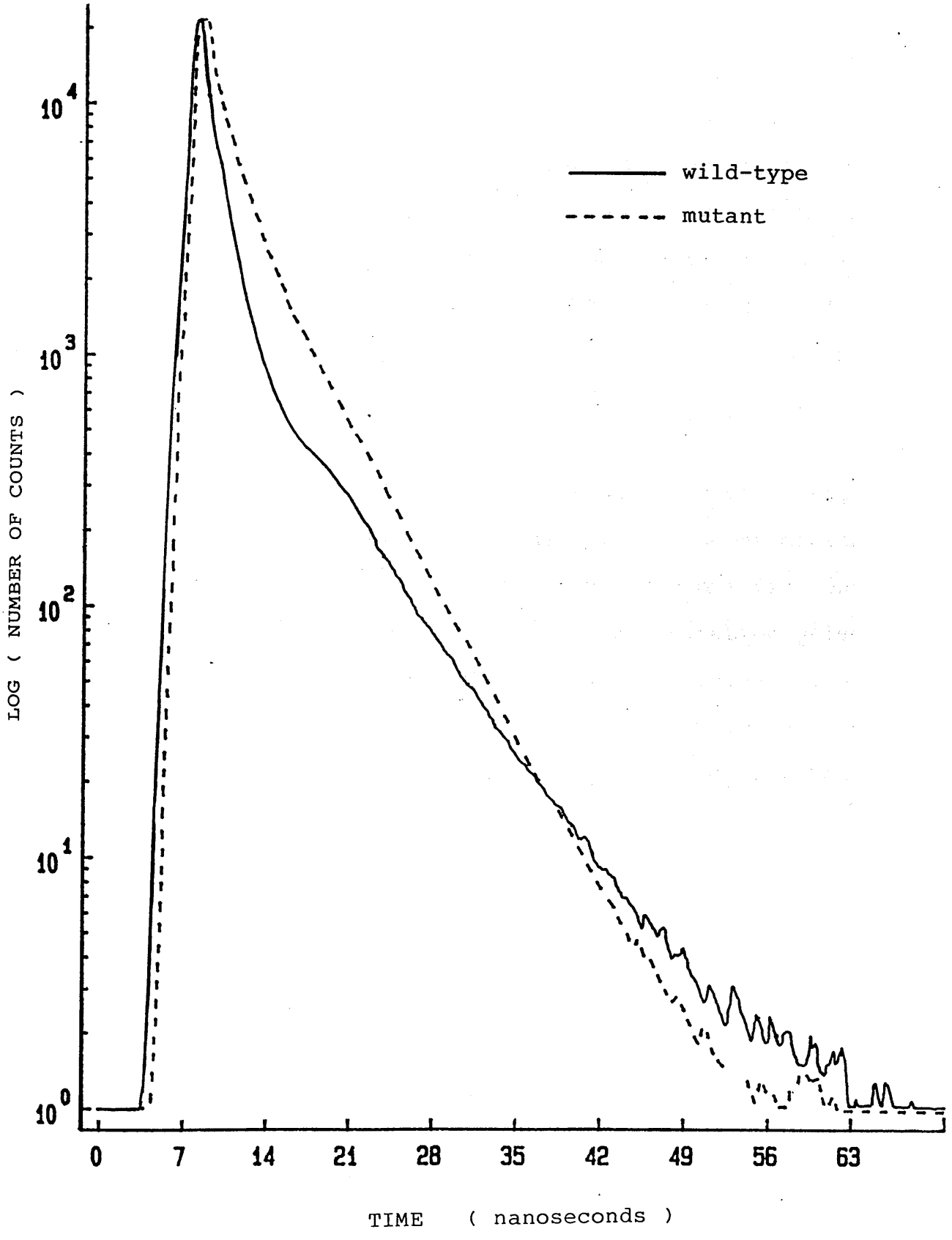

Fig.8.9 Fluorescence decay curves of wild-type and mutant PGK - excited at 295 nm.

τ_1 to the fluorescence intensity has fallen from over 67% in the wild-type enzyme to just less than 36% for mutant PGK. Comparing the τ_3 and α_3 results for both forms of PGK,there are large differences. τ_3 for mutant PGK is approximately 4.7 nanoseconds which is much shorter than the corresponding life -time of just greater than 6.5nanoseconds exhibited by the wild-type enzyme. A comparison of the contributions of this particular fluorescence decay for both enzymes shows that in most cases α_3 for mutant PGK is greater than three times as large as the same value for wild-type PGK.

It has been observed that the fluorescence decay curve of a species may vary depending on the wavelength of excitation (Weber,1961). To investigate this, the previous fluorescence lifetime experiments were repeated using excitation pulses of wavelength 280nm. The result was that the decay curves for mutant and wild-type enzyme were essentially independent of the excitation wavelength, where λ_{ex} = 280nm or 295nm (see Figs.8.10, 8.11 and 8.12). At wavelengths above 300nm and below 270nm however, τ_2 and τ_3 become slightly longer. This behaviour is even more pronounced for wild-type PGK (Dr. Dryden, personal communication) and is probably due to preferential excitation of the surface tryptophan (Trp308) which will have different absorption characteristics from the buried tryptophan (Trp333).

Fig.8.10 Fluorescence decay of mutant PGK-excited at 280nm

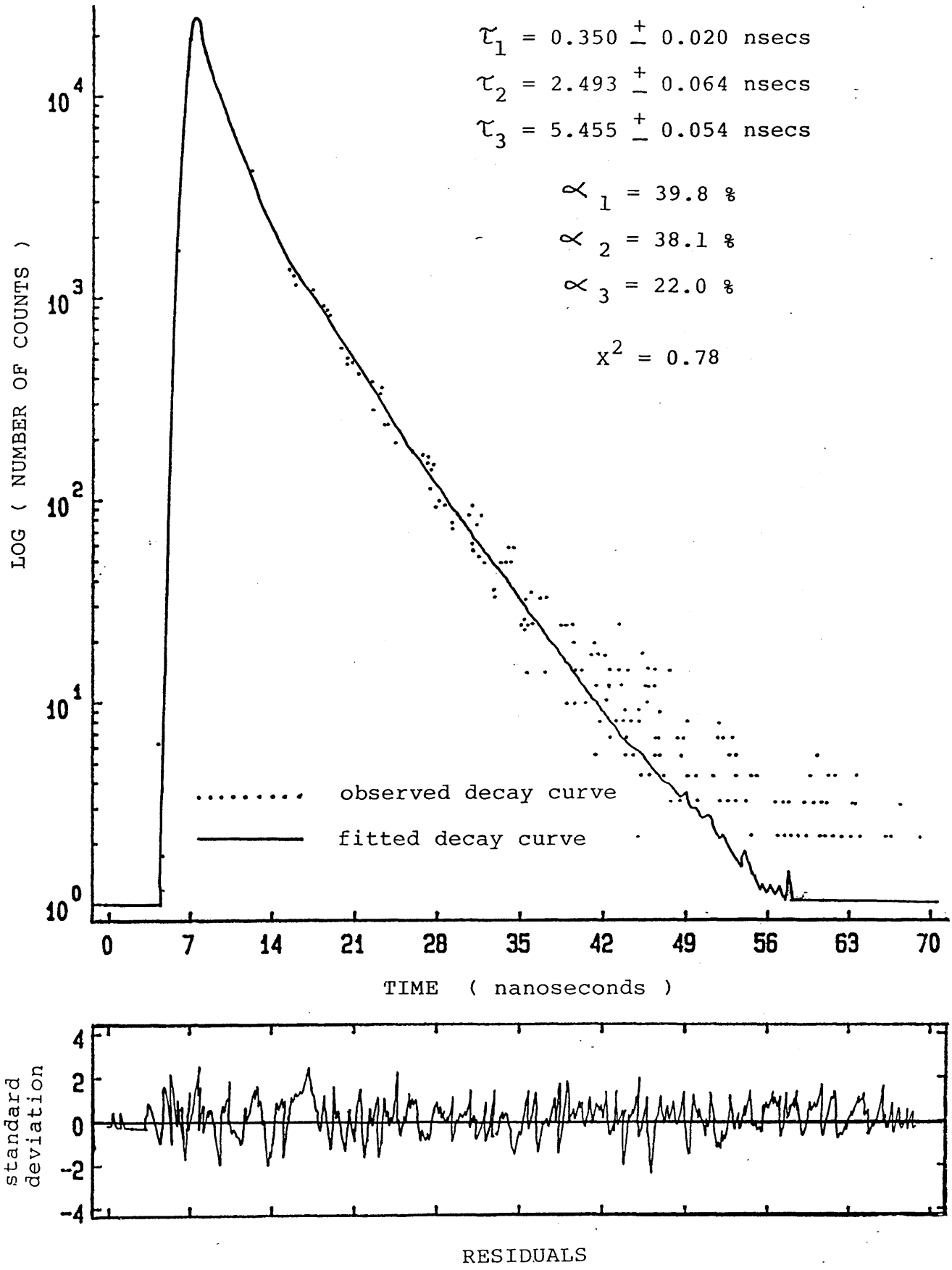

Fig. 8.11 Fluorescence decay of wild-type PGK-excited at 280nm

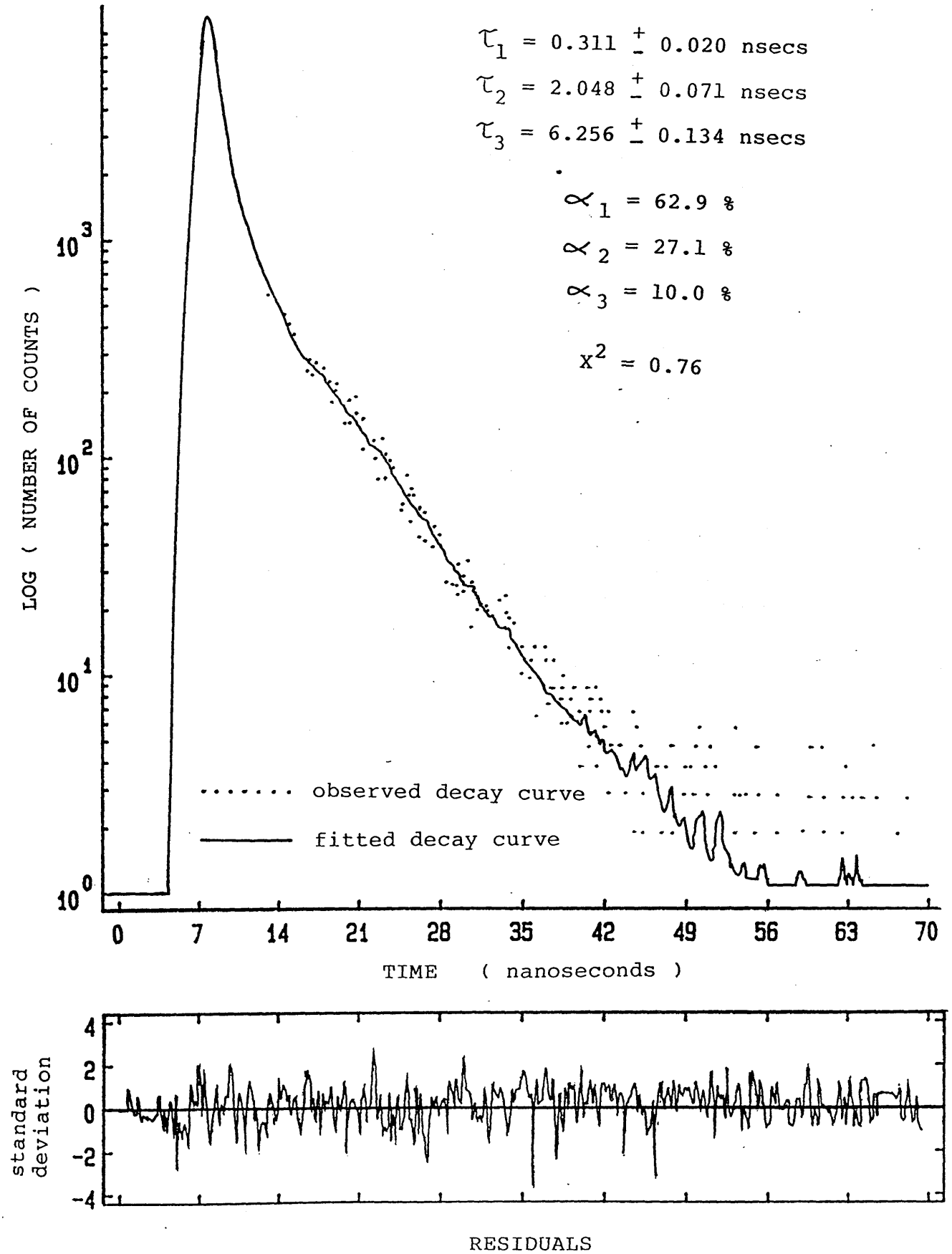

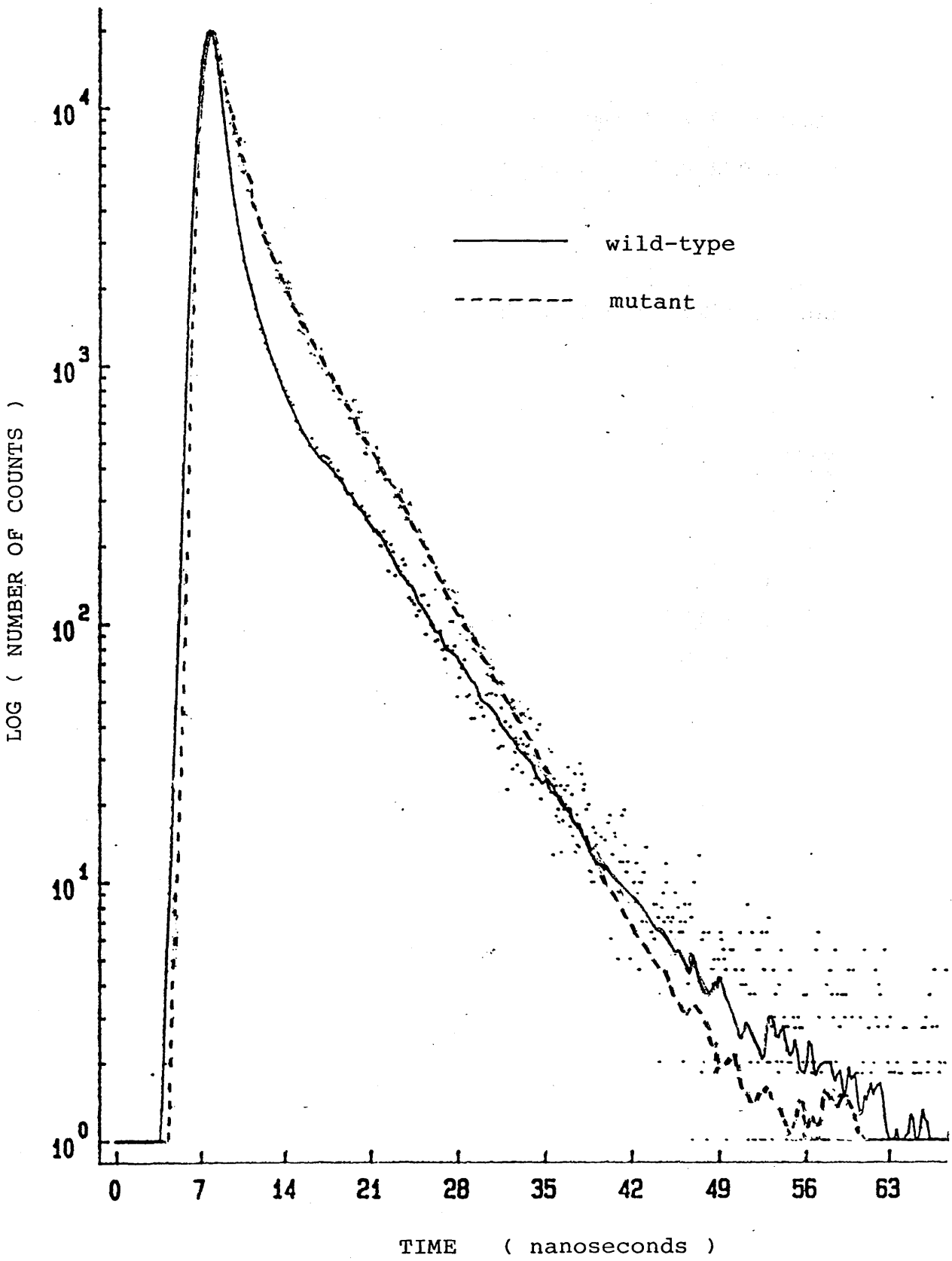

Fig.8.12 Fluorescence decay curves of wild-type and mutant PGK - excited at 280 nm.

8.5 Effect of Substrate Binding on the Fluorescence Lifetimes of PGK

8.5.1 Experimental

To 980 µl of 2mg mutant PGK per ml of 10mM Tris/90mM NaCl/1mM EDTA.Na_2,pH7.27 buffer was added 20µl of 100mM ATP and 20µl of 125mM $MgCl_2$ in the same buffer.

Fluorescence decay results were calculated as before (section 8.4).

An identical experiment was carried out when 20µl, 100mM 3PG in buffer was added to 980 µl of mutant PGK solution, identical to that used previously.

8.5.2 Results and Discussion

The pulse excitation wavelength was 295nm and all other parameters were similar to those mentioned in section 8.4.1. The results obtained are shown in Figs.8.13, 8.14 and Table8.3. As this fluorescence data indicates, the binding of ATP and 3PG do not have a large effect on the magnitude of the calculated parameters. This is a reasonable result since the two tryptophans are distant from the substrate binding sites and so the environment surrounding Trp308 and Trp333 should not be significantly altered when ATP and 3PG bind to the enzyme.

A trend similar to mutant PGK was found when the fluorescence decay results are calculated for ATP and 3PG binding to wild-type PGK (Dr.Dryden, personal communication).

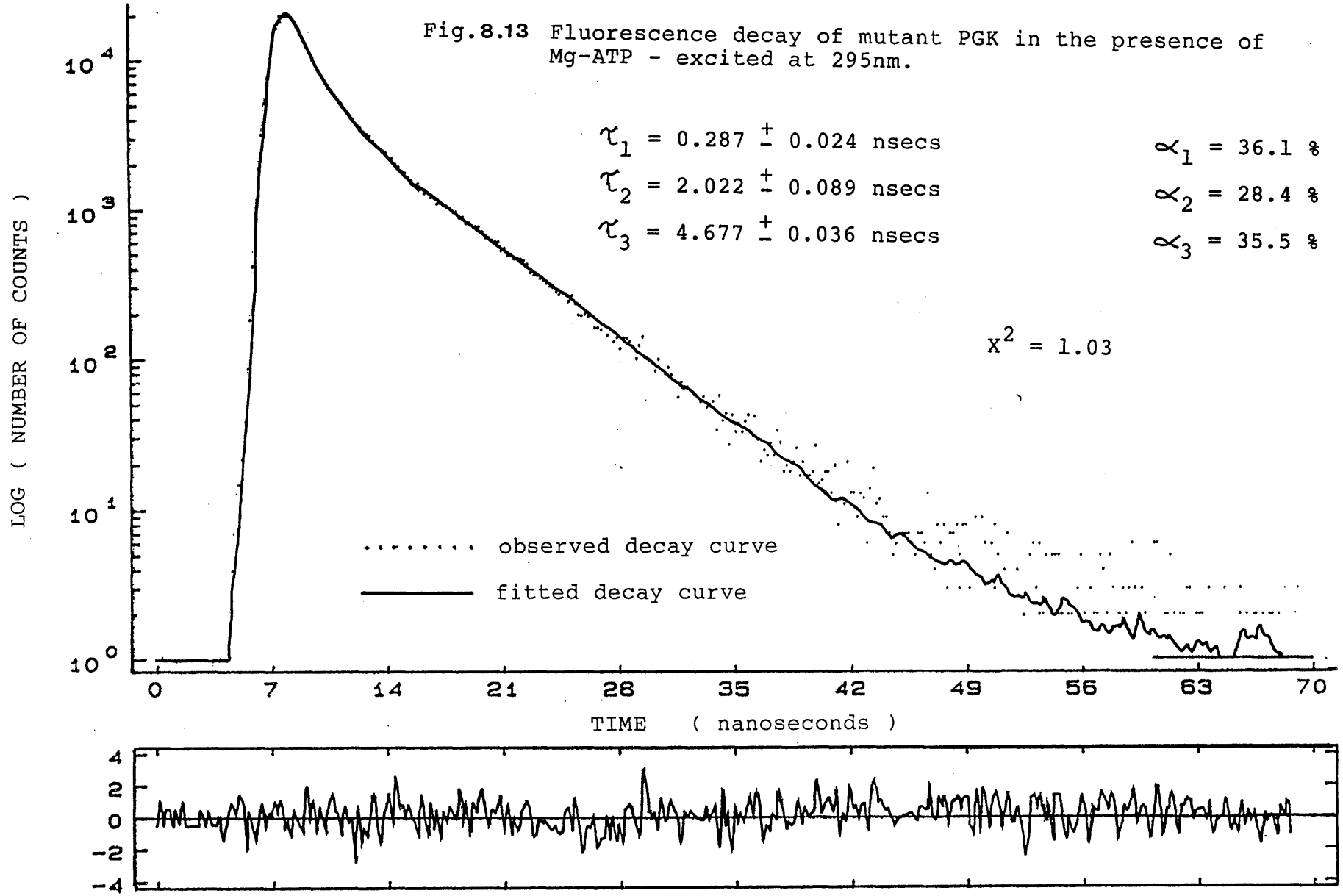
Fig.8.13 Fluorescence decay of mutant PGK in the presence of Mg-ATP - excited at 295nm.
τ_1 = 0.287 ± 0.024 nsecs
τ_2 = 2.022 ± 0.089 nsecs
τ_3 = 4.677 ± 0.036 nsecs
α_1 = 36.1 %
α_2 = 28.4 %
α_3 = 35.5 %
X^2 = 1.03
observed decay curve
fitted decay curve
LOG (NUMBER OF COUNTS)
10^4
10^3
10^2
10^1
10^0
0 7 14 21 28 35 42 49 56 63 70
TIME (nanoseconds)
4 2 0 -2 -4

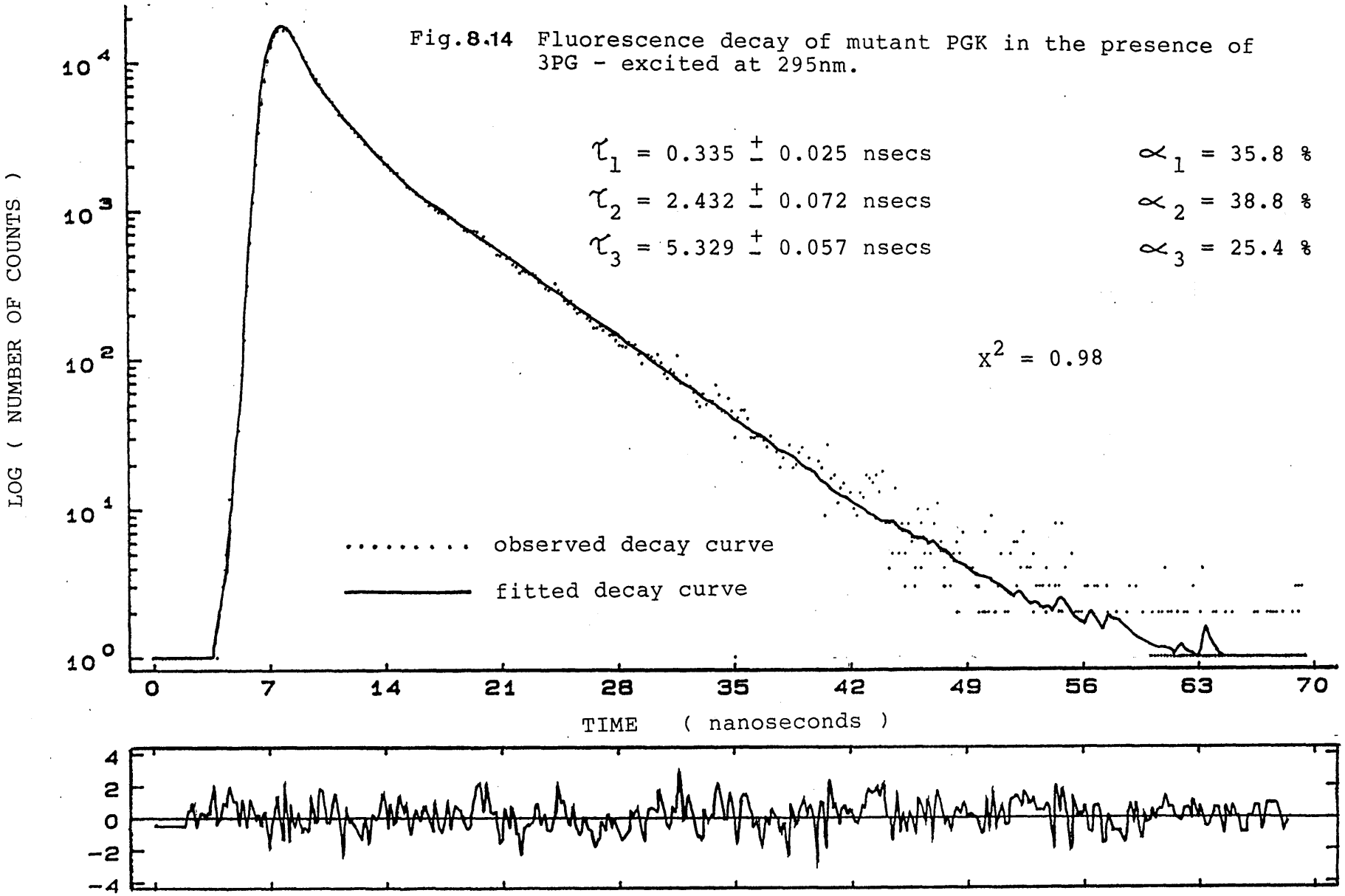
Fig.8.14 Fluorescence decay of mutant PGK in the presence of 3PG - excited at 295nm.
τ_1 = 0.335 ± 0.025 nsecs
τ_2 = 2.432 ± 0.072 nsecs
τ_3 = 5.329 ± 0.057 nsecs
α_1 = 35.8 %
α_2 = 38.8 %
α_3 = 25.4 %
x^2 = 0.98
observed decay curve
fitted decay curve
LOG (NUMBER OF COUNTS)
10^4
10^3
10^2
10^1
10^0
0 7 14 21 28 35 42 49 56 63 70
TIME (nanoseconds)
4 2 0 -2 -4

Table 8.3 Fluorescence decay data for mutant PGK with and without substrate - excited at 295nm.

	SUBSTRATE		NO SUBSTRATE
	MgATP	3PG	
τ_1 (nsec)	0.287 ± 0.024	0.335 ± 0.025	0.325 ± 0.020
τ_2 (nsec)	2.022 ± 0.089	2.423 ± 0.072	2.133 ± 0.074
τ_3 (nsec)	4.677 ± 0.036	5.329 ± 0.057	4.723 ± 0.038
α_1 (%)	36.1	35.8	35.8
α_2 (%)	28.4	38.8	31.3
α_3 (%)	35.5	25.4	33.0
χ^2	1.03	0.98	0.99

Since it is thought that fluorescence lifetime values are closely related to the tertiary structure and the dynamic properties of a protein, the lifetime results observed here imply that there has been a change in the dynamic and/or conformational properties of the enzyme, upon the introduction of a mutation. This is implied by the change in the values of α_1, α_2, α_3 and τ_3. These results are consistent with the data collected from the PGK fluorescence emission experiments - implying a dynamical change.

Assuming now that the low frequency Raman results obtained for mutant PGK do genuinely represent changes in the dynamic properties of PGK, so much so that different substrates affect the dynamics to different extents. Then if this is true, upon binding substrate to mutant PGK, it would be expected that fluorescence lifetime values for this enzyme, with and without substrate, would not be the same. This is not in fact the case - the lifetime values did not alter appreciably.In an attempt to explain these contradictory observations,the time scales over which each of the two techniques measures must be considered. In the low frequency Raman range that is being investigated (and in which changes are being observed upon substrate binding)-1 to 50cm^{-1}-the technique is able to detect fluctuations below the picosecond time scale (30 psec to 0.67psec). The fluorescence technique on the other hand is such that it can only detect processes on the nanosecond range.The fact that changes have been observed by the Raman method but not by the fluorescence technique, when substrate binds to PGK, may be as a

consequence of the time scale in which these theoretically altered fluctuations occur. Since the low frequency Raman method is capable of detecting much faster motions than can the fluorescence method, it may be that the fluctuations of interest to us are happening too quickly to be detected by the latter analysis. This would explain the conflicting results obtained by the two different methods.

CHAPTER 9

Summary and Conclusions

CHAPTER 9

SUMMARY AND CONCLUSIONS

In the past there has been extensive examination of the properties of PGK by techniques such as X-ray crystallography NMR and fluorescence spectroscopy, as well as many kinetic studies (sectionl.3). However, the dynamic and thermodynamic properties of the enzyme have not been widely considered and it is details of these investigations by microcalorimetry, laser Raman and fluorescence spectroscopies and differential scanning calorimetry that are reported within this thesis. As well as these results being important in obtaining a more complete understanding of the function of all the properties of PGK, they are also of particular importance in the pursuit of a greater understanding of the function of specific amino acids and in particular the role of non-covalent interactions occurring between them, in the control of the function and stability of the enzyme.

Flow calorimetric results indicate that the mutation has little effect on the thermodynamic parameters of substrate binding. However, preliminary thermodynamic data obtained by DSC suggests that the mutant enzyme is less thermally stable than the wild-type form.

Comparison of the conventional Raman spectra of solid samples of mutant and wild-type PGK show no major differences and this implies that introduction of the mutation has effected no gross conformational change in the macromolecule. On the

other hand,results obtained using a newly developed technique to analyse the depolarized Rayleigh scattering of solutions of mutant and wild-type PGK suggest that there may be changes in the dynamics of the enzyme upon substrate binding - for mutant PGK at least. Differences were also observed in the results of the fluorescence emission and lifetime experiments performed using both forms of PGK, although substrate binding had no detectable effect upon the original results.

The technique of flow microcalorimetry permitted the direct measurement of the thermodynamic binding parameters ΔH^{o}, K_{dis}, ΔG^{o} and ΔS^{o} when ATP, ADP and 3PG bind to PGK. Upon comparison of these binding parameters for both forms of the enzyme, the results were found to be very alike. This finding was in part expected since the mutation is in the hinge region of the molecule and not in the area of the substrate binding sites.However, it was thought that the energy for ATP binding might be slightly different for the two forms of the enzyme as it had previously been found by kinetic measurements that the K_{m} value for ATP was three times larger for binding to wild-type than binding to mutant PGK (0.23mM and 0.07mM, respectively).

The contrasting results of 3PG binding to PGK published by Hu and Sturtevant (1987) and those printed within this thesis were initially thought to have arisen because differing buffer systems were used - PIPES and Tris/MOPS respectively. However complimentary results for 3PG binding by a different calorimetric method are very similar to those reported here

and an explanation as to the source of the contradictory values has still to be sought.

Comparing the heats of binding of 3PG to PGK in two buffer systems - Tris/MOPS and PIPES - the results obtained are respectively,-20.5 and -16.0 $kJmol^{-1}$.By taking into consideration the heats of ionization of these buffers and the available pk_a data relating to 3PG bound to PGK and 3PG free in solution, the binding enthalpies imply that proton loss from the substrate (approximately 1/2 mole protons per mole of substrate) may be occurring upon formation of the enzyme-substrate complex.

Differential scanning calorimetric experiments, carried out using wild-type PGK with and without substrate bound,provided valuable information relating to the enzyme's thermal stability, heat capacity changes and the mechanism of unfolding.

PGK is observed to unfold, irreversibly at a temperature of about 53^{o}C.The presence of sulphate increases the temperature at which denaturation occurs - to about 57^{o}C. This apparent, additional stabilisation is probably due to the unfolding being accompanied by the dissociation of the bound sulphate ($T_{1/2}$ increases with increasing sulphate concentration).

Heat capacity changes are unobserved upon denaturation of the PGK sample prepared within this laboratory.

Calculation of the $\Delta H_{vH}/\Delta H_{cal}$ ratio for each experiment provides information relating to the unfolding mechanism of the PGK molecule.For example, this ratio for wild-type PGK is found to be approximately equal to 0.9 which indicates that there may be one or more intermediates occurring between the native and denatured states. In the presence of sulphate however, $\Delta H_{vH}/\Delta H_{cal}$ increases to over unity implying that there may be some degree of molecular association now occurring.This value becomes even higher, with the addition of continuously greater sulphate concentrations.

As yet successful results from the mutant enzyme have not been attained. Preliminary unfolding experiments performed on this enzyme in Prof. Sturtevant's laboratory have provided results that are not clear-cut but they do imply that this form of the enzyme is less thermally stable than the wild-type form. The fact that these results are difficult to reproduce leads to the conclusion that the PGK transition mechanism is probably fairly complicated.

Further experiments are in progress and it will be necessary to obtain this data to discover how replacement of His388 with Gln has affected the stability of the enzyme or any of the other parameters measurable by DSC.

Investigation of the dynamics of the mutant and wild-type forms of PGK using fluorescence and Raman spectroscopies produces various interesting but sometimes inexplicable results.

Low frequency Raman spectroscopy in theory provides a technique to study the collective motions of large numbers of different atoms within a protein-for example,the hinge-bending motion thought to occur with PGK. There may also be additional contributions to the Raman spectrum from rotational motions. The experiments reported within Chapter6 are the first of this kind known to be carried out and are therefore entirely exploratory.

Completely reproducible low frequency spectra of wild-type PGK, with and without substrates bound, are observed to be very alike - suggesting that no change in the dynamic properties, observable by this technique, has occurred upon substrate binding. When the same experiments are repeated with mutant PGK,small but not always reproducible,differences can be detected. These alterations involve exchanges of the distributions of the higher and lower frequency vibrations and it is tentatively concluded that there are indeed spectral changes occurring when substrate is added. As to establishing a trend however and deciding what is happening, from a dynamical viewpoint, is difficult. It can only provisionally be described as the increase in the number of lower frequency vibrations (for example with 3PG) at the cost of losing some of the higher frequency vibrations.(The opposite effect is observed with some other substrates). If this is in fact what is happening then it seems likely that it is as a direct consequence of the flexibility in the hinge region of PGK being altered, due to replacement of the His residue.

Direct comparison of the fluorescence emission and lifetime measurements for the two forms of PGK show quite different results. The high wavelength shift of the λ_{max} for tyrosine fluorescence emission, observed for mutant PGK but not for wild-type PGK is indicative of energy transfer occurring. This transfer of energy is possibly permitted in the mutant enzyme by a change in the flexibility of the polypeptide's structure - caused by the destruction of the His388-Glu190 electrostatic interaction which is thought to hold the enzyme in an "open" conformation until substrates bind.

The binding of the substrates 3PG and MgATP to mutant PGK exhibits little or no effect on the emission maximum observed for mutant PGK alone. This is a feasible result since the two tryptophans which are being excited are thought to be distinct from the substrate binding sites and so the environment surrounding Trp308 and Trp333 should not be dramatically altered when ATP and 3PG bind.

Fluorescence lifetime and emission measurements for both forms of the enzyme are also quite different and since tryptophan lifetimes are usually highly dependent upon the protein's tertiary structure, these results also support the suggestion that there has been an alteration in the enzyme's structure - possibly coincidental with a change in dynamics. Again the binding of MgATP and 3PG does not have a large effect on the magnitude of the measured parameters.For mutant PGK this observation is contrary to the results from low frequency Raman experiments which implied that the dynamic

properties of the mutant enzyme were affected by substrate binding. However the fact that no such trends are observable from the fluorescence results may arise because this technique is not capable of detecting fluctuations on the subnanosecond time scale whereas the Raman technique can.

The suggestion that there has been a change in the tryptophan environment in the mutant enzyme,as compared to the wild-type enzyme, is also partially supported by the difference in the dimensions of peaks at approximately 1335cm^{-1} and 1525cm^{-1} of the conventional Raman spectra of mutant and wild-type PGK.
To sum up therefore - the aim of the research reported within this thesis was to determine the importance of the His388-Glu 190 interaction on the dynamic and thermodynamic properties of PGK and thereby provide an experimental basis for the study of other enzymes using such techniques.

Many of the findings reported here are preliminary and any clearly defined conclusions cannot be made until further experimentation can be achieved.

SUGGESTIONS FOR FUTURE WORK

Experiments reported within this thesis have been useful in the obtainment of dynamic and thermodynamic information relating to PGK.Before continuing with these methods however, some of them require refinements, for example, maintenance of the clarity of the enzyme solution may alleviate the problems encountered when recording low frequency Raman spectra.Use of a Raman spinning cell permits for example, the direct comparison of enzyme solutions, wild-type and mutant.The cell consists of a cylindrically-shaped glass vessel, divided into two identical parts by a glass wall.In this instance one half of the cell would contain wild-type enzyme and the other half would contain mutant enzyme. The cell can be rotated by an external synchronous motor which would expose the laser beam alternately to wild-type and mutant enzyme. Thus the spectrometer and detector alternately receive signals from the two different liquids.Signal subtraction can then be accomplished electronically and a Raman difference spectrum generated.

Relating to the dynamic properties of PGK, quenching experiments similar to those performed with wild-type PGK (Pain and Dryden, personal communication) would provide information detailing whether one or both tryptophans is responsible for the change in the combined lifetime measurements observed for mutant PGK. These facts would relate directly to the changes in the tryptophans environments and possibly provide details of the conformational change of the whole molecule.

DSC measurements on mutant PGK would indicate if there has been a change in the thermal stability of the enzyme or any of the other thermodynamic properties measurable by this technique when they are compared to the results reported in chapter5 for wild-type PGK.

Investigations of 1,3-diphosphoglycerate (1,3-DPG) binding have been very limited because of the instability of this molecule - a half life of one hour.Past experiments involving 1,3-DPG (Scopes,1978b) indicate that it binds approximately one thousand times more strongly than the other three substrates and its dissociation from the enzyme is thought to be the rate determining step of the back reaction. The energetics of binding of this substrate to PGK and its effects on the dynamic properties of the enzyme would be of interest. Firstly however, it would be necessary to modify either the experiments to accomodate for the problems of 1,3-DPG instability or the method of preparation and storage of the substrate.

It would also be of interest to analyse the effect of binding model substrates to the enzyme. For example, a molecule with an "ATP-like" end and a "3PG-like" end, which was approximately 12Å long, would presumably bind to the two active sites and remain there, securing the enzyme in the open conformation. The opening and closing conformational fluctuations would,in theory,be prevented and so the dynamic properties of the open form of PGK could be analysed. Calorimetric heats of binding of this simple bifunctional molecule

could be investigated with reference to the binding of ATP and 3PG.

As well as the mutant PGK investigated within this thesis, many more are or will be available in the near future. These include PGK's with changes of amino acid residues at substrate binding sites, the hinge region and various other positions thought to be important in the catalytic process. The work proposed here should lead to a greater understanding of the action of PGK and other enzymes which employ major molecular movements to effect catalysis.

APPENDICES

A Isolation of Wild-Type PGK from Freeze-Dried Bakers Yeast

B Media used for the Growth of Bakers Yeast

C Tests for Phosphate Esters

D Surface Enhanced Raman Scattering

APPENDIX A

Isolation of Wild-Type PGK from Freeze-Dried Bakers Yeast

The initial method used to isolate PGK was from dried bakers yeast (Sigma Chemical Co.) following the published method by Scopes (1971 and 1975). This involved overnight autolysis of the yeast followed by four ammonium sulphate precipitation steps. The enzyme solution was then dialysed, treated with protamine sulphate and eluted from a CM-cellulose column by gradient elution. Upon a further ammonium sulphate precipitation step, the precipitate was dissolved in buffer and passed through a Sephadex gel-filtration column to allow collection of the almost pure protein.

Other purification procedures were also investigated (Conroy, 1983; B.Adams, PhD Thesis, University of Newcastle upon Tyne) -derivations of Scopes' method-and each one was carried out separately. It was not possible however to reproduce the quantities of purified PGK which had been obtained by the named authors-about 1g of PGK per 500g dried yeast. Even by combination of these methods it was still not possible to perfect a procedure which produced consistent results.

APPENDIX B

Media used for the Growth of Bakers Yeast

(1) amino acid stock solutions

AMINO ACID	CONCENTRATION (mg/ml)
Adenine	10
Histidine	10
Methionine	10
Tryptophan	10
Uracil	10

(2) Media

	COMPONENTS	CONCENTRATION (g/l)
YPG	Glucose	20
	Bactopeptone	10
	Yeast extract	10
YO	Yeast nitrogen base (without amino acids)	6.7
	Glucose	20
Top Agar	Glucose	20
	Yeast nitrogen base (without amino acids)	6.5
	Agar	30
	Sorbitol	220
	(+ amino acids at 50 μg/ml)	

Bottom Agar	Glucose	20
	Yeast nitrogen base (without amino acids)	6.5
	Agar	20
	Sorbitol	220
	(+ amino acids at 50 µg/ml)	

(3) Transformation solutions

(a) 1M Sorbitol/0.025M EDTA,pH8.0

(b) 1.2M Sorbitol/0.01M EDTA/0.1M NaCitrate,pH5.8

(c) 1.2M Sorbitol

(d) 1.2M Sorbitol/0.01M $CaCl_2$

(e) 0.01M $CaCl_2$/0.01M Tris,pH7.5

(f) YPG/Sorbitol :

COMPONENT	CONCENTRATION (g/l)
Glucose	20
Bactopeptone	10
Yeast extract	10
Sorbitol	220

APPENDIX C

Tests for Phosphate Esters

(1) Molybdate-perchloric acid (Dawson et al,1969)

This method depends on the hydrolysis of phosphate ester to inorganic phosphate in the presence of molybdic acid,followed by reduction of the phosphomolybdate formed to produce blue spots.

method

Spot the solutions to be tested onto filter paper, then spray with the mixture:

60% (w/v) perchloric acid : HCl : 4% ammonium molybdate : H_2O

= 5 : 10 : 25 : 60

The paper is then dried at 85°C for one minute and exposed to U.V. radiation. All organic phosphates including those hydrolysed with difficulty, now give blue spots whereas inorganic phosphate gives a yellow spot.

(2) Test-tube method

Three stock solutions were required:

(a) 70% Perchloric acid

(b) 5% Ammonium molybdate

(c) 0.5g 1-amino-2-naphthol-sulphonic acid + 30g $NaHCO_3$ + 6g Na_2SO_4,dissolved in 250ml water and then filtered.

method

Place 1ml of sample to be analysed with 0.2ml of solution (a) and heat to boiling for about one hour. Allow the mixture to cool before adding 0.2ml solution (b) and then 0.1ml solution (c). If the solution turns blue this implies the presence of organic phosphate.

APPENDIX D

Surface Enhanced Raman Scattering

Normal solution Raman scattering (NSRS) has already been introduced in chapter2. The effects observed are relatively inefficient processes, about 10^{-3} of the intensity of the incident exciting radiation appears as Rayleigh scattering and approximately 10^{-6} as Raman scattering. Fleischmann et al (1974) however, discovered that pyridine adsorbed on a silver surface produced an anomalously intense Raman spectrum of this molecule. This is now a well established phenomenon and in his early review on SERS, Van Duyne (1977) estimated that the expected scattering intensity from the adsorbed molecules is 10^5 to 10^6 times stronger than for non-adsorbed species at the same bulk concentration.

The most common, suitable substrates for adsorbed molecular species, in addition to the roughened silver electrodes on which this phenomenon was first observed (Fleischmann et al, 1974;Albrecht and Creighton,1977;Pettinger and Wenning,1978; Allen et al,1980), include colloidal metal particles (Creighton et al,1979; Von Raben et al,1981; Siiman et al, 1983) and vacuum-deposited metal island films (Yamada and Yamamoto,1981; Pockrand,1982). As well as these substrates, other experimental methods which produce similar results have been used (Kerker,1984).

The initial observations of SERS for adsorbates on gold (Creighton et al,1979; Wetzel and Gerischer,1980; Blatchford et al,1982), silver (Fleischmann et al,1974; Creighton et al,

1978 and 1979; Kerker et al,1980a; Lepp and Siiman,1985) and copper (Allen et al,1980; Temperini et al,1981; Creighton et al,1983) have been extended to include hydrosols and organosols of aluminium, cadmium, lithium, nickel (Yamada and Yamamoto,1981), palladium and platinum, as well as copper and iron derivatives (De Rooy et al,1980).

In the past few years there has been an enthusiastic interest aimed at elucidating the origin of SERS (Chang and Furtak, 1982). The most important information found indicates that the degree of Raman intensity enhancement is dependent on the state of division of the metal surface and is greatest for surfaces which have been electrochemically roughened. The enhanced Raman scattering for silver surfaces prepared in this way shows a marked increase in the excitation wavelength through the visible region (Creighton et al, 1978).It is also notable that particles of the copper, silver and gold group metals exhibit strong electronic plasma resonances in the visible region and as a result of this, colloidal dispersions or island films have distinct colours. The wavelengths of these resonances are highly dependent upon the size and shape of the particles and on their proximity to each other, and thus the colours of the colloids vary depending on the method of preparation and the state of aggregation (Blatchford et al,1982).

Metal sols are characterised by a special type of scattering called Mie scattering which is due to resonant excitation of the conduction electrons in the metal particles. Enhancement

is greatest when the excitation wavelength is close to that of the Mie band (Mie,1908). Since then, Kerker et al (1980a and 1980b) have developed a theory which shows that the Raman scattering by molecules adsorbed at the surface of a metal sphere may be enhanced by the order of up to 10^6 by large local fields near the surface, if the radius of the sphere is much less than the wavelength of the exciting light. Ideally, the radius should be less than 0.02 λ (Wang and Kerker,1981). In addition, it has been clearly demonstrated by measurements on silver and gold colloids (Blatchford et al,1972; Creighton et al,1979) and on silver island films (Weitz et al,1982) that if the absorption spectrum is changed of a dye coating on the island films, there is a related change in the surface Raman profiles.

Although it has been the consensus of opinion that at least the major proportion of SERS intensity arises from the large electromagnetic fields that occur at the surface of small metal particles, or the bumps and undulations of roughened electrodes and thin metal films, one universal model to describe these effects has not yet been agreed upon (Philpott,1975; Moscovits,1978; Furtak and Reyes,1980; Blatchford et al,1983). It has also been argued that although electromagnetic resonances and superatomic roughness do contribute to the overall enhancement in Raman spectroscopy from adsorbates on metal surfaces, there are many results which cannot be understood exclusively on the basis of electromagnetic resonance. One conclusion that has been reached is that there must exist at least one additional

enhancement mechanism, which is called the "chemical effect". One model for such a chemical effect is a dynamical charge transfer excitation of an electron from the metal to the adsorbate, giving rise to a resonance effect in the Raman cross-section of the adsorbate (Persson,1981; Ueba,1983a and 1983b). A different approach was described by Burstein et al (1979) and Otto et al (1984), involving the movement of an electron from the metal to the adsorbed molecule resulting in a negative ion, which has a different equilibrium geometry compared with the neutral adsorbate. This charge transfer process induces a nuclear relaxation in the adsorbate which, after the return of the electron to the metal, results in a vibrationally excited neutral molecule. Such a resonance scattering type of mechanism would result in the observed short-range enhancement of the Raman scattering.

Hence, speculations to account for SERS falls into two major categories.A purely physical mechanism in which the molecules are presumed to respond to gigantic electromagnetic fields generated locally by collective oscillations of the free electrons in small metal structures. In addition, so-called chemical mechanisms are envisioned as charge transfer processes, between metal and adsorbate or else formation of a molecule-metal atom complex with consequent molecular resonances. Contributions to SERS from each of these two mechanisms, electromagnetic and chemical, are not mutually exclusive.

SERS of Biomolecules

The phenomenon of SERS has been widely used in the study of small molecules binding to metal surfaces (Kerker et al, 1980a; Lippitsch,1980; McQuillan and Pope,1980; Garrell et al,1981) but more recently it has been used in order to elucidate the behaviour of chemisorbed biomolecules (Koglin and Sequaris,1986). This method of studying biomolecules has several advantages. Firstly, the high enhancement factor of the Raman scattering intensity by the adsorbed biomolecules creates a new technique for obtaining high resolution vibrational spectra of biomolecules from very dilute aqueous solutions; down to micromolar concentrations and below (Lippitsch,1981; Cotton and Van Duyne,1982; Suh et al,1983). Consequently, only very small amounts of material are needed and this is especially important if the compounds are not available in large amounts, because they are difficult to prepare or very expensive. A second advantage of the SERS method arises from the fact that many biomolecules have a very low solubility in water and normal Raman spectroscopy usually requires an aqueous solution of biomolecules with concentrations greater than 2%, in order to obtain a reasonable signal-to-noise ratio. For example,obtaining NSR spectra of some anabolic agents is impossible. Vibrational spectra of these compounds have been obtained however, by means of SERS in the presence of colloidal silver particles (Koglin and Sequaris,1986).

A further use is in the application of SERS to fluorescent products which provides discrimination of the fluorescence

with respect to Raman scattering, by surface enhancement of the latter (Lippitsch,1981).

One limiting factor of this method arises from the observation that there is a very rapid decay of SERS with increasing distance of the molecule under investigation from the metal surface (Gersten and Nitzan,1980; Kerker et al, 1980c). Thus in small molecules such as benzene, with dimensions of approximately 0.6nm, all vibrations of the molecule can be enhanced (Lippitsch,1980). In large biomolecules, on the other hand, with diameters of several nanometers-haemoglobin for example is 6nm in diameter-only groups which are attached directly to the surface will yield SERS (Koglin et al,1985). SERS, however, is still a potentially useful technique and has been widely used to investigate modified DNA (Sequaris et al,1985) and its interactions with antitumor agents (Sequaris et al,1984) as well as many other biological substances (Cotton et al,1980 and 1982; Lippitsch, 1981; Takahashi et al,1986). There have also been a number of recent investigations involving proteins, the SERS signals from which can provide specific information about the direct interaction of the surface active protein sites with a charged surface (Koglin and Sequaris,1986). These spectra show strong bands corresponding to the aromatic amino acid side chains (Nabiev et al,1983).

A considerable number of investigations have been carried out involving biological chromophores excited at a suitable wavelength, resulting in combined resonance Raman and surface

enhanced resonance Raman scattering (SERRS) (Itabashi et al, 1983; Copeland et al,1984; Nabiev et al,1985).

Given this background, it was thought that this technique might help solve some of the technical difficulties-such as aggregation at high concentrations encountered in Raman studies of PGK and other proteins of interest.

EXPERIMENTAL

Preparation of Silver Colloids

method 1

Silver sol was prepared following the procedure adopted by Creighton et al (1979). Solutions of 2mM sodium borohydride and lmM silver nitrate were made up in distilled water and cooled to ice temperature. One volume of the $AgNO_3$ solution was slowly added, dropwise to three volumes of $NaBH_4$. The mixture was continuously stirred, to aid monodispersity, and a clear, yellow-brown solution formed as all the $AgNO_3$ was added.

Visible absorption spectra of the resultant solution, for example Fig.D.1, obtained with a Pye Unicam SP 8-200 spectrophotometer, indicate a strong absorption peak at 398nm. This is characteristic of silver particles substantially smaller than the wavelength of light (Doremus,1964).The colloid was stable for several months if stored at $4^{o}C$.

method 2

Method 1 was repeated using potassium borohydride as a replacement for sodium borohydride.

Fig.D.1 Absorption spectrum of aqueous silver colloid

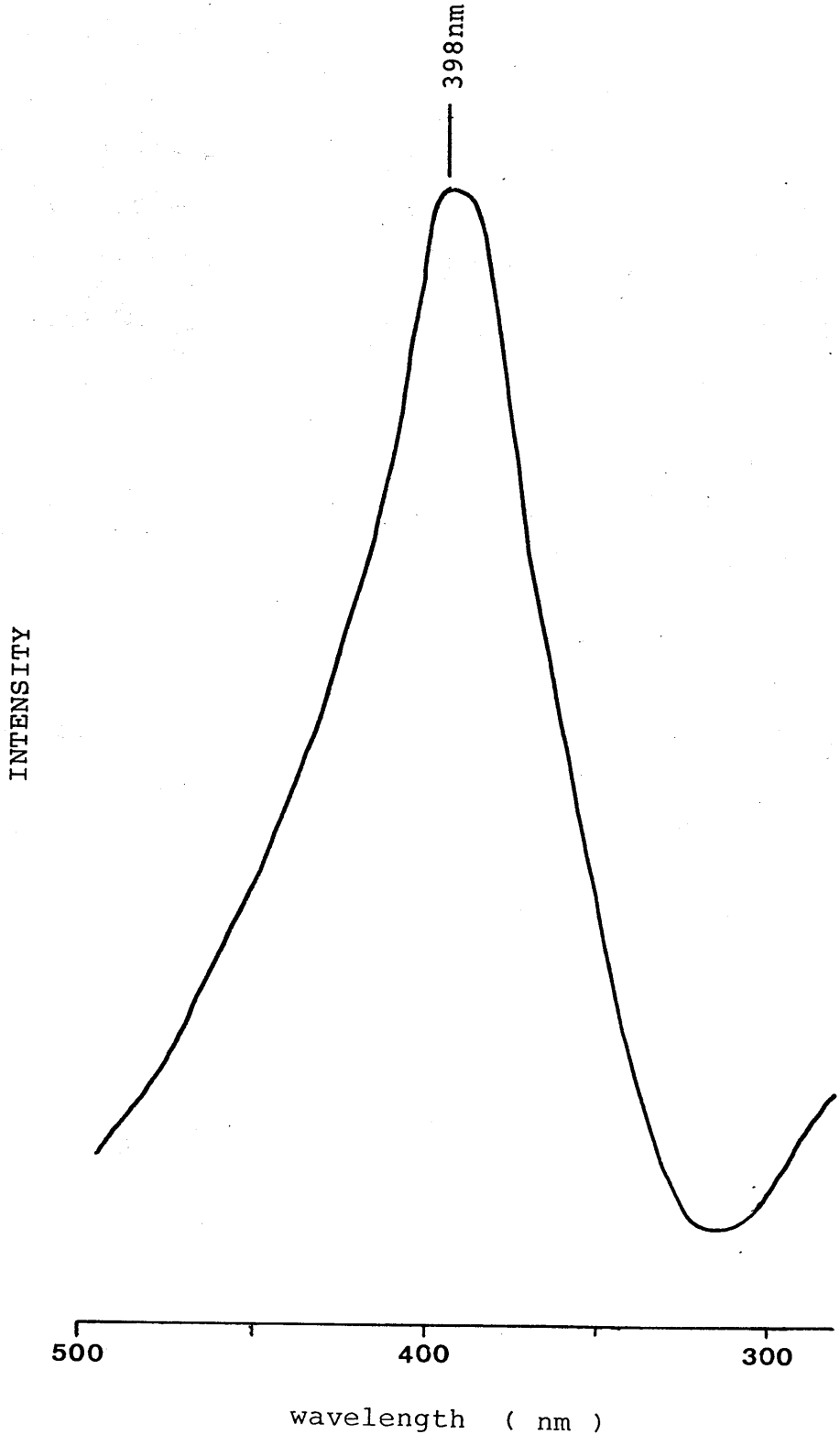

A clear yellow-brown colloid was produced with an absorption maximum at 398nm. This colloid, however, was not as stable as that prepared using $NaBH_4$ and overnight the solution acquired a greenish tint.

Preparation of Copper Colloids

This preparation was originally carried out by Creighton et al (1983). An aqueous solution of copper (II) sulphate (5ml, $2X10^{-2}M$) was added to a trisodium citrate solution (60ml, $2.8X10^{-3}M$). Into this mixture was stirred 30ml of freshly prepared $2X10^{-2}M$ $NaBH_4$ in $1.9X10^{-2}M$ sodium hydroxide. The resulting colloid, originally dark yellow-brown in colour, turned yellow-green overnight due to aggregation.
Substituting KBH_4 for $NaBH_4$ and repeating this preparation resulted in a pale green colloid forming which turned cloudy after one hour.

From the observations made on each of the colloids formed by the various methods, it was decided that the silver colloid prepared by method 1 would be used in subsequent experiments because it was easiest to prepare, the most stable and its properties correlated well with those described by Creighton et al (1979) and other authors using this preparation.

SERS of Pyridine + Silver Colloid

Pyridine was added to a sample of the Ag sol such that the final concentration of the pyridine is 25 μM. The yellow coloured colloid immediately turned red and the resulting absorption spectrum is reproduced in Fig.D.2. The appearance

Fig.D.2 Absorption spectra of silver colloid and silver colloid + 25 μM pyridine

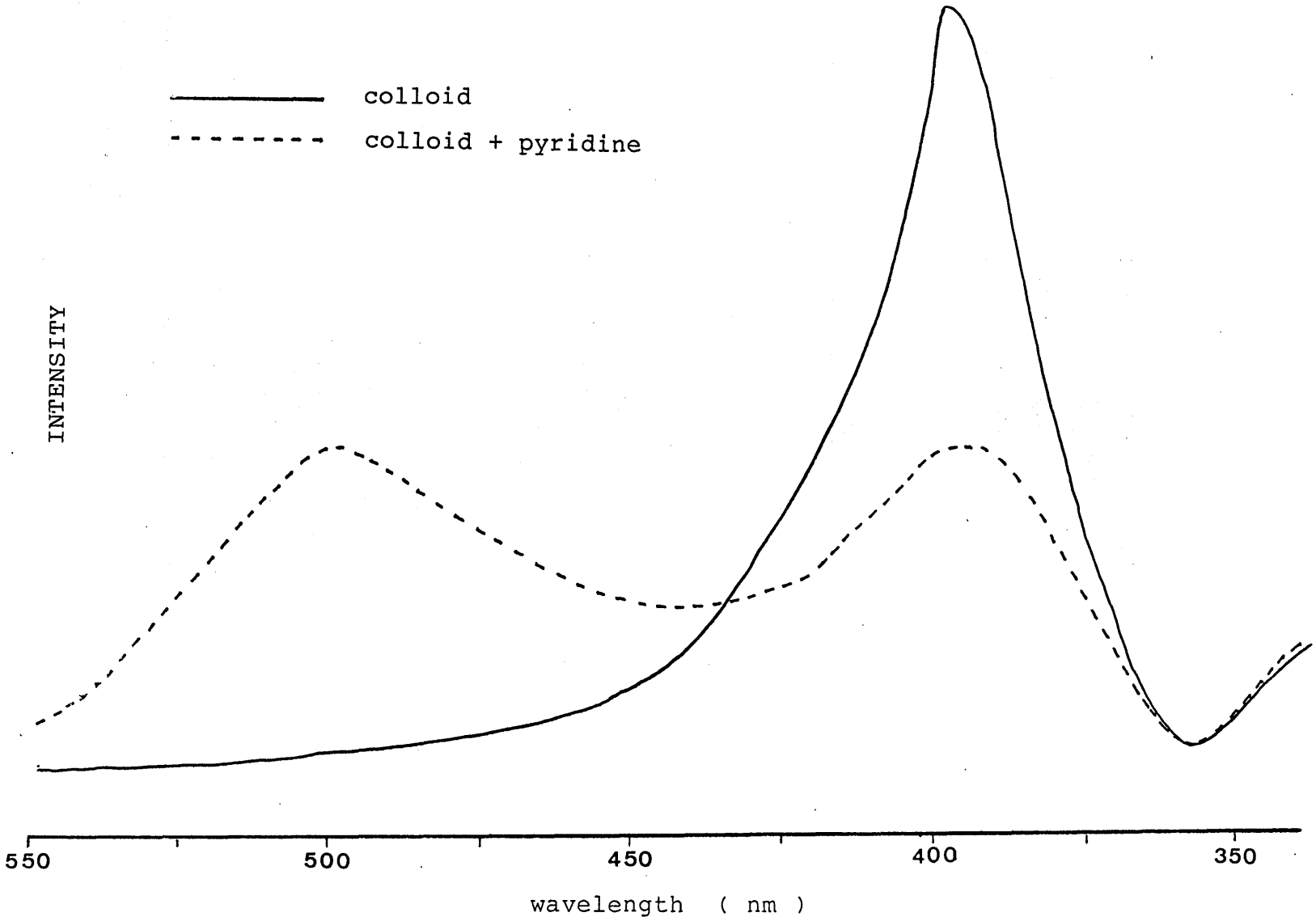

of the shoulder on the long-wavelength side of the 398nm band of the absorption spectrum is indicative of particle growth and coagulation. This has been confirmed by electron microscopy (Creighton et al,1983).

The resulting SERS spectrum is shown in Fig.D.3 and the bands observed are consistent with those published for SERS (Creighton et al,1979) and NSRS (Stidman and Dilella,1979) spectra of pyridine.

The spectrometer settings used to record the spectrum of pyridine and subsequent SERS spectra detailed within this appendix are shown in TableD.1.

SERS of Amino Acids + Silver Colloid

A typical protein chain is formed by the peptide repeating unit $(-CO-NH-C_{\alpha}HR-)_n$ where R is an aliphatic or aromatic side chain of the amino acid. Most of the observed Raman bands of proteins come from these side chains, particularly the aromatic side chains. For the interpretation of SERS spectra of proteins it is first necessary to discuss the surface enhanced Raman spectra of aromatic amino acids. These spectra were first presented by Nabiev et al (1983) and have been repeated within this appendix, using concentrations of two orders of magnitude less than those required for obtaining the non-resonance Raman spectra of amino acids.

D-Tyrosine

D-tyrosine (Sigma Chemical Co.Ltd.) solutions were made up in Ag colloid to a final concentration of $0.2-0.5 mgml^{-1}$. The

Fig.D.3 Raman spectrum of silver colloid and silver colloid + 25 μM pyridine

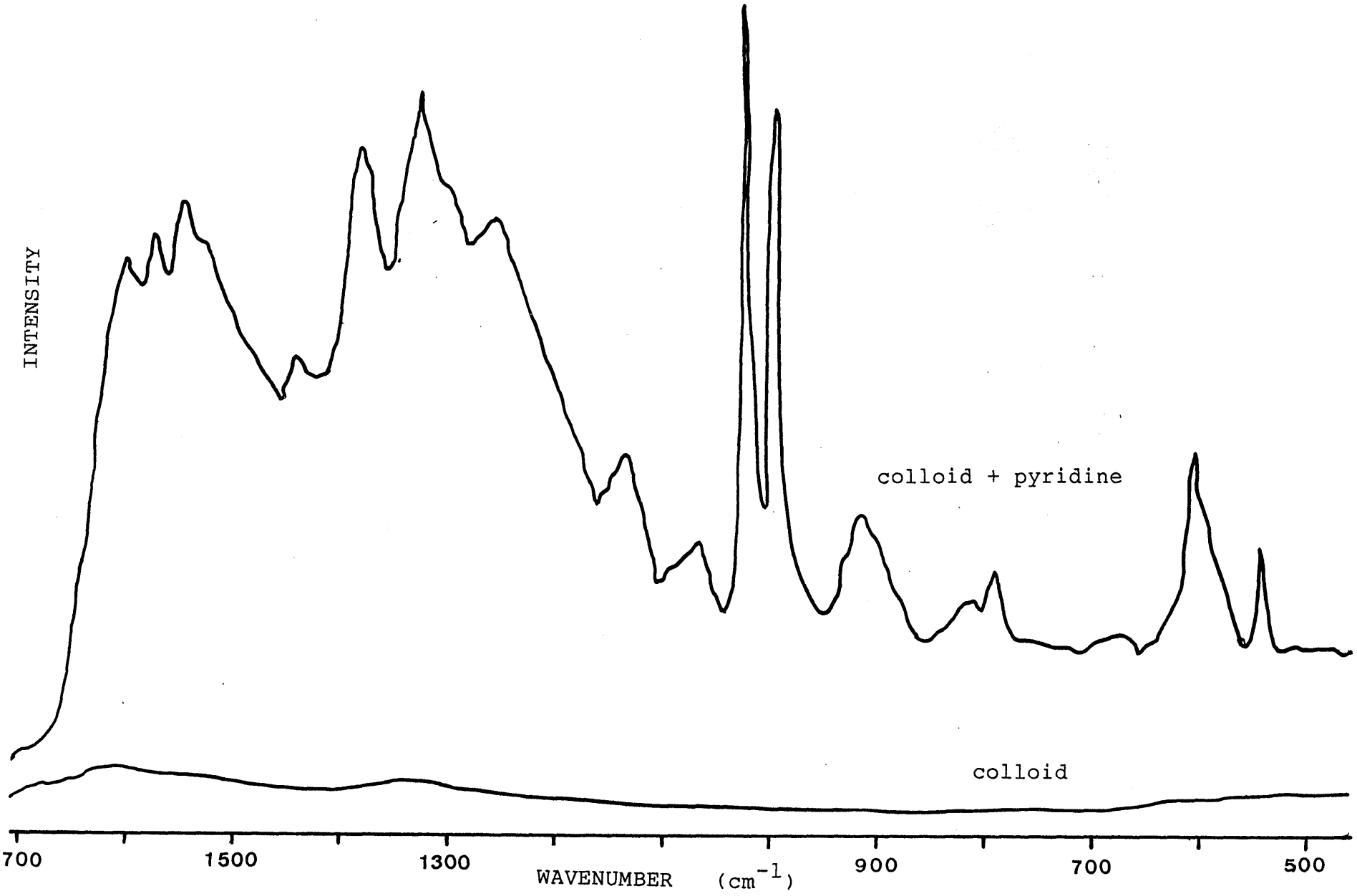

Table D.1 Raman spectrometer settings for recording SERS spectra

Laser line (nm)	488
Power (mW)	200
PM voltage (V)	1.5
Scan rate (cm^{-1} min^{-1})	50
Slits (μm)	500,500,500,500
Count time (secs)	1.2

solution was orange in colour and the absorption and SERS spectra obtained are reproduced in Figs.D.4 and D.5, respectively.

There is acceptable similarity between the SERS bands and those bands observed in the Raman spectra of solid tyrosine. In some cases it was noticed that the colour of the colloid + tyrosine solution changed slightly while it sat in the path of the laser beam and so the absorption spectrum was rerun after each SERS spectrum had been recorded (Fig.D.4).

L-Tryptophan

L-tryptophan (Sigma Chemical Co.Ltd.) solutions were prepared in Ag colloid to a final concentration of $0.5 mgml^{-1}$. Upon addition of the adsorbate, the colloid changed colour to orange with a decrease in the main absorption band of the sol at approximately 398nm and the appearance of a long-wavelength band at about 490nm (Fig.D.6). Fig.D.7 indicates the SERS spectrum recorded.This plot also corresponded favourably with those previously published.

L-Phenylalanine

L-phenylalanine (Sigma Chemical Co.Ltd.) solutions of concentration $0.5 mgml^{-1}$ were made up in siver colloid and the resulting solution was orange-red in colour. The observed absorption spectrum and SERS spectrum are reproduced in Figs.D.8 and D.9, respectively. Raman bands observed for the SERS spectrum were found at similar frequency shifts to those occurring in the spectra of solid and concentrated solutions of phenylalanine (Nabiev et al,1983).

Fig.D.4 Absorption spectra of silver colloid and silver colloid + 0.2 mg/ml tyrosine

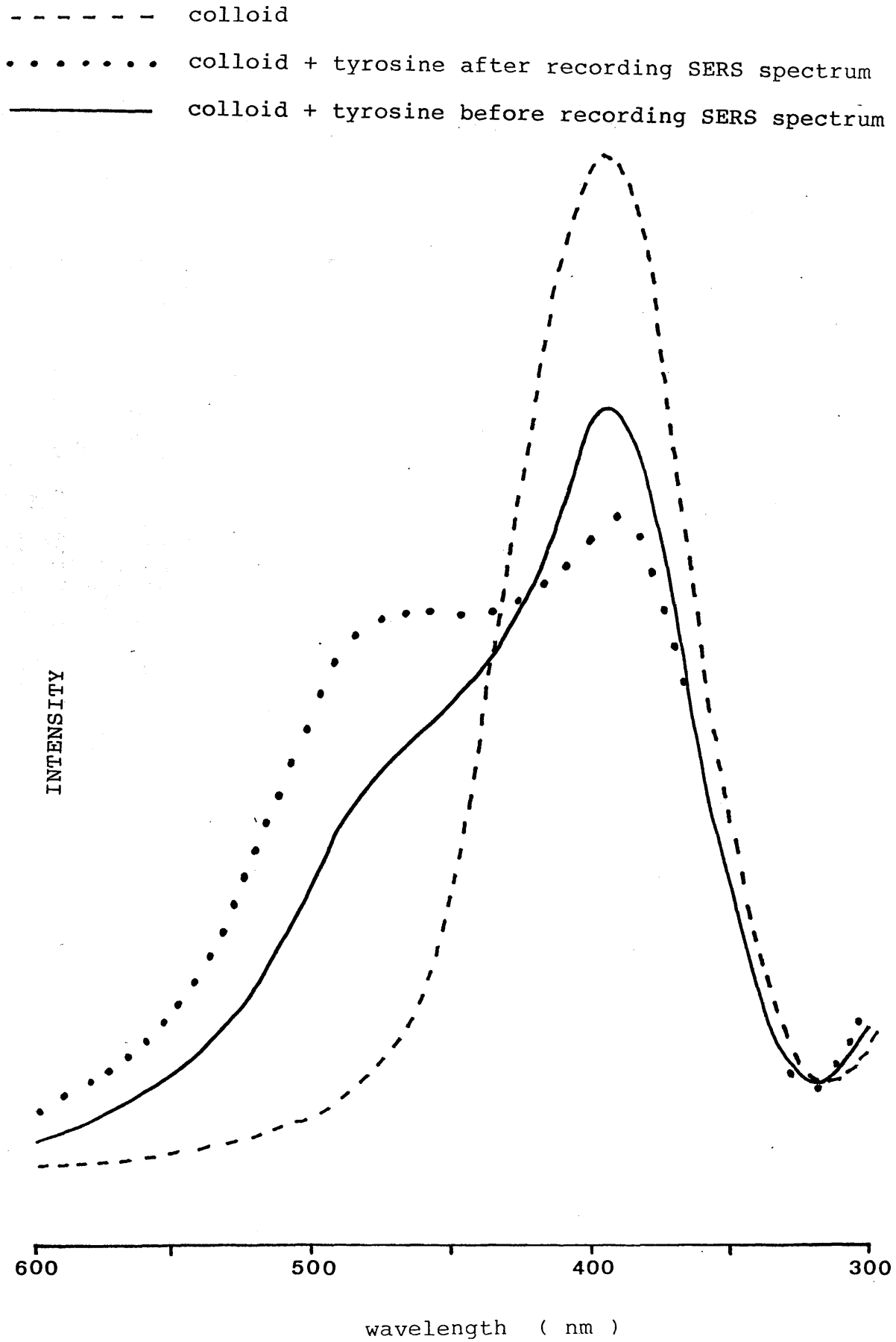

Fig.D.5 Raman spectra of colloid - tyrosine complex and aqueous tyrosine solution

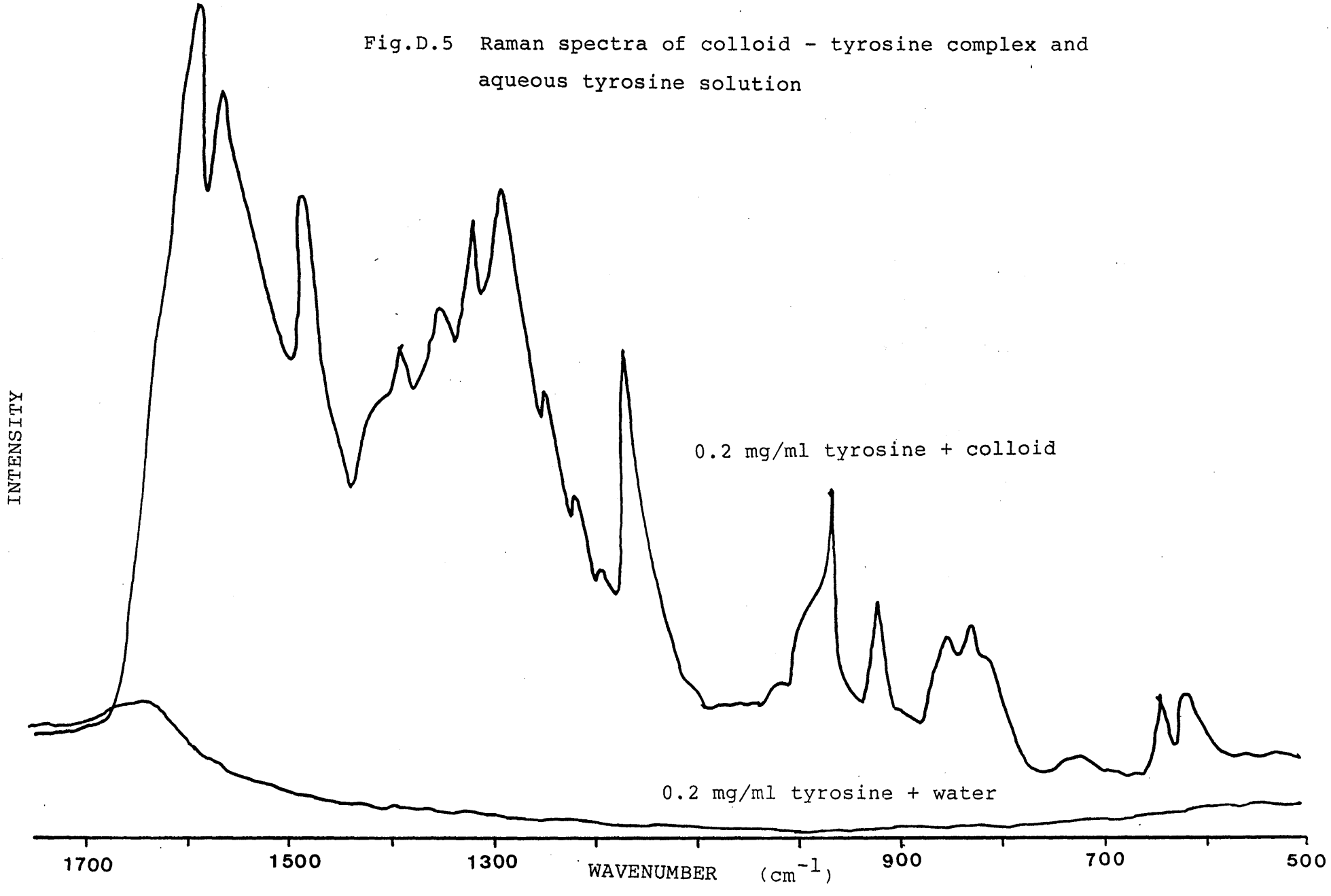

Fig.D.6 Absorption spectra of silver colloid and silver colloid + 0.5 mg/ml tryptophan

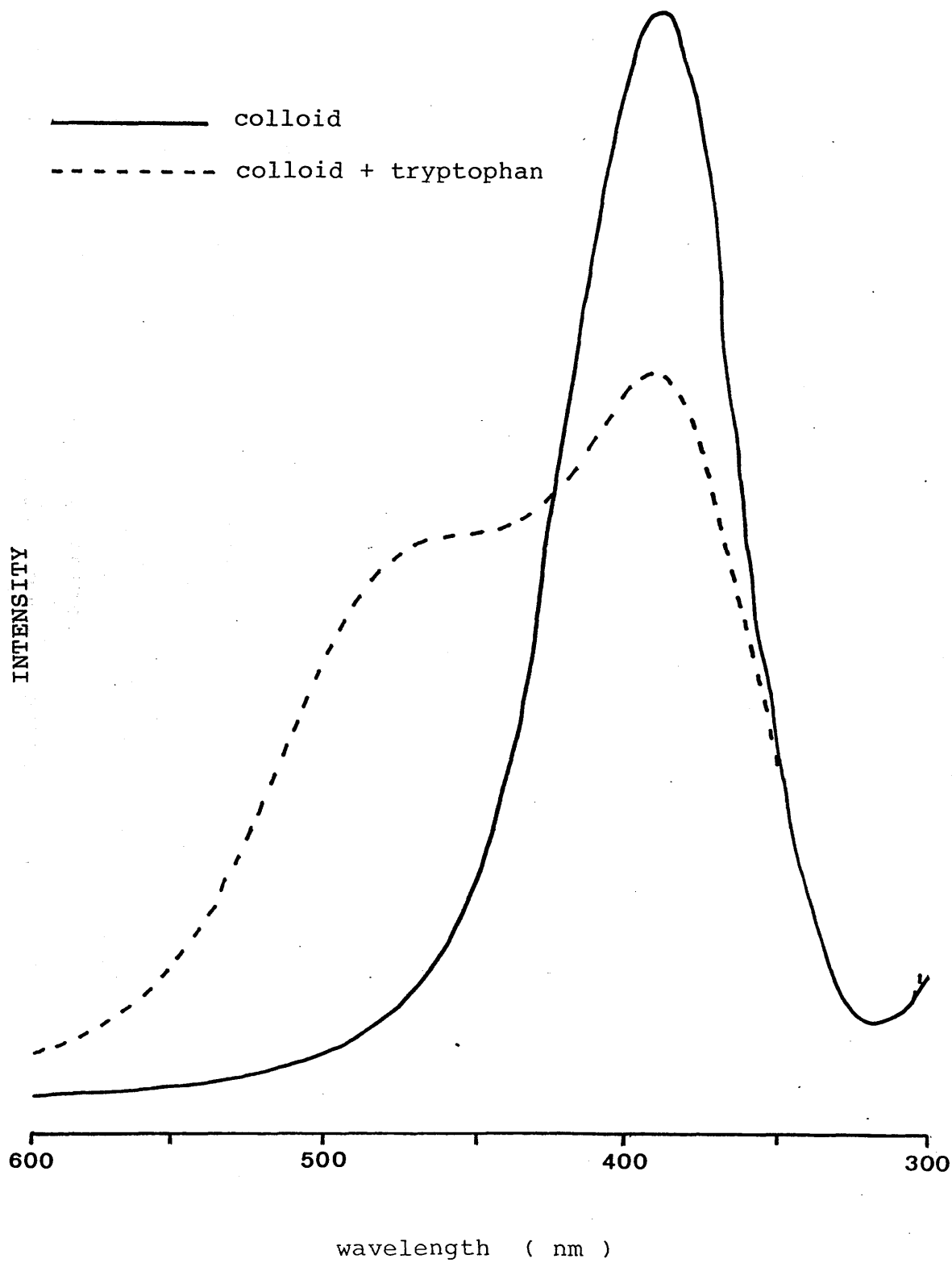

Fig.D.7 Raman spectra of colloid - tryptophan complex and aqueous tryptophan solution

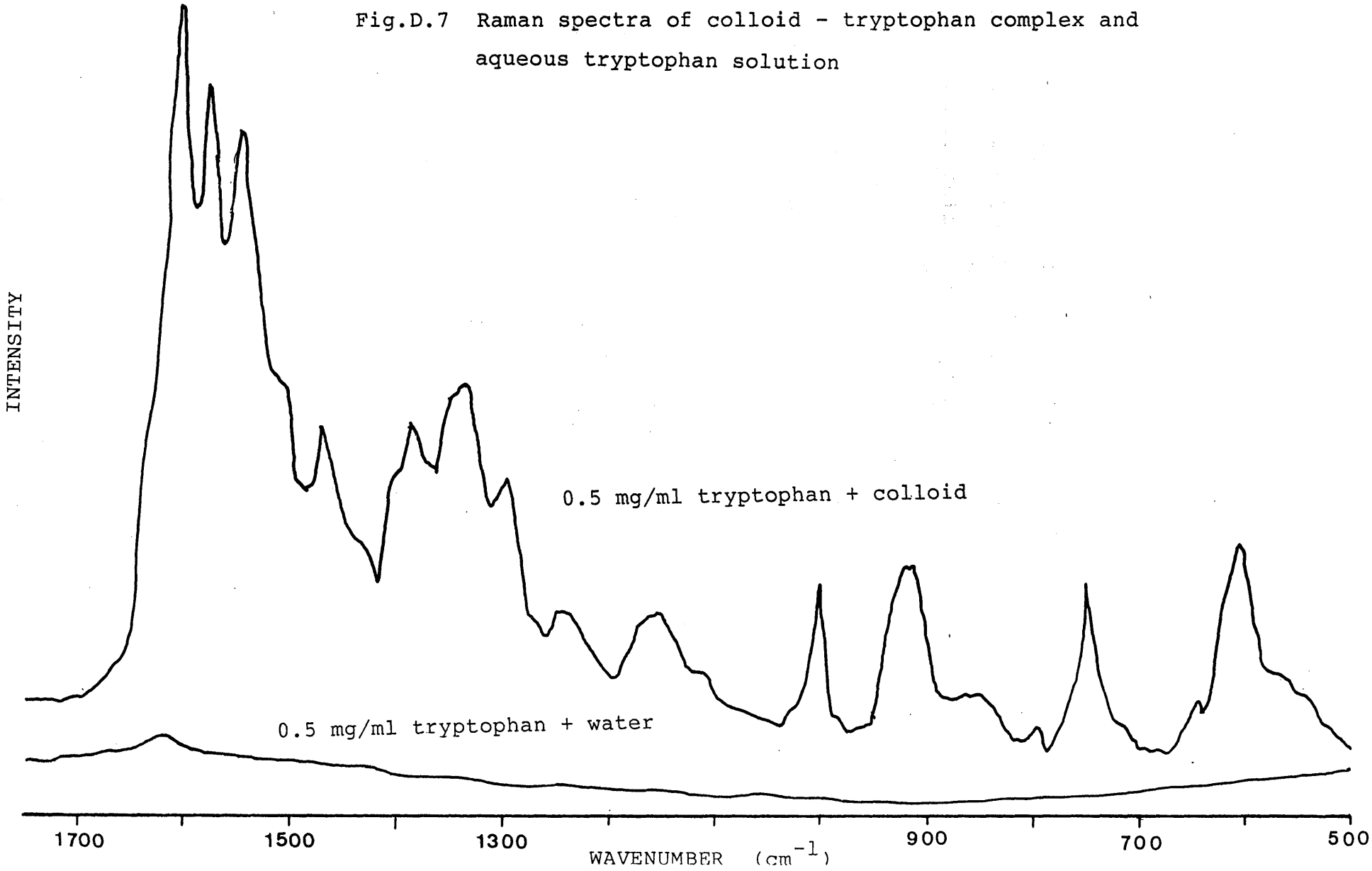

Fig.D.8 Absorption spectra of silver colloid and silver colloid + 0.5mg/ml phenylalanine

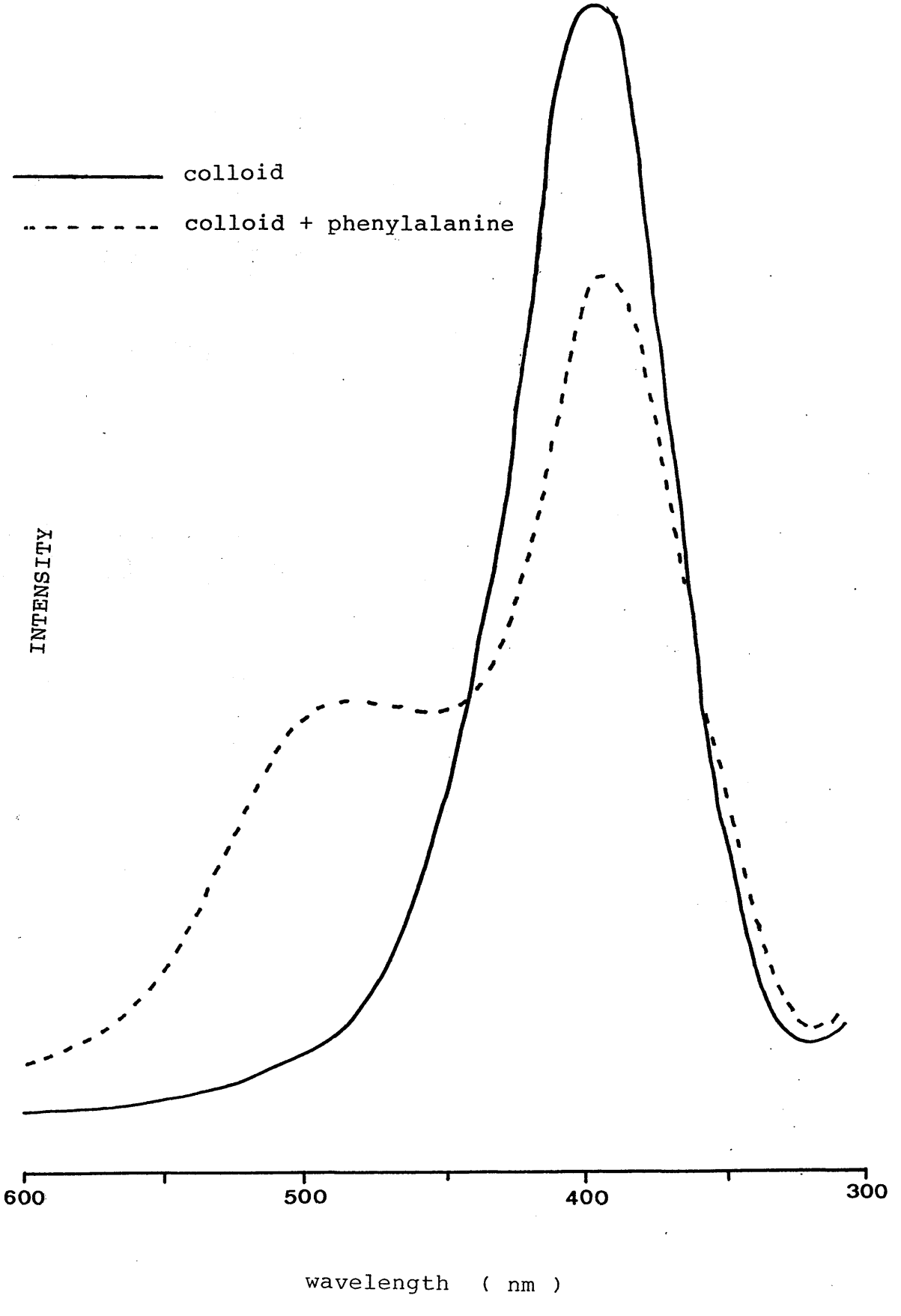

Fig.D.9 Raman spectra of colloid - phenylalanine complex and aqueous phenylalanine solution

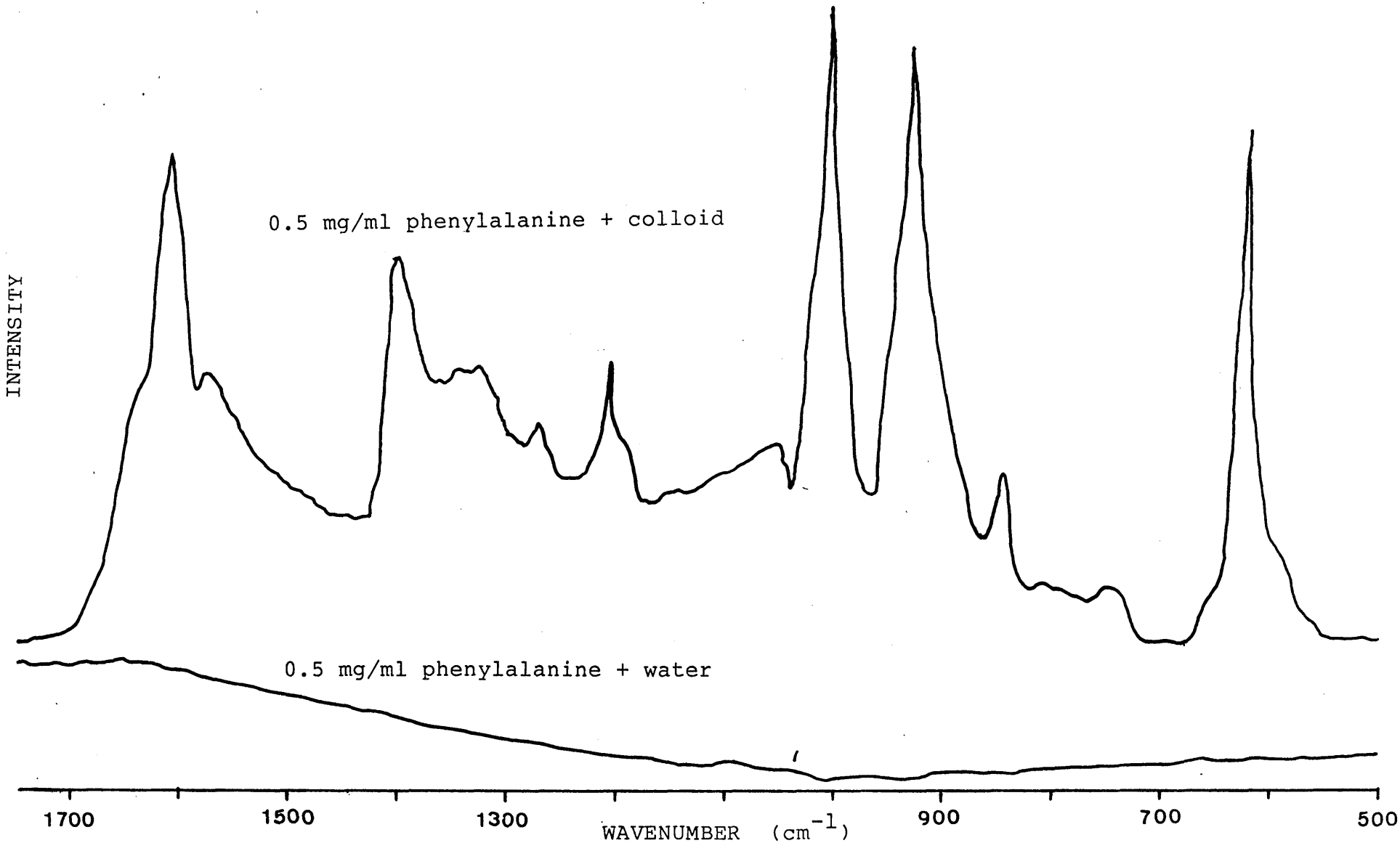

This method of recording the Raman spectra of biological molecules of this type and dimension is therefore ideal - intense spectra are usually obtained which correspond fairly closely to those recorded for the species in concentrated solution or solid form, using a fraction of the amount of material. Applying the SERS technique to record protein spectra should therefore be of great advantage - for the reasons mentioned previously.

SERS of Lysozyme + Silver Colloid

The result obtained for 0.15μM lysozyme in silver colloid is described in Fig.D.10. It was not possible to obtain a more detailed spectrum by adding greater amounts of lysozyme. This may be because of the decrease in scattering enhancement observed with increasing distance of lysozyme groups from the silver surface, it might be that the adsorbed lysozyme is denatured in some way or perhaps the lysozyme is existing free in solution and is not adsorbed to the metal. This final suggestion is partly eliminated by the Raman spectrum of 0.15 μM lysozyme in water which for the most part is devoid of any significant features. The first step was therefore to check if the enzyme was still active and this was carried out using an assay procedure involving the bacterium micrococcus lysodeikticus, the cell walls of which are particularly susceptible to lysozyme.

Assay Procedure using the Lysozyme Substrate Micrococcus Lysodeikticus

The following solutions were pipetted into a cuvette:

Fig.D.10 Raman spectrum of 0.15 μM lysozyme - colloid complex

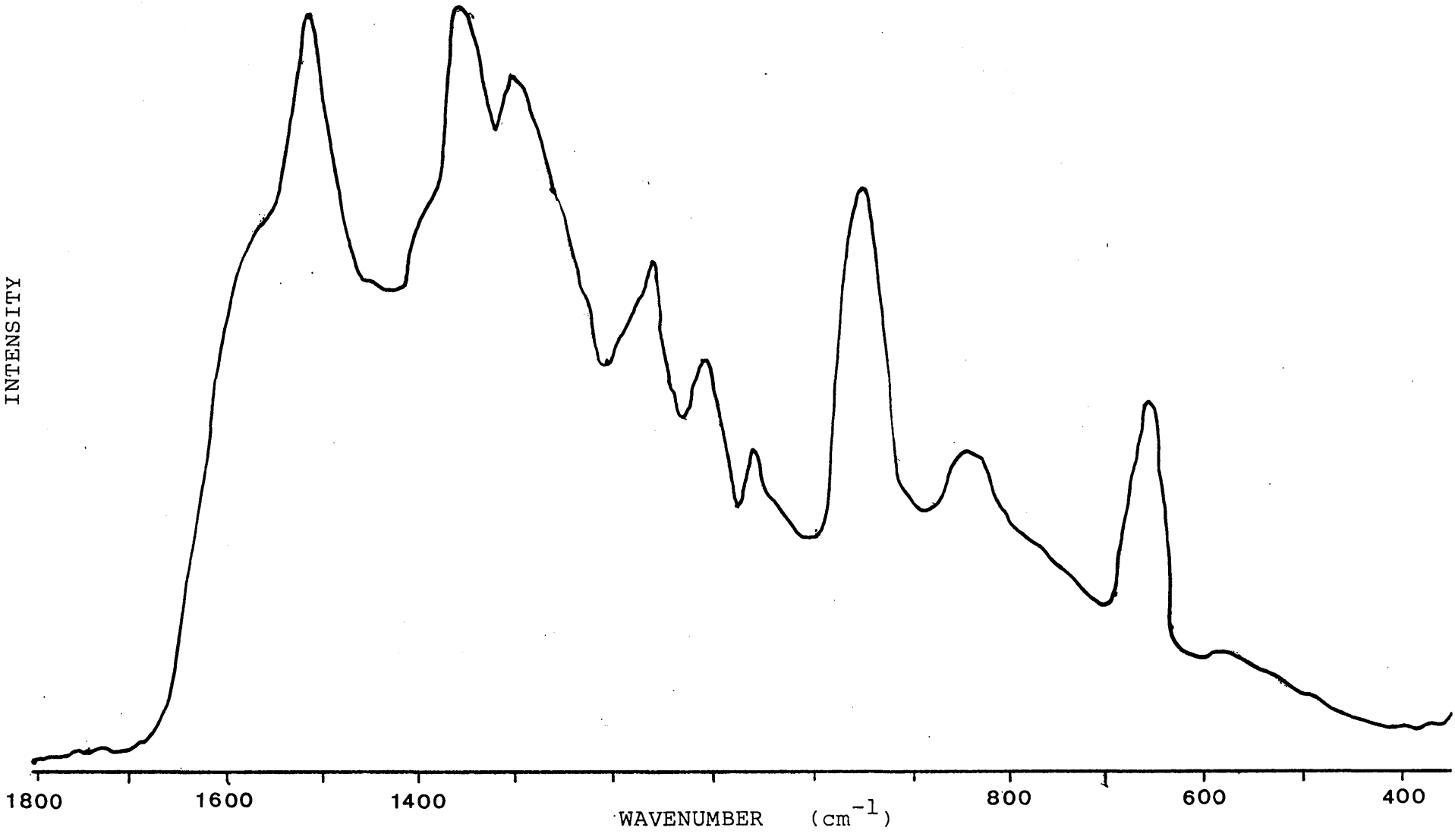

2.5ml of a suspension of micrococcus lysodeikticus (Sigma Chemical Co.Ltd.) in 0.066M potassium phosphate buffer, pH6.24. (The potassium phosphate buffer was prepared to the correct pH by adding amounts of 0.066M di-potassium hydrogen orthophosphate, trihydrate to 0.066M potassium dihydrogen orthophosphate). The $O.D._{450}$ of this suspension was between 0.60 and 0.70; the exact reading was recorded as the zero time reading.

The cuvette was left to equilibrate to $25^{o}C$.

0.1ml of lysozyme solution in 0.066M phospate buffer, pH6.24, containing 0.1-0.2$mgml^{-1}$, was added to the cuvette and mixed by inversion. The cuvette was then quickly placed in the spectrophotometer and the decay of absorbance at 450nm followed for approximately three minutes.

Activity of the lysozyme was defined as one unit being equal to the amount of enzyme which caused a $\Delta O.D._{450}$ of 0.001 in the micrococcus lysodeikticus suspension in one minute, at pH 6.24, in 2.6ml reaction mix and 1cm path length.
The calculation used was:

$$O.D._{450} \text{ per min}/\ 0.0001(X) = \text{units.mg}^{-1}$$

where X equals the concentration of lysozyme solution in $mgml^{-1}$.(Calculations are based on the initial rate since the rate may decrease as the reaction proceeds).

Specific activity of the lysozyme sample used was found to be approximately 16,000 $unitsmg^{-1}$.

Lysozyme Test Solution

A 0.5 μM lysozyme solution in phosphate buffer was prepared and 0.1ml added to 2.5ml of the assay mixture, producing a solution of final lysozyme concentration 0.019 μM. The absorbance at 450nm was seen to decay over five minutes and the resulting activity measurement indicated that the assay mixture contained 13 units of activity. A similar result was obtained when the lysozyme sample was prepared in water rather than buffer.

The $O.D._{450}$ was observed to decrease with time, even before lysozyme was added, implying that there was some impurity within the lysodeikticus solution itself.

Lysozyme + Silver Colloid

0.1ml of 0.5μM lysozyme solution in silver colloid was added to the assay medium. The $O.D._{450}$ decreased rapidly, showing that the assay solution contained 12 units of activity. Since this is close in value to the result observed for lysozyme solution prepared in water, the implication arises that the presence of silver colloid has not had a major effect on the active site of the enzyme.This result suggests therefore that denaturation has not occurred but still does not provide information as to whether the lysozyme is adsorbed to the silver colloid or is "free" in solution.(If the former situation is prevalent, the fact that some lysozyme may be adsorbed onto the silver atoms by its active site may account for the apparent loss in activity - 13 units in aqueous solution to 12 units in colloid).

To determine if the lysozyme is adsorbed, 0.5 μM lysozyme solution was made up in silver colloid and this was centrifuged at 16,500 rpm for 20minutes. The supernatant was decanted and when assayed, found to contain a negligible amount of enzyme.The solid portion of the centrifuged colloid -lysozyme solution was redispersed in distilled water and assayed. A lysozyme activity of 11.4 units were present in the redispersed solution, which is a decrease from the activity value calculated before centrifugation. In calculating the activity value however, it has been assumed that the solid was completely and evenly redispersed. In fact this is probably unlikely since some aggregation of the silver-lysozyme complex is bound to occur and large particles could clearly be seen in the solution. This could account for the decreased activity.

One observation made by Smulevich and Spiro (1985) when investigating SERS of haem proteins was that denaturation can occur upon adsorption to silver particles. However, from the results reported here, it would appear that this is not the case with lysozyme adsorbed on silver. Lysozyme is not unique in this respect since it was clearly demonstrated that glucose oxidase showed undiminished activity while bound to colloid (Copeland et al,1984).

It would appear therefore that the Raman spectra obtained for lysozyme in silver colloid solution were of active and adsorbed lysozyme. Hence it is likely that detail has been lost on the spectra because it is only the groups of the

enzyme that are in close proximity to the surface of the silver particle which have their scattered signals enhanced. Presumably all of the enzyme molecules will not adsorb to the colloid via precisely the same amino acids and so this would explain the broad, overlapping peaks which are a feature of the SERS spectrum.

SERS of N-retinylidene-n-butylamine

As mentioned previously, the SERS technique is potentially of great importance for the study of species which are available in limited quantities. However, it has also been of use for recording spectra of biological molecules which have limited solubility in aqueous solution. One example of this is the study of the Schiff bases formed from retinal, the chromophoric group of the visual pigment which undergoes conformational change after it has absorbed a photon. The visual pigment-called rhodopsin-consists of the prosthetic group retinal bound by a Schiff-base linkage to a protein, opsin. Schiff-bases of retinal bound to "simple" molecules such as butylamine have been used in the past as model compounds to investigate the properties of rhodopsin itself. While these molecules are not soluble in aqueous solution, it is reported here that a Raman spectrum can be obtained in this medium using the SERS technique.(Previous SERS experiments have been carried out by Nabiev et al (1985) involving the membrane protein bacteriorhodopsin, found in some bacteria, which functions as a light driven proton pump).

Experimental

10ml of a $5X10^{-5}M$ stock solution of retinal in ethanol was prepared and to this was added 100 μl of redistilled butylamine. The solution was left at room temperature for approximately 20minutes, to allow the Schiff-base to form. This was confirmed by recording the absorption spectrum of the sample-the peak maximum shifted from 380nm for retinal to about 360nm for unprotonated Schiff-base (Fig.D.11).
50 μl of the $5X10^{-5}M$ N-retinylidene-n-butylamine solution was added to 25ml of silver colloid and the same volume to 25ml of water. Raman spectra were recorded for each of the solutions and the results obtained are reproduced in Fig. D.12. As expected the spectrum of Schiff-base in water is virtually featureless due to insolubility problems. The spectrum,however, obtained for Schiff-base in colloid corresponds well to the NSRS spectrum of retinal in ethanol (Fig.D.13) and published data (Curry et al,1982).

Future Work

While this technique may be useful to study PGK-especially since a low concentration of enzyme is required, possibly therefore easing the aggregation problems encountered at high PGK concentration-there was insufficient time to carry out these examinations.

SERS would probably be of use for investigating the higher frequency spectra of PGK but it is unlikely to be suitable for the low frequency work mentioned in chapter6, since the colloid itself exhibits large Rayleigh scattering.

Fig.D.11 Absorption spectra of 5 X 10^{-5}M retinal and 5 X 10^{-5}M retinal - Schiff base

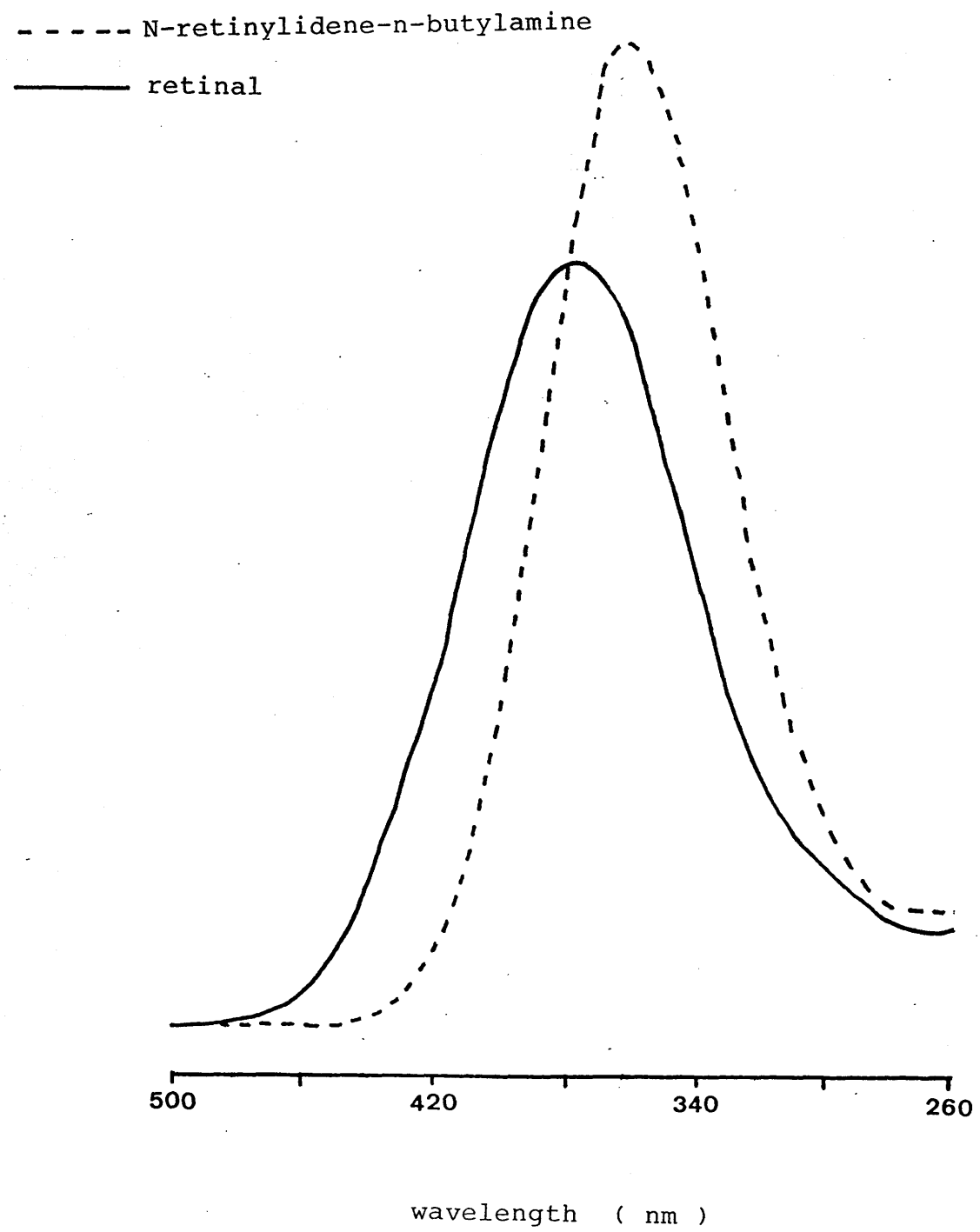

Fig.D.12 Raman spectra of 10^{-7}M N-retinylidene-n-butylamine in silver colloid and water

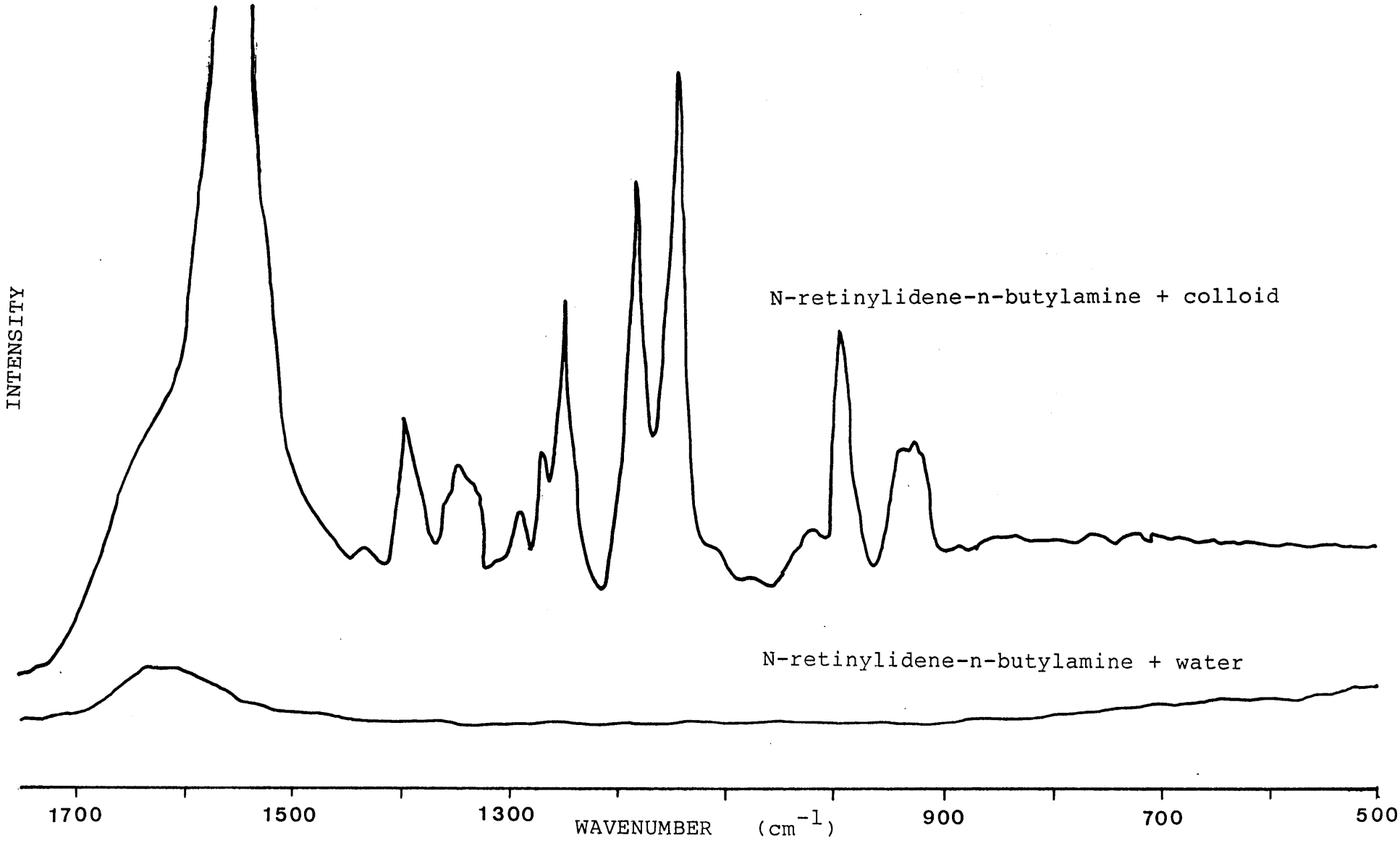

Fig.D.13 Raman spectrum of 10^{-4}M retinal in ethanol

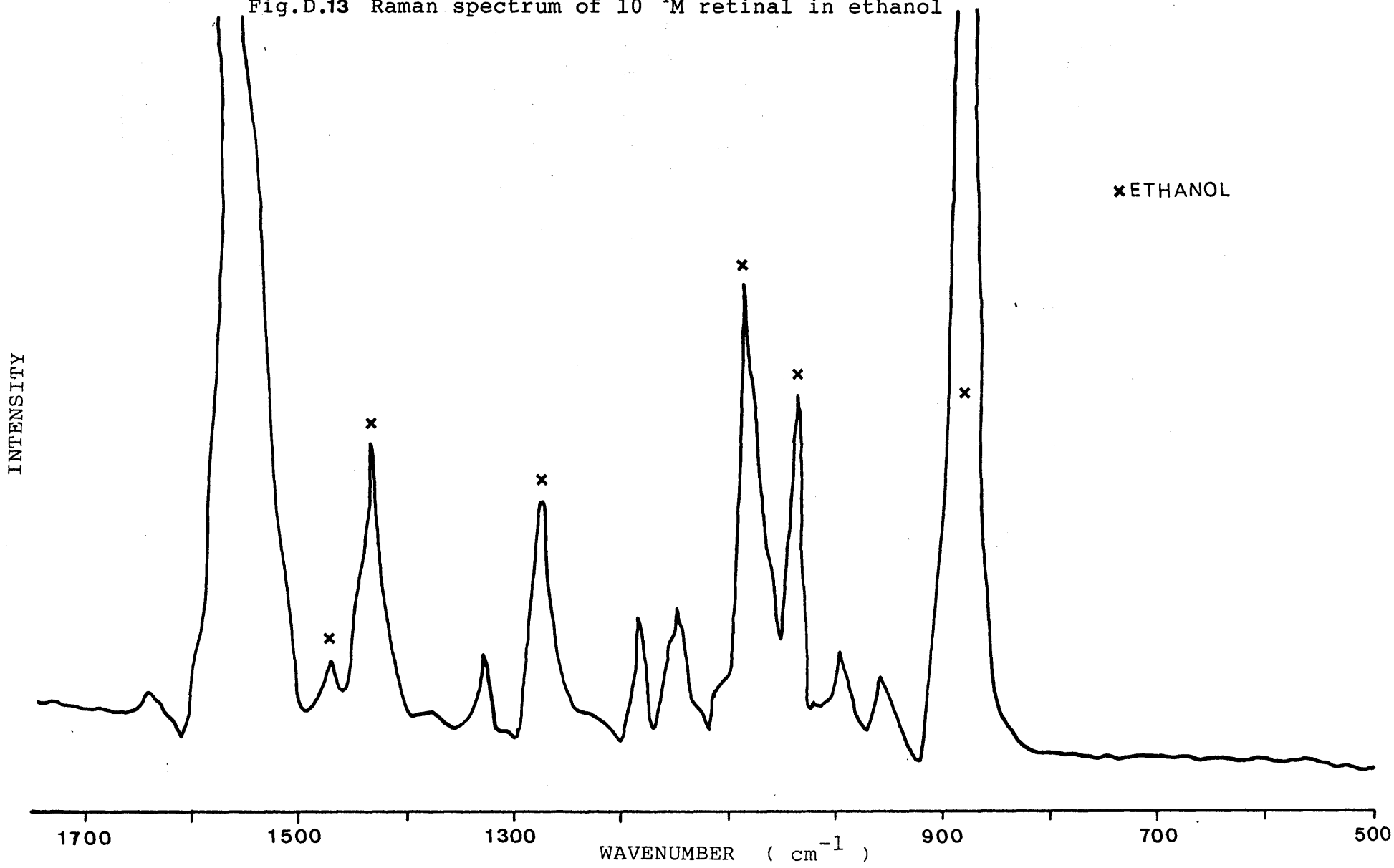

Adams B., Burgess R.J. and Pain R.H. (1985) Eur. J. Biochem. 152, 715.

Adams B. and Pain R.H. (1986) FEBS letters 196, 361.

Albrecht M.G. and Creighton J.A. (1977) J.Am.Chem.Soc. 99, 5215.

Ali M. and Brownstone Y.S. (1976) Biochim.Biophys.Acta 445, 89.

Allen C.S., Schatz G.C. and Van Duyne R.P. (1980) Chem. Phys. letters 75, 201.

Anderson C.M.,Zucker F.H. and Steitz T.A. (1979) Science 204, 375.

Armstrong G.T. (1964) J.Chem.Educ. 41, 297.

Artymiuk P.J.,Blake C.C.F.,Grace D.E.P.,Oatley S.J.,Phillips D.C. and Sternberg M.J.E. (1979) Nature 280, 563.

Atkins P.W. (1983) In Physical Chemistry,2nd edition. Oxford University Press, London.

Badea M.G. and Brand L. (1971) Methods Enzymol. 61, 378.

Banks R.D.,Blake C.C.F.,Evans P.R.,Haser R.,Rice D.W.,Hardy G.W., Merret M. and Phillips A.W (1979) Nature 279, 773.

Bartunik D., Jolles P., Berthou J. and Dianoux A.J. (1982) Biopolymers 21, 43.

Beck K., Gill S.J. and Downing M. (1965) J.Am.Chem.Soc. 87, 901.

Beece D.,Eisenstein L.,Frauenfelder H.,Good D.,Marden,M.C., Reinisch L.,Reynolds A.H.,Sorensen,L.B. and Yue,K.T. (1980) Biochemistry 19, 5147.

Beggs J.D. (1978) Nature 275, 104.

Beissner R.S. and Rudolph F.B. (1979) J.Biol.Chem. 254,6273.

Berger R.L.,Fok Chick Y. and Davids N. (1968) Rev. Scient. Instrum. 39, 362.

Bjurulf C., Laynez J. and Wadso I. (1970) Eur.J.Biochem. 14, 47.

Bjurulf C. and Wadso I. (1972) Eur.J.Biochem. 31, 95.

Blake C.C.F.,Johnson L.N.,Mair G.A.,North A.C.T.,Phillips D. C. and Sarma V.R. (1967) Proc.Roy.Soc. (London) Ser.B 167, 378.

Blake C.C.F. and Evans P.R. (1974) J.Mol.Biol. 84, 585.

Blatchford C.G.,Campbell J.R. and Creighton J.A. (1982) Surf. Sci. 120, 435.

Blatchford C.G., Kerker M. and Wang D.S. (1983) Chem. Phys. Letts. 100, 230.

Blatz L.A. (1967) J.Chem.Phys. 47, 841.

Blatz L.A. and Waldstein P. (1968) J.Phys.Chem. 72, 2614.

Blazyk J.F. and Steim J.M. (1972) Biochim. Biophys. Acta 266, 737.

Breslauer K.J.,Frank R.,Blocker H. and Marky L.A. (1986) PNAS 83, 3746.

Broach J.R. (1982) Cell 28, 203.

Brown K.G.,Erfurth S.C.,Small E.W. and Peticolas W.L. (1972) PNAS 69, 1467.

Bryant T.N.,Watson H.C. and Wendell P.L. (1974) Nature 247, 14.

Bucaro J.A. and Litovitz T.A. (1971a) J.Chem.Phys. 54, 3846.

Bucaro J.A. and Litovitz T.A. (1971b) J.Chem.Phys. 55, 3585.

Bucher T. (1947) Biochim. Biophys. Acta 1, 292.

Bucher T. (1955) Methods Enzymol. 1, 415.

Burstein E., Chen Y.J., Chen C.Y., Lundquist S. and Tosath E. (1979) Solid State Commun. 29, 567.

Byrne R.H. and Bryan W.P. (1970) Anal. Biochem. 33, 414.

Careri G., Fasella P. and Gratton E. (1979) Ann.Rev.Biophys. Bioeng. 8, 69.

Carey P.R. (1982) In Biochemical Applications of Raman and Resonance Raman Spectroscopies.New York,Academic Press.

Chang R.K. and Furtak T.E (1982) Eds. Surface Enhanced Raman Scattering.Plenum Press, New York.

Chen R.F. (1967) In Fluorescence:Theory,Instrumentation and Practice. Ed.G.G.Guilbault. Edward Arnold (Publishers) Ltd., London.

Chen M.C.,Lord R.C. and Mendelsohn R. (1974) J.Am.Chem.Soc. 96, 3038.

Chothia L. (1975) Nature 254, 304.

Cohen S.N. (1975) Scientific American 233, 24.

Conroy S.C. (1983) PhD Thesis, University of Aberdeen.

Conroy S.C.,Adams B.,Pain R.H. and Fothergill L.A. (1981) FEBS letters 128, 353.

Cooper A. (1974) Biochemistry 13, 2853.

Cooper A. (1976) PNAS 73, 2740.

Cooper A. (1984) Prog.Biophys.Molec.Biol. 44, 181.

Cooper A. and Dryden D.T.F. (1984) Eur.BiophysJ. 11, 103.

Copeland R.A.,Fodor S.P.A. and Spiro T.G. (1984) J.Am.Chem. Soc. 106, 3872.

Cotton T.M.,Schultz S.G. and Van Duyne R.P. (1980) J.Am.Chem. Soc. 102, 7960.

Cotton T.M.,Schultz S.G. and Van Duyne R.P. (1982) J.Am.Chem. Soc. 104, 6528.

Cotton T.M. and Van Duyne R.P. (1982) FEBS letters 147, 81.

Craik C.S., Largman C., Fletcher T., Roczniak S., Barr P.J., Fletterick R. and Rutter W.J. (1985) Science 228,291.

Creighton J.A.,Albrecht M.G.,Hester R.E. and Matthew J.A.D. (1978) Chem.Phys.Letts. 55, 55.

Creighton J.A.,Blatchford C.G.,Albrecht M.G. (1979) J.Chem. Soc.,Faraday Trans. 75, 790.

Creighton J.A.,Alvarez M.S.,Weitz D.A.,Garoff S. and Kim M.W. (1983) J.Phys.Chem. 87, 4793.

Curry B., Broek A., Lugtenburg J. and Mathies R. (1982) J.Am. Chem.Soc. 104, 5274.

Danforth R.,Krakauer H. and Sturtevant J.M. (1966) Rev. Sci. Instr. 38, 484.

Dardy H.D.,Volterra V. and Litovitz T.A. (1973) J.Chem.Phys. 59, 4491.

Dawson R.M.C.,Elliot D.C.,Elliot W.H. and Jones K.M. (1969) In Data for Biochemical Research, 2nd edition. Oxford University Press.

De Rooy N.,De Bruyn P.L. and Overbeek J.T.G. (1980) J.Colloid and Interface Science 75, 542.

Devlin G.E.,Davis J.L.,Chase L. and Geschwind S. (1971) App. Phys. letters 19, 138.

Dobson M.J.,Tuite M.F.,Roberts N.A.,Kingsman A.J.,Kingsman S.M.,Perkins R.E.,Conroy S.C.,Dunbar B. and Fothergill L.A. (1982) Nuc. Acid Res. 10, 2625.

Dodd J.W. and Tonge K.H. (1987) In Thermal Methods.Analytical Chemistry by Open Learning. John Wiley and Sons, London.

Doddrell D.,Glushko V. and Allerhand A. (1972) J.Chem.Phys. 56, 3683.

Donahue J. (1953) PNAS 39, 470.

Donovan J.W. and Ross K.D. (1973) Biochemistry 12, 512.

Doremus R.H. (1964) J.Appl.Phys. 35, 3456.

Dryden D.T.F. and Pain R.H. (1988),personal communication.

Eftink M.R. and Ghiron C.A. (1975) PNAS 72, 320.

Eftink M.R. and Ghiron C.A. (1977) Biochemistry 16, 5546.

Englander S.W.,Downer N.W. and Teitelbaum H. (1972) Ann. Rev. Biochem. 41, 903.

Englander S.W. and Englander J.J. (1972) Methods Enzymol. 26 406.

Fanconi B.,Small E.W. and Peticolas W.L. (1971) Biopolymers 10, 1277.

Fanconi B. and Peticolas W.L. (1971)Biopolymers 10,2223.

Fersht A. (1985)In Enzyme Structure and Mechanism.2nd edition Freeman,San Francisco.

Fifis T. and Scopes R.K. (1978) Biochem.J. 175, 311.

Fleischmann M.,Hendra P.J. and McQuillan A.J. (1974) Chem. Phys. letters 26, 163.

Frank H.S. and Evans M.W. (1945) J.Chem.Phys. 13, 507.

Frauenfelder H.,Petsko G.A. and Tsernoglou D. (1979) Nature 280, 558.

Fujita T.,Iwasa J. and Hansch C. (1964) J. Am. Chem. Soc. 86, 5175.

Furtak T.E. and Reyes J. (1980) Surf.Sci. 93, 351.

Garrell R.L., Shaw K.D. and Krimm S. (1981) J.Chem.Phys. 75 4155.

Gelin B.R. and Karplus M. (1975) PNAS 72, 2002.

Genzel L.,Keilmann F.,Martin T.P.,Winterling G.,Yacoby Y., Frohlich H. and Makinen M.W. (1976) Biopolymers 15, 219.

Gersten J. and Nitzan A. (1980) J.Chem.Phys. 73, 3023.

Gill S.J. and Beck K. (1965) Rev. Sci. Instr. 36, 274.

Gilson T.R. and Hendra P.J. (1970) In Laser Raman Spectroscopy, chapter2. Wiley, New York.

Go N. (1978) Biopolymers 17, 1373.

Grenthe I.,Ots H. and Ginstrup,O. (1970) Acta.Chem.Scand. 24, 1067.

Grinvald A. and Steinberg I.Z. (1974) Anal. Biochem. 59, 583.

Grinvald A. and Steinberg I.Z. (1976) Biochim. Biophys. Acta 427, 663.

Gross E. and Vuks M. (1935) Nature 135, 100.

Gucker F.T.,Pickard H.B. and Planck,R.W. (1938) J.Am.Chem. Soc. 61, 454.

Gurd F.R.N. and Rothgeb T.M. (1979) Adv.Prot.Chem. 33,73.

Hjelmgren T., Arvidsson L. and Larsson-Raznikiewicz M. (1976) Biochim.Biophys.Acta 445, 342.

Holland M.J. and Holland J.P. (1978) Biochemistry 17, 4900.

Hu C.Q. and Sturtevant J.M. (1987) Biochemistry 26, 178.

Hu C.Q. and Sturtevant J.M. (1988) submitted to Biochemistry.

Hutchinson C.A.,Phillips S.,Edgell M.H.,Gillam S.,Jahnke P. and Smith M. (1978) J.Biol.Chem. 253, 6551.

Hvidt A. and Nielsen S.O. (1966) Adv.Prot.Chem. 21, 287.

Itabashi M.,Kato K. and Itoh K. (1983) Chem. Phys. Letters 97,528.

Itoh K. and Shimanouchi T. (1970) Biopolymers 9, 383.

Itoh K. and Shimanouchi T. (1971) Biopolymers 10, 1419.

Jenkins F. (1974) PhD Thesis, University of Oxford.

Kaiser E.T. and Lawrence D.S. (1984) Science 226, 505.

Karplus M. and McCammon J.A. (1979) Nature 277, 578.

Karplus M. and McCammon J.A. (1981) CRC Crit.Rev.Biochem. 9, 293.

Kauzmann W. (1959) Adv. Prot. Chem. 14, 1.

Kerker M., Siiman O., Bumm L.A. and Wang D.S. (1980a) App. Optics 19, 3253.

Kerker M.,Wang D.S. and Chew H. (1980b) App. Optics 19, 3373.

Kerker M.,Wang D.S. and Chew H. (1980c) App. Optics 19, 4159.

Kerker M. (1984) Acc. Chem. Res. 17, 271.

Khamis M.M. and Larsson-Raznikiewicz M. (1981) Biochim. Biophys. Acta 657, 190.

Klapper M.H. (1971) Biochim. Biophys. Acta 229, 557.

Koglin E.,Lewinsky H.H. and Sequaris J.M. (1985) Surf. Sci. 158, 370.

Koglin E. and Sequaris J.M. (1986)Topics in Current Chemistry 134, 1.

Kowalski C.J. and Schimmel P.R. (1969) J.Biol.Chem. 244 3900.

Kresheck G.C. and Klotz I.M. (1969) Biochemistry 8, 8.

Krietsch W.K.G. and Bucher T. (1970) Eur.J.Biochem. 17, 568.

Krishnan C.V. and Friedman H.L. (1969) J.Phys.Chem. 73, 1572.

Lakowicz J.R. and Weber G. (1973) Biochemistry 12, 4171.

Lakowicz J.R. (1983) In Principles of Fluorescence Spectroscopy. Plenum Press, New York.

Langerman N. and Biltonen R.L. (1979) Methods Enzymol. 61, 261.

Larsson-Raznikiewicz M. (1964) Biochim.Biophys.Acta 85,60.

Larsson-Raznikiewicz M. (1967) Biochim.Biophys.Acta 132, 33.

Larsson-Raznikiewicz M. (1970a) Eur.J.Biochem. 15, 574.

Larsson-Raznikiewicz M. (1970b) Eur.J.Biochem. 17, 183.

Larsson-Raznikiewicz M. and Jansson J.R. (1973) FEBS letters 29, 345.

Lee B. and Richards F.M. (1971) J.Mol.Biol. 55, 379.

Lehrer S.S. (1971) Biochemistry 10,3254.

Leo A.,Hansch C. and Elkins D. (1971) Chem.Revs. 71, 525.

Lepp A. and Siiman O. (1985) J. Phys. Chem. 89, 3494.

Lesk A.M. and Chothia C. (1984) J. Mol. Biol. 174, 175.

Levitt M. (1983a) J. Mol. Biol. 168, 595.

Levitt M. (1983b) J. Mol. Biol. 168, 621.

Linderstrom-Lang K.U. and Schellman J.A. (1959)The Enzymes 1. Eds. P.D.Boyer, H.Lardy and K.Myrback. 2nd edition.

Lippitsch M.E. (1980) Chem. Phys. letters 74, 125.

Lippitsch M.E. (1981) Chem. Phys. letters 79, 224.

Lord R.C. and Yu N.T. (1970a) J. Mol. Biol. 50, 509.

Lord R.C. and Yu N.T. (1970b) J. Mol. Biol. 50, 203.

Markland F.S., Bacharach A.D.E., Weber B.H., O'Grady T.C., Saunders G.C. and Unemura N. (1975) J.Biol.Chem. 250, 130.

Mas M.T., Chen C.Y., Hitzeman R.A. and Riggs A.D. (1986) Science 233, 788.

Mas M.T., Resplandor Z.E. and Riggs A.D. (1987) Biochemistry 26, 5369.

Mas M.T.,Bailey J.M. and Resplandor Z.E. (1988) Biochemistry 27, 1168.

McCammon J.A., Gelin B.R., Karplus M. and Wolynes P.G. (1976) Nature 262, 325.

McCammon J.A. and Karplus M. (1977) Nature 268, 765.

McCammon J.A. and Harvey S.C. (1987) In Dynamics of Proteins and Nucleic Acids. Cambridge University Press, London.

McDevitt N.T. and Fateley W.G. (1970) J.Mol.Struct. 5, 477.

McQuillan A.J. and Pope C.G. (1980) Chem. Phys. letters 71, 349.

Merrett M. (1981) J. Biol. Chem. 256, 10293.

Mie G. (1908) Ann. Physik. 25, 377.

Monk P. and Wadso I. (1968) Acta.Chem.Scand. 22, 1842.

Mooradian A. (1970) Science 169, 20.

Mori N.,Singer-Sam J. and Riggs A.D. (1986) FEBS letters 204, 313.

Moscovits M. (1978) J. Chem. Phys. 69, 4159.

Nabiev I.R., Savchenko V.A. and Efremov E.S. (1983) J. Raman Spect. 14, 375.

Nabiev I.R., Efremov R.G., Chumanov G.D. and Kuryatav A.B. (1985) Biol. Membranes 2, 1003.

Norton I.T.,Goodall D.M.,Morris E.R. and Rees D.A. (1983) J. Chem. Soc.,Faraday Trans.I 79, 2475.

O'Connor D.V.O., Ware W.R. and Andre J.C. (1979) J.Phys.Chem. 83, 1333.

Otto A.,Billmann J.,Eickmans J.,Erturk U. and Pettenkofer C. (1984) Surf. Sci. 138, 319.

Painter P.C. and Mosher L.E. (1979) Biopolymers 18,3121.

Painter P.C.,Mosher L.E. and Rhoads C. (1981) Biopolymers 20 243.

Painter P.C.,Mosher L.E. and Rhoads C. (1982) Biopolymers 21 1469.

Parak F., Frolov E.N., Mossbauer R.L. and Goldanskii V.I. (1981) J. Mol. Biol. 145, 825.

Pauling L. and Corey R.B. (1951) PNAS 37, 256.

Perkins R.E.,Conroy S.C.,Dunbar B.,Fothergill L.A.,Tuite M.F, Dobson M.J., Kingsman S.M. and Kingsman A.J. (1983) Biochem.J. 211, 199.

Persson B.N.J. (1981) Chem. Phys. letters 82, 561.

Peticolas W.L. (1979) Methods Enzymol. 61, 425.

Pettinger B. and Wenning U. (1978) Chem. Phys. letters 56, 253.

Philpott M.R. (1975) J. Chem. Phys. 62, 1812.

Pickover C.A.,McKay D.B.,Engelman D.M. and Steitz T.A. (1979) J. Biol. Chem. 254, 11323.

Pockrand I. (1982) Chem. Phys. letters 85, 37.

Privalov P.L., Plotnikov V.V. and Filimonov V.V. (1975) J. Chem. Thermodyn. 7, 41.

Privalov P.L. (1979) Adv. Prot. Chem. 33, 167.

Privalov P.L. (1980) Pure Appl. Chem. 52 479.

Privalov P.L. and Potekhin S.A. (1986) Methods Enzymol. 131, 4.

Privat J.P.,Wahl P.,Auchet J.C. and Pain R.H. (1980) Biophys. Chem. 11, 239.

Radda G.K. and Dodd G.H. (1968) In Luminescence in Chemistry. Ed. E.J. Bowen. D.van Nostrand Company Ltd., London.

Razin A.,Hirose T.,Itakura K. and Riggs A.D. (1978) PNAS 75, 4269.

Reid D.S.,Quickenden M.A.J. and Franks F. (1969) Nature 224, 1293.

Richards F.M. (1974) J. Mol. Biol. 82, 1.

Richarz R.,Sehr P.,Wagner G. and Wuthrich K. (1979) J. Mol. Biol. 130, 19.

Richarz R.,Nagayama K. and Wuthrich K. (1980) Biochemistry 19, 5189.

Roustan C.,Fattoum A. and Pradel L.A. (1976) Biochemistry 15, 2172.

Roustan C., Fattoum A., Jeanneau R. and Pradel L.A. (1980) Biochemistry 19, 5168.

Sass J.K.,Sen R.K.,Meyer E. and Gerischer H. (1974) Surf.Sci. 44, 515.

Saviotti M.L., and Galley W.C. (1974) PNAS 71, 4154.

Schierbeck M. and Larsson-Raznikiewicz M. (1979) Biochim. Biophys. Acta 568, 195.

Schott H. and Kossel H. (1973) J.Am.Chem.Soc. 95, 3778.

Schulz G.E. and Schirmer R.H. (1979) In Principles of Protein

structure. Ed. C.R. Cantor. Springer-Verlag.

Scopes R.K. (1969) Biochem. J. 113, 551.

Scopes R.K. (1971) Biochem. J. 122, 89.

Scopes R.K. (1975) Methods of Enzymol. 42, 127.

Scopes R.K. (1978a) Eur. J. Biochem. 85, 503.

Scopes R.K. (1978b) Eur. J. Biochem. 91, 119.

Scopes R.K. and Algar E. (1979) FEBS letters 106, 239.

Sequaris J.M.,Koglin E. and Malfoy B. (1984) FEBS letters 173 95.

Sequaris J.M.,Fritz J.,Lewinsky H.H. and Koglin E. (1985) J. Coll. Interface Sci. 105, 417.

Siiman O.,Bumm L.A.,Callaghan R.,Blatchford C.G. and Kerker M. (1983) J. Phys. Chem. 87, 1014.

Singer S.J. and Nicolson G.L. (1972) Science 175, 720.

Skinner H.A. (1979) In Biochemical Microcalorimetry. Ed. H.A. Brown. Academic Press, New York.

Small E.W.,Fanconi B. and Peticolas W.L. (1970) J.Chem.Phys. 52, 4369.

Smulevich G. and Spiro T.G. (1985) J.Phys.Chem. 89,5168.

Spragg S.P., Wilcox J.K., Roche J.J. and Barnett W.A. (1976) Biochem. J. 153, 423.

Steim J.M.,Tourtellotte M.E.,Reinert J.C.,McElhaney R.N. and Rader R.L. (1969) PNAS 63, 104.

Stein D.L. (1985) PNAS 82, 3670.

Stidman H.D. and Dilella D.P. (1979) J.Raman Spect. 8, 181.

Strey G. (1969) Spectrochim. Acta 25A, 163.

Stryjewski W. and Wasylewski Z. (1986) Eur. J. Biochem. 158, 547.

Sturtevant J.M. (1987) Ann. Rev. Phys. Chem. 38, 463.

Suh J.S.,Dilella D.P. and Moskovits M. (1983) J. Phys. Chem.

87, 1540.

Takahashi M.,Sakai Y.,Fujita M. and Ito M. (1986) Surf. Sci. 176, 351.

Tanford C. (1968) Adv. Prot. Chem. 23, 122.

Tanford C. (1970) Adv. Prot. Chem. 24 1.

Tanford C. (1973) In The Hydrophobic Effect. John Wiley, New York.

Tanswell P.,Westhead E.W. and Williams R.J.P. (1976) Eur. J. Biochem. 63, 249.

Teale F.W.J. and Weber G. (1957) Biochem. J. 65, 476.

Teale F.W.J. (1960) Biochem. J. 76, 381.

Temperini M.L.A.,Chagas H.C. and Sala O. (1981) Chem. Phys. letters 79, 75.

Thomas P.G., Russel A.J. and Fersht A.R. (1985) Nature 318 375.

Tobin M.C. (1971) In Laser Raman Spectroscopy.Wiley,New York.

Tompa P., Hong P.T. and Vas M. (1986) Eur. J. Biochem. 154, 643.

Ueba H. (1983a) Surf. Sci. 131, 328.

Ueba H. (1983b) Surf. Sci. 131, 347.

Ulmer K.M. (1983) Science 219, 666.

Valentine R.C. and Green N.M. (1967) J.Mol.Biol. 27, 615.

Van Duyne R.P. (1977) J.Phys. (Paris) 38, C-5, 239.

Vas M. and Batke J. (1984) Eur. J. Biochem. 139, 115.

Von Raben K.U.,Chang R.K. and Laube B.L. (1981) Chem. Phys. letters 79, 465.

Wadso I. (1968) Acta Chem. Scand. 22, 927.

Wadso I. (1970) Quart. Rev. Biophys. 3, 383.

Wadso I. (1972) MTP International review of science,physical chemistry, vol.10. Ed. H.A.Skinner.Butterworth,London.

Wadso I. (1976) Methods of Biochemical Analysis 23, 1.

Wagner G. and Wuthrich K. (1978) Nature 275, 247.

Wagner G. and Wuthrich K. (1979) J. Mol. Biol. 130, 31.

Wagner G. (1983) Quart. Rev. Biophys. 16, 1.

Wallace R.B.,Johnson P.F.,Tanaka S.,Schold M.,Itakawa K. and Abelson J. (1980) Science 209, 1396.

Wang D.S. and Kerker M. (1981) Phys. Rev. B. 24, 1777.

Watson H.C.,Walker N.P.C.,Shaw P.J.,Bryant T.N.,Wendell P.L., Fothergill L.A., Perkins R.E., Conroy S.C., Dobson M.J., Tuite M.F.,Kingsman A.J. and Kingsman S.M. (1982) EMBO J. 1, 1635.

Webb M.R. and Trentham D.R. (1980) J.Biol.Chem. 255,1775.

Weber G. (1961) Nature 190, 27.

Weber G. (1975) Adv. Prot. Chem. 29, 1.

Weitz D.A., Garoff S. and Gramila T.J. (1982) Opt. letters 7, 168.

Wetlaufer D.B. (1962) Adv. Prot. Chem. 17, 304.

Wetzel H. and Gerischer H. (1980) Chem.Phys.letters 76, 460.

Wilson C.A.B., Tuite M.F., Dobson M.J.,Kingsman S.M.,Kingsman A.J.,Glover L.A., Hardman N., Watson H.C. and Fothergill L.A. (1984) Biochem. Soc. Trans. 12, 278.

Wilson C.A.B. (1985) PhD Thesis, University of Aberdeen.

Wilson C.A.B.,Hardman N.,Fothergill-Gilmore L.A.,Gamblin S.J. and Watson H.C. (1987) Biochem. J. 241, 609.

Wilson E.B., Decius J.C. and Cross P.C. (1955) In Molecular Vibrations. McGraw-Hill, New York.

Wilson H.R.,Williams R.J.P.,Littlechild J.A. and Watson H.C. (1988) Eur. J. Biochem. 170, 529.

Woodward C.K and Hilton B.D. (1979) Ann.Rev.Biophys.Bioeng. 8, 99.

Wuthrich K. and Wagner G. (1979) J. Mol. Biol. 130, 1.

Wuthrich K. (1979) In Protein Folding. Eds. A.Balaban and R. Jaenicke.

Yamada H. and Yamamoto Y. (1981) Chem. Phys. letters 77, 520.

Yguerabide J. (1972) Methods of Enzymol. 26, 498.

Yu N.T. (1974) J. Am. Chem. Soc. 96, 4664.

Yu N.T. (1977) CRC Critical Reviews in Biochemistry 4, 229.